

Durham E-Theses

Can biochar retain water holding capacity in United Arab Emirates (UAE) soils?

Naeema Al Nofeli and Fred Worrall and Chris Greenwell

How to cite:

Al Nofeli, Naeema and Worrall, Fred and Greenwell, Chris (2026) Can biochar retain water holding capacity in United Arab Emirates (UAE) soils? Doctoral thesis, Durham University.

Use policy

The full-text may be used and/or reproduced, and given to third parties in any format or medium, without prior permission or charge, for personal research or study, educational, or not-for-profit purposes provided that:

- a full bibliographic reference is made to the original source
- a <https://etheses.durham.ac.uk/id/eprint/16671/> is made to the metadata record in Durham E-Theses
- the full-text is not changed in any way

The full-text must not be sold in any format or medium without the formal permission of the copyright holders.

Please consult the [full Durham E-Theses policy](#) for further details.

Can biochar retain water holding capacity in United Arab Emirates (UAE) soils?

Naeema Al Nofeli

Abstract

Water scarcity has a huge impact on global food security, particularly in countries with arid climates and less fertile soils. Recently, there has been increasing interest in the production of biochar from agricultural wastes as a potential solution for improving soil quality. Studies have shown that biochar can enhance carbon sequestration, plant growth and soil pH. Although there are many reported benefits of biochar, there has been limited research into the behaviour of biochar in arid environments, where water retention is a critical factor in improving soil health. The aim of this research was to investigate the potential of Date Palm Fronds (DPF) and biochar to improve water holding capacity and plant growth in the context of an arid climate. The aim was approached by 4 main experiments: 1) Investigate the physiochemical properties of the materials; 2) A mesocosm experiment to measure the water holding capacity of the soils with biochar amendments; 3) Pot trial experiments to evaluate plant growth, and 4) Analysis of water retention using Thermal Gravimetric Analysis (TGA). The experiments took place in two different locations: the Department of Earth Science in Durham University, UK and the United Arab Emirates (UAE), Abu Dhabi. UAE sandy soils were amended with both date palm fronds and biochar derived from DPF. The effects of the treatments were assessed using Analysis of

Variance (ANOVA). The results demonstrate that biochar improves plant growth and soil quality, while DPF can be equally effective and in some cases more effective in enhancing water retention. Biochar exhibited greater porosity, a higher carbon to nitrogen ratio and increased thermal stability compared to DPF. Both biochar and DPF enhanced soil moisture retention, with biochar showing greater effectiveness during wet cycles and supporting plant growth under extreme conditions. The combined application of biochar and DPF further improved soil moisture and plant growth, with lower application rates proving more effective.

These findings support the use of biochar and DPF as a sustainable soil amendment to address water scarcity and soil degradation in arid regions. Further research should focus on long-term field studies as well as the economic and environmental implications of large-scale biochar application. This study provides valuable insights into using biochar and DPF for sustainable soil improvement and agricultural productivity in a challenging environment.

Can biochar retain water-holding capacity in United Arab Emirates (UAE) soils?

Naeema Al Nofeli

Thesis submitted in fulfilment for the degree of Doctor of Philosophy
Department of Earth Sciences, Durham University

2026

Table of content

| | |
|--|----|
| Declaration | 1 |
| Statement of copyright | 1 |
| Acknowledgement..... | 2 |
| Chapter 1: Introduction and Literature Review | 4 |
| 1.1 Introduction..... | 4 |
| 1.1.1 Biochar..... | 5 |
| 1.1.1.1 Biochar definition | 5 |
| 1.1.1.2 Biochar benefits..... | 5 |
| 1.1.1.3 Climate change..... | 7 |
| 1.1.1.4 Biochar production..... | 9 |
| 1.1.1.5 Biochar properties..... | 11 |
| 1.1.1.6 Biochar application..... | 13 |
| 1.2 Biochar Application in UAE Sandy Soils: The UAE Context..... | 13 |
| 1.3 Research gap | 15 |
| 1.4 Novelty of the study | 16 |
| 1.5 Aim and objectives..... | 16 |
| 1.6 Outline of the thesis..... | 17 |
| Chapter 2: Physiochemical properties of UAE sand, sharp sand, DPF and Biochar..... | 19 |
| 2.1 Introduction | 19 |
| 2.2 Materials and methods..... | 19 |
| 2.2.1 Sample Collection | 19 |
| 2.2.1.1 <i>Sandy Soil Collection</i> | 19 |
| 2.2.1.2 <i>Land soil survey</i> | 20 |
| 2.2.1.3 <i>Date Palm Waste Collection</i> | 21 |
| 2.2.1.4 <i>Date Palm Frond preparation</i> | 21 |
| 2.2.1.5 <i>Biochar production</i> | 22 |
| 2.2.2 Physical Characterization | 23 |
| 2.2.2.1 Scanning Electron Microscopy (SEM) and the energy dispersive spectroscopy (EDS) | 23 |
| 2.2.2.2 Light Optical Microscope..... | 23 |
| 2.2.2.3 Brunauer–Emmett–Teller (BET) experiment | 24 |

| | | |
|---------|--|----|
| 2.2.2.4 | Sieving Analysis | 24 |
| 2.2.3 | Chemical Characterization..... | 24 |
| 2.2.3.1 | Elemental analysis for Carbon, Hydrogen, and Nitrogen (CHN)..... | 24 |
| 2.2.3.2 | Thermogravimetric analysis (TGA) | 25 |
| 2.3 | Results | 25 |
| 2.3.1 | SEM | 25 |
| 2.3.1.1 | SEM of DPF | 25 |
| 2.3.1.2 | SEM of biochar | 27 |
| 2.3.1.3 | SEM of Sharp Sand | 29 |
| 2.3.1.4 | SEM of UAE sand..... | 30 |
| 2.3.2 | Light Optical Microscopy | 31 |
| 2.3.2.1 | Sharp Sand | 31 |
| 2.3.2.2 | UAE Sand | 32 |
| 2.3.3 | BET..... | 32 |
| 2.3.4 | Sieving Analysis of Sharp Sand and UAE Sand | 33 |
| 2.3.5 | Chemical Analysis..... | 33 |
| 2.3.5.1 | ESM EDS..... | 33 |
| 2.3.5.2 | CHN analysis..... | 34 |
| 2.3.5.3 | Thermogravimetric Analysis (TGA) | 34 |
| 2.4 | Discussion | 36 |
| 2.5 | Conclusion..... | 47 |
| 3.1 | Introduction | 49 |
| 3.2 | Approach Statement | 50 |
| 3.3 | Materials and methods..... | 50 |
| 3.3.1 | <i>Sample collection</i> | 50 |
| 3.3.2 | <i>Date Palm frond preparation</i> | 50 |
| 3.3.3 | <i>Sandy soil preparation</i> | 50 |
| 3.3.4 | <i>Mesocosms experimental design</i> | 51 |
| 3.3.4.1 | <i>Measuring Temperature & Humidity</i> | 54 |
| 3.3.5 | <i>Statistical Analysis</i> | 55 |
| 3.4 | Results | 55 |
| 3.4.1 | <i>Weight loss</i> | 55 |
| 3.4.2 | <i>Moisture content</i> | 55 |
| 3.4.3 | <i>ANOVA results</i> | 63 |
| 3.5 | Discussion | 72 |
| 3.6 | Conclusion..... | 76 |

| | | |
|---------|--|-----|
| 4.1 | Introduction | 78 |
| 4.2 | Approach..... | 79 |
| 4.3 | Materials and method | 79 |
| 4.3.1 | <i>Sample collection</i> | 79 |
| 4.3.2 | <i>Laboratory pot trial experiment (controlled conditions)</i> | 80 |
| 4.3.3 | <i>Field pot trial experimental (uncontrolled conditions)</i> | 87 |
| 4.3.4 | <i>Statistical Analysis</i> | 88 |
| • | Growth rate calculation | 90 |
| 4.4 | Results | 91 |
| 4.4.1 | <i>Height</i> | 91 |
| 4.4.1.1 | Plant growth in controlled condition (laboratory based)..... | 91 |
| 4.4.1.2 | Plant growth in uncontrolled conditions (field based)..... | 95 |
| • | <i>Growth Rate</i> | 99 |
| a. | <i>Growth Rate in controlled experiment</i> | 99 |
| b. | <i>Growth Rate in uncontrolled experiment</i> | 100 |
| 4.4.2 | <i>Moisture level</i> | 101 |
| 4.4.2.1 | Moisture level in the controlled experiment. | 101 |
| 4.4.2.2 | Moisture level in the uncontrolled experiment..... | 105 |
| 4.4.3 | <i>Soil temperature</i> | 109 |
| 4.4.3.1 | Soil temperature in controlled experiment. | 109 |
| 4.4.3.2 | Soil temperature in uncontrolled experiment..... | 113 |
| 4.4.4 | <i>Soil pH</i> | 117 |
| 4.4.4.1 | Soil pH in controlled experiment..... | 117 |
| 4.4.4.2 | Soil pH in uncontrolled experiment | 119 |
| 4.4.5 | <i>Light</i> | 122 |
| 4.4.5.1 | Light in controlled experiment | 122 |
| 4.4.5.2 | Light in uncontrolled experiment..... | 122 |
| 4.4.6 | <i>Canopeo</i> | 123 |
| 4.4.7 | <i>ANOVA results</i> | 124 |
| 4.4.7.1 | Controlled | 124 |
| 4.4.7.2 | Uncontrolled..... | 147 |
| 4.5 | Discussion | 158 |
| 4.6 | Conclusion..... | 163 |
| 6.1 | Introduction | 178 |
| 6.2 | Approach..... | 178 |
| 6.3 | Materials and methods..... | 179 |

| | | |
|---------|-----------------------------------|-----|
| 6.3.1 | <i>Sample collection</i> | 179 |
| 6.3.2 | <i>Mesocosms</i> | 179 |
| 6.3.3 | <i>Pot trial</i> | 180 |
| 6.3.4 | <i>Statistical Analysis</i> | 183 |
| 6.4 | Results | 184 |
| 6.4.1 | <i>Mesocosms experiment</i> | 184 |
| 6.4.1.1 | <i>Moisture content</i> | 184 |
| 6.4.2 | <i>Pot trial experiment</i> | 187 |
| 6.4.2.1 | Plant height | 187 |
| • | Growth rate calculation | 189 |
| 6.4.2.2 | Moisture level..... | 190 |
| 6.4.2.3 | Soil temperature | 191 |
| 6.4.2.4 | Soil pH | 193 |
| 6.4.2.5 | Light..... | 193 |
| 6.4.3 | <i>ANOVA results</i> | 195 |
| 6.4.3.1 | <i>Mesocosm experiment</i> | 195 |
| 6.5 | Discussion | 216 |
| 6.6 | Conclusion..... | 219 |
| 7.1 | Overview of thesis..... | 220 |
| 7.2 | Key objectives and findings..... | 220 |
| 7.3 | Implications..... | 221 |
| 7.4 | Limitations | 222 |
| 7.5 | Future work..... | 223 |
| 8.1 | References | 224 |

List of figures

| | |
|--|----|
| Figure 1.1. The benefits of biochar ((International Biochar Initiative, 2018)..... | 6 |
| Figure 1.2. Biochar meets Sustainable Goal Developments at least 12 goals (Kumar and Bhattacharya, 2021). | 8 |
| Figure 1.3. The different types of pyrolysis process (slow, fast and flash) (Bhaskar et al., 2019). | 10 |
| Figure 2.1. The image indicates the Soil Group Classification of the UAE and specifies the Al Nahda East soil collection. | 20 |
| Figure 2.2. Location of Date Palm Waste Collection (Dubai- Abu Dhabi Road)..... | 21 |
| Figure 2.3. Date Palm Frond preparation in the Lab..... | 22 |
| Figure 2.4. (a) DPF weighed before being charred and (b) is DPF after being charred which is called biochar. | 22 |
| Figure 2.5. SEM imaging of Date Palm Frond (DPF) that shows the left side (a) taken in 10 μ m and the right side (b) was taken in 50 μ m. | 26 |
| Figure 2.6. The pore size distribution of DPF and pore count. | 26 |
| Figure 2.7. SEM imaging of biochar that shows the left side (a) taken in 10 μ m and the right side (b) was taken in 50 μ m. | 27 |
| Figure 2.8. The pore size distribution of biochar and pore count. | 27 |
| Figure 2.9. Comparison of the pore size distribution of DPF and biochar. | 28 |
| Figure 2.10. SEM imaging of sharp sand..... | 29 |
| Figure 2.11. The particle size distribution of sharp sand. | 29 |
| Figure 2.12. SEM imaging of UAE sand. | 30 |
| Figure 2.13. The particle size distribution of UAE sand..... | 31 |
| Figure 2.14. Sharp sand images taken 10x magnification on image (A) and 40x magnification (B). .. | 31 |
| Figure 2.15. UAE sand images taken 10x lens magnification on image (A) and 40x lens magnification on image (B). | 32 |
| Figure 2.16. Grain size distribution of Sharp Sand. | 33 |
| Figure 2.17. TGA curve for Date Palm fronds and biochar at heating rate 5oC/min. | 34 |
| Figure 2.18. TGA curve for Sharp Sand and UAE Sand at heating rate 5oC. | 35 |
| Figure 2.19 Carbon content of biochar and no charged materials | 41 |
| Figure 2.20 Carbon and nitrogen ratio versus pyrolysis temperature. | 43 |
| Figure 3.1. Mesocosms PVC tube experimental design for biochar application..... | 54 |
| Figure 3.2. (a) shows the 3 materials used, which are: Sand, DPF and biochar. (b) shows the treatments of biochar and DPF. (c) The samples were placed on a tray, then in the oven for 3 weeks at 40° C..... | 54 |
| Figure 3.3. The boxplot of the moisture content (% by weight) of the materials measured during the wet cycle. Box-and-whisker plots show the interquartile range, with the box representing the first quartile (Q1) to the third quartile (Q3), and the whiskers extending from the minimum to the maximum values. The median is represented by a line within the box, and the cross symbol (x) indicates the mean moisture content. | 56 |
| Figure 3.4. The boxplot of the moisture content (% by weight) of the treatment*material interaction for the wet cycle. Box-and-whisker plots show the interquartile range, with the box representing the first quartile (Q1) to the third quartile (Q3), and the whiskers extending from the minimum to the maximum values. The median is represented by a line within the box, and the cross symbol (x) indicates the mean moisture content. | 57 |

| | |
|--|----|
| Figure 3.5. The boxplot of the moisture content (% by weight) of the materials measured during the dry cycle. Box-and-whisker plots show the interquartile range, with the box representing the first quartile (Q1) to the third quartile (Q3), and the whiskers extending from the minimum to the maximum values. The median is represented by a line within the box, and the cross symbol (x) indicates the mean moisture content. | 58 |
| Figure 3.6. The boxplot of the moisture content (% by weight) of the treatment*material interaction measured during the dry cycle. Box-and-whisker plots show the interquartile range, with the box representing the first quartile (Q1) to the third quartile (Q3), and the whiskers extending from the minimum to the maximum values. The median is represented by a line within the box, and the cross symbol (x) indicates the mean moisture content. | 59 |
| Figure 3.7. The boxplot of the moisture content (% by weight) of the materials measured during the dry cycle (waw). Box-and-whisker plots show the interquartile range, with the box representing the first quartile (Q1) to the third quartile (Q3), and the whiskers extending from the minimum to the maximum values. The median is represented by a line within the box, and the cross symbol (x) indicates the mean moisture content. | 60 |
| Figure 3.8. The boxplot of the moisture content (% by weight) of the treatment*material interaction measured during the dry cycle (waw). Box-and-whisker plots show the interquartile range, with the box representing the first quartile (Q1) to the third quartile (Q3), and the whiskers extending from the minimum to the maximum values. The median is represented by a line within the box, and the cross symbol (x) indicates the mean moisture content. | 61 |
| Figure 3.9. QQ' plot of the observed value of the moisture content. Log MC =log(Moisture Content). | 63 |
| Figure 3.10. Main effects plot of the Cycle factor with respect to moisture content. Error bars are the 95% confidence interval. | 65 |
| Figure 3.11. Main effects plot of the Treatment factor on moisture content. Error bars are the 95% confidence interval and may be smaller than the plotted point. | 66 |
| Figure 3.12. Main effects plot of the Material factor with respect to moisture content. Error bars are the 95% confidence interval. | 67 |
| Figure 3.13. Main effects plot of the Day factor with respect to moisture content moisture content. Error bars are the 95% confidence interval. | 68 |
| Figure 3.14. The interaction plot of moisture content between Day and Treatment factors. | 70 |
| Figure 3.15. The interaction plot of moisture content between the Material and Cycle factors. | 71 |
| Figure 4.1. (a) first germination during the wet cycle, (b) plant growth results by the end of the wet cycle and (c) dry cycle results. | 86 |
| Figure 4.2. (a) the first stage of wet cycle field experiment (pots were uncovered). Figure (b) the pots were covered to reduce direct sunlight. (c) first germination of watermelon and figure (d) shows the results of watermelon growth. | 87 |
| Figure 4.3. Boxplot of plant height (cm) relative to the Material factors measured during the wet cycle. Box show the interquartile range, with the box representing the first quartile (Q1) to the third quartile (Q3), and the median is represented by a line within the box, and the cross symbol (x) indicates the mean plant height. | 91 |
| Figure 4.4. Boxplot of plant height (cm) relative to the Treatment*Material interaction measured during the wet cycle. Box show the interquartile range, with the box representing the first quartile (Q1) to the third quartile (Q3), and the median is represented by a line within the box, and the cross symbol (x) indicates the mean plant height. | 92 |
| Figure 4.5. Boxplot of height (cm) relative to the Material factors measured during the dry cycle. Box plots show the interquartile range, with the box representing the first quartile (Q1) to the third quartile (Q3), and the median is represented by a line within the box, and the cross symbol (x) indicates the mean plant height. | 93 |

Figure 4.6. Boxplot of height (cm) relative to the Treatment*Material interaction measured during the dry cycle. Box plots show the interquartile range, with the box representing the first quartile (Q1) to the third quartile (Q3), and the median is represented by a line within the box and the cross symbol (x) indicates the mean plant height. 94

Figure 4.7. Boxplot of height (cm) relative to the Material factors measured during the wet cycle. Box plots show the interquartile range, with the box representing the first quartile (Q1) to the third quartile (Q3). The median is presented by a line within the box, although in some cases the median coincides with the quartile boundary and may not be visually distinguishable. The cross symbol (x) indicates the mean plant height. 95

Figure 4.8. Boxplot of height (cm) relative to the Treatment*Material interaction measured during the wet cycle. Box plots show the interquartile range, with the box representing the first quartile (Q1) to the third quartile (Q3). The median is presented by a line within the box, although in some cases the median coincides with the quartile boundary and may not be visually distinguishable. The cross symbol (x) indicates the mean plant height. 96

Figure 4.9. Boxplot of height (cm) relative to the Material factors measured during the dry cycle. Box plots show the interquartile range, with the box representing the first quartile (Q1) to the third quartile (Q3). The median is presented by a line within the box, although in some cases the median coincides with the quartile boundary and may not be visually distinguishable. The cross symbol (x) indicates the mean plant height. 97

Figure 4.10. Boxplot of height (cm) relative to the Treatment*Material interaction measured during the dry cycle. Box plots show the interquartile range, with the box representing the first quartile (Q1) to the third quartile (Q3). The median is presented by a line within the box, although in some cases the median coincides with the quartile boundary and may not be visually distinguishable. The cross symbol (x) indicates the mean plant height. 98

Figure 4.11. Plant growth rate (cm/day) under controlled laboratory conditions during wet and dry cycles. Growth rates were calculated from incremental changes in plant height over time. Values represent pooled data across all material treatments (DPF, biochar and UAE sand)..... 99

Figure 4.12. Plant growth rate (cm/day) under uncontrolled field conditions during wet and dry cycles. Growth rates were calculated from incremental changes in plant height over time. Values represent pooled data across all material treatments (DPF, biochar and UAE sand)..... 100

Figure 4.13. Boxplot of moisture level relative to the Material factors measured during the wet cycle. Box-and-whisker plots show the interquartile range, with the box representing the first quartile (Q1) to the third quartile (Q3), and the whiskers extending from the minimum to the maximum values. The median is represented by a line within the box and the cross symbol (x) indicates the mean moisture level..... 101

Figure 4.14. Boxplot of moisture level of the Treatment*Material interaction measured during the wet cycle. Box-and-whisker plots show the interquartile range, with the box representing the first quartile (Q1) to the third quartile (Q3), and the whiskers extending from the minimum to the maximum values. The median is represented by a line within the box and the cross symbol (x) indicates the mean moisture level. 102

Figure 4.15. Boxplot of the moisture level relative to the Material factors measured during the dry cycle. Box-and-whisker plots show the interquartile range, with the box representing the first quartile (Q1) to the third quartile (Q3), and the whiskers extending from the minimum to the maximum values. The median is presented by a line within the box, although in some cases the median coincides with the quartile boundary and may not be visually distinguishable. The cross symbol (x) indicates the mean moisture level. 103

Figure 4.16. Boxplot of the moisture level relative to the Treatment*Material interaction measured during the dry cycle. Box-and-whisker plots show the interquartile range, with the box representing the first quartile (Q1) to the third quartile (Q3), and the whiskers extending from the minimum to the maximum values. The median is presented by a line within the box, although in some cases the

| | |
|---|-----|
| median coincides with the quartile boundary and may not be visually distinguishable. The cross symbol (x) indicates the mean moisture level..... | 104 |
| Figure 4.17.Boxplot of the uncontrolled moisture level relative to the Material factors measured during the wet cycle. Box-and-whisker plots show the interquartile range, with the box representing the first quartile (Q1) to the third quartile (Q3), and the whiskers extending from the minimum to the maximum values. The median is presented by a line within the box, although in some cases the median coincides with the quartile boundary and may not be visually distinguishable. The cross symbol (x) indicates the mean moisture level..... | 105 |
| Figure 4.18.Boxplot of the moisture level relative to the Treatment*Material interaction measured during the wet cycle. Box-and-whisker plots show the interquartile range, with the box representing the first quartile (Q1) to the third quartile (Q3), and the whiskers extending from the minimum to the maximum values. The median is represented by a line within the box and cross symbol (x) indicates the mean moisture level. | 106 |
| Figure 4.19. Boxplot of the moisture level relative to the Material factors measured during the dry cycle. Box-and-whisker plots show the interquartile range, with the box representing the first quartile (Q1) to the third quartile (Q3), and the whiskers extending from the minimum to the maximum values. The median is presented by a line within the box, although in some cases the median coincides with the quartile boundary and may not be visually distinguishable. The cross symbol (x) indicates the mean moisture level. | 107 |
| Figure 4.20. Boxplot of the moisture level relative to the Treatment*Material interaction measured during the dry cycle. Box-and-whisker plots show the interquartile range, with the box representing the first quartile (Q1) to the third quartile (Q3), and the whiskers extending from the minimum to the maximum values. The median is presented by a line within the box, although in some cases the median coincides with the quartile boundary and may not be visually distinguishable. The cross symbol (x) indicates the mean moisture level..... | 108 |
| Figure 4.21. Boxplot of the soil temperature relative to the Material factors measured during the wet cycle. Box-and-whisker plots show the interquartile range, with the box representing the first quartile (Q1) to the third quartile (Q3), and the whiskers extending from the minimum to the maximum values. The median is represented by a line within the box, and the cross symbol (x) indicates the mean soil temperature. | 109 |
| Figure 4.22. Boxplot of the soil temperature relative to the Treatment*Material interaction measured during the wet cycle. Box-and-whisker plots show the interquartile range, with the box representing the first quartile (Q1) to the third quartile (Q3), and the whiskers extending from the minimum to the maximum values. The median is represented by a line within the box and the cross symbol (x) indicates the mean soil temperature. | 110 |
| Figure 4.23. Boxplot of the soil temperature relative to the Material factors measured during the dry cycle. Box-and-whisker plots show the interquartile range, with the box representing the first quartile (Q1) to the third quartile (Q3), and the whiskers extending from the minimum to the maximum values. The median is represented by a line within the box and the cross symbol (x) indicates the mean soil temperature. | 111 |
| Figure 4.24. Boxplot of the soil temperature relative to the Treatment*Material interaction measured during the dry cycle. Box-and-whisker plots show the interquartile range, with the box representing the first quartile (Q1) to the third quartile (Q3), and the whiskers extending from the minimum to the maximum values. The median is represented by a line within the box and the cross symbol (x) indicates the mean soil temperature. | 112 |
| Figure 4.25. Boxplot of the uncontrolled soil temperature relative to the Material factors measured during the wet cycle. Box-and-whisker plots show the interquartile range, with the box representing the first quartile (Q1) to the third quartile (Q3), and the whiskers extending from the minimum to the maximum values. The median is represented by a line within the box and the cross symbol (x) indicates the mean soil temperature. | 113 |

| | |
|--|-----|
| Figure 4.26. Boxplot of the soil temperature relative to the Treatment*Material interaction measured during the wet cycle. Box-and-whisker plots show the interquartile range, with the box representing the first quartile (Q1) to the third quartile (Q3), and the whiskers extending from the minimum to the maximum values. The median is represented by a line within the box and the cross symbol (x) indicates the mean soil temperature. | 114 |
| Figure 4.27. Boxplot of the soil temperature relative to the Material factors measured during the dry cycle. Box-and-whisker plots show the interquartile range, with the box representing the first quartile (Q1) to the third quartile (Q3), and the whiskers extending from the minimum to the maximum values. The median is represented by a line within the box and the cross symbol (x) indicates the mean soil temperature. | 115 |
| Figure 4.28. Boxplot of the soil temperature relative to the Treatment*Material interaction measured during the dry cycle. Box-and-whisker plots show the interquartile range, with the box representing the first quartile (Q1) to the third quartile (Q3), and the whiskers extending from the minimum to the maximum values. The median is represented by a line within the box and the cross symbol (x) indicates the mean soil temperature. | 116 |
| Figure 4.29. Boxplot of the soil pH relative to the Material factors measured during the wet cycle. Box-and-whisker plots show the interquartile range, with the box representing the first quartile (Q1) to the third quartile (Q3), and the whiskers extending from the minimum to the maximum values. The median is represented by a line within the box and the cross symbol (x) indicates the mean soil pH. | 117 |
| Figure 4.30. Boxplot of the soil pH relative to the Treatment*Material interaction measured during the wet cycle. Box-and-whisker plots show the interquartile range, with the box representing the first quartile (Q1) to the third quartile (Q3), and the whiskers extending from the minimum to the maximum values. The median is represented by a line within the box and the cross symbol (x) indicates the mean soil pH. | 118 |
| Figure 4.31. Boxplot of the soil pH relative to the material factors measured during the wet cycle. Box-and-whisker plots show the interquartile range, with the box representing the first quartile (Q1) to the third quartile (Q3), and the whiskers extending from the minimum to the maximum values. The median is presented by a line within the box, although in some cases the median coincides with the quartile boundary and may not be visually distinguishable. The cross symbol (x) indicates the mean soil pH. | 119 |
| Figure 4.32. Boxplot of the soil pH relative to the Treatment*Material interaction measured during the wet cycle. Box-and-whisker plots show the interquartile range, with the box representing the first quartile (Q1) to the third quartile (Q3), and the whiskers extending from the minimum to the maximum values. The median is represented by a line within the box, and the cross symbol (x) indicates the mean soil pH. | 120 |
| Figure 4. 33. Boxplot of the soil pH relative to the Treatment*Material interaction measured during the dry cycle. Box-and-whisker plots show the interquartile range, with the box representing the first quartile (Q1) to the third quartile (Q3), and the whiskers extending from the minimum to the maximum values. The median is represented by a line within the box and the cross symbol (x) indicates the mean soil pH. | 121 |
| Figure 4. 34. QQ' plot of the observed value of the height. | 124 |
| Figure 4.35. Main effects plot of the Cycle factor on height. Error bars are the 95% confidence interval. | 126 |
| Figure 4. 36. The main effect plot of the Day factor on height. Error bars are the 95% confidence interval and may be smaller than the plotted point. | 127 |
| Figure 4.37. The main effect plot of the Treatment factor on height. Error bars are the 95% confidence interval but may be smaller than the plotted point. | 129 |
| Figure 4. 38. The main effect plot of the Material factor on height. Error bars are the 95% confidence interval and may be smaller than the plotted point. | 131 |
| Figure 4.39. QQ' plot of the observed value of the moisture. | 132 |

| | |
|--|-----|
| Figure 4.40. Main effects plot of the Cycle factor on moisture content. Error bars are the 95% confidence interval..... | 134 |
| Figure 4.41. Main effects plot of the Treatment factor on moisture content. Error bars are the 95% confidence interval and may be smaller than the plotted point..... | 135 |
| Figure 4.42. Main effects plot of the Material factor on moisture content. Error bars are the 95% confidence interval..... | 137 |
| Figure 4.43. QQ' plot of the observed values of the pH..... | 138 |
| Figure 4.44. Main effects plot of the Cycle factor on moisture content. Error bars are the 95% confidence interval..... | 140 |
| Figure 4.45. Main effects plot of the Treatment factor on moisture content. Error bars are the 95% confidence interval and may be smaller than the plotted point..... | 141 |
| Figure 4.46. Main effects plot of the Material factor on moisture content. Error bars are the 95% confidence interval..... | 143 |
| Figure 4.47. The interaction plot of the soil pH between Materials and Treatment factors..... | 144 |
| Figure 4.48. QQ' plot of the observed value of the temperature..... | 145 |
| Figure 4.49. QQ' plot of the observed value of the height..... | 147 |
| Figure 4.50. Main effects plot of the Treatment factor on plant height. Error bars are the 95% confidence interval and may be smaller than the plotted point..... | 149 |
| Figure 4.51. QQ' plot of the observed value of the soil moisture..... | 151 |
| Figure 4.52. QQ' plot of the observed value of the pH..... | 153 |
| Figure 4.53. The interaction plot for pH between Material and Treatment factor..... | 155 |
| Figure 4.54. QQ' plot of the observed value of the temperature..... | 156 |
| Figure 5.1. The rate of mass loss of Date Palm Fronds (DPF) at different heat rates (K/min)..... | 166 |
| Figure 5.2. The rate of mass loss of biochar in different heat rate (K/min)..... | 167 |
| Figure 5.3. The rate of mass loss of water in different heat rates (K/min)..... | 168 |
| Figure 5.4. The rate of mass loss of wet DPF in different heat rates (K/min)..... | 169 |
| Figure 5.5. The rate of mass loss of wet biochar in different heat rates (K/min)..... | 170 |
| Figure 5.6. The rate of mass loss of wet sharp sand in different heat rates (K/min)..... | 171 |
| Figure 5.7. The rate of mass loss of wet UAE sand in different heat rates (K/min)..... | 172 |
| Figure 6.1. The boxplot of the moisture content (% by weight) of the Treatment*Materials interaction measured during the wet cycle. Box-and-whisker plots show the interquartile range, with the box representing the first quartile (Q1) to the third quartile (Q3), and the whiskers extending from the minimum to the maximum values. The median is represented by a line within the box, and the cross symbol (x) indicates the mean moisture content..... | 184 |
| Figure 6.2. The boxplot of the moisture content (% by weight) of the Treatment*Materials interaction measured during the dry cycle. Box-and-whisker plots show the interquartile range, with the box representing the first quartile (Q1) to the third quartile (Q3), and the whiskers extending from the minimum to the maximum values. The median is represented by a line within the box, and the cross symbol (x) indicates the mean moisture content..... | 185 |
| Figure 6.3. The boxplot of the moisture content (% by weight) of the Treatment*Materials interaction measured during the dry cycle waw. Box-and-whisker plots show the interquartile range, with the box representing the first quartile (Q1) to the third quartile (Q3), and the whiskers extending from the minimum to the maximum values. The median is represented by a line within the box, and the cross symbol (x) indicates the mean moisture content..... | 186 |
| Figure 6.4. The boxplot of the height (cm) of the Treatment*Material interaction measured during the wet cycle. Box-and-whisker plots show the interquartile range, with the box representing the first quartile (Q1) to the third quartile (Q3), and the whiskers extending from the minimum to the maximum values. The median is represented by a line within the box, and the cross symbol (x) indicates the mean plant height..... | 187 |
| Figure 6.5. The boxplot of the height (cm) of the Treatment*Material interaction measured during the dry cycle. Box-and-whisker plots show the interquartile range, with the box representing the first | |

| | |
|--|-----|
| quartile (Q1) to the third quartile (Q3), and the whiskers extending from the minimum to the maximum values. The median is represented by a line within the box, and the cross symbol (x) indicates the mean plant height. | 188 |
| Figure 6.6. Plant growth rate (cm/day) during wet and dry cycles in mixed amendment pot trial experiment. Growth rates were calculated from incremental changes in plant height over time. | 190 |
| Figure 6.7. The boxplot of the soil temperature of the Treatment*Material interaction measured during the wet cycle. Box-and-whisker plots show the interquartile range, with the box representing the first quartile (Q1) to the third quartile (Q3), and the whiskers extending from the minimum to the maximum values. The median is represented by a line within the box, and the cross symbol (x) indicates the mean soil temperature. | 191 |
| Figure 6.8. The boxplot of the soil temperature of the Treatment*Material interaction measured during the dry cycle. Box-and-whisker plots show the interquartile range, with the box representing the first quartile (Q1) to the third quartile (Q3), and the whiskers extending from the minimum to the maximum values. The median is represented by a line within the box, and the cross symbol (x) indicates the mean soil temperature. | 192 |
| Figure 6.9. QQ' plot of the observed value of the moisture content. Log MC =log(Moisture Content). | 195 |
| Figure 6.10. Main effects plot of the Cycle factor with respect to moisture content. Error bars are the 95% confidence interval. | 197 |
| . Figure 6.11. Main effects plot of the Day factor with respect to moisture content. Error bars are the 95% confidence interval. | 198 |
| Figure 6. 12. The interaction plot of moisture content between Day and Cycle factors. | 200 |
| . Figure 6.13. QQ' plot of the observed value of plant height. LogOutcome is log(Height). | 201 |
| . Figure 6.14. Main effects plot of the Cycle factor with respect to plant height. Error bars are the 95% confidence interval. | 203 |
| . Figure 6.15. Main effects plot of the Day factor with respect to moisture content. Error bars are the 95% confidence interval. Sometimes the error bars are smaller than the plotted point. | 204 |
| . Figure 6.16. The interaction plot of plant height between Cycle and Treatment factors. | 205 |
| . Figure 6.17. QQ' plot of the observed value of the moisture content. LogOutcome =log(Moisture Content). | 206 |
| Figure 6.18. QQ' plot of the observed value of the soil temperature. LogOutcome =log(Temperature). | 208 |
| . Figure 6.19. Main effects plot of the Cycle factor with respect to soil temperature. Error bars are the 95% confidence interval. | 210 |
| . Figure 6.20. Main effects plot of the Treatment factor on soil temperature. Error bars are the 95% confidence interval and may be smaller than the plotted point. | 211 |
| . Figure 6.21. Main effects plot of the Day factor with respect to soil temperature. Error bars are the 95% confidence interval. | 212 |
| . Figure 6.22. The interaction plot of soil temperature between Cycle and Treatment factors. | 213 |
| Figure 6.23. QQ' plot of the observed value of the soil pH. LogOutcome =log(pH). | 214 |

List of tables

| | |
|--|-----|
| Table 2.1. The standard biochar pore type (Lehmann and Joseph, 2015)..... | 23 |
| Table 2.2. BET surface area proximate results of DPF, biochar, Sharp Sand and UAE Sand. | 32 |
| Table 2.3. The chemical analysis of the biochar and DPF using SEM ESD. | 33 |
| Table 2.4. The percentage by mass CHN composition of sands, biochar and DPF..... | 34 |
| Table 2.5. Material pore size comparison with other studies..... | 37 |
| Table 2.6. Carbon, Hydrogen and Nitrogen (CHN) Analysis comparison with other studies. | 39 |
| Table 2.7. BET surface area for study materials comparison with other published studies. | 45 |
| Table 3.1. Amended treatments used in the mesocosm experiments (composition by dry weight). | 52 |
| Table 3.2. The percentage of variance explained for factors and interactions of the Day, Treatment and Cycle factors for on the moisture content. | 64 |
| Table 3.3. Results of Tukey’s post hoc test for the different cycles. | 65 |
| Table 3.4. Results of post hoc test of treatment levels for moisture content. | 67 |
| Table 3.5. Results of post hoc analysis for between the levels of the Materials factor..... | 68 |
| Table 3.6. Results of post hoc analysis on the moisture content between the levels of the Day factor..... | 69 |
| Table 4.1. Treatment combinations used in the pot trial experiments (composition by dry weight)... | 83 |
| Table 4.3. The percentage coverage of canopy monitored during the controlled pot trial experiment. | 123 |
| Table 4.4. The percentage of variance explained for significant ($P < 0.05$) factors and interactions for the Treatment, Material, Cycle, and Day factors for height..... | 125 |
| Table 4.5. Results of Tukey’s post hoc test for height between levels of the Day factor. Levels not significantly different from each other share a common letter grouping. | 128 |
| Table 4.6.. Results of Tukey’s post hoc test for the height between levels of the Treatment factor. Levels not significantly different from each other share a common letter grouping. | 130 |
| Table 4.7. The percentage of variance explained for significant ($P < 0.05$) factors and interactions for the Treatment, Material and Cycle factors on the moisture content. | 133 |
| Table 4.8. Results of Tukey’s post hoc test for the Moisture between levels of the Treatment factor. Levels not significantly different from each other share a common letter grouping. | 136 |
| Table 4.9. The percentage of variance explained for significant ($P < 0.05$) factors and interactions for the Treatment, Material and Cycle factors on the pH. | 139 |
| Table 4.10. Results of Tukey’s post hoc test for the pH between levels of the Treatment factor. Levels not significantly different from each other share a common letter grouping. | 142 |
| Table 4.11. The percentage of variance explained for significant ($P < 0.05$) factors and interactions for the Treatment, Material and Cycle factors on the temperature. | 146 |
| Table 4.12. The proportion of significant ($P < 0.05$) factors for the treatment, material, cycle and day. | 148 |
| Table 4.13. Results of Tukey’s post hoc test for the height of the Treatment factor. Levels not significantly different from each other share a common letter grouping. | 150 |
| Table 4.14. The proportion of significant ($P < 0.05$) factors for the treatment, material, and cycle... | 152 |
| Table 4.15. The proportion of significant ($P < 0.05$) factors for the treatment, material and cycle.... | 154 |
| Table 4.16. The proportion of significant ($P < 0.05$) factors for the treatment, material and cycle.... | 157 |
| Table 6.1. Mixed amendment treatments used in the mesocosm and pot trial experiments (composition by dry weight)..... | 182 |

| | |
|---|-----|
| Table 6.2. Summary of plant growth rates (cm/day) during wet and dry cycles in the mixed treatment material pot trial experiment. Growth rate was calculated from changes in plant height between measurement intervals. | 189 |
| Table 6.3. The percentage of variance explained for factors and interactions of the Day, Treatment and Cycle factors for on the moisture content. | 196 |
| Table 6.4. Results of post hoc analysis on Moisture content between Cycle factor. | 199 |
| Table 6.5. The percentage of variance explained for factors and interactions of the Day, Treatment and Cycle factors for on the plant height. | 202 |
| Table 6.6. The percentage of variance explained for factors and interactions of the Day, Treatment and Cycle factors for on the moisture content. | 207 |
| Table 6.7. The percentage of variance explained for factors and interactions of the Day, Treatment and Cycle factors for soil temperature. | 209 |
| Table 6.8. The percentage of variance explained for factors and interactions of the Day, Treatment and Cycle factors for on the soil pH. | 215 |

Declaration

I declare that this thesis, which I submit for the degree of Doctor of Philosophy at Durham University, is my own work and not substantially the same as any which has been submitted previously at this or any other university.

This work was funded by the United Arab Emirates Ministry of Education.

Statement of copyright

The copyright of this thesis rests with the author. No quotation from it should be published without the author's prior written consent and information derived from it should be acknowledged.

Acknowledgement

I would like to express my sincere gratitude to my supervisor, Professor Fred Worrall, for guiding me through this journey, particularly during the uncertainty of the COVID-19 period. This work began as an evolving idea, and I am thankful for the freedom to explore it creatively and independently. Although the journey was not always straightforward and took longer than expected, I truly appreciate the patience and support that allowed me to see it through.

I am deeply grateful to my co-supervisor, Professor Chris Greenwell, for his encouragement and moral support. His guidance, particularly in shaping my perspective on future research, has been invaluable.

I would also like to extend my sincere thanks to my examiners, Professor Karen Johnson and Professor Yit Arn Teh, for their thoughtful and constructive feedback during my viva. It was a valuable and engaging experience, and their insights have greatly strengthened this thesis.

My heartfelt thanks go to the Department of Earth Sciences for creating such a warm and welcoming environment. As an international student, this sense of belonging meant more than words can express, and the supportive atmosphere made this journey both manageable and enriching.

I would like to extend my special thanks to Professor Stephan Nielson and Ms Louise Bowron for their continuous care, support, and administrative guidance. I am also sincerely grateful to my annual review team Professor James Baldini, Professor Richard Hobbs, and Associate Professor Julia Knapp for their support in helping me stay on track throughout my PhD.

I would also like to thank all the professors I worked with as a demonstrator. Through them, I discovered the joy of teaching, learned different ways of sharing knowledge, and came to

appreciate the art of giving. My thanks also go to the IT team for their support, and to the wonderful cleaners whose kindness and warm smiles were a constant reminder that there is always more to life beyond research.

To my friends, both within and outside the department, thank you for your companionship, laughter, and quiet support during difficult moments your presence has meant more than I can express.

I would also like to extend my deepest gratitude to my sponsors, the Ministry of Education and the Cultural Attaché at the UAE Embassy in London, for their continued support throughout my academic journey.

To my family, especially my parents, thank you for being my foundation and constant source of strength. I hold a special place in my heart for my father, whom I dearly wish were here to witness this moment I know he would have been proud.

To my sister, Dr. Khadija Al Nofeli, my greatest support system thank you for always standing by me. Sharing this journey with you makes this achievement even more meaningful.

To my husband, Mohamed Dhiri, the love of my life thank you for your patience, understanding, and unwavering support. Through every challenge, you have been my strength. With the arrival of our son, I am deeply grateful for the love and care you have given our family.

Lastly, I thank myself. There were moments of doubt, but I did not give up. I persevered, and this journey has taught me resilience that I will carry forward.

Chapter 1: Introduction and Literature Review

1.1 Introduction

Chapter 1 introduces biochar as a soil amendment and examines its potential role in improving soil properties, particularly in arid environments. Biochar has gained increasing attention due to its ability to enhance soil structure, increase water retention and contribute to climate change mitigation through carbon sequestration. Despite extensive global research, the behaviour and effectiveness of biochar in arid and sandy soils remain insufficiently understood.

Arid regions such as the United Arab Emirates (UAE) face significant environmental challenges, including water scarcity, poor soil fertility and land degradation. These conditions limit agricultural productivity and increase reliance on unsustainable water and soil management practices. Therefore, there is a critical need for low-cost, sustainable solutions that can improve soil water retention and support plant growth under extreme climatic conditions.

This chapter reviews the existing literature on biochar production, properties and applications with a particular focus on its relevance to arid soils. It also introduces the use of date palm fronds (DPF), an abundant agricultural waste in the UAE as a potential alternative or complementary soil amendment. The chapter concludes by outlining the research gap, study aims and structure of the thesis.

1.1.1 Biochar

1.1.1.1 Biochar definition

Biochar is a term used to describe a charcoal-like substance that is produced from a thermochemical decomposition of organic material at high temperatures in the absence of oxygen (Lehmann and Joseph, 2015). Biochar is characterised as a porous material with very low bulk density and is an inert form of carbon (Jouiad *et al.*, 2015). It has been used for centuries to improve soil fertility, increase crop yields, and reduce greenhouse gas emissions. The use of biochar as soil amendment was discovered by Amazonian civilisation in South America (Yu *et al.*, 2019), where indigenous people used to call biochar Terra Preta or Dark Earth (Ippolito *et al.*, 2012). The carbon stored in biochar is highly stable and can remain in the soil for hundreds to thousands of years (Lehmann and Joseph, 2009). In recent years, biochar has gained attention as a means of climate change mitigation and as a soil conditioner because biochar is considered inexpensive, sustainable material and could be a good option for improving the agricultural waste management (Lehmann, 2015); (Jouiad *et al.*, 2015) and because biochar can be produced with large-scale pyrolysis technologies that are commercially available across the world (Woolf *et al.*, 2010).

1.1.1.2 Biochar benefits

There are multiple reported benefits of biochar application to soil (ref - Figure 1.1). These benefits include improving soil texture, enhancing plant growth, increasing nutrient retention, and promoting microbial activity (Zheng *et al.*, 2022). Studies have shown that biochar can increase soil pH and reduce soil acidity, which helps plant growth (Grünzweig *et al.*, 2022). Biochar can also reduce greenhouse gas emissions such as methane and nitrous oxide by enhancing the stability of organic matter (Liu *et al.*, 2013). Furthermore, biochar was noticed

to increase soil aggregation and enhance water holding capacity, which is essential for soils that lack nutrients and have difficulty in holding water, such as arid regions (Biederman and Harpole, 2013). Biochar is being considered a sustainable fertiliser rather than using chemical fertilisers that would harm the environment (Jeffery *et al.*, 2011). Although biochar has many reported benefits when applied to soil, it has also been noticed that it can be used for livestock management to reduce odours and improve air quality in animal production systems and feed for the digestive system (Tomczyk *et al.*, 2020). Other benefits include: being used for building materials; urban applications, wall capping to assist in flood management; anaerobic digestion during the wastewater treatment; and for batteries (Benyoucef *et al.*, 2020).

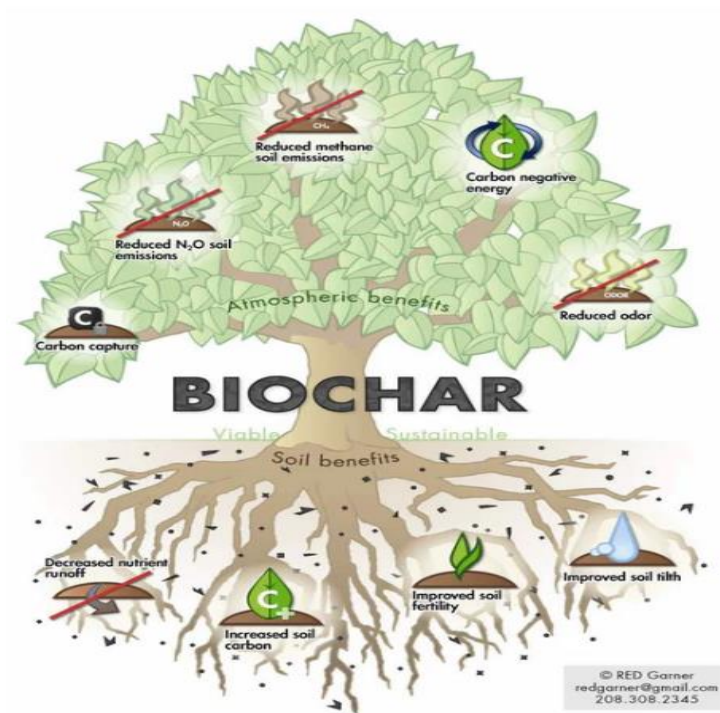


Figure 1.1. The benefits of biochar ((International Biochar Initiative, 2018).

1.1.1.3 Climate change

Worldwide soils contain over 3000 G tonnes of carbon, which is almost four times as much carbon as in the atmosphere and all of the world's plants (Thunberg, 2022). This soil store controls the global carbon cycle, which benefits food production, biodiversity, resistance to drought and flooding, and ecosystem health (Grünzweig *et al.*, 2022). It is understood that human dependence on the existing carbon will cause danger to the atmospheric carbon pool CO₂ emission, which will lead to climate change (Thunberg, 2022). Due to climate change, air temperature is rising every year, and more disasters may occur, such as water scarcity and soil degradation (Haider *et al.*, 2017).

According to Kumar and Bhattacharya (2021), it is believed that biochar has the potential to meet not less than 12 Sustainable Development Goals (SDGs), as illustrated in Figure 1.2.

The SDGs have 17 goals that are designed to prevent poverty and protect the environment by 2030. Where the use of biochar could contribute to most of the goals, for example:

- i) Goals 1 and 2 - by increasing crop production, which would lead to reducing poverty and hunger (Karim, 2020).
- ii) Goal 3 - using biochar as a sustainable fertiliser instead of chemical fertiliser to increase production of healthier crops, which falls into healthier food and wellbeing (Kochanek *et al.*, 2022).
- iii) Goal 6 – biochar is a sustainable solution for the prevalent problem of water pollution, as it can absorb heavy metals, dyes, organic molecules, oil, etc. ((Jha *et al.*, 2023).
- iv) Goals 7 & 12 - as biochar production process is considered as a source of renewable energy, it aids in producing heat, electricity, biofuels, and gas (Neogi *et al.*, 2022).
- v) Goal 8 - biochar production and application help develop careers for farmers and investors (Kochanek *et al.*, 2022).

- vi) Goal 9 - biochar used in building infrastructure, which is believed to have a good lifespan in the materials mixed with concrete, bricks, and asphalt (Zhang *et al.*, 2022).
- vii) Goal 11 - biochar use has been expanding between communities by developing water management systems and green buildings (Novotný *et al.*, 2023).
- viii) Goal 13 - biochar has a huge contribution to climate action by reducing carbon emissions (Neogi *et al.*, 2022).
- ix) Goal 14 - adding biochar into soil helps retain water and reserve nutrients from leaching (Seyedsadr *et al.*, 2022).
- x) Goal 15 - biochar can be used to restore, reclaim, and remediate land (Wang *et al.*, 2017).



Figure 1.2. Biochar meets Sustainable Goal Developments at least 12 goals (Kumar and Bhattacharya, 2021).

One potential solution to the negative impacts of drought and heatwaves on the ecosystem is the use of biochar (Quan *et al.*, 2023). Biochar has been shown to not only reduce N₂O and NO₃ emissions in sandy soil (Borchard *et al.*, 2019), but also to have efficient CO₂ capture and storage capabilities, which can contribute to reducing greenhouse gas emissions resulting from CO₂ sequestration storage (Salem *et al.*, 2021). Given the significant challenges faced by the implementation of carbon capture and storage technology due to its high cost, the development of low-cost CO₂ adsorption materials such as biochar has become desirable (Eickemeier *et al.*, 2019). However, the potential benefits of biochar in reducing the negative impacts of drought and heatwaves on the ecosystem require further investigation, particularly in dryland areas, which cover 37%-46% of the global land and require more attention (Badawi, 2019).

1.1.1.4 Biochar production

Biochar is the product of heating biomass above 250°C with the absence or with limited access to oxygen; this process is called pyrolysis (Lehmann and Joseph, 2015). There are many ways of producing biochar, which range from the traditional method by which different feedstocks are set on fire and then covered with soil (Artiola and Wardell, 2017) to the mechanised production of biochar with the advantage of also producing co-products such as fuel and gas. There are three pyrolysis processes: slow, fast, and flash (Figure 1.3). The different pyrolysis processes are distinguished by the duration of heating and temperature used (Ragula *et al.*, 2016). Slow pyrolysis is a process of converting biomass that uses slow heating temperatures from 300°C with the absence of oxygen (Bruun, 2011). The heating of the material and duration can extend up to hours, which can result in changing biochar properties such as pore size, composition, and heat value. The biochar yield is in the range of 50% for slow pyrolysis. Fast pyrolysis, also known as gasification, is an intermediate-fast heating process from (600-725°C) which results having 60% yield of bio-oil, 20% biochar and 20% syngas. The heating of the

material and duration is 1-200 K/sec, and the process duration is up to 1 min. Finally, flash pyrolysis, also a gasification, is a very fast heating process from (725-1000°C) which results in achieving up to 75% of bio-oil yield. The heating of the material and duration is 1000 K/sec, and of the process <1 sec. However, the fast pyrolysis has limitations of poor thermal stability and can produce solids in the oil (Al-Rumaihi *et al.*, 2022).

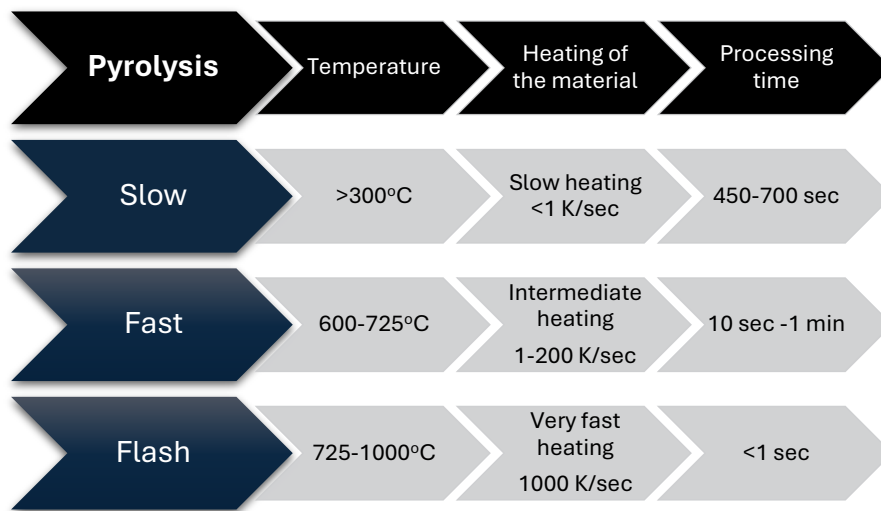


Figure 1.3. The different types of pyrolysis processes (slow, fast and flash) (Bhaskar *et al.*, 2019).

Studies have shown that lower temperature produced biochar in the range 300-400°C have the potential to increase crop yield by 19% and increase water retention by 46% (Alotaibi and Schoenau, 2019). On the other hand, biochar produced from higher temperatures (500-600°C) increases the porosity and alkalinity but decreases the essential nutrients that would benefit the crop. In addition, the higher the porosity, the better impact on soil physical, chemical and biological properties (Salem *et al.*, 2021).

1.1.1.5 Biochar properties

Biochar properties are controlled by various factors, including the types of feedstocks used and the pyrolysis temperature applied during its production (Tomczyk *et al.*, 2020). These factors contribute to the variation in physical, chemical, and biological properties exhibited by biochar (Rutherford *et al.*, 2012). In addition, the behaviour of biochar in the soil will depend on the interaction between the properties of the biochar and the properties of the soil (Gopal *et al.*, 2020).

The physical properties of biochar are mostly affected by the pyrolysis temperature used in the production of the biochar (Barrera-zapata, 2017). The biochar particle size can differ from finer powder (micropore < 2 nm) to larger particles (macropore >50 nm) (Lehmann and Joseph, 2015) and can easily be changed post-pyrolysis by crushing/grinding, or by fusing biochar dust. The particle size can influence the porosity, surface area and water holding capacity of biochar (Bruun, 2011). The smaller the particles, the greater the surface area: the larger the pore size, the greater the water holding capacity (Edeh and Mašek, 2022). (Tomczyk *et al.*, (2020) observed that biochar can exhibit a wide pore size distribution that includes both macropores and micropores. Large pores, also known as macropores, contribute to a high surface area which helps in adsorption of water, nutrients, contaminants and microorganisms (Tomczyk *et al.*, 2020). The bulk density of biochar is reported as ranging between 0.2 - 0.6 g/cm³ (Blanco-Canqui, 2017). The low density of biochar, relative to mineral soils, can improve water infiltration into the soils where biochar has been applied. Therefore, biochar enhances soil structure and reduces soil compaction (Bhat *et al.*, 2022). A higher density of 0.6 g/cm³, would lead to increased carbon storage, improved soil amendments and enhanced filtration (Yu *et al.*, 2019). The physical properties relevant to this study will be reviewed in Chapter 2.

As for chemical properties, biochar generally exhibits a pH ranging from neutral to slightly alkaline, which may serve to mitigate soil acidity and restore pH balance (Oni *et al.*, 2019). In addition, biochar may contain useful amounts of vital plant nutrients, namely nitrogen, phosphorus, and potassium (Gao *et al.*, 2021). The cation exchange capacity (CEC) of biochar is relatively high, implying its capacity to attract and hold cations, including plant nutrients, within the soil matrix (Som *et al.*, 2012). The chemical composition of the feedstock experiences transformation during the pyrolysis, resulting in influencing the composition of the lignocellulose (Gopal *et al.*, 2020). Understanding the physiochemical properties of biochar helps understand the ability of biochar to remediate various soils (Tomczyk *et al.*, 2020). The chemical properties relevant to this study will be reviewed in Chapter 2.

When blended into soil, biochar creates a favourable habitat for microorganisms (Biederman and Harpole, 2013). Biochar's porous structure is beneficial for improving plant health and growth (Clough *et al.*, 2013). Also, biochar increases soil quality by creating soil aggregation, which leads to sustaining nutrients from microbes, plants (Rosa, 2020). Biochar also supports biological nitrogen fixation and may limit harmful soil-borne pathogens (Clough *et al.*, 2013). The biological properties relevant to this study will be reviewed in Chapter 4.

1.1.1.6 Biochar application

Biochar application to soil is a widely researched topic, and a wide range of application rates have been reported (Brtnicky *et al.*, 2021). According to Liu *et al.*, 2017 biochar percentage application rates range from 1%- 10% by weight of soil. Bouchard *et al.* (2015) showed that a 1%-5% biochar application improved water and nutrient retention and soil structure. Nair and Mukherjee, (2022) reported that the greater the percentage of biochar application, up to 10% by soil weight, the greater the benefits to the soil. It is important to notice that the optimal biochar application rate will vary depending upon soil type, crop type and other factors (Kocsis *et al.*, 2022). Some biochar variants exhibit higher nutrient concentrations, making them particularly suitable for enhancing soil fertility and water retention (Hagemann *et al.*, 2017). Although there are many studies focusing on biochar application to soils, the majority of these studies were conducted indoors (laboratory-based), and far fewer were conducted in the field (Zhang *et al.*, 2023).

1.2 Biochar Application in UAE Sandy Soils: The UAE Context

Date Palm trees are one of the most popular raw materials in the Middle East & North Africa, where they are still used as a source of food, shelter and decoration (Heine, 2004). The Middle East produces over 70% of the World's date palm trees: around 120 million trees (Cybulska *et al.*, 2017). The United Arab Emirates alone has more than 40 million palm trees, and each year, 10 thousand palm trees are cloned in a Tissue Culture Centre (Bardsley, 2017). With the increasing production of date palm, there comes an increasing volume of waste. There are approximately 20 kg of palm frond waste per tree annually, and currently this waste is sent to landfill (Jouiad *et al.*, 2015). Khalifa and Yousef, (2015) have suggested that date palm fronds could be used as an alternative fertiliser by converting them into biochar.

Besides agricultural waste issues faced in the UAE, the country also suffers from water scarcity, extreme weather conditions and land degradation. The UAE is heavily reliant on groundwater as its main water resource (Shahin and Salem, 2015). Scientists from the UAEU (United Arab Emirates University) observed groundwater tables that have declined over a 20-year period (1990-2010) by 60 m as a result of 70% increase in groundwater consumption (Shahin and Salem, 2015). The annual mean rainfall in the UAE is 78 mm and ranges from 40 mm in the southern desert region of the Emirates to 160 mm in the north-eastern mountains (Ouarda *et al.*, 2014). The UAE's average rainfall is considered quite low compared to other countries. Moreover, the characterisation of the UAE climate is arid; a very hot and dry summer that goes up to 48°C, with a mild winter of 13°C (Shahin and Salem, 2015). Given that the UAE in the past was not as hot as today, climate change played a role in soil degradation that limits vegetation and plant productivity (Alsuwaidi and Ramos, 2017), for example, the low organic carbon content and poor nutrient content of UAE soil (Abdelfattah *et al.*, 2009). The UAE soil classification divides the country into 47 soil series and 2 phases, and the soil texture varies from one emirate to another, where some areas are more gravel dominated, and others are either sandy with more or less salinity in the soils (Abdelfattah *et al.*, 2014). Humans are the main cause of land degradation within the UAE, and this human impact has created various water quality issues that include saline irrigation water, fertilisers, pesticides, and oil contamination (Alsuwaidi and Ramos, 2017). The development of human activities that lead to land degradation in the UAE it causes negative effects such as salinisation in agricultural farms, soil compaction by off-road vehicles, loss of vegetation through uncontrolled overgrazing, poor wildlife habitat and ecosystem destruction (Abdelfattah *et al.*, 2009). There have been natural causes that have contributed to land degradation; these natural causes include drought, wind erosion and sand encroachment (AbdelRahman, 2023).

Even though the UAE has barren vegetation, the society continues growing their crops in their gardens or farms. Common soil amendments used are animal manures for improving the soil productivity, and salt correctors for supporting better growth in saline soils and many more agricultural practices. Most fertiliser applications take no account of water saving, even though this would be possible, for example, Desalt Innovation Middle East, which created a soil system that may last up to 30 years to help soil salinity and save a thousand gallons of water (Malek, 2014). Therefore, the purpose of this study was to enhance water retention in domestic garden wastewater and improve water-holding amendments.

Date Palm Tree are considered resilient crops with nearly 105 million trees across the world. They are mostly grown in arid and semi-arid regions, and they survive in hot summers, low rainfall and relatively humid (Salem *et al.*, 2021).

Despite the availability of these potential solutions, there remains limited research evaluating the effectiveness of biochar derived from date palm waste under UAE-specific conditions. In particular, the comparison between unamended date palm fronds and biochar in improving water retention and plant growth has not been fully explored. Furthermore, there is a lack of integrated studies combining laboratory, mesocosm and field experiments in arid environments. Therefore, this study aims to address these limitations.

1.3 Research gap

Although biochar has been widely studied as a soil amendment, most existing research has focused on temperate soils and controlled laboratory conditions. There remains a limited understanding of how biochar performs in arid environments characterised by sandy soils, high temperatures and low organic matter content.

Furthermore, few studies have directly compared biochar with its original feedstock, such as date palm fronds (DPF), to evaluate whether pyrolysis is necessary to achieve improvements

in soil water retention and plant growth. In addition, most studies have focused on single experimental approaches with limited integration of laboratory characterisation, mesocosm experiments and field trials.

Therefore, there is a need for a comprehensive investigation that:

- Evaluates biochar performance specifically in UAE sandy soils
- Compares biochar with raw agricultural waste (DPF)
- Integrates multiple experimental approaches to assess water holding capacity and plant growth

This study addresses these gaps by combining physiochemical characterisation, controlled mesocosm experiments, pot trials and thermal analysis.

1.4 Novelty of the study

This study is novel in that it:

- Investigates biochar derived specifically from UAE date palm waste
- Compares biochar with its raw feedstock (DPF)
- Integrates laboratory, mesocosm and field experiments
- -Applies thermogravimetric analysis (TGA) to evaluate water retention behaviour.

This combination approach provides a more comprehensive understanding of biochar performance in arid sandy soils than previous studies.

1.5 Aim and objectives

The aim of this study is to evaluate the effectiveness of biochar derived from date palm fronds in improving water holding capacity and plant growth in sandy soils representative of arid environments.

It is hypothesised that biochar will enhance soil water retention and plant growth more effectively than unamended date palm fronds due to its increased porosity and stability.

To achieve this aim, the following objectives were defined:

- To characterise the physical and chemical properties of biochar, date palm fronds (DPF) and sandy soils.
- To quantify the effect of biochar and DPF on soil water holding capacity under controlled conditions.
- To evaluate the impact of biochar and DPF on plant growth under both controlled and field conditions.
- To analyse the thermal behaviour and moisture retention characteristics of the material using thermal gravimetric analysis (TGA).

To assess whether combining biochar and DPF provides synergistic benefits for soil improvement. The study aligns with the Abu Dhabi Economic Vision 2030 and COP 28, which prioritises sustainability in 2023 in the UAE. The use of biochar has the potential to address several environmental concerns related to agriculture in the UAE, such as reducing the need for waste disposal sites and minimising water usage while adding value to waste products.

1.6 Outline of the thesis

The aim of this research was to investigate the differences in water holding capacity between Date Palm Frond (DPF) and biochar treatments in sandy soils, specifically, by establishing the correlation between these treatments under extreme temperature conditions.

Chapter One focuses on outlining the primary objectives of the research and providing a comprehensive literature review relating to biochar production and application. This includes the potential benefits of biochar in arid soils and investigates its impact on the climate.

Chapter two details the characterisation of the physiochemical properties of biochar produced from date palm fronds. The experimental materials were characterised by a range of techniques. Scanning electron microscopy (SEM) was used to examine the pore structure. The BET method was used to look at the pore size distribution, and sieving analysis also took place to measure the particle size. Elemental Analysis of CHNO was used for measuring the chemical composition of biochar, DPF, UAE sand and Sharp Sand.

Chapter three reports mesocosm experiments on the hydrological effect of biochar application in the UAE soil. The experiment was to investigate its capability of holding water in different controlled cycle conditions, such as wet cycle and dry cycles, comparing DPF, biochar and soil.

Chapter four examines crop response to biochar application. The aim was to look at plant growth under controlled conditions in the laboratory using a growth tent in comparison to plant growth in uncontrolled conditions that took place in the field in the United Arab Emirates. Both experiments were pot trial experiments using different biochar and DPF percentage applications to soil.

Chapter five measures the water holding capacity of the experimental materials using thermal gravimetric analysis (TGA).

Chapter six seeks to optimise the combination of biochar and DPF to enhance plant growth and soil condition. The study will also include the mesocosms and pot trial experiment. To help see if combining both samples could result in a better solution for plant growth and water retention.

Chapter seven summarises and concludes the research findings. It also suggests future work that could help future researchers. The reference and appendices are also included.

Chapter 2: Physiochemical properties of UAE sand, sharp sand, DPF and Biochar

2.1 Introduction

Chapter 1 gave an overview of previous studies performed on biochar properties characterisation and its potential role in soil improvement. Building on that foundation, this chapter focuses on determining the physical and chemical properties of the materials used in this study: date palm fronds (DPF), biochar, UAE sand and sharp sand. Understanding these properties is important for evaluating how each material can influence the performance of sandy soils when used as soil amendments. Therefore, the objective of this chapter is to characterise the physiochemical properties of these materials to assess their suitability for improving sandy soil performance. There were two parts to the characterisation in this chapter. Firstly, the physical characterisation to assess size distribution, morphology and surface area using Scanning Electron Microscopy (SEM), Light Optical Microscope, Brunauer- Emmett-Teller surface area (BET) and sieve analysis. Secondly, the chemical characterisation to examine the elemental composition and thermal stability through Carbon, Hydrogen and Nitrogen (CHN) Analysis, Scanning Electron Microscopy Energy Dispersive X-ray Spectroscopy (SEM EDS) and Thermogravimetric Analysis (TGA).

2.2 Materials and methods

2.2.1 Sample Collection

2.2.1.1 Sandy Soil Collection

Sandy soils were collected from Al Nahda East, Abu Dhabi, and the site coordinates collected were at (54°43'19.7"E, 24°15'26.4"N).

2.2.1.3 Date Palm Waste Collection

Date palm fronds (DPF) waste were collected from beside the Abu Dhabi- Dubai Road (55°01'41.3"E, 24°52'17.1"N- Figure 2.2) during the month of December 2018. Normally, the fronds fall during the beginning of the winter season (October to December), which allows workers from the waste management centre to collect the waste and send it to the landfills. Therefore, for this research, the waste collected was packed and shipped to the UK to the Department of Earth Sciences- Durham University for conducting the experiments.



Figure 2.2. Location of Date Palm Waste Collection (Dubai- Abu Dhabi Road).

2.2.1.4 Date Palm Frond Preparation

The date palm fronds (DPF) were found air-dried (Figure 2.3). The DPF were cut into 5-8 cm, and then they were chopped into smaller pieces using a blender (Philips Viva Blender HR 2170/50). The samples were weighed before being charred (Figure 2.4).



Figure 2.3. Date Palm Frond preparation in the Lab.

2.2.1.5 Biochar production

The metal container was weighed separately before adding the DPF; this is to determine the weight loss before and after being charred. DPFs were weighed on a metal container, then charred at 250° C and left for processing on a Carbolite Furnace for 4 hours. After this process, biochar was produced from DPF it was allowed to cool for 1.5 hours. Biochar was then weighed to measure its weight loss (Figure 2.4).

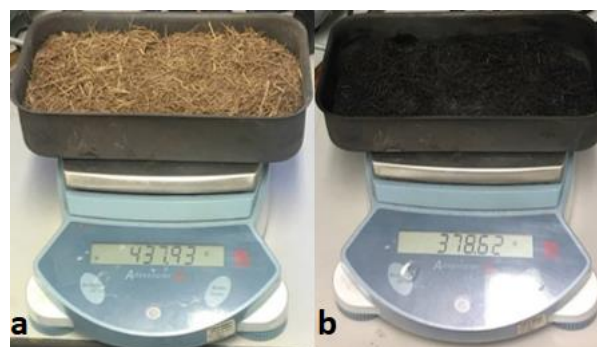


Figure 2.4. (a) DPF is weighed before being charred, and (b) is DPF after being charred, which is called biochar.

2.2.2 Physical Characterization

2.2.2.1 Scanning Electron Microscopy (SEM) and the energy dispersive spectroscopy (EDS)

SEM observations were conducted using Carl Zeiss Sigma VP300. The microscope is equipped with Bruker® QuantaX (EDS) and XsenseWD (WDS) detectors. The SEM was operated at 5 kV (imaging) and 10 kV (EDS). The samples were carbon-coated for EDS and gold-coated for Imaging. To perform a quantitative EDS microanalysis, ImageJ software was used to measure the porosity and the particle size distribution. The targeted chemical elements in this experiment were Carbon, Nitrogen, Oxygen, Sodium, Magnesium, Aluminium, Silicon and Phosphorus. After the SEM images were measured, the porosity was classified according to the pore types given in *Table 2.1*.

Table 2.1. The standard biochar pore type (Lehmann and Joseph, 2015).

| <i>Pore Type</i> | <i>Pore-Diameter</i> |
|------------------|----------------------|
| <i>Micropore</i> | <2nm |
| <i>Mesopore</i> | 2nm- 50nm |
| <i>Macropore</i> | >50nm |

2.2.2.2 Light Optical Microscope

The samples used in this analysis were only the UAE sand and the sharp sand. A small amount of each sand was added to the petri dish. The samples were already air-dried. The microscope used was the SWIFT SW380B Professional Binocular Compound Microscope. The images were taken from the SWIFT EP5R, 5MP Eyepiece Camera. The magnification used for the lenses was 10x and 40x.

2.2.2.3 Brunauer–Emmett–Teller (BET) experiment

The Brunauer–Emmet–Teller method (BET) was used for measuring the surface area of the catalysts. The BET was obtained from the P/P_0 relative nitrogen pressure <0.4 and adsorption isotherms at 77 K using a Quantachrom Autosorb instrument. The mesopore volume and the pore size distribution were computed using the nonlinear density function theory (NLDFT) model. The values obtained were scaled to the mass of the activated samples.

2.2.2.4 Sieving Analysis

The soil sieving analysis was conducted using wire sieving screens that are designed to measure coarse-grained soils. The dry samples were weighed to 230 g, and the weights of the sieves and the pan were recorded. The sieves were assembled in ascending order, placing those with larger openings on top. Therefore, the 710 μm screen was at the top, and the following were the 600 μm , 250 μm , 60 μm and 53 μm . The sample (sharp sand, UAE sand, DPF or biochar) was placed into the top sieve. The stack was manually shaken by hand for between 3 and 7 minutes. After shaking, the weight of each sieve was measured along with the pan of the remaining at the bottom of the sack (Geoengineering, 2015).

2.2.3 Chemical Characterization

2.2.3.1 Elemental analysis for Carbon, Hydrogen, and Nitrogen (CHN)

The elemental composition was determined using a Thermo Scientific Flash 2000 organic elemental analyser. The furnace heating temperature used was 900°C at GC Column and the TCD detector oven at 65°C. The samples were analysed in duplicates and using Helium carrier gas flow of 140ml/min, Oxygen flow 250 ml/min with Helium reference flow 100ml/min. The

sample ran for 720 seconds, and a sample delay of 12 seconds was injected for 5 seconds with Oxygen.

2.2.3.2 Thermogravimetric analysis (TGA)

The TGA was used in this section for analysing the weight loss of organic matter and inorganic matter, such as the Biochar, DPF, UAE sand and Sharp Sand. The instrument used for conducting TGA was the SGA TGH 1200, and the samples were run from ambient to 700°C using different heat ramps of 10 K min⁻¹ within a micro furnace using N₂ as a gas reaction. The heat ramp temperature used for each material was 5°C. The measured values were adjusted to a common temperature scale and cut to a temperature range between 50°C and 700°C. To start up the experiment, the alumina pan was placed to balance in a controlled furnace at a temperature. Then the TGA experiment was run using the organic and inorganic materials.

2.3 Results

2.3.1 SEM

2.3.1.1 SEM of DPF

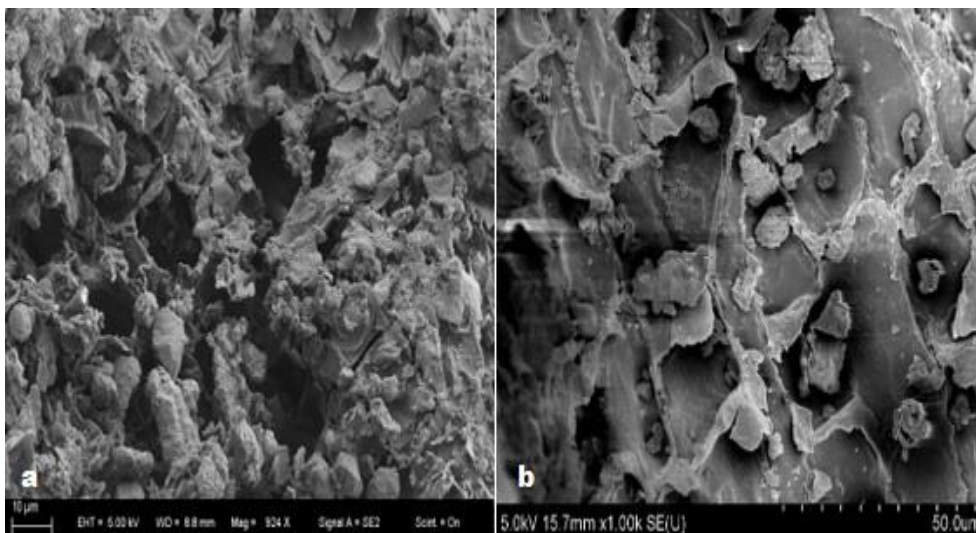


Figure 2.5. SEM imaging of Date Palm Frond (DPF) that shows the left side (a) taken in $10\mu\text{m}$ and the right side (b) was taken in $50\mu\text{m}$.

The imagery of the Date Palm Frond (DPF – Figure 2.5) shows that the surface area was undecomposed and that it had a less porous structure than biochar (Figure 2.5) due to no temperature exposure (Figure 2.5). It also indicates the presence of cellulose, hemicellulose, and lignin (Salem, Gamal, *et al.*, 2021) (Som, Wang and Al-Tabbaa, 2013).

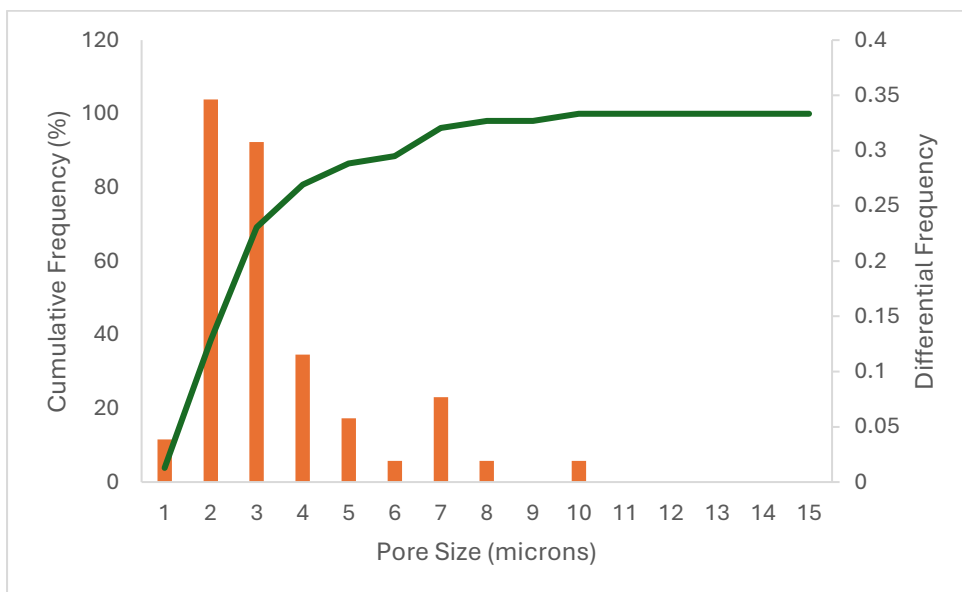


Figure 2.6. The pore size distribution of DPF and pore count.

The pore size distribution of the biochar was rising between $1\mu\text{m}$ - $10\mu\text{m}$ but mostly the rise was between $2\mu\text{m}$ - $3\mu\text{m}$. This would also indicate the pore type would be mostly micropores and a few of mesopores $5\mu\text{m}$ - $10\mu\text{m}$ (Table 2.1 - Figure 2.6).

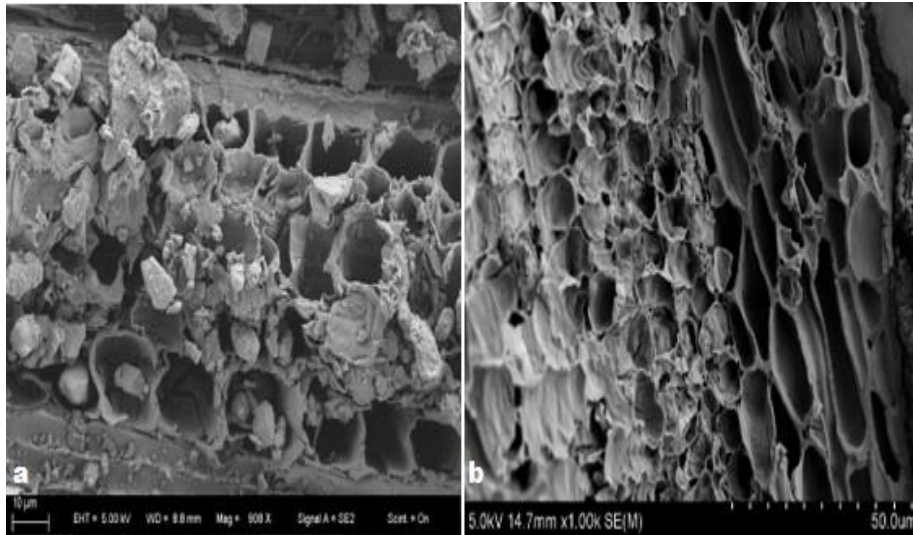


Figure 2.7. SEM imaging of biochar that shows the left side (a) taken in 10µm and the right side (b) taken in 50µm.

The morphology of biochar shows that the surface area had a graphitic pore structure after being exposed to higher temperature at 250°C (Figure 2.7) and that the pore size has increased both in terms of structure and quantity (Tomczyk, Sokołowska and Boguta, 2020).

2.3.1.2 SEM of biochar

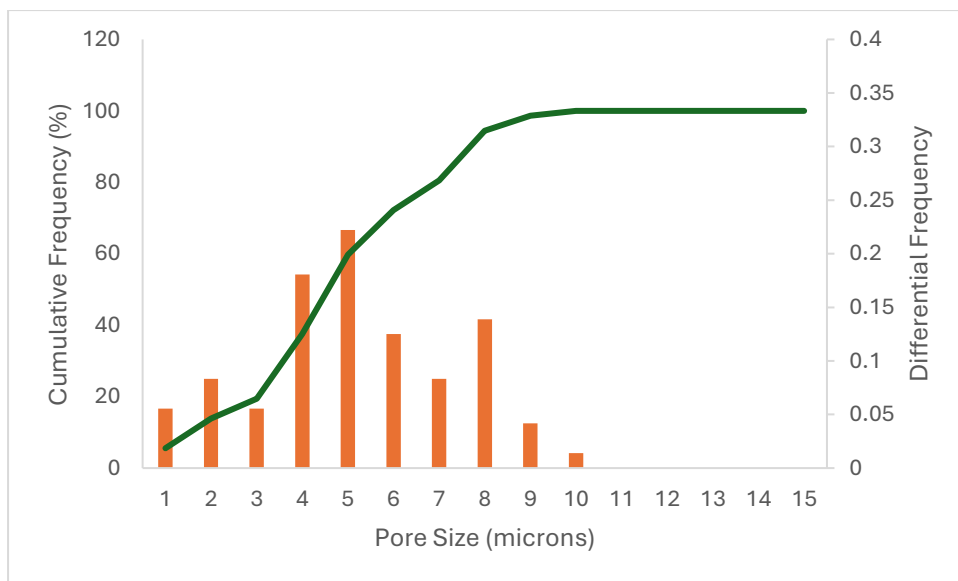


Figure 2.8. The pore size distribution of biochar and pore count.

The pore size distribution of the biochar began between 1 μ m-10 μ m but rose between 4 μ m-8 μ m. This would indicate that the pore type would be mostly mesopores (Table 2.1) (Figure 2.8).

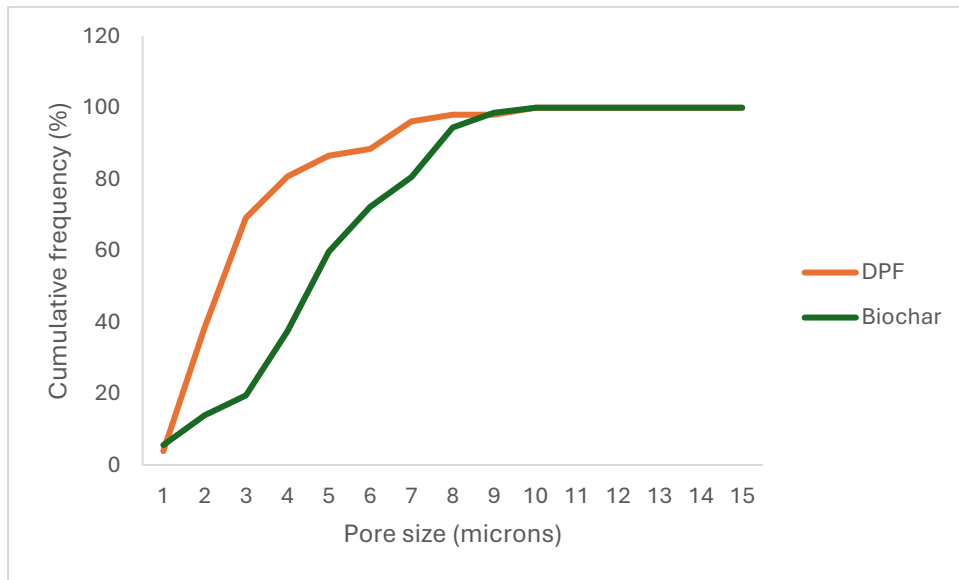


Figure 2.9. Comparison of the pore size distribution of DPF and biochar.

The graph shows the pore size distribution comparison between DPF and biochar (Figure 2.9). The results show that both materials have the same pore type, which was mesopores, but differ in different stages. The pore sizes of the biochar had more macropores when compared to DPF.

2.3.1.3 SEM of Sharp Sand

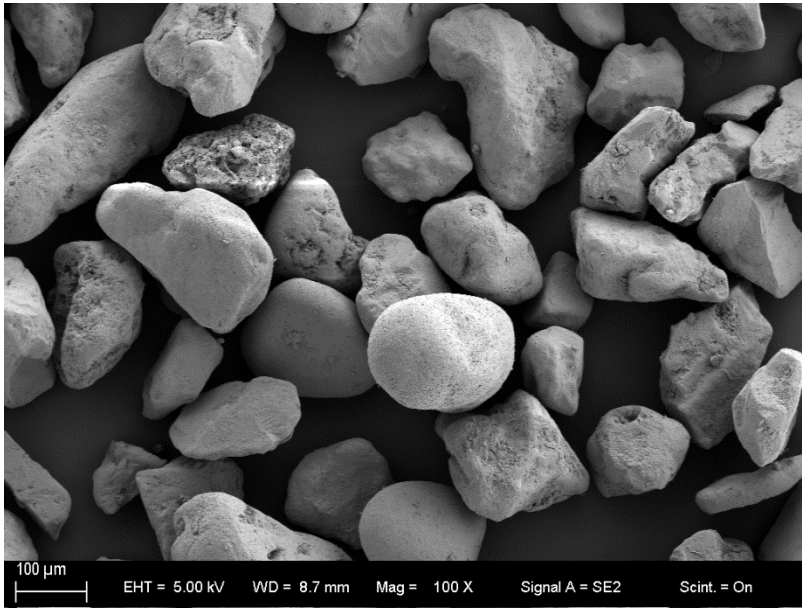


Figure 2.10. SEM imaging of sharp sand.

The different morphology of the sharp sand grains varies from well-rounded grains to sharp silica fracture surfaces (Figure 2.10).

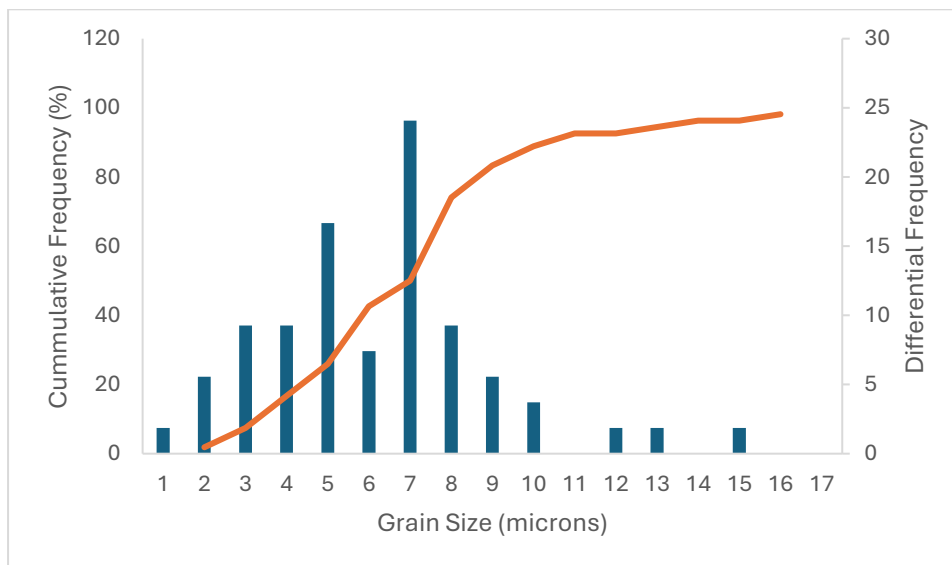


Figure 2.11. The particle size distribution of sharp sand.

The Figure (Figure 2.11) shows that the grain size of the sharp sand was rising between 2 μ m-9 μ m but the most obvious grain sizes that occurred highest were 5 μ m and 7 μ m. The lowest grain size ranges from 1 μ and between 12 μ m-15 μ m at a percentage frequency between 1%-96% (Figure 2.11).

2.3.1.4 SEM of UAE sand

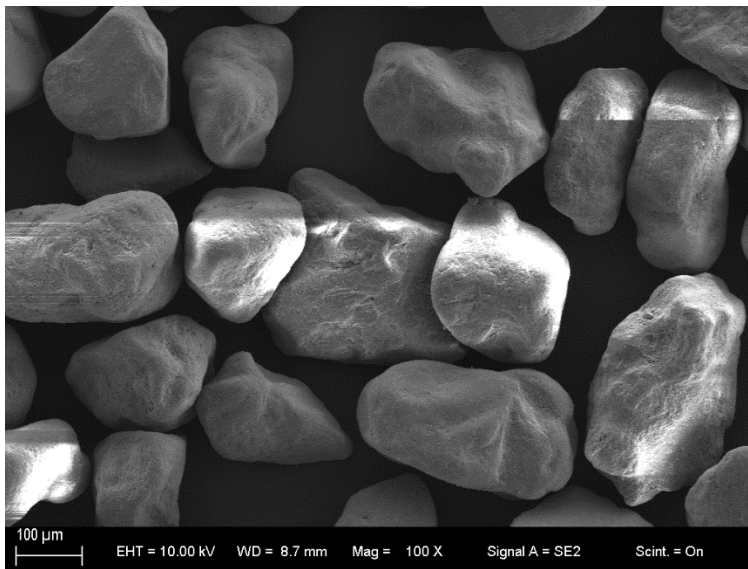


Figure 2.12. SEM imaging of UAE sand.

The UAE sand morphology shows the same in shape and size, which indicates the presence of quartz (SiO_2) (Figure 2.12).

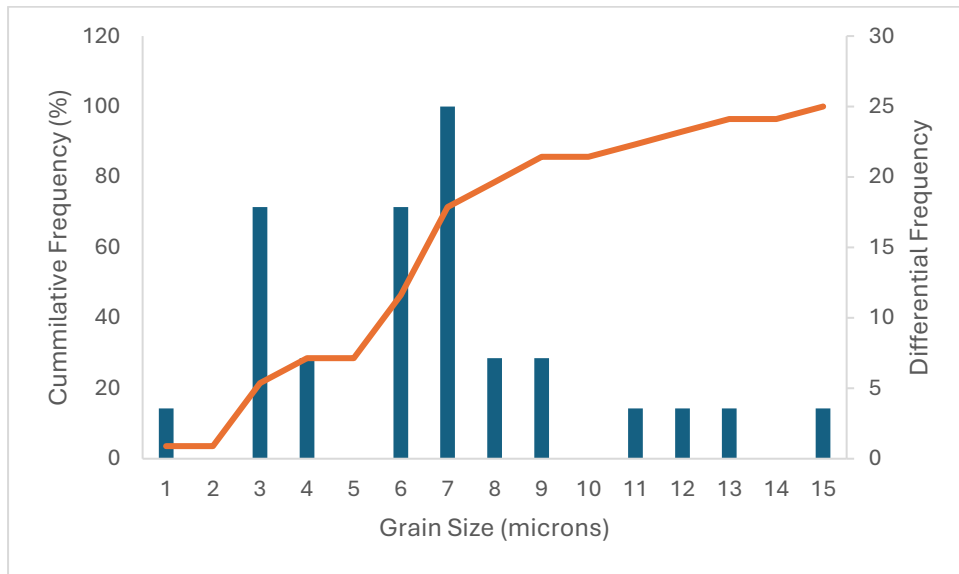


Figure 2.13. The particle size distribution of UAE sand.

The Figure (2.12) shows the grain size of UAE sand rises in the range from 3 μ , 6 μ - 7 μ with a lower percentage frequency. The lowest grain size, which ranges from 8 μ - 15 μ had a higher percentage frequency from 85%- 97% (Figure 2.13).

2.3.2 Light Optical Microscopy

2.3.2.1 Sharp Sand

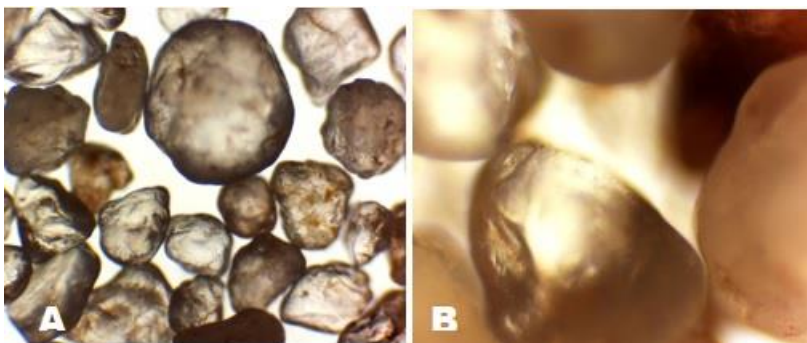


Figure 2.14. Sharp sand images taken at 10x magnification on image (A) and 40x magnification (B).

The sharp sand grains appear white, which indicates a predominant quartz composition (silicon dioxide, SiO₂) (Figure 2.14). The colour red and greyish green could also indicate the existence of iron and magnesium (Vossen, 2022).

2.3.2.2 UAE Sand

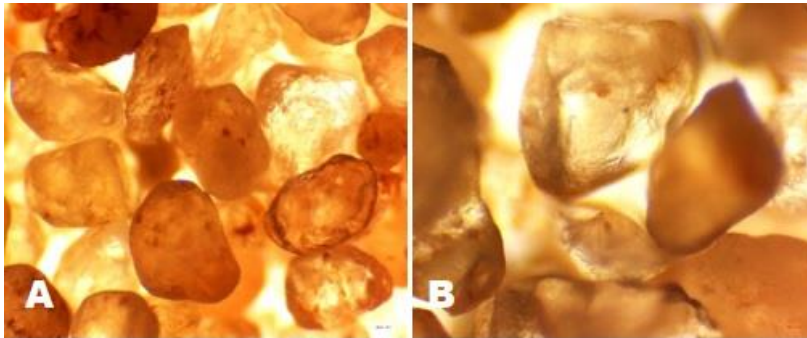


Figure 2.15. UAE sand images taken with a 10x lens magnification on image (A) and 40x lens magnification on image (B).

The UAE sand shows grains of two different colours (white and red), which could indicate having both quartz and iron minerals (Figure 2.15) (Vossen, 2022).

2.3.3 BET

Table 2.2. BET surface area proximate results of DPF, biochar, Sharp Sand and UAE Sand.

| <i>Material</i> | <i>BET (m²/g)</i> |
|--------------------|----------------------------------|
| <i>Palm Fronds</i> | 6.2 |
| <i>Biochar</i> | 6.3 |
| <i>Sharp Sand</i> | 1.2 |
| <i>UAE Sand</i> | 5.7 |

The transformation of DPF to biochar increased the BET surface area by 0.1 m²/g (Table 2.2).

The surface area of the UAE sand was greater than that of sharp sand by 4.5 m²/g.

2.3.4 Sieving Analysis of Sharp Sand and UAE Sand

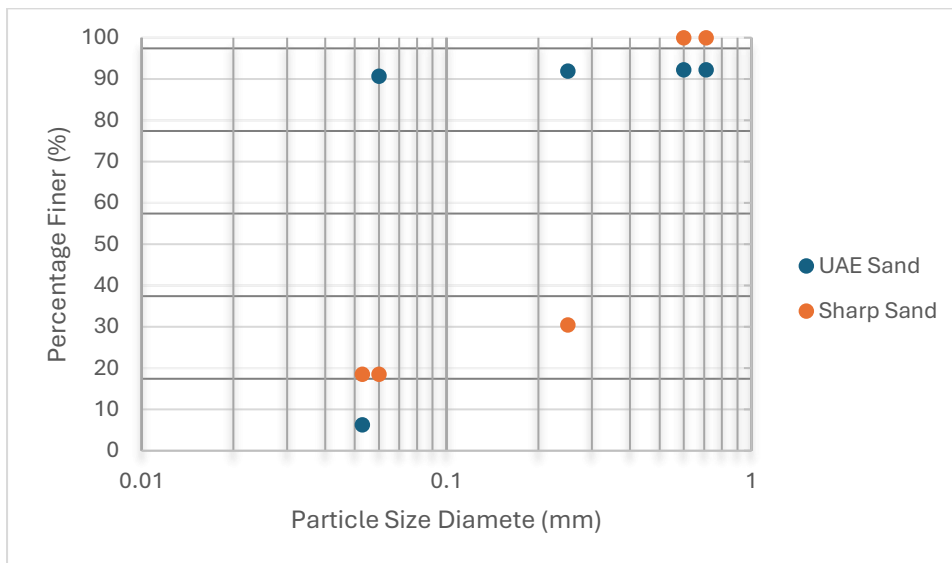


Figure 2.16. Grain size distribution of Sharp Sand.

From the graph (Figure 2.16), the UAE Sand and Sharp sand would both be classified as sandy soil (Figure 2.16). Figure 2.16 shows that the UAE sand had a finer particle size than the sharp sand (Particle Size Distribution Curve, 2019).

2.3.5 Chemical Analysis

2.3.5.1 ESM EDS

Table 2.3. The chemical analysis of the biochar and DPF using SEM ESD.

| Element | Biochar (wt %) | DPF (wt%) |
|---------|----------------|-----------|
| N | 32.58 | 24.38 |
| O | 42.75 | 50.46 |
| Na | 2.90 | 0 |
| Mg | 6.18 | 2.04 |
| Al | 0.86 | 2.35 |
| Si | 5.99 | 14.09 |
| P | 8.74 | 6.69 |

The result of the chemical analysis in Table 2.3 shows that biochar had a greater proportion of Nitrogen, Sodium, Magnesium and Phosphorus than found in the DPF. Conversely, the DPF had a higher proportion of Oxygen, Aluminium and Silicon than found in the biochar.

2.3.5.2 CHN analysis

Table 2.4. The percentage by mass CHN composition of sands, biochar and DPF.

| Material | N (wt%) | C (wt%) | H (wt%) |
|------------|---------|---------|---------|
| DPF | 2.59 | 37.72 | 5.37 |
| Biochar | 1.54 | 56.33 | 4.28 |
| Sharp Sand | 0.00 | 0.15 | 0.03 |
| UAE Sand | 0.01 | 4.49 | 0.12 |

As would be expected, the biochar had the highest concentration of C with an increase of 49% in C over the DPF (Table 2.4). Equally, the %N decreases in the biochar both in absolute and relative terms, with C:N ratio of the biochar being 36.6 compared to 14.6 in the DPF. The UAE sand had 4.5% C but negligible %N implying that the C present in the UAE sand is as carbonate.

2.3.5.3 Thermogravimetric Analysis (TGA)

- **DPF and Biochar**

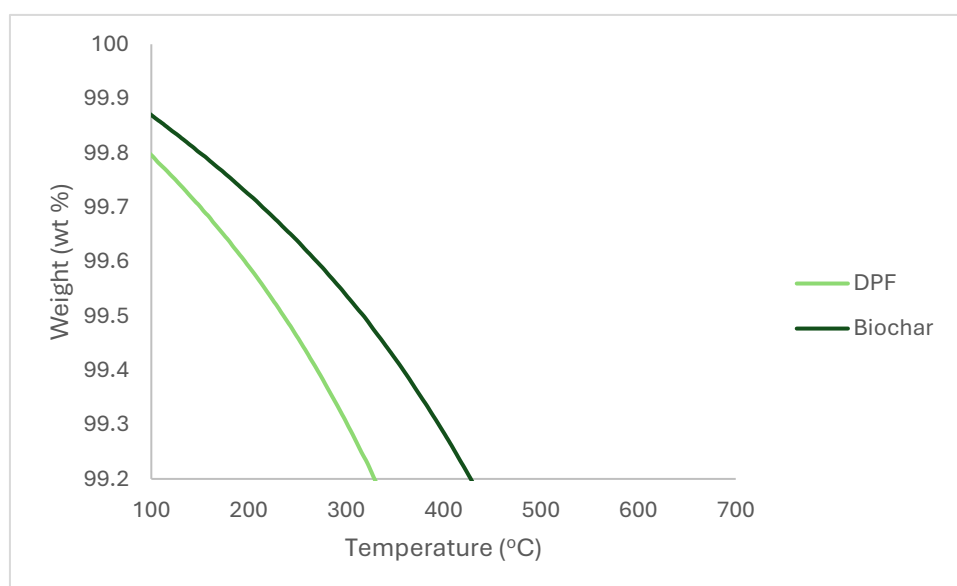


Figure 2.17. TGA curve for Date Palm fronds and biochar at heating rate 5°C/min.

The TGA curve for biochar demonstrates its high thermal stability, showing minimal mass loss up to 429°C and DPF begins degradation at lower temperatures at 330°C (Figure 2.17). The first single degradation of DPF from 8°C- 159°C was dehydration of hemicellulose- cellulose of 0.6. whereas biochar first degrades at a temperature 10°C- 127°C of cellulose of 0.7% mass loss (Figure 2.17).

- **Sharp Sand and UAE Sand**

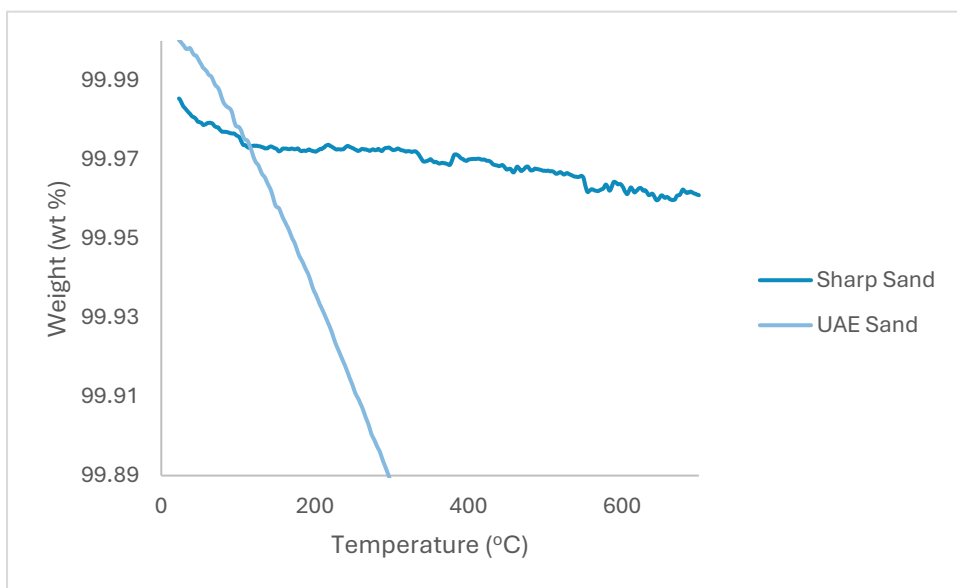


Figure 2.18. TGA curve for Sharp Sand and UAE Sand at heating rate 5°C.

The TGA curves for both sharp and UAE sands showed different mass loss across the temperature range tested. At 225°C, the UAE sand has more mass loss than the sharp sand. Figure 2.18 exhibits multiple peaks, and the highest peaks were highlighted. The first degradation of UAE sand was between 2°C- 200°C of 0.05%. The degradation of sharp sand was quite steady between 6°C- 176°C of 0.01% weight loss (Figure 2.18).

2.4 Discussion

This chapter has characterised the physiochemical properties of date palm fronds (DPF), biochar, sharp sand and UAE sand. The motivation to use DPF was to find alternative solutions for agricultural waste in the UAE and explore the advantages to improve sandy soil productivity, considering the specific ecological circumstances.

According to IBI (International Biochar Initiative, 2015), there are several parameters to assess and compare when considering biochar. Examples of these analyses are BET surface area, SEM, TGA and CHNO elemental analysis. Each analysis serves its purpose for identifying the chemical and physical properties of the biochar (Lehmann and Joseph, 2015). To determine the pore size and structure, materials were examined using scanning electron microscopy (SEM). Thermogravimetric Analysis (TGA) was used to evaluate the thermal stability, decomposition behaviour, composition of biochar, DPF, sharp sand and UAE sand. For biochar and DPF it helps to determine thermal degradation of the materials and. It's composition its essential for understanding it benefit in application to soil. Whereas, the sharp sand and UAE sand to determine thermal stability and understand its effective use of these materials in various environmental contexts (Rajisha *et al.*, 2011).

The Brunauer–Emmet–Teller (BET) analysis was conducted to assess the distribution of pore sizes and surface area. To determine the chemical composition of biochar, DPF, UAE sand, and sharp sand, elemental analysis of CHNO was used.

The biochar pore size was measured in this study to gain an insight into its potential to enhance the water-holding capacity of sandy soil. The results of SEM images of this study confirm the results of Jouiad *et al.* (2015), where the DPF had a smaller pore size than biochar (Table 2.5-Figure 2.7). Pore size distribution for both DPF and biochar was dominated by mesopores. The only difference was that biochar had a greater proportion of macropores compared to DPF. Som

et al, (2013) also showed that DPF and its biochar were dominated by mesopores. This increase in pore volume is significant because mesopores and macropores improve the capacity of soil amendments to store moisture and provide microhabitats for beneficial microorganisms. This improved pore structure is particularly advantageous for improving soil structure and fertility in arid UAE soils, where water retention is limited.

Table 2.5. Material pore size comparison with other studies.

| Material | Temperature (°C) | Pore Size (µm) | Pore Type | References |
|----------------------------------|------------------|----------------|------------|--------------------------------|
| DPF | - | >2 | Mesopores | This study |
| Biochar | 250°C | >4 | Mesopores | This study |
| Biochar | 300°C | >1.9 | Macropores | (Som, <i>et al.</i> , 2013) |
| DPF | - | >1.3 | | (Jouiad <i>et al.</i> , 2015) |
| Biochar | 400°C | | Mesopores | (Jouiad <i>et al.</i> , 2015) |
| Oak | - | >0.02 | | (Heydari <i>et al.</i> , 2023) |
| Oak biochar | 550°C | >0.89 | Mesopores | (Heydari <i>et al.</i> , 2023) |
| Pine wood biochar (raw) | 525°C | >25.7 | Macropores | (Taheran <i>et al.</i> , 2016) |
| Pine wood biochar (activated) | 525°C | >12.25 | Macropores | (Taheran <i>et al.</i> , 2016) |

The results of this study found that C:N ratio of biochar was 36.6 compared to 14.6 in the DPF. A study conducted by Yang et al., (2019) provides evidence that Enteromorpha biochar production at 250°C with a C:N ratio of 32.91 closely aligns with the results obtained in this study. This higher C:N indicates greater carbon stability and lower decomposition compared to original DPF material, Materials with higher C:N ratios are generally more resistant to microbial decomposition and tend to persist longer in soil (Lehmann and Joseph, 2015), suggesting that biochar may contribute to longer term carbon storage when applied to sandy soils (Jouiad *et al.*, 2015). The higher pyrolysis temperature used to produce biochar the higher carbon and nitrogen will occur (Chatterjee et al., 2020). Another study done by Jouiad et al., (2015), it was noticed that biochar produced at 400 °C exhibited a slightly higher carbon content at 50.17 % compared to the current study, accompanied by a lower nitrogen content of

0. Table 2.6 shows a comparison of various hardwood and softwood materials with the results of our study. Specifically, Taheran et al., (2016) observed that Pinewood biochar exhibited the highest carbon content at 80.73% while rice husk biochar displayed a carbon content of 37.66%. As for the raw materials (uncharred), such as in our study, DPF and rice husk have the lowest carbon content when compared to the Elm Sawdust, which has the highest carbon content (Wang, Yin and Liu, 2014).

This study also considered the CHNO composition of UAE sand and sharp sand so as to confirm the nature of any organic matter in the materials. UAE sand was found to have a higher C: N ratio than Sharp sand. Although Sharp sand and UAE sand were analysed for CHN, there were no prior investigations, nor scholarly research was found in the literature that has characterised CHN content within the sand samples.

In a separate investigation of this study, SEM EDS was conducted to check the chemical composition of the materials. The findings revealed that biochar had a higher proportion of Carbon, Nitrogen, Sodium, Magnesium and Phosphorus than DPF. DPF had a higher proportion of Oxygen, Aluminium, Silicon and Hydrogen (Table 2.3 and Table 2.4). A comprehensive literature review was conducted to identify the chemical composition of biochar and DPF using SEM, but for the ESM EDS experiment, studies were found for DPF and its biochar, but for sand, few studies were found.

Although both SEM EDS and CHN analysis were conducted to assess elemental composition. SEM EDS provided semi-quantitative data on surface elemental distribution and is considered less sensitive to light elements such as carbon and nitrogen, which cannot accurately represent total bulk composition. In contrast to CHN analysis, which measures total elemental content with high precision using combustion analysis, resulting in higher

concentrations of carbon and nitrogen. Therefore, CHN analysis is considered the primary quantitative method for assessing carbon and nitrogen.

Table 2.6. Carbon, Hydrogen and Nitrogen (CHN) Analysis comparison with other studies.

| Material | Temperature | Elemental composition (weight %) | | | | References |
|--------------------------------|-------------|----------------------------------|------|-------|--------|--------------------------------|
| | | C | H | N | C/N | |
| <i>DPF</i> | - | 37.72 | 5.37 | 2.59 | 14.56 | This study |
| <i>Biochar</i> | 250°C | 56.33 | 4.28 | 1.54 | 36.58 | This study |
| <i>DPF</i> | - | 43 | 5.83 | 0.70 | 61.43 | (Usman <i>et al.</i> , 2015) |
| <i>Biochar</i> | 300°C | 57.99 | 4.08 | 0.54 | 107.39 | (Usman <i>et al.</i> , 2015) |
| <i>DPF</i> | - | 45.4 | 5.6 | 0 | 0 | (Jouiad <i>et al.</i> , 2015) |
| <i>Biochar</i> | 400°C | 60.9 | 2.5 | 1.2 | 50.75 | (Jouiad <i>et al.</i> , 2015) |
| <i>DPF</i> | - | 41.9 | 5.8 | 0.2 | 209.5 | (Burezq and Davidson, 2023) |
| <i>Biochar</i> | 400°C | 46.9 | 3.5 | 0.1 | 469 | (Burezq and Davidson, 2023) |
| <i>Oak biochar</i> | 550°C | 72.62 | 2.12 | 1.01 | 71.90 | (Heydari <i>et al.</i> , 2023) |
| <i>Neem wood biochar</i> | 300°C | 58.09 | - | 14.10 | 4.12 | (Boraah <i>et al.</i> , 2023) |
| <i>Neem wood biochar</i> | 500°C | 63.84 | - | - | 0 | (Boraah <i>et al.</i> , 2023) |
| <i>Pine wood biochar (raw)</i> | 525°C | 78.28 | - | - | 0 | (Taheran <i>et al.</i> , 2016) |

| | | | | | | |
|--------------------------------------|-------|-------|------|------|--------|--------------------------------|
| <i>Pine wood biochar (activated)</i> | 525°C | 80.73 | | | 0 | (Taheran <i>et al.</i> , 2016) |
| <i>Enteromorpha biochar</i> | 250°C | 70.2 | 4.5 | 2.2 | 32.91 | (Yang <i>et al.</i> , 2019) |
| <i>Rice Husk Char</i> | 700°C | 43.43 | 24.3 | 1.96 | 22.16 | (Konneh <i>et al.</i> , 2021a) |
| <i>Coconut Husk Char</i> | 700°C | 38.46 | 29.1 | 2.31 | 16.65 | (Konneh <i>et al.</i> , 2021b) |
| <i>Coffee Husk Char</i> | 700°C | 43.03 | 27.6 | 2.22 | 19.38 | (Konneh <i>et al.</i> , 2021b) |
| <i>Rice husk</i> | - | 35.15 | 4.16 | 0.36 | 97.64 | (Wang, Yin and Liu, 2014) |
| <i>Rice husk Biochar</i> | 550°C | 37.66 | 1.83 | 0.30 | 125.53 | (Wang, Yin and Liu, 2014) |
| <i>Elm Sawdust</i> | - | 47 | 5.39 | 0.29 | 162.07 | (Wang, Yin and Liu, 2014) |
| <i>Elm Sawdust Biochar</i> | 550°C | 67.98 | 3.78 | 0.39 | 174.31 | (Wang, Yin and Liu, 2014) |
| <i>Sharp Sand</i> | - | 0.15 | 0.03 | 0.00 | 0 | This study |
| <i>UAE sand</i> | - | 4.49 | 0.12 | 0.01 | 449 | This study |

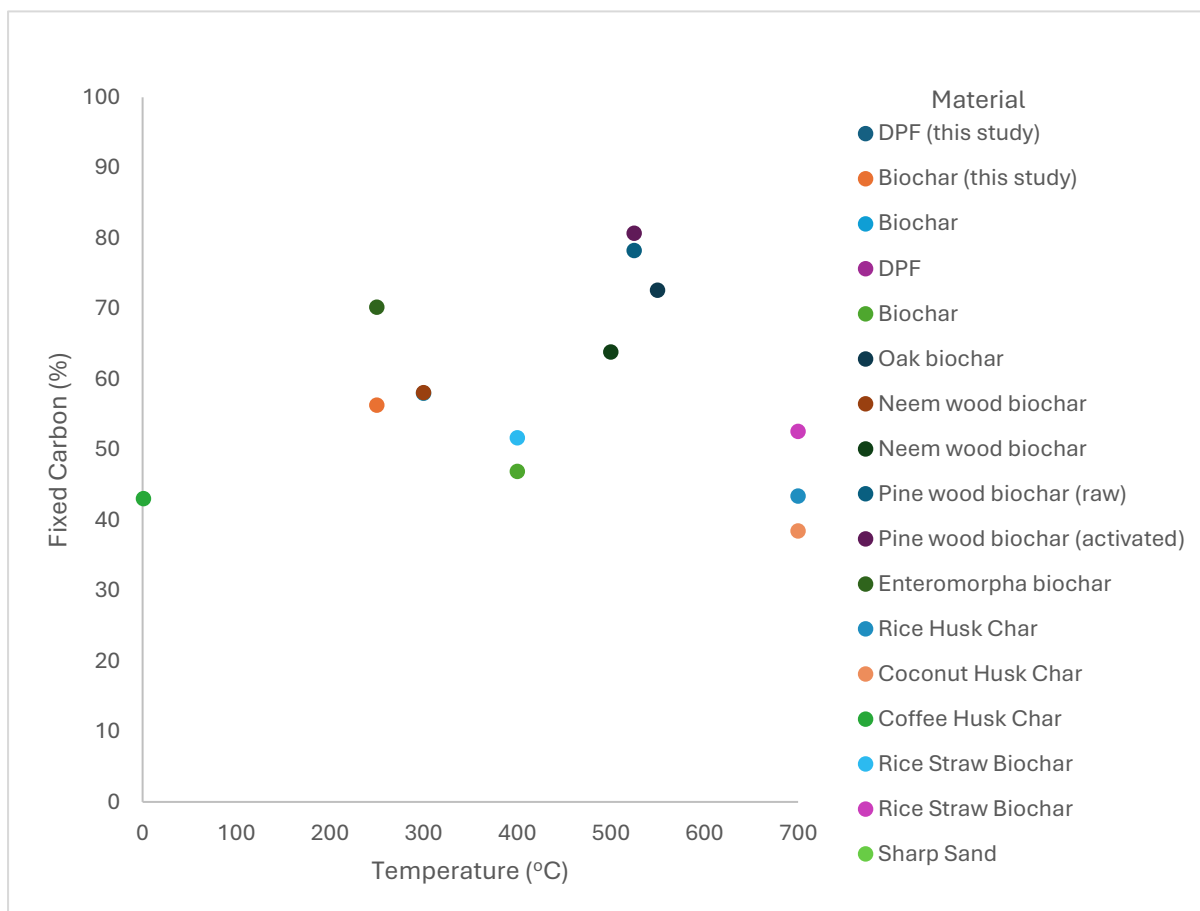


Figure 2.19 Carbon content of biochar and non-charred materials

The abundance of carbon shows on the graph was between 250°C-700°C pyrolysis temperatures (

Figure 2.19). The highest carbon content was at 500°C and the lowest was at 550°C. This is due to the different feedstock presented in (Table 2.6).

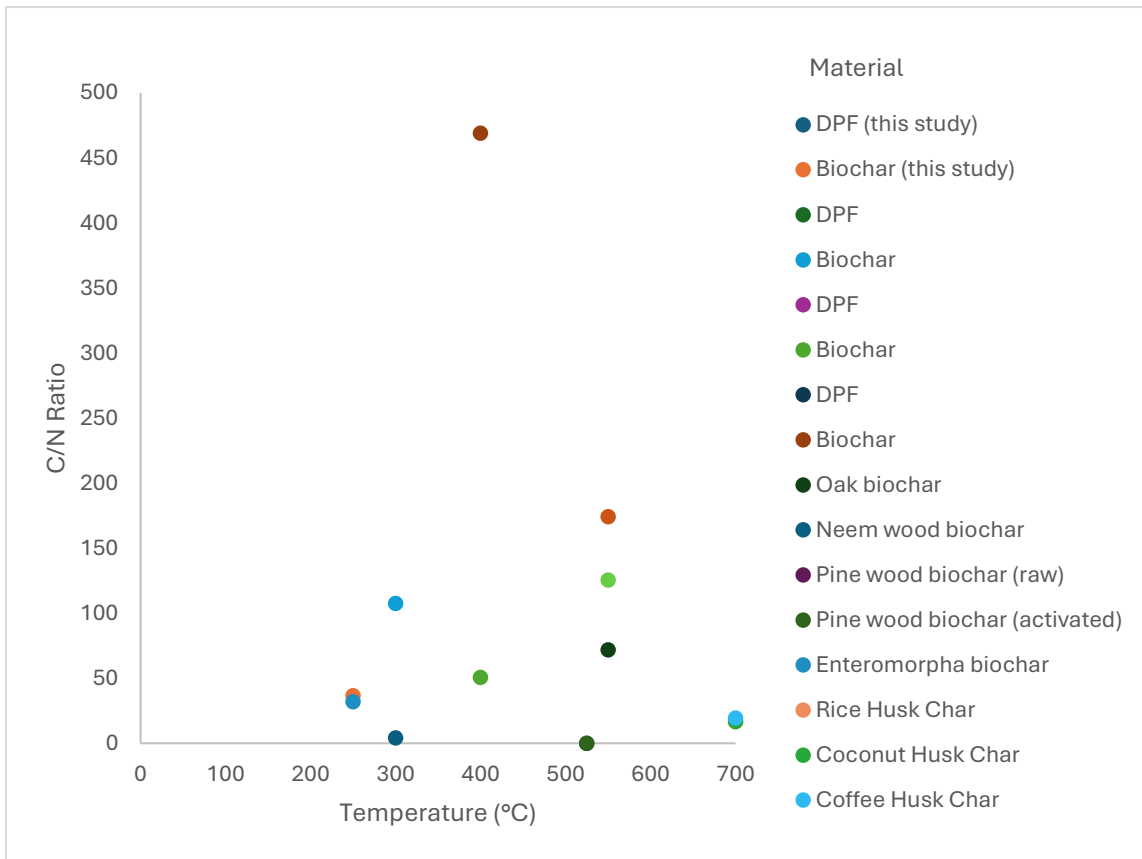


Figure 2.20 Carbon and nitrogen ratio versus pyrolysis temperature.

The carbon and nitrogen ratio shown on the graph was between 250°C-700°C pyrolysis temperatures (Figure 2.20). The highest C:N ratio was at 400°C and the lowest was at 500°C. This is due to the different feedstock presented in (Table 2.6).

The BET analysis was conducted in this study to determine the surface area and pore size distribution of the materials. The obtained results from the BET analysis revealed that the biochar exhibited slightly higher surface area than the DPF (Table 2.7). The surface area of the DPF in this study was larger than found in previous studies (Table 2.7). The highest surface area for biochar was reported in a study conducted by Som *et al.*, (2013), which measured a value of 9 m²/g. The increase in surface area observed in biochar compared to DPF is particularly important because it reflects the formation of new pore structures during the pyrolysis process. A higher surface area enhances the material's capacity for water adsorption, nutrient retention and microbial habitats when applied to soil (Lehmann and Joseph, 2009). This property is beneficial in arid regions such as the UAE, where soils are characterised by low organic matter and limited water holding capacity (Inayat *et al.*, 2023). The great surface area of biochar will create microbial activity that will act like a sponge to reserve nutrients and water, which prevents nutrients from leaching out of sandy soil (Konneh *et al.*, 2021a). In addition, the increased surface area contributes to chemical stability and carbon sequestration as more carbon is locked in graphitic structures that resist decomposition (Davidson and Janssens, 2006). Therefore, the higher BET surface area of biochar not only differentiates it physically from DPF but also enhances its functional potential as a soil amendment for improving fertility, moisture retention and long-term carbon storage. Although there are some variations in the results, a study conducted by (Elnour *et al.*, 2019) reported a surface area for biochar, with a difference of 0.8 m²/g compared to the findings. A study conducted by Taheran *et al.*, (2016) found that pinewood biochar had a higher surface area by 8.56 m²/g.

As for the surface area of the sands, it was noticed that UAE sand had a higher surface area than sharp sand. (Mecheri *et al.*, 2015) examined Algerian sand, where the only study found to have measured desert sand on BET, which shows a lower surface area than UAE sand by 2.66 m²/g and higher than sharp sand by 1.84 m²/g. These results show no major difference between

different palm fronds. This study was also compared with other hardwood and softwood materials to see if there were possible similarities, and it was noticed that Pine wood biochar conducted by Taheran et al., (2016) was only 8.56 higher. Other studies showed with much higher surface area when compared to this study, such as the oak biochar, pinewood activated, cedar wood biochar, Sawdust, and Sawdust activated carbon. This could be due to having its biochar produced at a higher temperature of 400°C- 900°C (Table 2.7). It is crucial to consider other differences to help understand more of the material behaviour, enabling identification of performance differences that may not be noticeable from the surface area measurements alone.

Table 2.7. BET surface area for study materials comparison with other published studies.

| <i>Material</i> | <i>Temperature</i> | <i>BET</i> <i>(m²/g)</i> | <i>References</i> |
|--------------------------|--------------------|--|---------------------------------|
| <i>DPF</i> | - | 6.2 | This study |
| <i>Biochar</i> | 250°C | 6.3 | This study |
| <i>Sharp Sand</i> | - | 1.2 | This study |
| <i>UAE Sand</i> | - | 5.7 | This study |
| <i>DPF</i> | - | 4 | (Som <i>et al.</i> , 2013) |
| <i>Biochar</i> | 300°C | 9 | (Som <i>et al.</i> , 2013) |
| <i>DPF</i> | - | 0.98 | (Jouiad <i>et al.</i> , 2015) |
| <i>Biochar</i> | 400°C | 1.99 | (Jouiad <i>et al.</i> , 2015) |
| <i>DPF</i> | - | 1.1 | (Sizirici <i>et al.</i> , 2021) |
| <i>Biochar</i> | 400°C | 3.8 | (Sizirici <i>et al.</i> , 2021) |
| <i>DPF</i> | - | 1.0 | (Elnour <i>et al.</i> , 2019) |
| <i>Biochar</i> | 400°C | 5.5 | (Elnour <i>et al.</i> , 2019) |
| <i>DPF</i> | - | 0.463 | (Taha and Daffalla, 2023) |
| <i>Biochar</i> | 600°C | 1.74 | (Taha and Daffalla, 2023) |
| <i>Oak biochar</i> | 550°C | 170.88 | (Heydari <i>et al.</i> , 2023) |
| <i>Neem wood biochar</i> | 300°C | 1.61 | (Boraah <i>et al.</i> , 2023) |

| | | | |
|--------------------------------------|-------|--------|--------------------------------|
| <i>Neem wood biochar</i> | 500°C | 88.7 | (Boraah et al., 2023) |
| <i>Pine wood biochar (raw)</i> | 525°C | 14.86 | (Taheran et al., 2016) |
| <i>Pine wood biochar (activated)</i> | 525°C | 852.95 | (Taheran et al., 2016) |
| <i>Sawdust</i> | | 108.81 | (Chikri et al., 2023) |
| <i>Activated carbon (sawdust)</i> | 500°C | 254.69 | (Chikri et al., 2023) |
| <i>Biochar (cedar wood)</i> | 400°C | 310 | (Bataillou et al., 2022) |
| <i>Biochar (cedar wood)</i> | 900°C | 136 | (Bataillou et al., 2022) |
| <i>Sharp Sand</i> | - | 1.2 | This study |
| <i>UAE Sand</i> | - | 5.7 | This study |
| <i>Algerian Sand</i> | - | 3.04 | (Mecheri <i>et al.</i> , 2015) |

The TGA measured in this study were different from other studies; this could be because of the biochar was produced from date palm fronds at a lower temperature (250°C) than in other studies. These results were compared with other studies done by Rutherford et al., (2012) and Gašparovič et al., (2010), who have highlighted that the dehydration reactions starts releasing moisture (up to 120°C). Therefore, the depolymerisation and volatilisation come next of the hemicellulose (220-315°C), cellulose (250-400°C) and Lignin (160-900°C) that follows over different stages depending on the biomass complexity.

2.5 Conclusion

The characterisation of this material has shown that both biochar and DPF are dominated by mesopores. The SEM images confirmed that biochar exhibited a greater proportion of macropores than the DPF starter material, while both materials were dominated by mesopores. In addition to these differences in pore structure, the chemical composition of the materials also differed; biochar had a higher C:N ratio than DPF. Moreover, SEM EDS analysis uncovered variations in the chemical composition, with biochar having higher levels of carbon, nitrogen, sodium, magnesium, and phosphorus, while DPF showed higher proportions of oxygen, aluminium, silicon, and hydrogen. The BET analysis indicated a slightly higher surface area for biochar than for DPF. The TGA experiment demonstrated that biochar had great thermal stability with minimal mass loss compared to DPF. Biochar primarily degrades cellulose, while DPF undergoes dehydration of hemicellulose-cellulose. The sharp and UAE sands exhibited different thermal degradation patterns. UAE sand experiences higher mass loss compared to sharp sand, indicating a wider temperature range of degradation. The sharp sand and UAE sand analyses revealed different thermal degradation patterns, with UAE sand exhibiting higher mass loss over a wider temperature range, featuring its variable mineral composition. These findings provide an important baseline for understanding the interaction between organic and inorganic components in improving soil amendment studies.

The BET analysis confirmed that biochar had a slightly higher surface area than DPF, representing an increase in pore development and a greater potential for water and nutrient adsorption.

Overall, this chapter establishes the foundational material properties that support the experimental work in later chapters. Understanding these physiochemical properties is

necessary for evaluating the effectiveness of biochar and DPF in improving sandy soil performance and for guiding their broader application in sustainable agricultural environment technologies.

Chapter 3: The hydrological effect of biochar application using sandy soil

3.1 Introduction

Chapter 2 focused on the physicochemical properties of DPF, biochar, sharp sand and UAE sand. The results in Chapter 2 provide the foundation for understanding how organic amendment may influence oil hydrological behaviour in an arid environment. Chapter 3 aimed to investigate the water holding capacity of sandy soil when amended with different percentages of DPF and biochar under controlled cycle conditions. To achieve this, mesocosm experiments were conducted, allowing for the controlled cycle manipulation of environment such as wet cycle, dry cycle and waw cycle (introducing humidity). The specific objectives of this chapter are to quantify soil moisture content under different moisture cycles, evaluate the effect of DPF and biochar amendments at varying application rates and compare their influence on moisture retention to unamended sandy soil.

3.2 Approach Statement

A quantitative research approach was conducted in this study using mesocosms to assess the factors controlling soil moisture content in amended and unamended sandy soils. The aim of the experiment was to examine what controlled the water content of biochar and precursor materials. The main research questions for this chapter were:

- Do soils amended with DPF, and biochar retain their water differently compared to unamended soils?
- Do DPF and biochar amendments improve soil moisture retention under different moisture regimes (wet, dry and dry cycle waw)?

3.3 Materials and methods

3.3.1 Sample collection

Chapter 2 explains Date Palm Fronds (DPF) waste collection seen in Figure (2.2) and the soil used for this experiment was the sharp sand only.

3.3.2 Date Palm frond preparation

The samples were prepared at the Department of Earth Science, Durham University, as shown in Chapter 2, Figure 2.3 and explain how DPF was transformed into biochar at 250°C.

3.3.3 Sandy soil preparation

The sandy soils from the United Arab Emirates were not accessible for the mesocosm experiment due to logistical challenges related to shipping. Instead of the UAE sandy soils, sharp sand, also known as builder's sand, was used as it has a similar texture. Prior to usage, the sharp sand was air-dried for 24 hours.

3.3.4 *Mesocosms experimental design*

The mesocosms were designed to simulate sandy soil conditions representative of arid environments such as those found in the UAE, under controlled temperature conditions. The experimental design includes four factors: material type, temperature level, wetting cycle and time. The material factor consisted of three levels: sharp sand, Date Palm Fronds (DPF) and biochar derived from DPF (Figure 3.2a).

The treatment factor represented the percentage of amendment material mixed with sharp sand on a dry weight basis. Seven treatment levels were used: 0%, 1%, 3%, 6%, 12%, 15% and 18%. The 0% treatment, consisting of sharp sand, DPF and biochar, served as the unamended control. The remaining treatment levels consisted of sharp sand amended with either DPF or biochar at the specified percentages. For example, the 1% treatment consisted of 1% amendment material and 99% sharp sand by dry weight, with higher amendment levels prepared accordingly. This design resulted in a total of 13 material-treatment combinations: one unamended control (sharp sand only), six DPF amendment levels and six biochar amendment levels. Each treatment combination was replicated three times within each moisture cycle.

The wetting cycle factor had three levels: wet cycle, dry cycle and dry cycle with a water bowl (hereafter referred to as dry cycle waw). During the wet cycle, each mesocosm was watered daily with 1 ml of tap water. During the dry cycle, no water was added. The dry cycle waw followed by the same procedure as the dry cycle, but a water bowl was placed inside the oven to increase humidity and influence soil moisture content. Each cycle was conducted separately in an electric oven maintained at 40°C for seven days.

Soil moisture content was measured gravimetrically by weighing each mesocosm daily using a precision balance. Moisture content was calculated as the percentage of water mass relative to the dry mass of the soil or amended material, based on the difference between the wet mass

and the initial dry mass. This gravimetric approach provides a direct and reliable measure of soil moisture content expressed as a percentage by weight.

Soil moisture content was measured daily over the seven-day period for each cycle using a gravimetric method. In this study, 'Day' referred to the sampling day within each cycle, 'Material' referred to the amendment type (DPF, biochar or sharp sand), 'Treatment' referred to the amendment percentage, and 'Cycle' referred to the moisture regime (wet, dry or dry cycle waw). These factors were included in the experimental design to assess the effects of amendment material, treatment level, moisture regime and time on soil moisture content. The material- treatment combinations used in the experiment are summarised in (*Table 3.1*).

Table 3.1. Amended treatments used in the mesocosm experiments (composition by dry weight).

| <i>Material type</i> | <i>Treatment level (%)</i> | <i>Composition (% by dry weight)</i> | <i>Description</i> |
|----------------------|----------------------------|--------------------------------------|--------------------|
| <i>Sharp sand</i> | 0 | 100% sharp sand | Unamended control |
| <i>DPF</i> | 0 | 100% DPF | Unamended control |
| <i>Biochar</i> | 0 | 100% biochar | Unamended control |
| <i>DPF</i> | 1 | 1% DPF + 99% sharp sand | Low amendment |
| <i>DPF</i> | 3 | 3% DPF + 97% sharp sand | Low amendment |
| <i>DPF</i> | 6 | 6% DPF + 94% sharp sand | Moderate amendment |
| <i>DPF</i> | 12 | 12% DPF + 88% sharp sand | Moderate amendment |
| <i>DPF</i> | 15 | 15% DPF + 85% sharp sand | High amendment |
| <i>DPF</i> | 18 | 18% DPF + 82% sharp sand | High amendment |
| <i>Biochar</i> | 1 | 1% biochar + 99% sharp sand | Low amendment |
| <i>Biochar</i> | 3 | 3% biochar + 97% sharp sand | Low amendment |
| <i>Biochar</i> | 6 | 6% biochar + 94% sharp sand | Moderate amendment |
| <i>Biochar</i> | 12 | 12% DPF + 88% sharp sand | Moderate amendment |
| <i>Biochar</i> | 15 | 15% DPF + 85% sharp sand | High amendment |
| <i>Biochar</i> | 18 | 18% DPF and 82% sharp sand | High amendment |

The mesocosms were 33 PVC tubes that were chopped into sections of 9-10 cm long and 4 cm in diameter. The plastic bungs were placed at the bottom of each tube to hold in the materials

and the treatments (Figure 3.1). The mesocosms material or treatment was triplicated in each cycle.

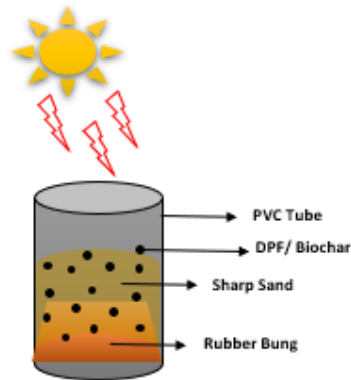


Figure 3.1. Mesocosms PVC tube experimental design for biochar application.



Figure 3.2. (a) shows the 3 materials used, which are: Sand, DPF and biochar. (b) shows the treatments of biochar and DPF. (c) The samples were placed on a tray, then in the oven for 3 weeks at 40° C.

3.3.4.1 Measuring Temperature & Humidity

Within the oven during the experiment, the air temperature and humidity were monitored. The device used for monitoring the temperature and the humidity was a Tinytag Explorer. The tiny tag was kept in the oven during all three cycles to assist in setting the desired temperature at 40° C and to record the humidity.

3.3.5 *Statistical Analysis*

In this study, the mesocosms experiment was conducted as a four-factor experiment: (i) soil amendment; (ii) wetting cycle; (iii) treatment; and (iv) time in the experiment. The temperature and humidity, as measured by Tinytag, were included as covariates. Day, Material, Treatment and Cycle were included as independent variables in the analysis of variance to assess their individual and interactive effects on soil moisture content. The results of the experiments were analysed by analysis of variance (ANOVA). The results were judged as statistically significant if they were different from zero with a probability (p) ≤ 0.95 . Before any ANOVA was performed, the data were Box-Cox transformed to remove outliers and tested for normality using the Anderson-Darling test (Anderson and Darling, 1952) – it did not prove necessary to transform the data for any of the metrics in this chapter. The homogeneity of the variance was tested using the Levene test, and if the test failed the data were log-transformed and re-tested – this did not prove necessary for any of the data in this chapter. The magnitude of the effects of each significant factor and interaction was calculated using the generalised ω^2 (Olejnik and Algina, 2003) and values were presented as least-square means (otherwise known as marginal means). Post hoc assessment of factors and interactions was carried out using the Tukey test.

3.4 Results

3.4.1 *Weight loss*

The conversion of Date Palm Frond (DPF) to biochar at a temperature of 250°C resulted in a weight loss of 5.7% relative to its initial dry weight.

3.4.2 *Moisture content*

This study measured moisture contents within the setting of a mesocosm experiment under controlled conditions (laboratory-based).

- Wet cycle

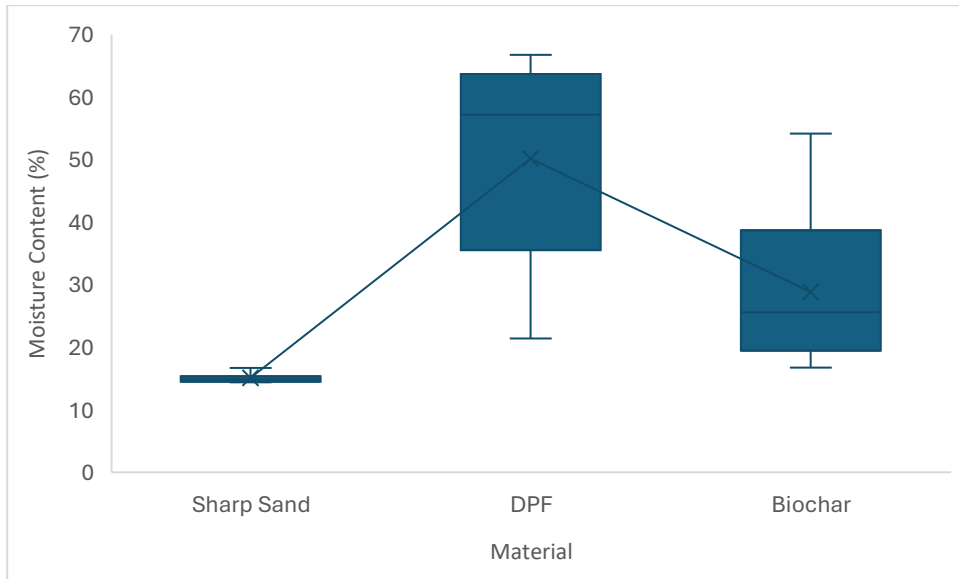


Figure 3.3. The boxplot of the moisture content (% by weight) of the materials measured during the wet cycle. Box-and-whisker plots show the interquartile range, with the box representing the first quartile (Q1) to the third quartile (Q3), and the whiskers extending from the minimum to the maximum values. The median is represented by a line within the box, and the cross symbol (x) indicates the mean moisture content.

During the wet cycle, the moisture content differs between the materials (Figure 3.3). The highest median represented by DPF recorded (57.17%) moisture content compared to the lowest moisture content was sharp sand (14.84%) (Figure 3.3). DPF also showed the highest mean moisture retention, recorded (50.14%), followed by biochar (28.83%) and sharp sand (15.08%). Statistical analysis confirmed that treatment level had a significant effect on moisture content ($p < 0.05$) (Figure 3.3).

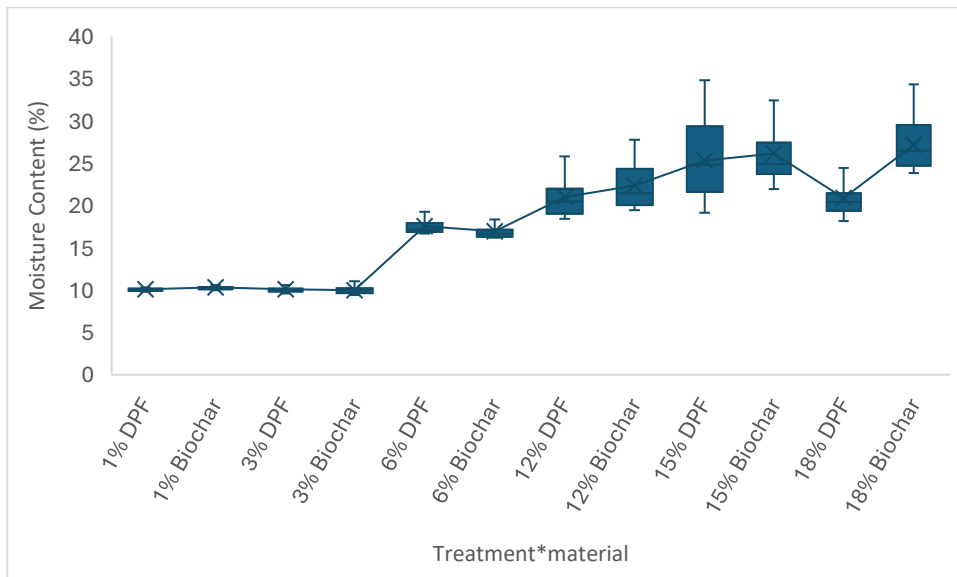


Figure 3.4. The boxplot of the moisture content (% by weight) of the treatment*material interaction for the wet cycle. Box-and-whisker plots show the interquartile range, with the box representing the first quartile (Q1) to the third quartile (Q3), and the whiskers extending from the minimum to the maximum values. The median is represented by a line within the box, and the cross symbol (x) indicates the mean moisture content.

During the wet cycle, the highest moisture content exhibited was the 18% biochar recorded (27.17%), and the lowest moisture content was the 1% DPF recorded (9.98%) (Figure 3.4). The highest mean moisture content was recorded for the 18% biochar treatment (27.17%) compared to the lowest treatments, such as 3% biochar (9.98%). Statistical analysis confirmed that treatment level had a significant effect on moisture content ($p < 0.05$) (Figure 3.4).

Figures 3.3 and 3.4 show that amended soils, particularly the DPF and biochar at higher amended levels, retained more moisture than the unamended control during the wet cycle. This supports the study hypothesis that amendment improved soil moisture retention. The differences observed between treatments and materials were statistically ($p < 0.05$), indicating that amendment type and level influenced moisture retention under wet conditions.

- Dry cycle

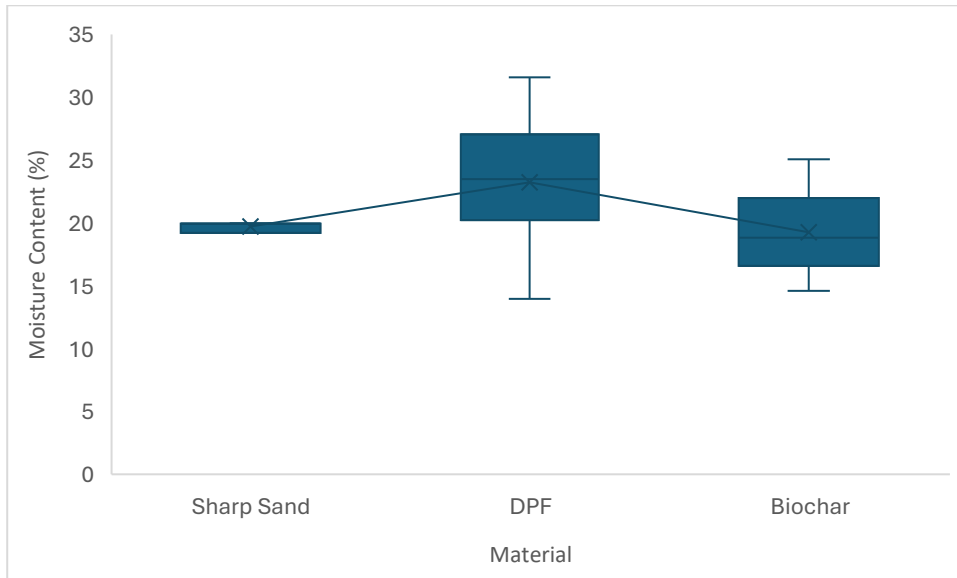


Figure 3.5. The boxplot of the moisture content (% by weight) of the materials measured during the dry cycle. Box-and-whisker plots show the interquartile range, with the box representing the first quartile (Q1) to the third quartile (Q3), and the whiskers extending from the minimum to the maximum values. The median is represented by a line within the box, and the cross symbol (x) indicates the mean moisture content.

During the dry cycle, DPF exhibited the highest moisture retention with a median moisture content of (23.24%), followed by sharp sand (19.95%) and biochar (18.81%). (Figure 3.5). DPF also showed the highest mean moisture retention, recorded (23.24%), compared to the lowest mean moisture retention, which was biochar (19.25%). Statistical analysis confirmed that treatment level had a significant effect on moisture content ($p < 0.05$) (Figure 3.5).

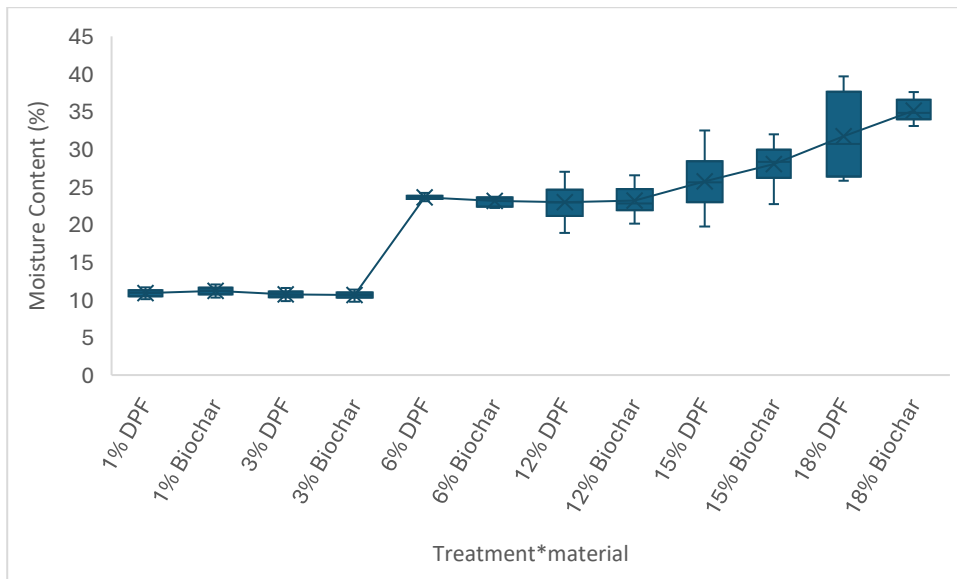


Figure 3.6. The boxplot of the moisture content (% by weight) of the treatment*material interaction measured during the dry cycle. Box-and-whisker plots show the interquartile range, with the box representing the first quartile (Q1) to the third quartile (Q3), and the whiskers extending from the minimum to the maximum values. The median is represented by a line within the box, and the cross symbol (x) indicates the mean moisture content.

During the dry cycle, moisture content differed across treatment levels (Figure 3.6). The highest mean moisture content exhibited was the 18% biochar recorded (34.82%), and the lowest mean exhibited was the 3% biochar (10.61%) (Figure 3.6). The 18% biochar exhibited the highest mean moisture content (35.12%), while the lower treatments, such as 3% biochar, showed lower moisture retention (10.61%). Statistical analysis confirmed that treatment level had a significant effect on moisture content ($p < 0.05$).

Figures 3.5 and 3.6 support the study hypothesis, demonstrating that soil amended with DPF and biochar at higher treatment levels, such as 15% and 18%, retained more moisture than the unamended control during the dry cycle. These differences were statistically significant ($p < 0.05$), confirming that the amendment improved soil moisture retention under dry conditions.

- Dry cycle (waw)

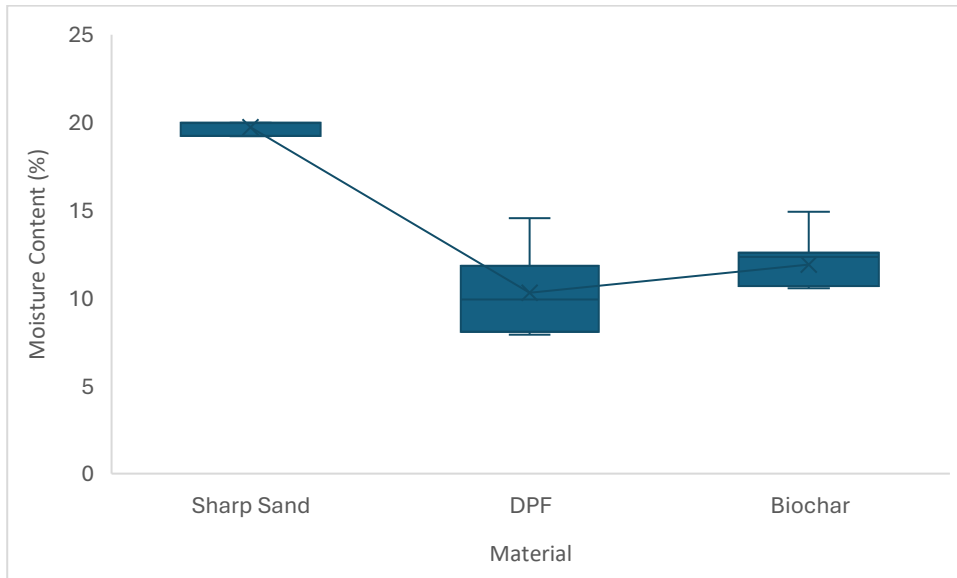


Figure 3.7. The boxplot of the moisture content (% by weight) of the materials measured during the dry cycle (waw). Box-and-whisker plots show the interquartile range, with the box representing the first quartile (Q1) to the third quartile (Q3), and the whiskers extending from the minimum to the maximum values. The median is represented by a line within the box, and the cross symbol (x) indicates the mean moisture content.

During the dry cycle waw, the moisture content varied between materials (Figure 3.7). Sharp sand showed the highest median moisture content recorded (19.97%), compared to the lowest median moisture content, which was the DPF (9.91%). As for the mean moisture content, sharp sand exhibited the highest mean recorded (19.72%) compared to the lowest mean, which was the DPF (10.28) (Figure 3.7). These differences were statistically significant ($p < 0.05$), confirming that amendment improved soil moisture retention under dry cycle waw conditions.

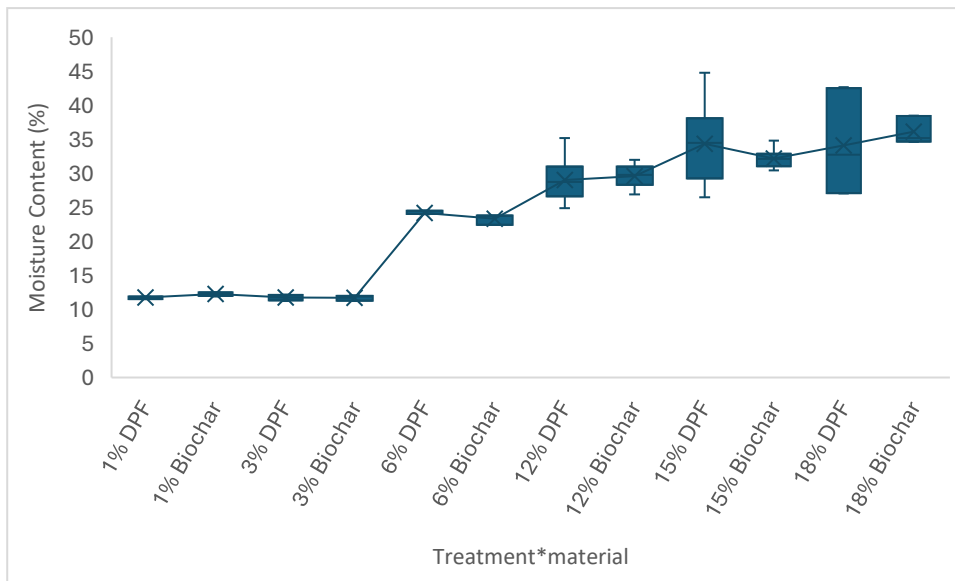


Figure 3.8. The boxplot of the moisture content (% by weight) of the treatment*material interaction measured during the dry cycle (waw). Box-and-whisker plots show the interquartile range, with the box representing the first quartile (Q1) to the third quartile (Q3), and the whiskers extending from the minimum to the maximum values. The median is represented by a line within the box, and the cross symbol (x) indicates the mean moisture content.

During the dry cycle (waw), varied across all moisture levels (Figure 3.8). The highest moisture median exhibited was the 18% biochar recorded (35.3%) compared to the lowest median, which was the 1% DPF (11.74%) (Figure 3.8). The 18% was highest mean moisture content (36.10%), while lower amendment levels such as 3% biochar showed lower moisture retention (11.73%). Statistical analysis confirmed that treatment level had a significant effect on soil moisture content ($p < 0.05$).

Figures 3.7 and 3.8 support the study hypothesis by showing that amendment with DPF and biochar influenced soil moisture retention during the dry cycle waw. Although the unamended soil exhibited higher overall moisture content under these conditions, higher amendment levels still demonstrated improved moisture retention compared to lower amendment levels. Statistical analysis confirmed that these differences were significant ($p < 0.05$).

The above data shows noticeable differences in moisture contents between the materials and treatment levels across the three moisture cycles. During the wet and dry cycles, soils amended with DPF and biochar retained more moisture than the unamended control, particularly at higher amendment levels, supporting the study hypothesis that amendment improves soil moisture retention. In contrast, during the dry cycle waw, the unamended sharp sand exhibited higher overall moisture content, indicating that amendment effects were influenced by environmental conditions. Higher amendment levels, particularly 12%, 15%, and 18%, showed greater moisture retention compared to lower amendment levels. Overall, these findings support the hypothesis that DPF and biochar amendments enhance soil moisture retention, especially under dry conditions, Statistical analysis confirmed that material type and treatment level had a significant effect on soil moisture content ($p < 0.05$).

3.4.3 ANOVA results

- Moisture

The Anderson-Darling test and the QQ' plot (Figure 3.9) showed that the data were not normally distributed, and so the data were log transformed. The QQ' plot indicates that some samples could be considered as outliers, and 0.08% of the samples were removed.

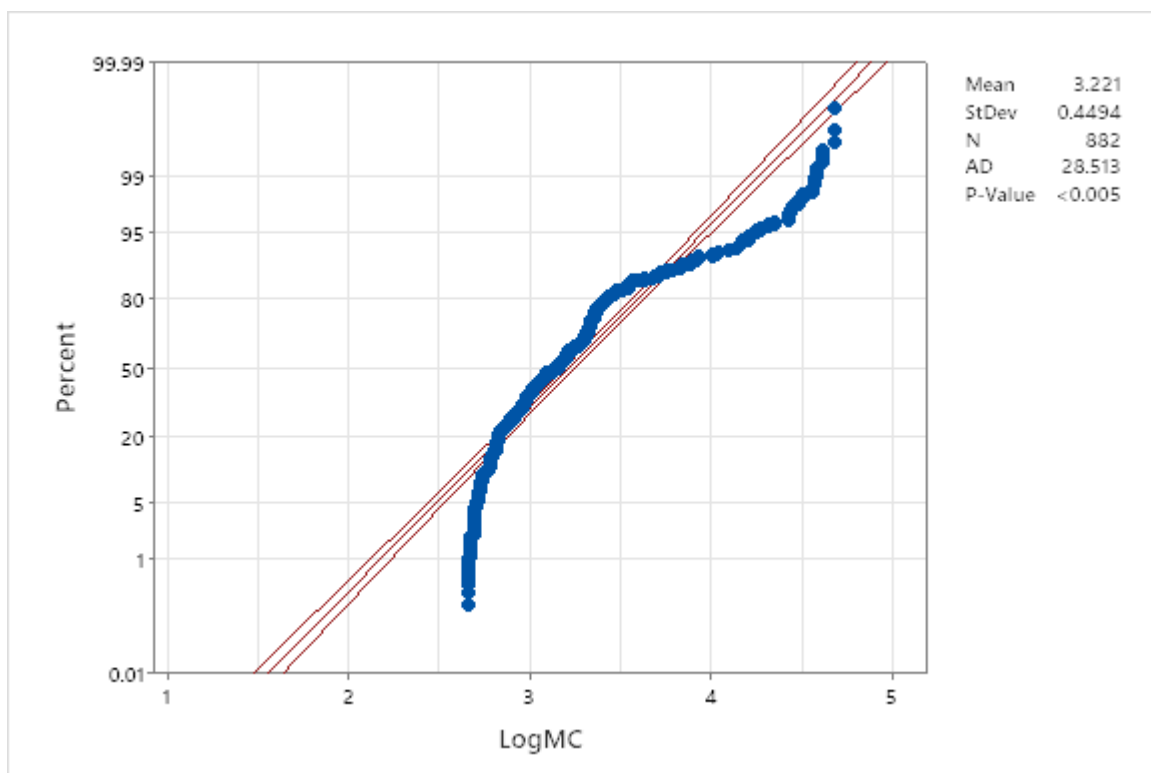


Figure 3.9. QQ' plot of the observed value of the moisture content. Log MC =log(Moisture Content).

The ANOVA, including all factors and two-way interactions, had an R^2 of 85.26%.

Table 3.2. The percentage of variance explained for factors and interactions of the Day, Treatment and Cycle factors for the moisture content.

| <i>Source</i> | <i>DF</i> | <i>P-Value</i> | <i>% of variance explained</i> |
|-----------------------|-----------|----------------|--------------------------------|
| <i>Day</i> | 6 | 0 | 6.08 |
| <i>Treatment</i> | 5 | 0 | 84.57 |
| <i>Cycle</i> | 2 | 0.045 | 0.10 |
| <i>Day*Treatment</i> | 30 | 0 | 6.39 |
| <i>Day*Cycle</i> | 12 | 1 | 0 |
| <i>Material*Cycle</i> | 4 | 0 | 1.79 |
| <i>Error</i> | 822 | 0 | 1.30 |

As measured by proportion of the original variance explained, the most important factor was Treatment, which explained 84.57% of the variance explained by the model (Table 3.2). As there were three levels of the Cycle factor, post hoc analysis was necessary for that factor.

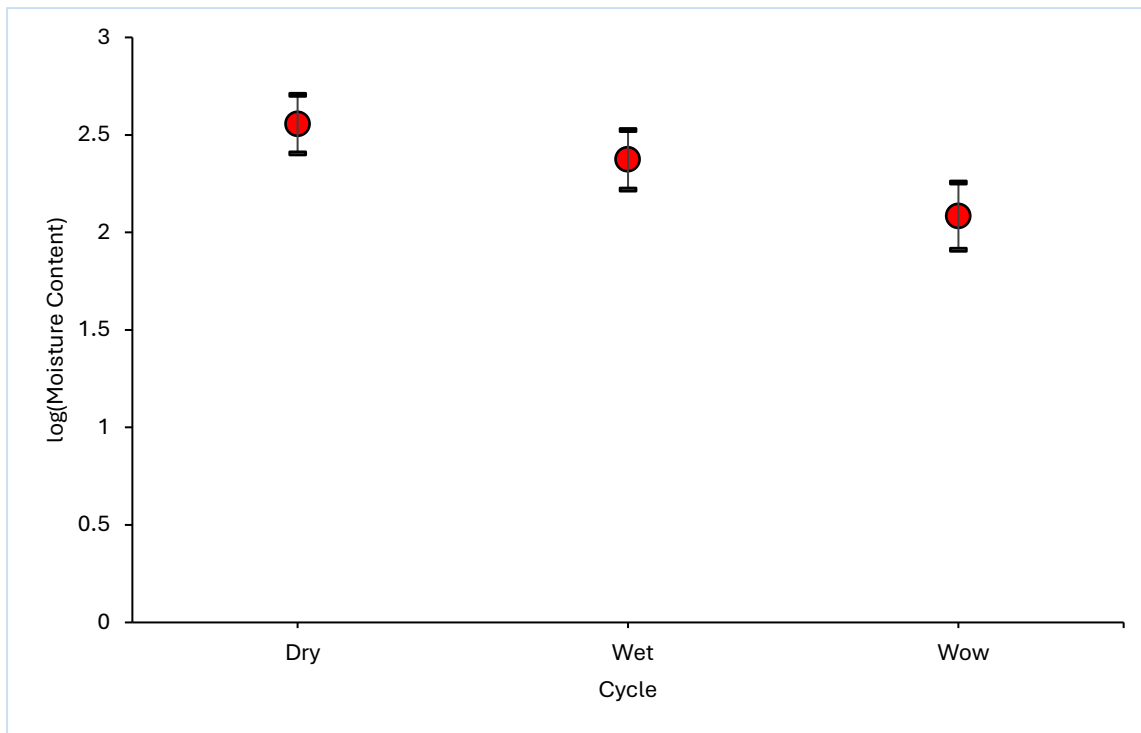


Figure 3.10. Main effects plot of the Cycle factor with respect to moisture content. Error bars are the 95% confidence interval.

The main effects plot of the Cycle factor (Figure 3.10) shows that the moisture content of the dry cycle was recorded as the highest mean moisture content, more than the wet cycle by 1.58 (w/w, %) and from the wow cycle by 3.16 (w/w, %).

Table 3.3. Results of Tukey's post hoc test for the different cycles.

| Cycle | N | Mean | Grouping |
|-------|-----|------|----------|
| wet | 441 | 3.14 | A |
| waw | 294 | 3.13 | A B |
| dry | 147 | 3.09 | B |

The moisture content was compared between the different wet cycles using *post hoc* analysis (Table 3.3). The post hoc analysis showed there were 2 groupings (indicated by the letters in Table 3.3). The waw cycle was not significantly different from either the wet or dry cycles, but the wet cycle was significantly different from the dry cycle (Table 3.3).

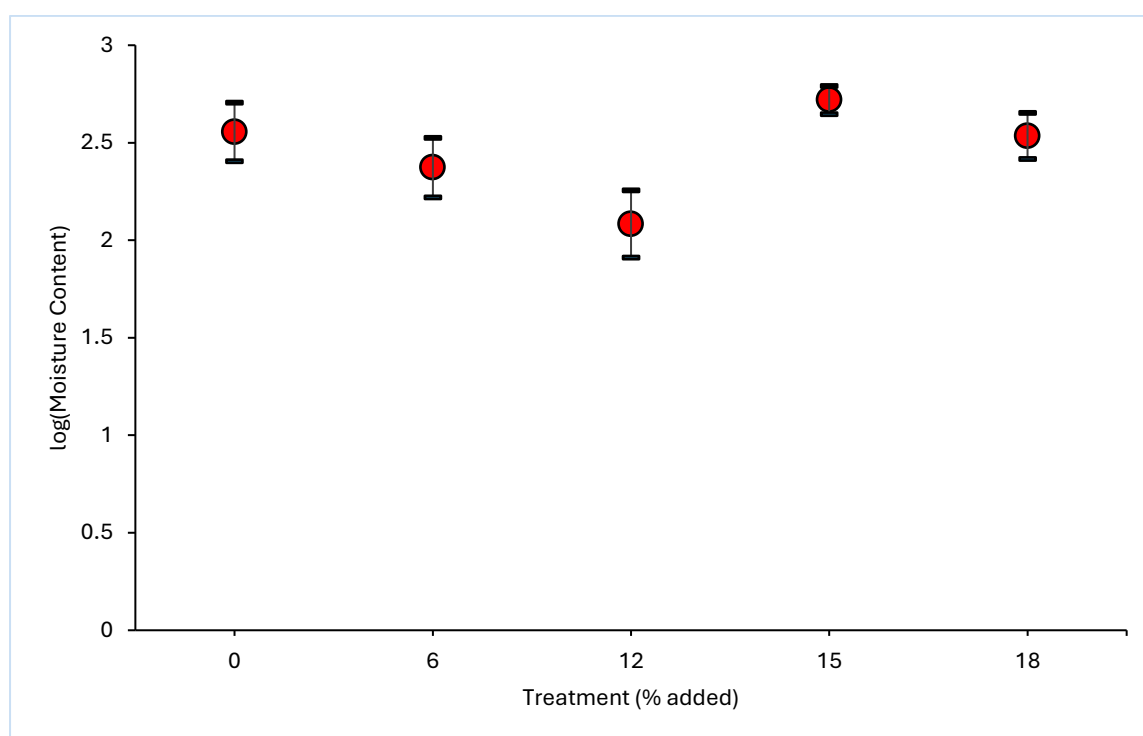


Figure 3.11. Main effects plot of the Treatment factor on moisture content. Error bars are the 95% confidence interval and may be smaller than the plotted point.

The highest mean recorded for the Treatment factor was for the 15% treatment (Figure 3.11). The lowest mean moisture content was for the 12% treatment (Figure 3.11). The Treatment factor referred to the amendment percentage applied to the soil (0%, 1%, 3%, 6%, 12%, 15% and 18%) irrespective of amendment material type. For this analysis, moisture content data values represent marginal means (least-square means) of moisture content for each amendment level, averaged across the other factors in the model.

Table 3.4. Results of post hoc test of treatment levels for moisture content.

| <i>Treatment</i> | <i>N</i> | <i>Mean</i> | <i>Grouping</i> | |
|------------------|----------|-------------|-----------------|---|
| 100 | 252 | 3.74 | A | |
| 15 | 126 | 3.23 | B | |
| 18 | 126 | 3.14 | | C |
| 12 | 126 | 3.07 | | C |
| 6 | 126 | 2.82 | | D |
| 0 | 126 | 2.74 | | E |

The post hoc analysis showed that there were 5 groups – denoted by letters in Table 3.3. Each level of the Treatment factor was different from each other except for the 18% and 12% treatments (group C - Table 3.4). The largest mean was for the 100% treatment, and the lowest was for the 0% treatment (Table 3.4).

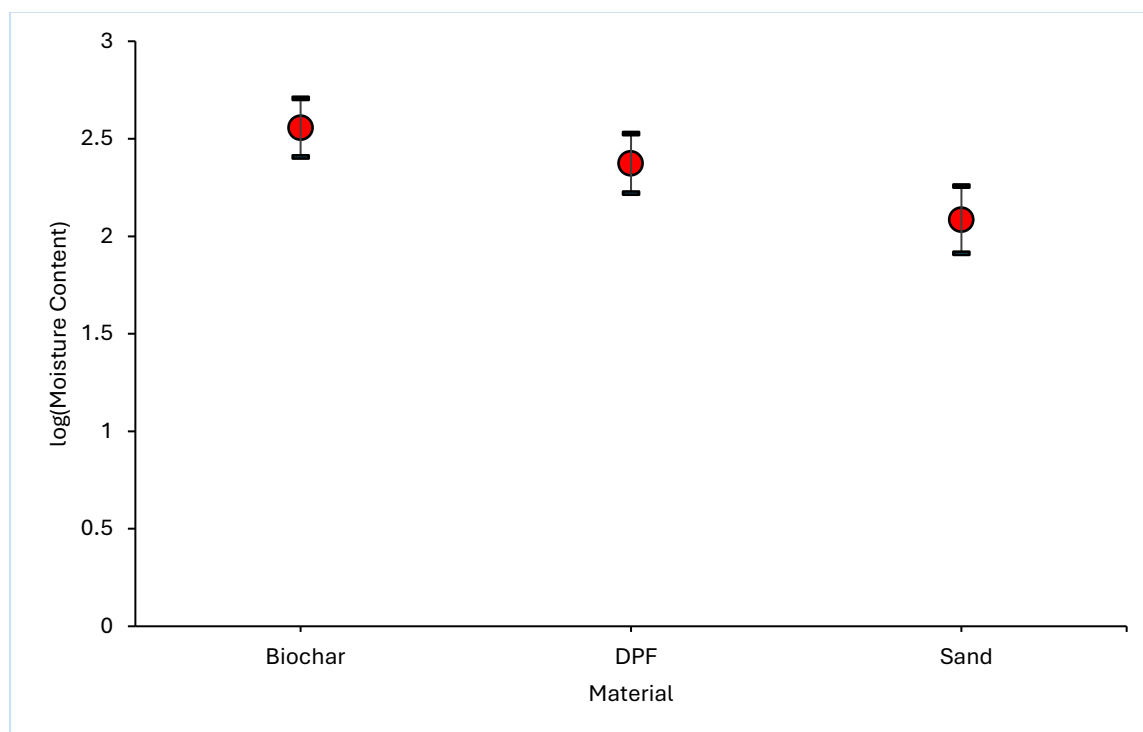


Figure 3.12. Main effects plot of the Material factor with respect to moisture content. Error bars are the 95% confidence interval.

Comparing between the levels of the Material factor, the highest mean moisture content was for biochar, and the lowest mean moisture content was for sand by 2.5 (w/w, %) difference (Figure 3.12).

Table 3.5. Results of post hoc analysis for between the levels of the Materials factor.

| Material | N | Mean | Grouping |
|----------|-----|------|----------|
| Biochar | 378 | 3.37 | A |
| DPF | 378 | 3.24 | B |
| Sand | 126 | 2.73 | C |

The post hoc analysis showed that each material was different from each other (Table 3.5).

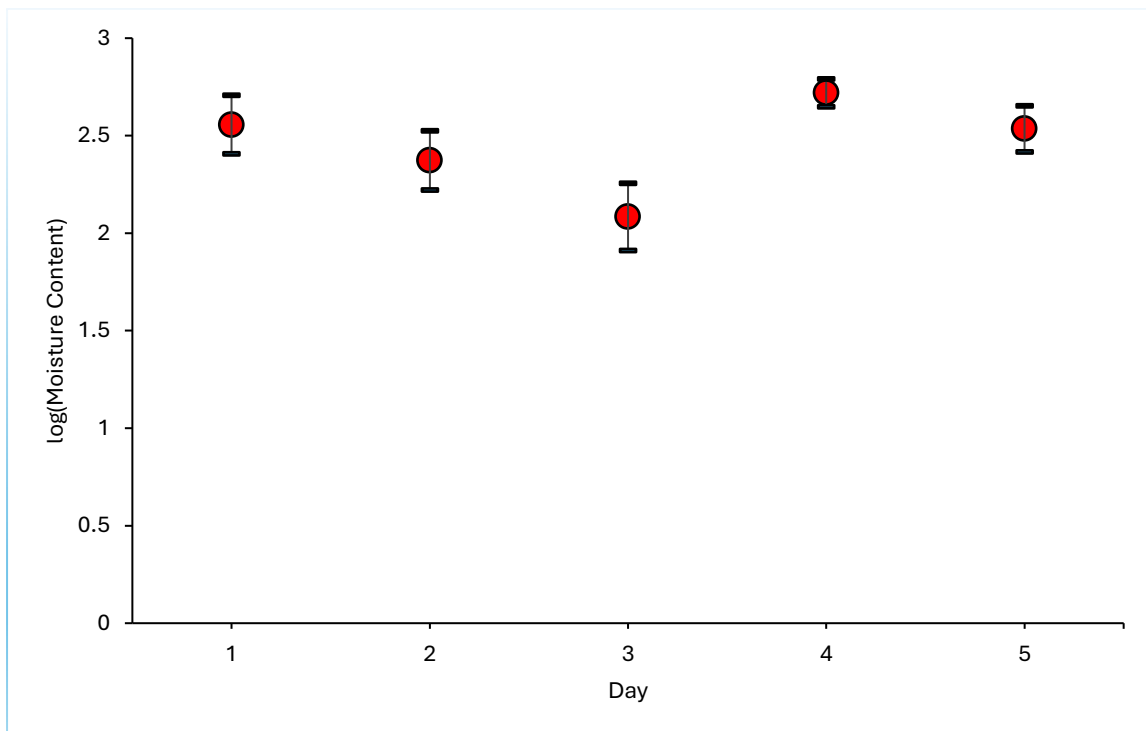


Figure 3.13. Main effects plot of the Day factor with respect to moisture content moisture content. Error bars are the 95% confidence interval.

The highest mean moisture content for the Day factor was on Day 4, and the lowest mean moisture content was recorded on Day 3, where Day represents the sampling time point across the wet and dry cycles (Figure 3.13).

Table 3.6. Results of post hoc analysis on the moisture content between the levels of the Day factor.

| <i>Day</i> | <i>N</i> | <i>Mean</i> | <i>Grouping</i> | | | |
|------------|------------|-------------|-----------------|----------|----------|----------|
| <i>1</i> | <i>126</i> | <i>3.36</i> | <i>A</i> | | | |
| <i>2</i> | <i>126</i> | <i>3.19</i> | | <i>B</i> | | |
| <i>3</i> | <i>126</i> | <i>3.14</i> | | <i>B</i> | <i>C</i> | |
| <i>4</i> | <i>126</i> | <i>3.07</i> | | | <i>C</i> | <i>D</i> |
| <i>5</i> | <i>126</i> | <i>3.05</i> | | | | <i>D</i> |
| <i>6</i> | <i>126</i> | <i>3.03</i> | | | | <i>D</i> |
| <i>7</i> | <i>126</i> | <i>3.01</i> | | | | <i>D</i> |

The post hoc analysis between the levels of the Day factor showed that there were 4 groups: A, B, C and D – Table 3.6. Days 1 and 2 were categorised into different groups, but Day 1 showed a higher mean moisture content compared to Day 2 (Table 3.6). However, Days 2 and 3 did not show significant differences in moisture content. From day 3 onwards, the moisture content decreased.

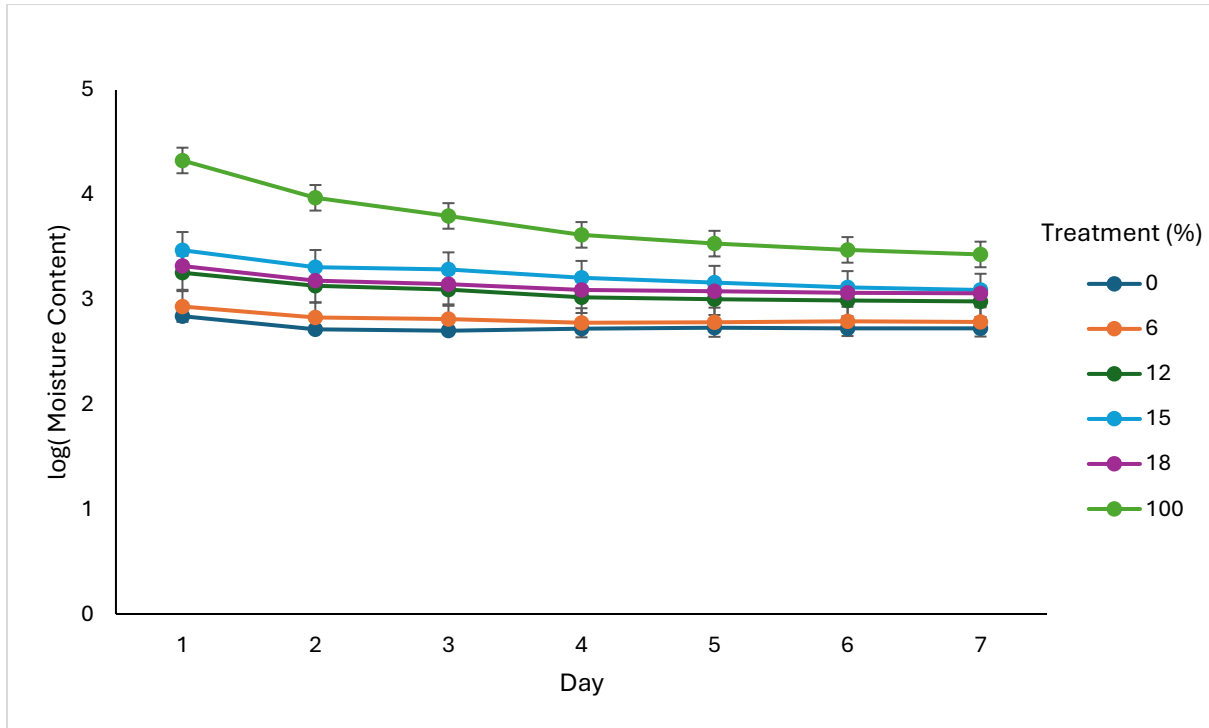


Figure 3.14. The interaction plot of moisture content between Day and Treatment factors.

Two interactions were found to be significant (Day*Treatment and Material*Cycle– (Table 3.2 & Figure 3.14). The plot suggests that the moisture content did not behave consistently between treatments across the whole week. The control (100%) showed the greatest moisture content from Day 1- to Day 7 (Figure 3.14). The second greatest moisture content shown was the 15% treatment, compared to the lowest moisture content, which was for the sand, which was 0% (Figure 3.14).

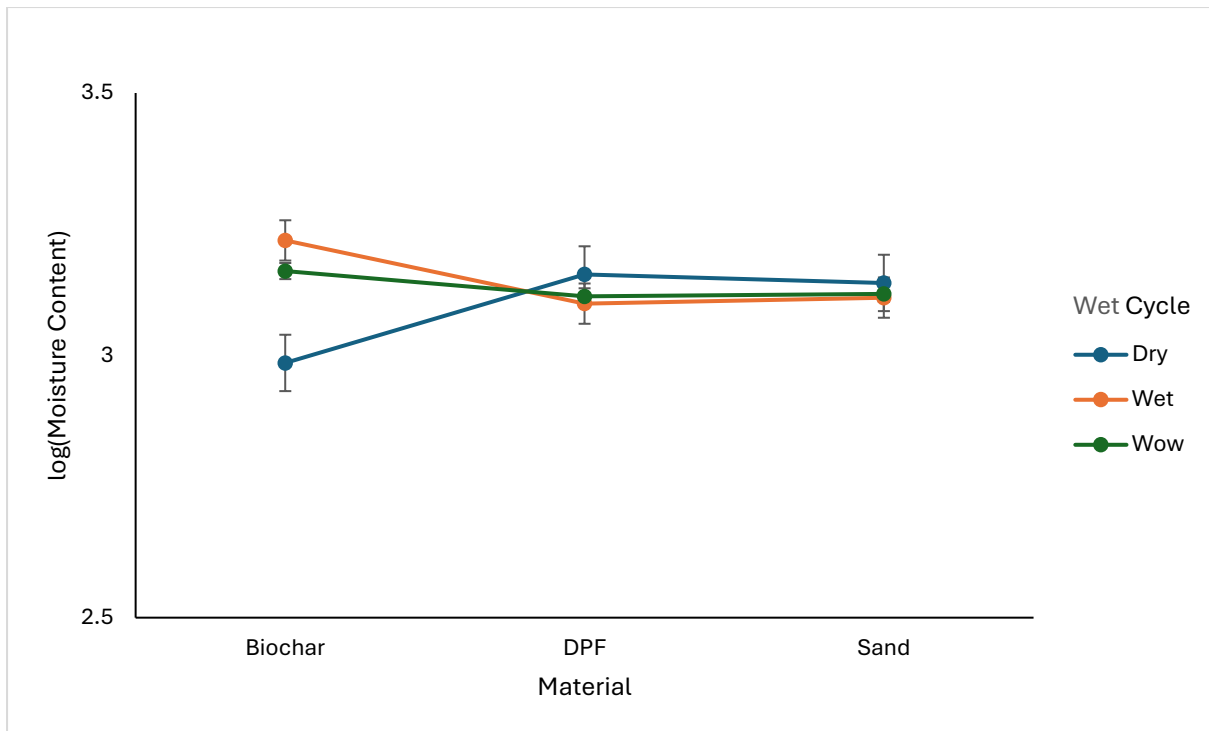


Figure 3.15. The interaction plot of moisture content between the Material and Cycle factors.

The other significant interaction was between the Material and Cycle factors (Figure 3.15). The plot suggests that the effect of the moisture content between different materials is not consistent across the three cycles (Wet, Dry and Waw). During the wet cycle biochar had a greater moisture content than DPF and sand, while for the dry cycle and dry cycle waw the DPF had a higher moisture content (Figure 3.15).

3.5 Discussion

The chapter represents the findings from a mesocosm investigation that examined the moisture content dynamics of biochar and precursor materials. This study hypothesised that soils amended with DPF and biochar would exhibit greater water retention capabilities relative to unamended soils, even under diverse wet temperature cycles (wet, dry and dry waw).

There have been various studies that have explored the behaviour of biochar in mesocosm experiments, these include: CO₂ flux measurements (Horák *et al.*, 2022); moisture content analysis; microbial activity with plant growth (Zhang *et al.*, 2021); and assessment of plant health to nutrient measurements (Stewart *et al.*, 2013). A study has shown that using mesocosm experiments has shown that water retention offers numerous benefits (Doan *et al.*, 2015). This study focused on investigating the moisture content and its impact on sandy soil under harsh climate conditions. The observations of this study indicate that different percentages of DPF and biochar treatment can enhance water retention under controlled temperatures ranging from 30°C to 40°C. The duration of this experiment represents a key limitation, as it captures only short-term effects of newly applied biochar and unprocessed DPF. Under field conditions, organic amendments are subject to ageing processes including microbial decomposition, surface oxidation and aggregation. These processes can alter porosity, surface area and water retention capacity over time. Microbial activity stimulated by organic inputs such as DPF may also enhance soil structure through biofilm and extracellular polymer production, potentially increasing water retention in the longer term. As a result, the findings presented initial responses rather than long-term soil behaviour. In addition to ageing processes, the persistence of biochar in soil under field conditions can be influenced by physical and biological loss mechanisms that are not fully captured in controlled mesocosm experiments. Processes such as leaching, erosion and microbial mineralisation can lead to redistribution or loss of processes that occur over longer time scales and under more complex environmental conditions than

those simulated in this laboratory study. The results presented here should be interpreted as representing initial soil responses rather than long-term field behaviour.

The results from data analysis demonstrated substantial differences in moisture content between the various treatment groups. Specifically, the soils amended with DPF and biochar were not significantly different during the wet cycles, except for higher treatment percentages (15% and 18%). However, there was a greater difference between the unamended material of DPF and biochar, with DPF showing greater water retention during both the wet and dry cycles than the biochar unamended soils, while biochar showed greater water retention during the waw cycle. This observation aligns with the findings of Saarnio *et al.* (2013) who monitored their samples during different cycles, wet and dry cycles and showed increased water retention on biochar during a dry cycle. However, their experiment used a hardwood feedstock and was performed at a larger scale than this experiment. Reynaert *et al.* (2024) focused on grassland soils and compared between sandy soil and loam soil water retention and noticed there was an increased weather persistence in terms of water holding capacity Chafik *et al.*, (2024) investigated five different feedstocks (palm fronds, citrus wood, eucalyptus chips, eucalyptus wood and argan nuts) and found that the highest water holding capacity was for biochar from a palm frond feedstock.

When interpreting these findings, it is important to recognise that differences in reported moisture retention arise partly from the analytical approach used. Material-specific comparison indicates that DPF generally exhibits higher moisture retention than biochar under wet and dry cycles. However, analyses based upon the ANOVA of the whole database across amended and unamended soils emphasise treatment level effects, where biochar can exhibit higher overall mean moisture content, particularly at higher amendment percentages and during specific

moisture cycles. These differences, therefore, reflect variation in data aggregation and statistical grouping rather than inconsistency in the experimental results.

There were several limitations to this study that should be taken into consideration. The mesocosm experiment yielded promising results, but concerns over its ecological validity may arise, potentially limiting its applicability in real-world situations. However, the experiment's controlled conditions enabled precise manipulation and measurement of variables, ensuring accurate capture of the fundamental mechanisms affecting soil moisture. Although the study's duration was short, which is crucial for soil moisture testing that may require longer time periods, the initial insights gained offer a valuable foundation for longer-term studies that can build upon these findings. Additionally, while the number of samples tested was limited, the statistical methods employed ensured robust and representative results that captured broader trends within the sample population. Despite not testing for soil microbial communities and nutrients, which significantly impact soil moisture dynamics, the focus on physical soil properties and moisture retention provides critical baseline data that future studies can expand upon by incorporating microbial and nutrient analyses. From the ecological perspective, the controlled nature of the mesocosm experiment inevitably limits its representation of field conditions. Natural soils experience spatial heterogeneity, variable rainfall, temperature fluctuations and repeated wetting-drying cycles that influence soil structure and moisture dynamics over time. In addition, the absence of vegetation and an active rhizosphere restricts root soil microbe interactions that can enhance aggregation and water retention through biological processes such as biofilm and mycelia formation. The use of UAE sand as a simplified soil proxy further limits ecological realism, as agricultural soils supporting date palms typically contain organic matter and exhibit higher biological activity. Consequently, while the mesocosm design was well-suited to isolating short-term physical responses, extrapolation of these findings to long-term field conditions should be undertaken with caution.

Thus, it is essential for future studies to address these limitations to improve our comprehension of the soil moisture dynamics of soils that have been amended with biochar and DPF. The following chapter will concentrate on the utilisation of biochar and DPF in sandy soils, particularly in determining the water-holding capacity of these amendments.

The UAE sand used in this study represents a simplified mineral analogue of soils found in arid regions rather than a fully developed agricultural soil. Soils in which date palms are grown typically contain a sandy mineral fraction but also include organic matter and biological components that influence water retention and soil processes. Differences in surface area between UAE sand and sharp sand may therefore influence soil behaviour as surface area is a key determinant of surface reaction, such as water adsorption and nutrient retention. These differences highlight the importance of organic amendments such as DPF and biochar in enhancing surface area and improving the functional properties of sandy soils.

This research has important implications for both theoretical understanding and practical applications in the fields of soil science and agricultural management. The study provides novel information about the effects of biochar and DPF amendments on soil moisture under different temperature conditions in wet cycles, which adds to our knowledge of how soil and water interact with varying percentages of these treatments. These findings hold considerable importance for sustainable land management practices, particularly in regions dealing with water scarcity or soil degradation. Based on the results of this study, several recommendations can guide future research. Hence, there is a need to investigate the long-term effects of biochar and DPF amendments on soil moisture. Broadening the scope to include a wider range of treatment levels and considering additional environmental factors, such as soil microbial activity, is crucial for a more comprehensive understanding of soil moisture regulation mechanisms. Moreover, monitoring the irrigation system and temperature exposure could aid

in identifying sustainable land use practices and enhancing resilience to environmental stressors. Moving forward, Chapter 4 will focus on crop response to biochar application, delving deeper into the practical implications of these findings for agricultural productivity.

3.6 Conclusion

In conclusion, the results of a mesocosm study conducted to explore the dynamics of moisture content in sandy soil amendment with biochar and Date Palm Fronds (DPF) under different controlled conditions (wet, dry and dry (waw) cycles).

The results aimed to test the hypothesis that soils amended with DPF and biochar can exhibit improved water retention capabilities compared to unamended soils under various wet temperature cycles. The results showed that different percentages of DPF and biochar treatments improved water retention at controlled temperatures.

The findings revealed significant differences in moisture content among the different treatment groups, with DPF showing higher water retention during wet and dry cycles, while biochar had higher retention during the waw cycle. Although the study had limitations due to its short-term duration and controlled laboratory setting, these conditions enabled precise measurement of soil moisture responses.

Future studies should address term field studies that incorporate microbial processes, ageing effects and nutrient dynamics to better represent real-world conditions. Overall, this study contributes valuable insights into the potential of biochar and DPF as soil amendments for improving water retention in arid and semi-arid environments. This research should further

explore the implications of biochar and DPF applications for sustainable agricultural management, as discussed in Chapter 4.

Chapter 4: Crop response to biochar application

4.1 Introduction

The results in Chapter 3 showed differences between biochar and DPF in water retention during the mesocosm experiment. Biochar exhibited greater moisture content during the wet cycle, while the DPF retained moisture during the dry cycles. The objective of this chapter was to evaluate plant growth responses to soil amendments (biochar and DPF) in sandy soil under controlled and uncontrolled environmental conditions, with particular focus on moisture availability and elevated temperature. The first experiment took place in the laboratory (henceforward referred to as control conditions) and the second experiment took place in the field in the United Arab Emirates (henceforward referred to as uncontrolled conditions). Both experiments monitored plant growth throughout the experiment by measuring plant height alongside soil moisture content. In Chapter 1, the literature review covers pot trial experiments conducted on sandy soil and their effects on climate change.

4.2 Approach

In this chapter, the quantitative research approach was conducted using two pot trial experiments. The aim of these experiments was to examine the plant growth in the context of climate, differing water content, and the addition of biochar. The main research questions for this chapter were:

- Would biochar application to a sandy soil influence plant growth?
- Would biochar control the water content of the soil and make a difference to plant growth even under elevated temperatures?

4.3 Materials and methods

4.3.1 *Sample collection*

The DPF and UAE sandy soil were collected from the UAE and shipped to the UK. Details of DPF and soils are given in Chapters 2 and 3.

4.3.2 Laboratory pot trial experiment (controlled conditions)

The controlled pot trial experiment took place in the laboratory of the Department of Earth Sciences, University of Durham. The experiment was a four-factor experiment to evaluate the effects of soil amendments and environmental conditions on plant growth. The first factor was soil amendment (henceforward referred to as Material), which consisted of two amendment types: biochar and date palm fronds (DPF). These materials were selected due to their contrasting physical and chemical properties and their potential influence on soil moisture retention and plant growth. The second factor was the proportion amendment used (henceforward referred to as Treatment). Five treatment levels were used: 100% (unamended controls, which is the absence of sand), 100%, 1%, 6%, 15% and 18% amended by weight. These levels were selected to evaluate both low and high amendment rates and to identify any optimal application level improving plant growth.

The amendment levels used in this experiment were informed by the mesocosm experiment presented in Chapter 3, which evaluated amendment levels of 1%, 3%, 6%, 12%, 15% and 18%. Based on those results, the 3% and 12% treatments were excluded from further testing, and four amendment levels (1%, 6%, 15% and 18%) were selected for the pot trial experiments. This refinement allowed the experiment to focus on amendment levels that showed more consistent effects on soil moisture and plant growth.

The third factor was the wetting cycle (referred to as Cycle), which consisted of two levels: a wet cycle and a dry cycle. The wet cycle involved daily irrigation to simulate favourable moisture conditions, while the dry cycle involved withholding water to simulate drought stress conditions. This factor allowed the assessment of amendment performance under contrasting moisture regimes.

The fourth factor was time in the experiment (referred to as Day), which represented measurements taken throughout the duration of the experiment. This factor allowed assessment of plant growth dynamics and changes in soil conditions over time.

In addition to these four main factors, four covariates were monitored throughout the experiment: soil pH, soil moisture, soil temperature and light intensity. These covariates were included to account for environmental variability and to better understand the mechanisms influencing plant growth response.

The dimension of the pot used was length 7.6 cm, top width 7.8 cm and bottom width 5.1 cm. The plant species used in this experiment was cat grass (sp. *Avena sativa*): grown from seed. This species was selected for several reasons. First, cat grass is commonly cultivated in the United Arab Emirates, and it can grow in sandy and low-nutrient soils. In addition, its rapid germination and growth allow measurable plant responses within a short experimental period, making it suitable for pot trials. Although it's known to be a fast-growing species, it may be more sensitive to drought stress, which was considered when interpreting plant responses during the dry cycle. All treatments were triplicated in this experiment. Cat grass was used because of its fast growth rates in laboratory experiments (Figure 4.1a). The soil used in the pots was mixed with the materials of interest and with sand. The sand was used as a neutral amendment that would be hypothesised to have negligible water holding capacity and so was used to see the impact of a physical amendment on a soil. The amendment materials (biochar and DPF) were mixed with UAE sandy soil at four amendment levels (1%, 6%, 15% and 18%) by dry weight. In addition, three control treatments were included: unamended UAE sand (100%), 100% biochar and 100% biochar. The full set of treatment combinations is summarised in (Table 4.1) below:

Table 4.1. Treatment combinations used in the pot trial experiments (composition by dry weight).

| <i>Material type</i> | <i>Treatment level (%)</i> | <i>Composition (% by dry weight)</i> | <i>Description</i> |
|------------------------|----------------------------|--------------------------------------|--------------------|
| <i>UAE sand</i> | 0 | 100% UAE sand | Unamended control |
| <i>DPF</i> | 0 | 100% DPF | Unamended control |
| <i>Biochar</i> | 0 | 100% biochar | Unamended control |
| <i>DPF</i> | 1 | 1% DPF + 99% UAE sand | Amended treatment |
| <i>DPF</i> | 6 | 6% DPF + 94% UAE sand | Amended treatment |
| <i>DPF</i> | 15 | 15% DPF + 85% UAE sand | Amended treatment |
| <i>DPF</i> | 18 | 18% DPF + 82% UAE sand | Amended treatment |
| <i>Biochar Biochar</i> | 1 | 1% biochar + 99% UAE sand | Amended treatment |
| <i>Biochar</i> | 6 | 6% biochar + 94% UAE sand | Amended treatment |
| <i>Biochar</i> | 15 | 15% biochar + 85% UAE sand | Amended treatment |
| <i>Biochar</i> | 18 | 18% biochar + 82% UAE sand | Amended treatment |

In this study, “unamended control” refers to materials tested in their pure form without mixing with sandy soil, consistent with the experimental design used in Chapter 3.

The mixed amended and unamended pots were kept in a growth tent (dimension: 129.5 cm height, 75 cm width and length), and an LED light was set to increase air temperature to 26° C and maintain a fixed light condition. The period of the experiment was 5 weeks, and this period was divided into two cycles: the wet cycle was for 3 weeks, and the dry cycle was for 2 weeks. The wet cycle was longer due to the time allowed for germination - germination occurred after 5 days. During the wet cycle, 10 ml of tap water was added to each pot daily, then soil moisture was checked using a moisture probe. After the completion of the wet cycle, the dry cycle began by not adding water (Figure 4.1), but the probe analysis of the pots was continued until the end of each cycle. The moisture probe used in this experiment was the Beslands Soil Tester 4 in 1 for measuring moisture (made in China). The probe measures moisture (5 levels), pH (4.0- 9.0), temperature (8.89° C- 50° C), and light intensity (9 levels).

The soil moisture and light intensity were measured using Bleslands Soil Tester 4- in- 1 probe, which provides semi- quantitative measurements using categorical scales. The moisture probe reports relative moisture levels: dry + (1), dry (2), normal (3), wet (4) and wet + (5). The light intensity is reported on a six-level scale: low + (1), low (2), nor (3), nor + (4), high (5) and high + (6). These values represent relative measurements based on electrical resistance sensing and provide an indication of soil moisture availability and light exposure rather than direct gravimetric or volumetric measurements. Gravimetric moisture measurements were conducted in Chapter 3 to provide a precise quantitative assessment of soil water retention properties. In contrast, the use of a portable moisture probe in this experiment was intended to explore an alternative and practical method for monitoring soil moisture during plant growth. Portable probes are widely used in agricultural and horticultural settings because they are inexpensive, rapid, easy to use and allow frequent monitoring without specialised laboratory equipment. Although probe measurements provide relative rather than absolute moisture values, they allow assessment of moisture dynamics over time and offer practical relevance for real-world soil management. The use of this method also complements the gravimetric analysis presented in Chapter 3 by providing additional insight into soil moisture behaviour under plant growth conditions. The plant growth was measured vertically using a 30 cm ruler. The moisture probe used in this experiment was factory calibrated by the manufacturer and designed for general soil moisture assessment using electrical resistance sensing. No additional calibration was performed prior to the experiment, as the objective was to monitor relative differences in soil moisture among treatments rather than obtain absolute gravimetric moisture values. To ensure consistency, measurements were taken under the same conditions across all treatments and baseline measurements were established using pure sand, biochar and DPF samples for reference.

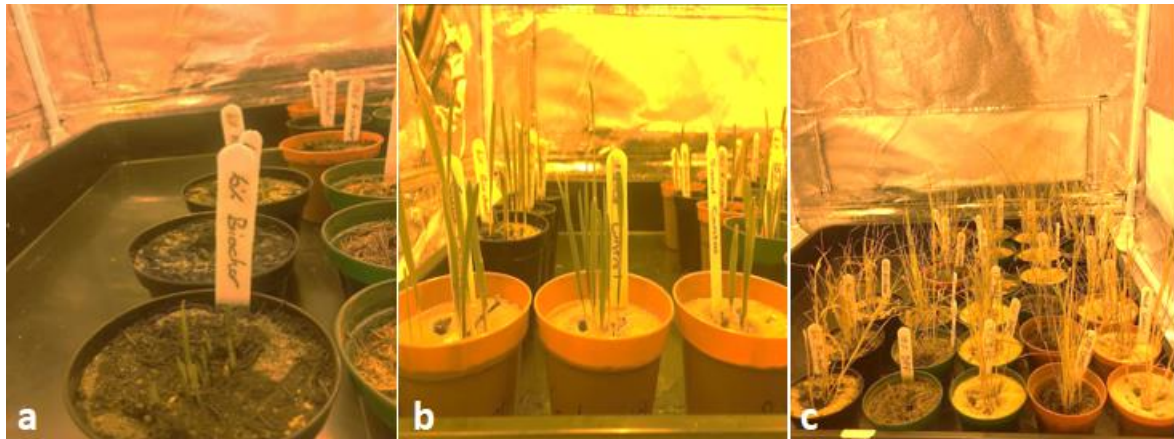


Figure 4.1. (a) first germination during the wet cycle, (b) plant growth results by the end of the wet cycle and (c) dry cycle results.

Canopy cover was assessed using the Canopeo application, a mobile-based image analysis tool developed by Oklahoma State University for measuring fractional green canopy cover. Canopeo uses digital photographs taken from directly above the vegetation and applies a colour thresholding algorithm to distinguish green vegetation from soil and other non-green background elements. The application calculates canopy cover as the percentage of green pixels in the image, providing an estimate of vegetation cover. This method provides a rapid, non-destructive and repeatable assessment of plant canopy development. The Canopeo application has been validated in previous studies and has been shown to provide reliable estimates of canopy cover comparable to traditional image analysis methods (Patrignani and Ochsner, 2015).

Therefore, in this study, canopy cover was measured during the controlled experiment on both wet cycles, but during the uncontrolled field experiment, canopy measurements could not be consistently obtained due to excessive light intensity, which affected image quality and vegetation.

4.3.3 Field pot trial experimental (uncontrolled conditions)

The field pot trial experiment took place in Abu Dhabi, UAE (24°15'11.5"N 54°43'13.1"E) (Figure 3). The pot preparation of the controls and materials was similar to the laboratory, controlled conditions experiment, but the difference was: the location in the field; a different plant had to be grown; the temperature conditions could not be controlled as the experiment was conducted outdoors; and the wet cycle was extended to two months until germination occurred. 10 ml of tap water was added daily during the wet cycle, and data were collected using the probe and plant height was measured. The dry cycle was analysed for 3 days only due to fast drying during the summer conditions in the UAE at the time. During the uncontrolled conditions pot trial experiment, there were three species used: cat grass, carrot (sp. *Daucus carota subsp. Sativus*), and watermelon (sp. *Citrullus lanatus*). Having noticed that seeds were not germinating, a shelter was created for the pots (Figure 4.2 a)



Figure 4.2. (a) The first stage of the wet cycle field experiment (pots were uncovered). Figure (b) the pots were covered to reduce direct sunlight. (c) First germination of watermelon and figure (d) shows the results of watermelon growth.

4.3.4 *Statistical Analysis*

In this study, the pot trials were conducted as four-factor experiments, where the four factors were: soil amendment, treatment, wetting cycle, and time in the experiment. The soil amendment factor (henceforward referred to as Material) had two levels: the date palm frond (DPF) and biochar. The treatment factor (henceforward referred to as Treatment) had 5 levels, and treatments were 0, 1, 6, 15, and 18% of each amendment in UAE sandy soil. The wetting cycle factor (henceforward as Cycle) had two levels: the wet cycle and the dry cycle. The time in the experiment, referred to as the day factor, had up to 60 levels (i.e., 60 days).

The results of both experiments were analysed by analysis of variance (ANOVA). The results were judged as statistically significant if they were different from zero with a probability (p) \leq 0.05. Before any ANOVA was performed, the data were Box-Cox transformed to remove outliers and tested for normality using the Anderson-Darling test (Anderson and Darling, 1952) – it did not prove necessary to transform the data for any of the metrics in this study. The homogeneity of the variance was tested using the Levene test, and if the test failed, the data were log-transformed and re-tested – this did not prove necessary. The magnitude of the effects of each significant factor and interaction was calculated using the generalised ω^2 (Olejnik and Algina, 2003), and values were presented as least-square means (otherwise known as marginal means). Post hoc assessment of factors and interactions was carried out using the Tukey test.

Main effects plots were generated from the ANOVA model and display these marginal means responses for each factor level, averaged across the levels of the other factors included in the model.

Outliers were assessed using normal probability (QQ) plots to evaluate deviations from normality in the model residuals. Observations that showed extreme deviation from the

expected distribution were excluded prior to analysis to satisfy the assumptions required for ANOVA. The removal procedure of 34.26% was applied consistently across the dataset to improve the robustness of the statistical analysis.

The relatively high proportion of removed observations reflects the variability associated with the uncontrolled field conditions, where extreme environmental factors such as high temperatures and rapid soil drying affected plant growth consistency. To ensure the validity of the ANOVA assumptions, removal of these extreme values was necessary to achieve approximate normality of residuals. Importantly, comparative analysis conducted before and after outlier removal showed consistent overall trends in the data, indicating that the exclusion of these observations did not alter the main conclusion of the study but improved the reliability of the statistical analysis.

ANOVA analyses were conducted in Minitab, and statistical tables presented in this chapter summarise the factors retained in the model output that contributed most strongly to explaining variation in the response variable. Therefore, not all possible factors and interaction terms are displayed in every table.

The unamended sand was treated as baseline control and was excluded from the factorial ANOVA because it does not present an amendment material and therefore cannot be included as a level within the “Material” factor (biochar vs DPF). When sand was included, the database became non-factorial/ corresponding unamended material level, not as its response to amended treatment material structure. For this reason, the factorial ANOVA was restricted to biochar and DPF treatments across the defined amendment levels, while the sand control was retained for descriptive comparison in the results.

- **Growth rate calculation**

Plant growth rate was calculated to measure the rate of height increase over time and to allow more accurate comparison of treatment effects than final plant height alone. Growth rate reports for differences in initial plant size provide a more reliable measure of plant response to environmental conditions and soil amendments.

Growth rate was calculated using the incremental growth rate formula:

$$\text{Growth rate} = \frac{H_{i+1} - H_i}{t_{i+1} - t_i}$$

where:

H_i = plant height at time point i (cm)

H_{i+1} = plant height at the subsequent time point (cm)

t_i and t_{i+1} = corresponding time points (days)

This calculation provides the change in plant height per day (cm/day) between measurement intervals.

Growth rates were calculated separately for the wet and dry cycles under both controlled and uncontrolled conditions. The values were derived using data from all material treatments combined (DPF, biochar and UAE sand) to evaluate plant growth response to moisture conditions.

4.4 Results

4.4.1 Height

4.4.1.1 Plant growth in controlled condition (laboratory based)

- Wet cycle

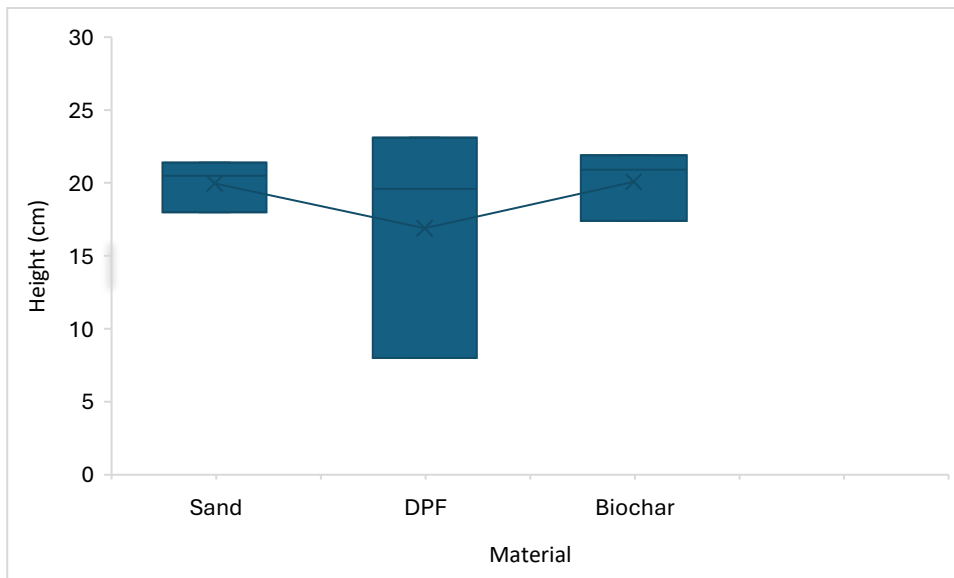


Figure 4.3. Boxplot of plant height (cm) relative to the Material factors measured during the wet cycle. The box shows the interquartile range, with the box representing the first quartile (Q1) to the third quartile (Q3), and the median is represented by a line within the box, and the cross symbol (x) indicates the mean plant height.

The plant growth under controlled conditions during the wet cycle showed differences among unamended materials (Figure 4.3). DPF exhibited the largest interquartile range of plant height, indicating greater variability compared to sand and biochar. In terms of central tendency, the median plant height was highest for biochar (20.9 cm), followed by sand (20.5 cm) and DPF (19.6 cm). The biochar exhibited the highest mean plant height (20.07 cm), followed closely by sand (19.97 cm), while DPF recorded the lowest plant height (16.9 cm). Statistical analysis indicated that unamended material had a significant effect on plant height during the wet cycle under controlled conditions ($p < 0.05$).

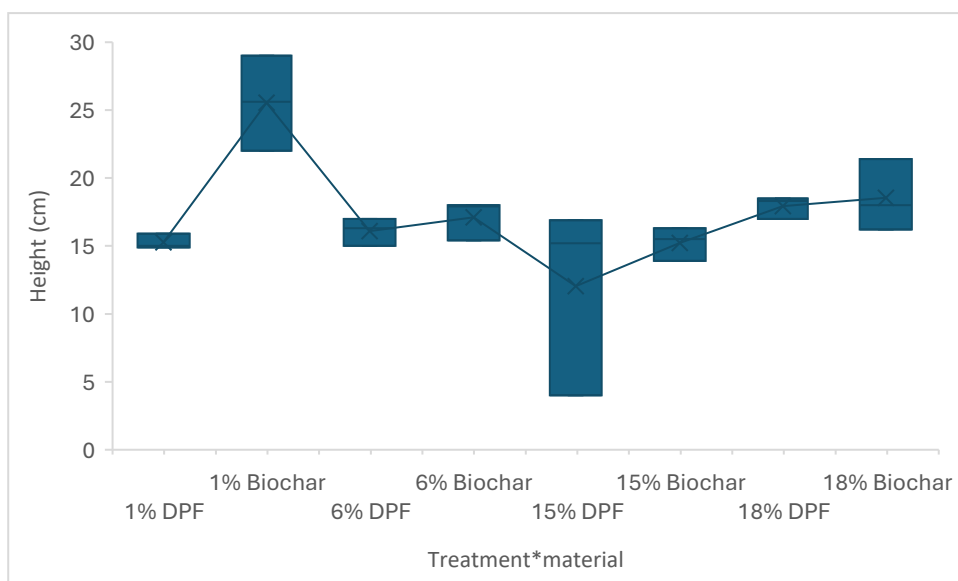


Figure 4.4. Boxplot of plant height (cm) relative to the Treatment*Material interaction measured during the wet cycle. The box shows the interquartile range, with the box representing the first quartile (Q1) to the third quartile (Q3), and the median is represented by a line within the box, and the cross symbol (x) indicates the mean plant height.

The plant growth under controlled condition during the wet cycle differed among the amendment treatment levels (Figure 4.4). The median plant height was highest at the 1% biochar (25.6 cm), and the lowest plant height was the 15% DPF (15.2 cm) (Figure 4.4). The 1% biochar exhibited the highest mean plant height recorded (25.53 cm), followed by the lowest plant height recorded (12.03 cm), which was the 15% DPF. Statistical analysis indicated that amended treatment material had a significant effect on plant height during the wet cycle under controlled conditions ($p < 0.05$).

From Figure 4.3 and Figure 4.4, both amended and unamended soils had an influence on plant growth during the wet cycle, though whether there was a clear statistical impact of treatment will be discussed below.

- Dry cycle

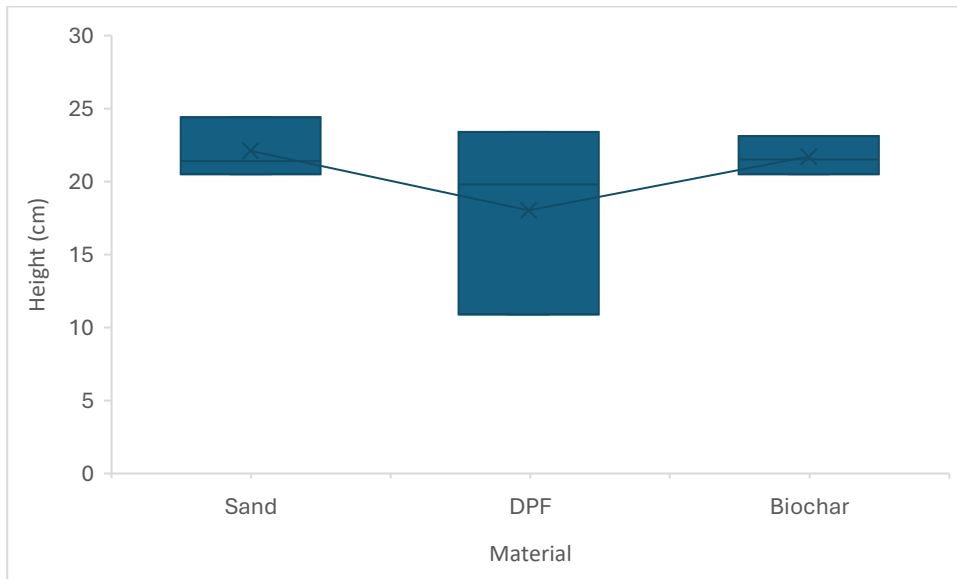


Figure 4.5. Boxplot of height (cm) relative to the Material factors measured during the dry cycle. Box plots show the interquartile range, with the box representing the first quartile (Q1) to the third quartile (Q3), and the median is represented by a line within the box, and the cross symbol (x) indicates the mean plant height.

The plant growth under controlled condition during the dry cycle showed differences among unamended materials (Figure 4.5). DPF exhibited the largest interquartile range of plant height, indicating greater variability compared to sand and biochar. In terms of central tendency, the median plant height was highest for biochar (21.5 cm), followed by sand (21.4 cm) and DPF (19.8 cm). The sand exhibited the highest mean plant height (22.1 cm), followed closely by biochar (21.7 cm), while DPF recorded the lowest plant height (18.03 cm). Statistical analysis indicated that unamended material had a significant effect on plant height during the dry cycle under controlled conditions ($p < 0.05$).

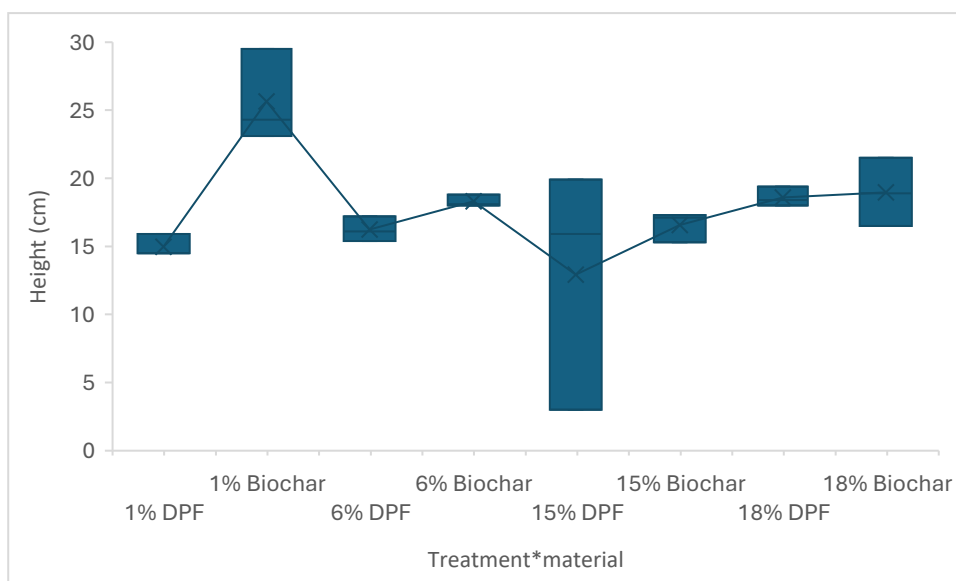


Figure 4.6. Boxplot of height (cm) relative to the Treatment*Material interaction measured during the dry cycle. Box plots show the interquartile range, with the box representing the first quartile (Q1) to the third quartile (Q3), and the median is represented by a line within the box, and the cross symbol (x) indicates the mean plant height.

Under controlled conditions during a dry cycle, plant growth measurements revealed that 1% biochar treatment resulted in the tallest plants with a median height of 24.3 cm, while 15% DPF treatment led to the shortest plants with a median height of 15.9 cm (Figure 4.6). The 1% biochar exhibited the highest mean plant height recorded (25.63 cm), followed by the lowest plant height, which was the 15% DPF (12.93 cm) (Figure 4.6). Statistical analysis indicated that amended treatment material had a significant effect on plant height during the wet cycle under controlled conditions ($p < 0.05$).

Figure 4.5 and Figure 4.6 show that both amended and unamended soils had an influence on plant growth during the dry cycle, though whether there was a clear statistical impact of treatment will be discussed below.

4.4.1.2 Plant growth in uncontrolled conditions (field based)

- Wet cycle

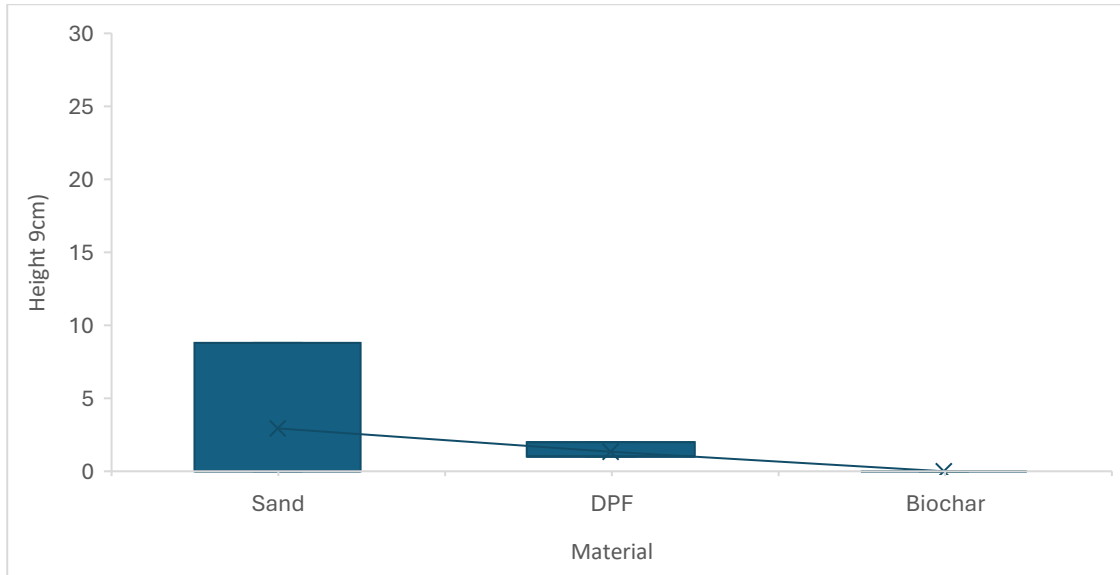
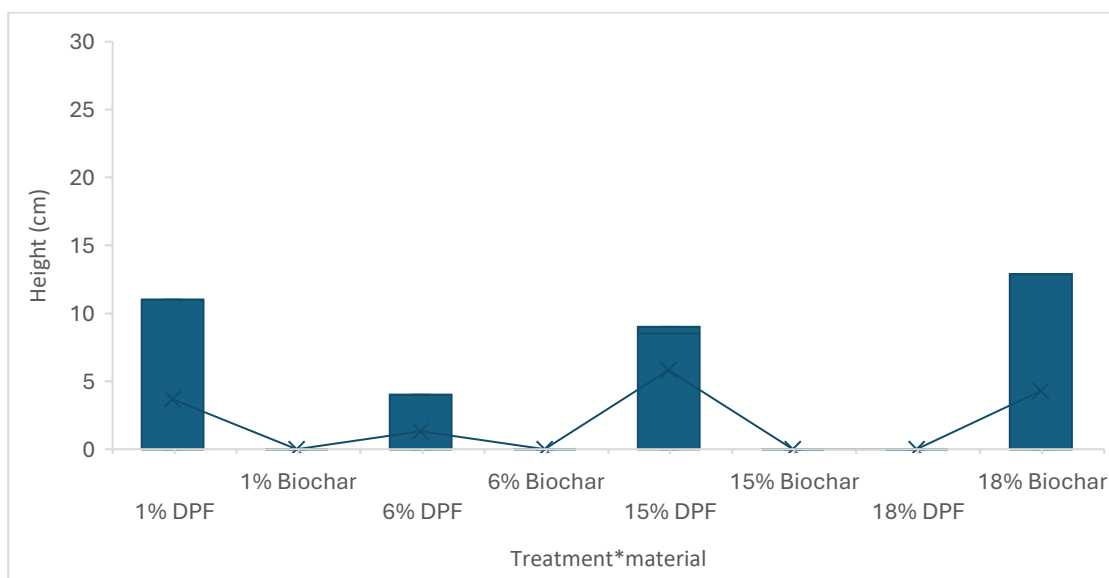


Figure 4.7. Boxplot of height (cm) relative to the Material factors measured during the wet cycle. Box plots show the interquartile range, with the box representing the first quartile (Q1) to the third quartile (Q3). The median is presented by a line within the box, although in some cases the median coincides with the quartile boundary and may not be visually distinguishable. The cross symbol (x) indicates the mean plant height.

During the wet cycle under uncontrolled conditions, sand exhibited the highest median plant height at 8.8 cm, followed by DPF (2 cm), and the lowest median was biochar, which showed no plant growth recorded (0 cm) (Figure 4.7). The UAE sand exhibited the highest mean plant height recorded (2.93 cm), followed by DPF (1.33 cm) and biochar (0 cm) (Figure 4.7). Statistical analysis indicated that unamended material had a significant effect on plant height during the wet cycle under uncontrolled conditions ($p < 0.05$).



*Figure 4.8. Boxplot of height (cm) relative to the Treatment*Material interaction measured during the wet cycle. Box plots show the interquartile range, with the box representing the first quartile (Q1) to the third quartile (Q3). The median is presented by a line within the box, although in some cases the median coincides with the quartile boundary and may not be visually distinguishable. The cross symbol (x) indicates the mean plant height.*

Under uncontrolled conditions during the wet cycle, the treatment with 18% biochar had the highest median plant height (12.9 cm) (Figure 4.8), and the lowest median plant height was (0 cm) for all the biochar treatments of 1%, 6%, 15% and 18% DPF. The 15% DPF exhibited the highest mean plant height recorded (5.83 cm), followed by the lowest mean plant height, which were the biochar's of 1%, 6%, 15%, and 18% DPF were recorded as (0 cm). Statistical analysis indicated that amended treatment material had a significant effect on plant height during the wet cycle under uncontrolled conditions ($p < 0.05$).

Figure 4.7 and Figure 4.8 show that both amended and unamended soil can influence plant growth during the wet cycle under uncontrolled condition though whether there was a clear statistical impact of treatment will be discussed below.

- Dry cycle

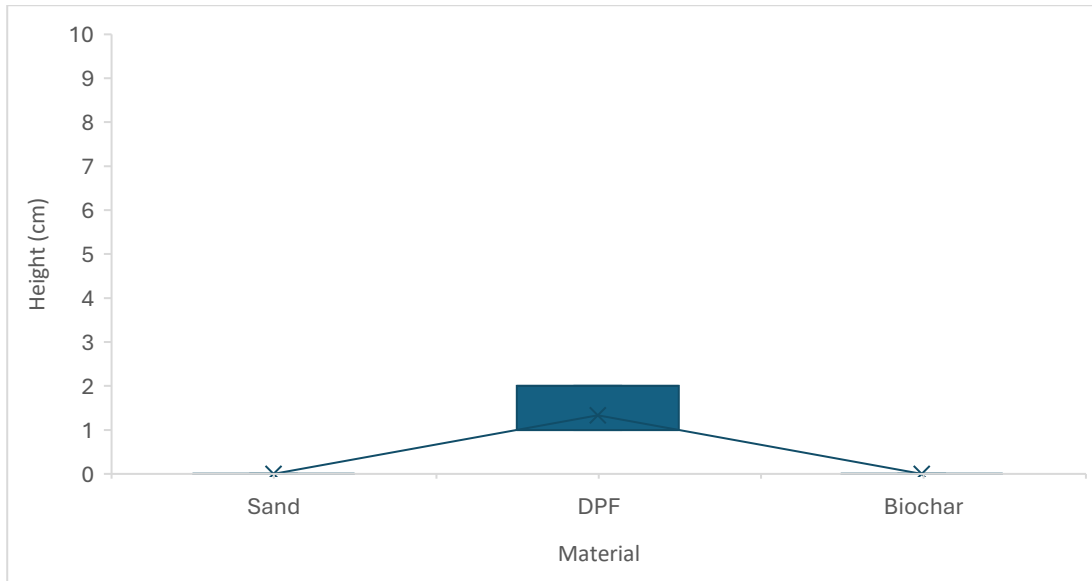
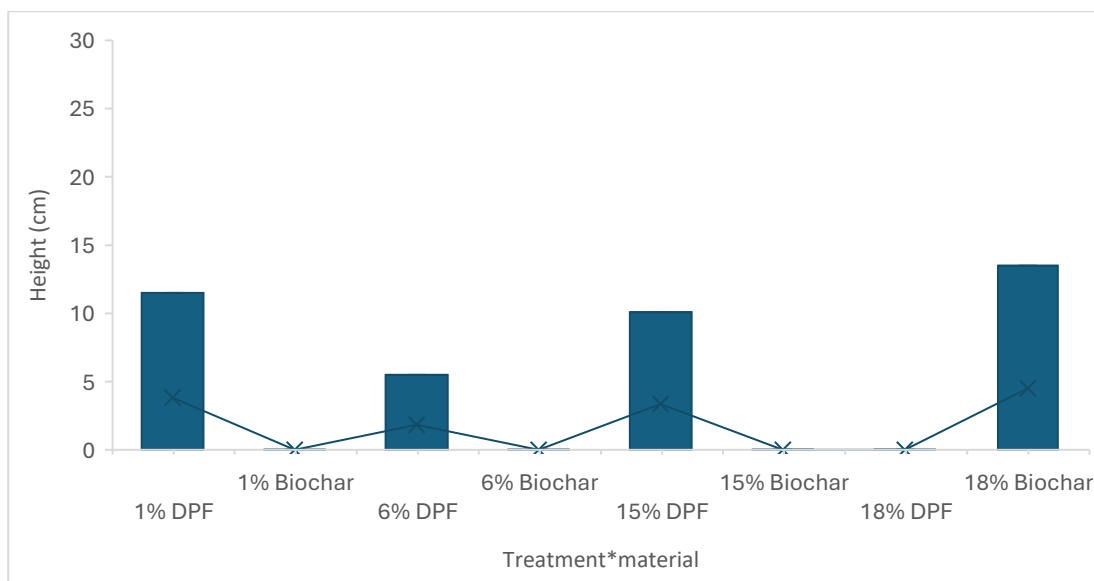


Figure 4.9. Boxplot of height (cm) relative to the Material factors measured during the dry cycle. Box plots show the interquartile range, with the box representing the first quartile (Q1) to the third quartile (Q3). The median is presented by a line within the box, although in some cases the median coincides with the quartile boundary and may not be visually distinguishable. The cross symbol (x) indicates the mean plant height.

During the dry cycle under uncontrolled conditions, DPF exhibited the highest median plant height at (2 cm) (Figure 4.9). The sand and biochar unamended soils did not exhibit any growth, and the medians were recorded (0 cm) (Figure 4.9). The DPF exhibited the highest mean plant height (1.33 cm), followed by UAE sand and biochar, which were recorded with no plant growth (0 cm). Statistical analysis indicated that amended material had a significant effect on plant height during the dry cycle under uncontrolled conditions ($p < 0.05$).



*Figure 4.10. Boxplot of height (cm) relative to the Treatment*Material interaction measured during the dry cycle. Box plots show the interquartile range, with the box representing the first quartile (Q1) to the third quartile (Q3). The median is presented by a line within the box, although in some cases the median coincides with the quartile boundary and may not be visually distinguishable. The cross symbol (x) indicates the mean plant height.*

Under uncontrolled conditions during the dry cycle, treatments with 18% biochar exhibited the highest median plant height (13.5 cm) (Figure 4.10). Conversely, the 6% DPF treatment had the lowest median plant height (5.5 cm). Notably, the 1% biochar, 6% biochar, 15% biochar, and 18% DPF treatments showed no plant growth (0 cm) (Figure 4.10). The 18% biochar exhibited the highest mean plant height recorded (4.5 cm), followed by the lowest plant height were the biochar's of 1%, 6%, 15% and 18% DPF, recorded as (0 cm). Statistical analysis indicated that amended treatment material had a significant effect on plant height during the dry cycle under uncontrolled conditions ($p < 0.05$).

Figure 4.9 and Figure 4.10 show that both amended and unamended soils had an influence on plant growth during the dry cycle in uncontrolled condition though whether there was a clear statistical impact of treatment will be discussed below.

- *Growth Rate*

A summary of the calculation growth rates is shown in Table 4.

Table 4.2. Summary of plant growth rates (cm/day) under controlled and uncontrolled conditions during wet and dry cycles. Growth rates were calculated from changes in plant height over time. Values represent pooled data across all materials treatments, including PDF, biochar and UAE sand.

| <i>Condition</i> | <i>Cycle</i> | <i>Maximum Growth Rate (cm/day)</i> | <i>Minimum Growth Rate (cm/day)</i> |
|---------------------|--------------|-------------------------------------|-------------------------------------|
| <i>Controlled</i> | <i>Wet</i> | 0.26 | 0.20 |
| <i>Controlled</i> | <i>Dry</i> | 0.35 | 0.19 |
| <i>Uncontrolled</i> | <i>Wet</i> | 0.85 | 0.00 |
| <i>Uncontrolled</i> | <i>Dry</i> | 0.20 | 0.00 |

a. Growth Rate in a controlled experiment

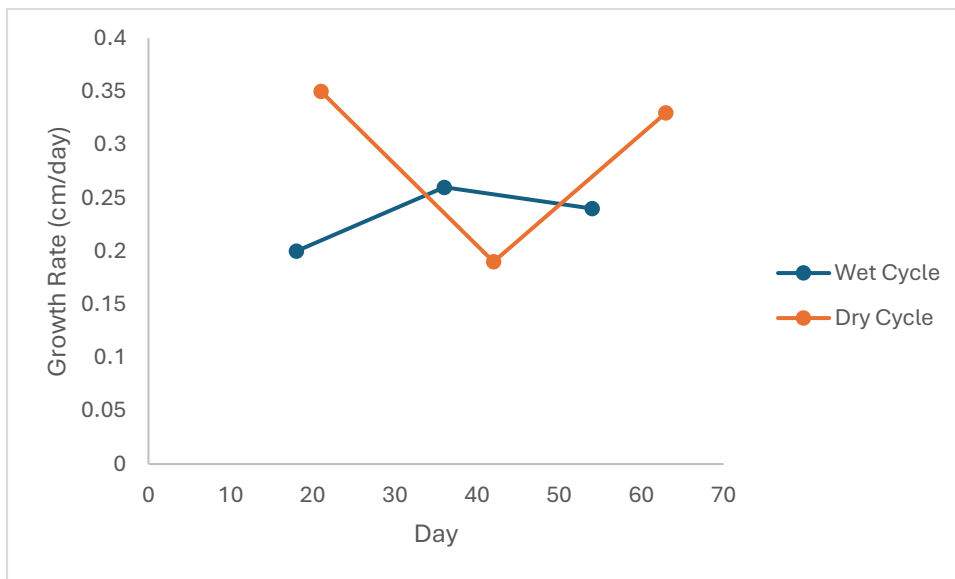


Figure 4.11. Plant growth rate (cm/day) under controlled laboratory conditions during wet and dry cycles. Growth rates were calculated from incremental changes in plant height over time. Values represent pooled data across all material treatments (DPF, biochar and UAE sand).

Under controlled laboratory condition, plant growth rates differed between wet and dry cycles.

During the wet cycle, growth rates ranged from (0.20- 0.26 cm/day), in contrast to the dry cycle, which showed more growth rates ranging from (0.19- 0.35 cm/day) (Figure 4.11).

b. Growth Rate in an uncontrolled experiment

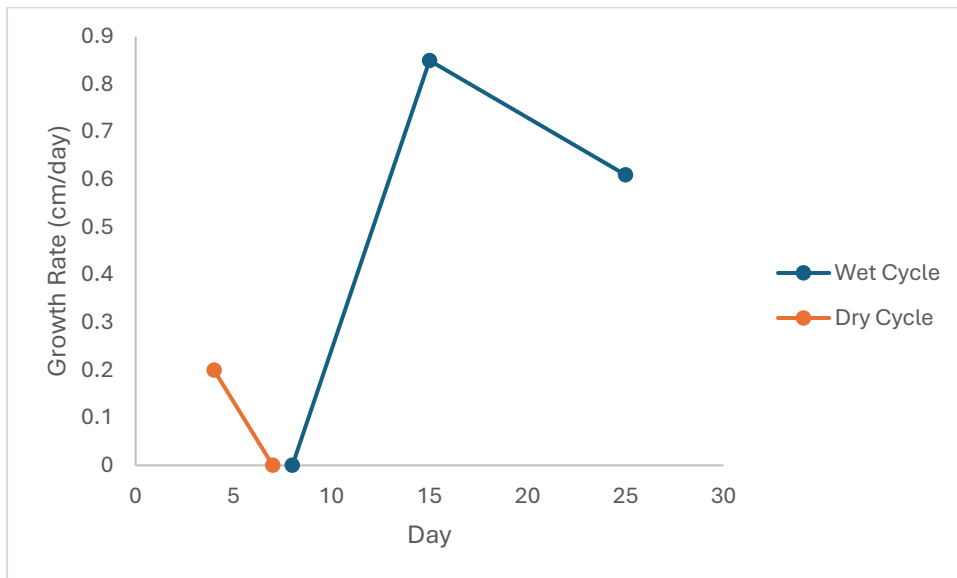


Figure 4.12. Plant growth rate (cm/day) under uncontrolled field conditions during wet and dry cycles. Growth rates were calculated from incremental changes in plant height over time. Values represent pooled data across all material treatments (DPF, biochar and UAE sand).

Under uncontrolled field conditions, plant growth rates were considerably higher during the wet cycle compared to the dry cycle. The wet cycle showed a peak growth rate of (0.85 cm/day), followed by a slight decline to (0.61 cm/day). In contrast to the dry cycle, which showed lower growth rates recorded (0 cm/day), indicating limited or no plant growth under dry conditions (Figure 4.12).

Minor fluctuations in plant height observed during the early measurement intervals likely reflect measurement variability or temporary changes in leaf orientation rather than an actual reduction in plant size. In addition, the apparent period in plant height towards the end of the dry cycle indicates that plant growth slowed or ended under reduced moisture availability. These patterns are therefore consistent with the calculated growth rate values and suggest that plant development was constrained during periods of limited water availability (Figure 4.12).

4.4.2 Moisture level

4.4.2.1 Moisture level in the controlled experiment.

- Wet cycle

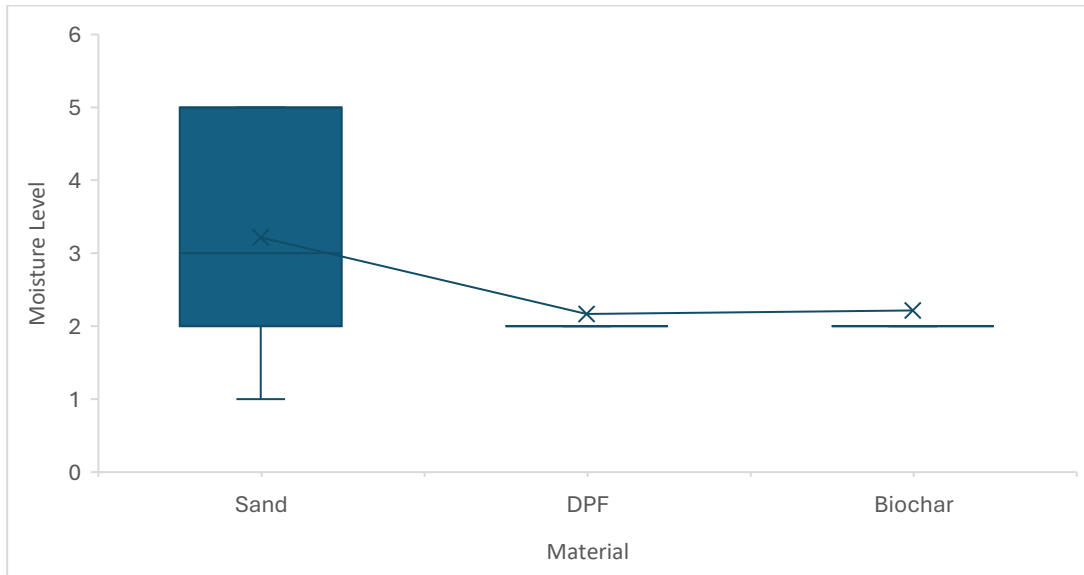


Figure 4.13. Boxplot of moisture level relative to the Material factors measured during the wet cycle. Box-and-whisker plots show the interquartile range, with the box representing the first quartile (Q1) to the third quartile (Q3), and the whiskers extending from the minimum to the maximum values. The median is represented by a line within the box, and the cross symbol (x) indicates the mean moisture level.

Under controlled conditions during the wet cycle, sand exhibited the highest median moisture level, which was recoded as (level 3) (Figure 4.13). DPF and biochar shared the lowest median moisture level, both at (level 2) (Figure 4.13). The UAE sand exhibited the highest mean moisture level recorded (3.2), followed by biochar (2.21) and DPF (2.17). Statistical analysis indicated that unamended material had a significant effect on moisture level during the wet cycle under controlled conditions ($p < 0.05$).

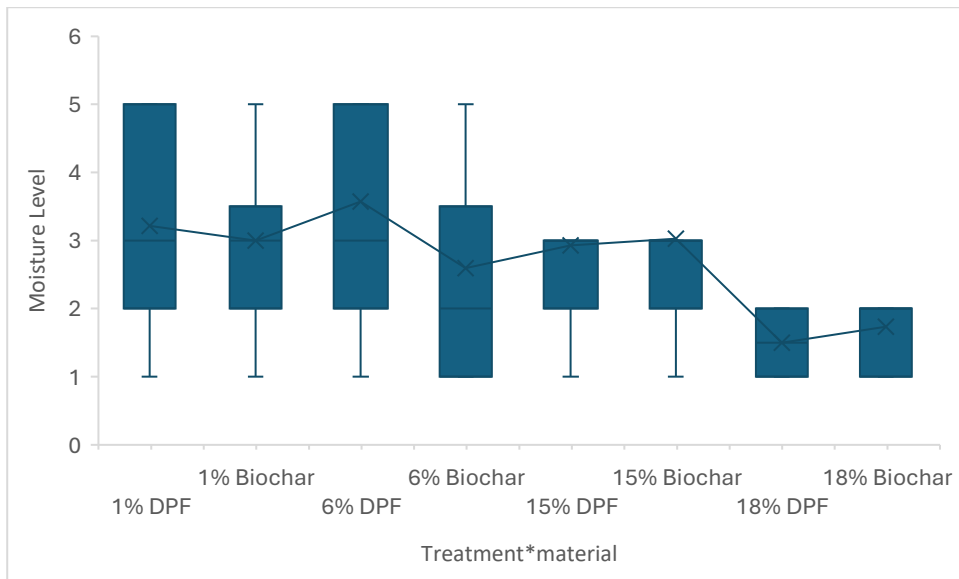


Figure 4.14. Boxplot of moisture level of the Treatment*Material interaction measured during the wet cycle. Box-and-whisker plots show the interquartile range, with the box representing the first quartile (Q1) to the third quartile (Q3), and the whiskers extending from the minimum to the maximum values. The median is represented by a line within the box, and the cross symbol (x) indicates the mean moisture level.

Under controlled conditions during the wet cycle, the 1% and 6% DPF treatments exhibited the highest median moisture levels (level 3) (Figure 4.14). Conversely, the 6% 18% DPF and biochar treatment showed the lowest median moisture level (level 2) (Figure 4.14). The 6% DPF exhibited the highest mean moisture level recorded (3.57), and the lowest moisture level was for the 18% DPF (1.5). Statistical analysis indicated that amended treatment material had a significant effect on moisture level during the wet cycle under controlled conditions ($p < 0.05$).

Figure 4.13 and Figure 4.14 show that both amended and unamended soils had an influence on moisture levels during the wet cycle in controlled condition though whether there was a clear statistical impact of treatment will be discussed below.

- Dry cycle

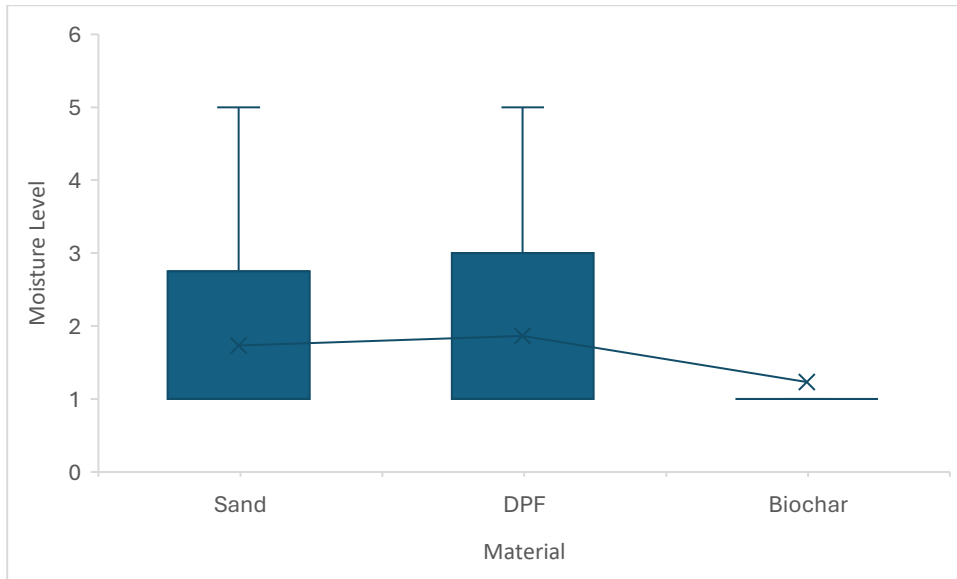


Figure 4.15. Boxplot of the moisture level relative to the Material factors measured during the dry cycle. Box-and-whisker plots show the interquartile range, with the box representing the first quartile (Q1) to the third quartile (Q3), and the whiskers extending from the minimum to the maximum values. The median is presented by a line within the box, although in some cases the median coincides with the quartile boundary and may not be visually distinguishable. The cross symbol (x) indicates the mean moisture level.

Under controlled conditions during the dry cycle, both sand and DPF reached the same median moisture level (level 5) (Figure 4.15). Biochar showed the lowest soil moisture level at (level 1) (Figure 4.15). The DPF exhibited the highest mean moisture level (1.87), followed by UAE (1.73) sand and biochar (1.23). Statistical analysis indicated that amended material had a significant effect on moisture level during the dry cycle under controlled conditions ($p < 0.05$).

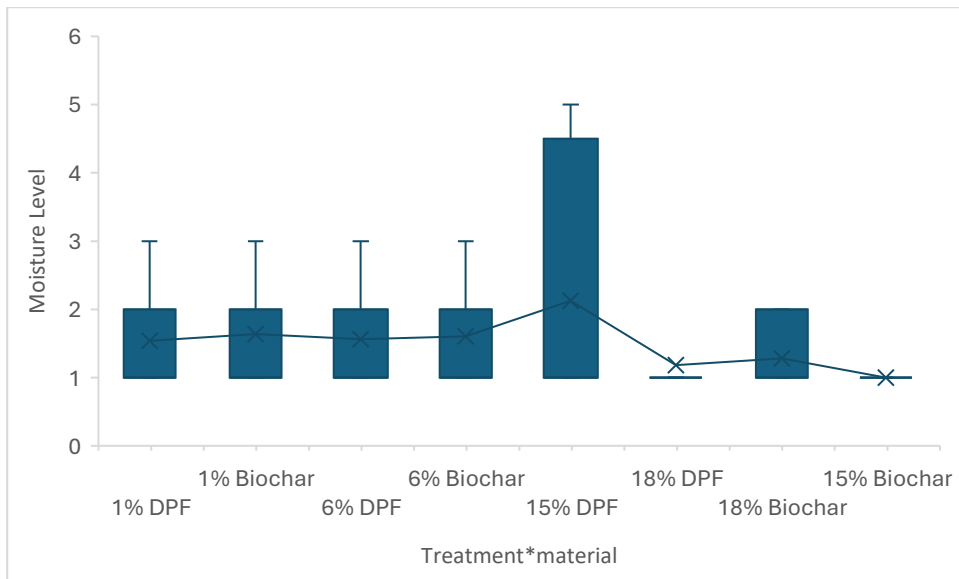


Figure 4.16. Boxplot of the moisture level relative to the Treatment*Material interaction measured during the dry cycle. Box-and-whisker plots show the interquartile range, with the box representing the first quartile (Q1) to the third quartile (Q3), and the whiskers extending from the minimum to the maximum values. The median is presented by a line within the box, although in some cases the median coincides with the quartile boundary and may not be visually distinguishable. The cross symbol (x) indicates the mean moisture level.

Under controlled conditions during the dry cycle, showed that 15% DPF showed the highest median m moisture level at (level5) (Figure 4.16). Conversely, the 15% biochar treatments showed the lowest median soil moisture recorded (level 1) (Figure 4.16). The with 15% DPF exhibited the highest mean moisture level recorded (2.13), followed by the lowest moisture level, the 15% biochar recorded (level 1). Statistical analysis indicated that amended treatment material had a significant effect on moisture level during the dry cycle under controlled conditions ($p < 0.05$).

The Figure 4.15 and Figure 4.16 show that both amended and unamended soil had an influence on moisture levels during the dry cycle in controlled condition though whether there was a clear statistical impact of treatment will be discussed below.

4.4.2.2 Moisture level in the uncontrolled experiment.

- Wet cycle

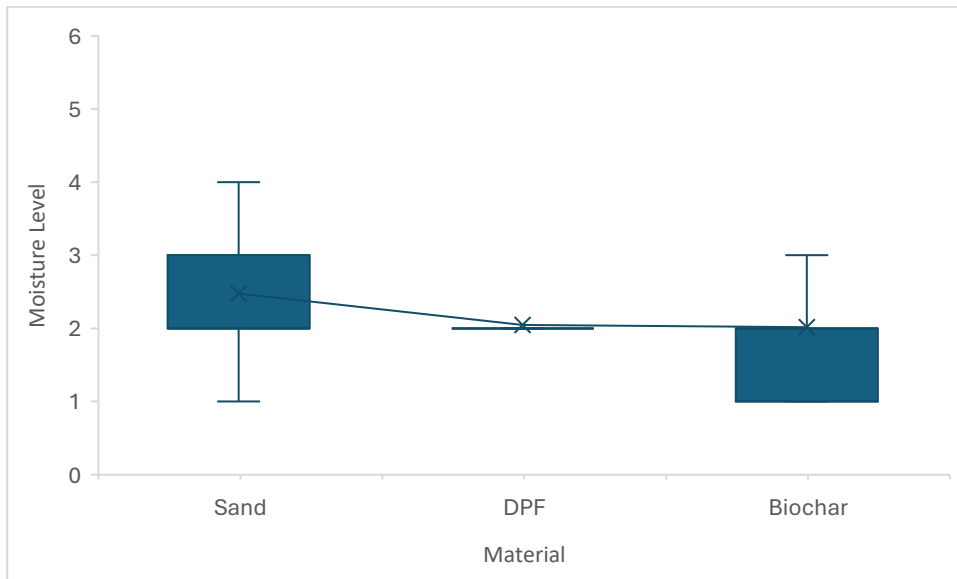
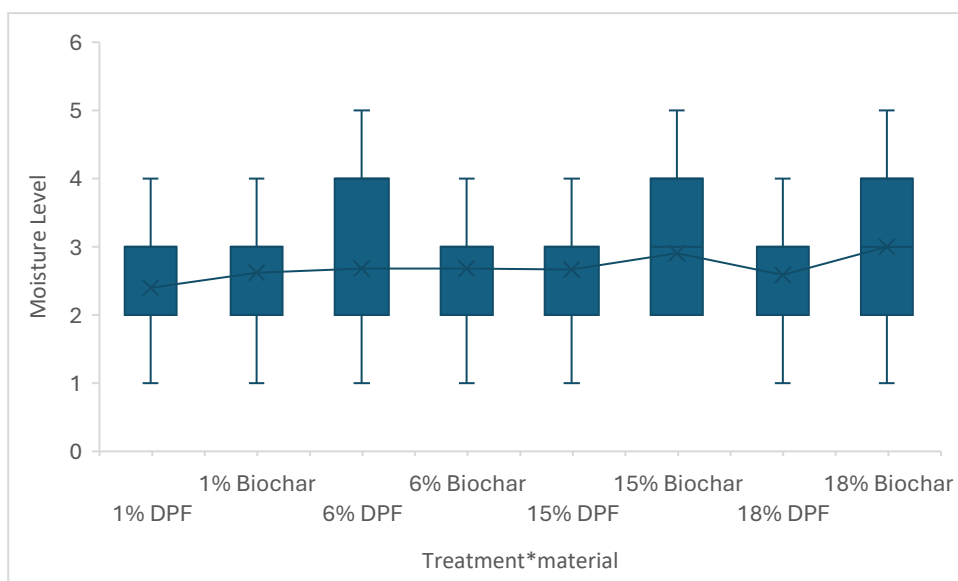


Figure 4.17. Boxplot of the uncontrolled moisture level relative to the Material factors measured during the wet cycle. Box-and-whisker plots show the interquartile range, with the box representing the first quartile (Q1) to the third quartile (Q3), and the whiskers extending from the minimum to the maximum values. The median is presented by a line within the box, although in some cases the median coincides with the quartile boundary and may not be visually distinguishable. The cross symbol (x) indicates the mean moisture level.

During the uncontrolled wet cycle, sand exhibited the highest median moisture level, reaching (level 4), as shown in (Figure 4.17). Conversely, both DPF and biochar had the lowest median moisture level at (level 1 (Figure 4.17)). The UAE sand exhibited the highest mean moisture level recorded (2.48), followed by DPF (2.05) and biochar (2.02). Statistical analysis indicated that unamended material had a significant effect on moisture level during the wet cycle under uncontrolled conditions ($p < 0.05$).



*Figure 4.18. Boxplot of the moisture level relative to the Treatment*Material interaction measured during the wet cycle. Box-and-whisker plots show the interquartile range, with the box representing the first quartile (Q1) to the third quartile (Q3), and the whiskers extending from the minimum to the maximum values. The median is represented by a line within the box, and the cross symbol (x) indicates the mean moisture level.*

Under uncontrolled wet cycle conditions, three treatments - 6% DPF, 15% biochar, and 18% biochar - shared the highest maximum moisture level, reaching level 5 (Figure 4.18). Interestingly, all treatments except 15% biochar exhibited the lowest minimum moisture level (Figure 4.18). The 15% biochar treatment had the lowest quartile moisture level at level 2, while both 15% and 18% biochar treatments had a median moisture level of 3.

Figure 4.17 and Figure 4.18 show that both treated and untreated soils had an influence on moisture levels during the wet cycle in uncontrolled condition though whether there was a clear statistical impact of treatment will be discussed below.

- Dry cycle

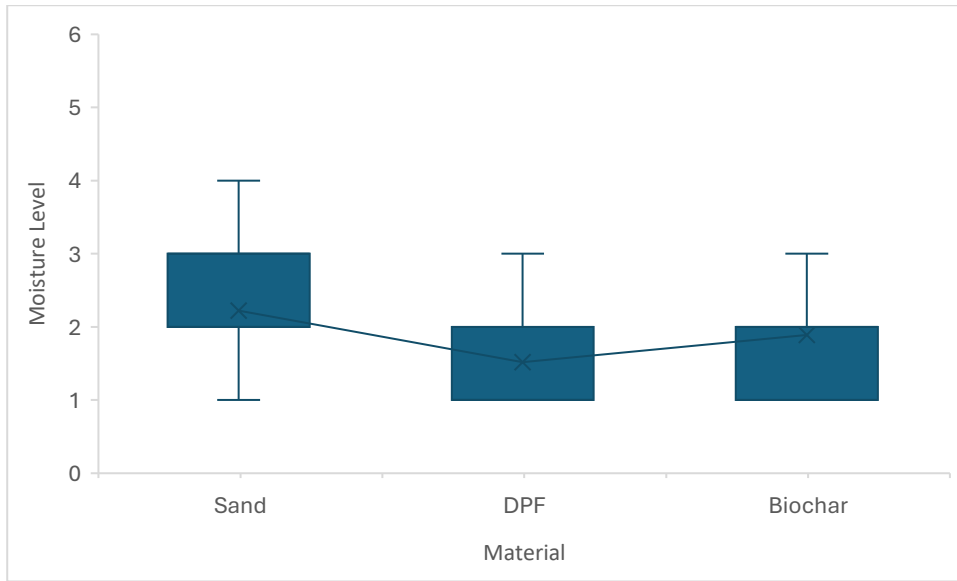


Figure 4.19. Boxplot of the moisture level relative to the Material factors measured during the dry cycle. Box-and-whisker plots show the interquartile range, with the box representing the first quartile (Q1) to the third quartile (Q3), and the whiskers extending from the minimum to the maximum values. The median is presented by a line within the box, although in some cases the median coincides with the quartile boundary and may not be visually distinguishable. The cross symbol (x) indicates the mean moisture level.

Under uncontrolled dry cycle conditions, sand exhibited the highest median moisture level, reaching (level 4) (Figure 4.19). Conversely, both DPF and biochar had the lowest median moisture level at (level 1) (Figure 4.19). The UAE sand exhibited the highest mean moisture level recorded (2.22), followed by biochar (1.89) and DPF (1.52). Statistical analysis indicated that unamended material had a significant effect on moisture level during the dry cycle under uncontrolled conditions ($p < 0.05$).

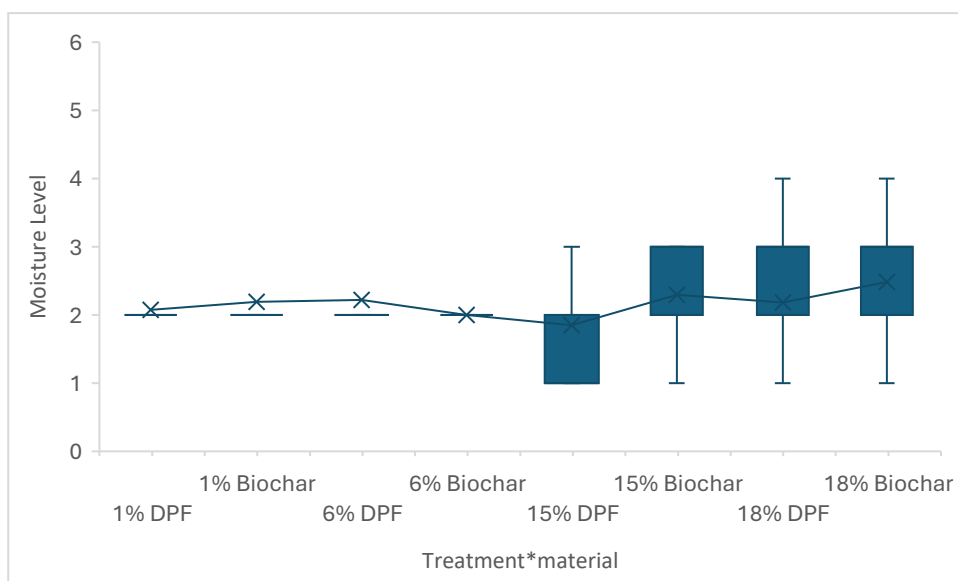


Figure 4.20. Boxplot of the moisture level relative to the Treatment*Material interaction measured during the dry cycle. Box-and-whisker plots show the interquartile range, with the box representing the first quartile (Q1) to the third quartile (Q3), and the whiskers extending from the minimum to the maximum values. The median is presented by a line within the box, although in some cases the median coincides with the quartile boundary and may not be visually distinguishable. The cross symbol (x) indicates the mean moisture level.

Under uncontrolled dry cycle conditions, two treatments, 18% DPF and 18% biochar, exhibited the highest median moisture level, reaching (level 4) (Figure 4.20). Conversely, the 1% DPF, 1% biochar, 6% DPF and 6% biochar showed the lowest median moisture level at (level 2) (Figure 4.20). The 18% biochar exhibited the highest mean moisture level recorded (2.48), followed by the lowest moisture level, the 15% DPF (1.85). Statistical analysis indicated that amended treatment material had a significant effect on moisture level during the dry cycle under uncontrolled conditions ($p < 0.05$).

Figures Figure 4.19 and Figure 4.20 show that both amended and unamended soils had an influence on moisture levels during the dry cycle in uncontrolled condition though whether there was a clear statistical impact of treatment will be discussed below.

4.4.3 Soil temperature

4.4.3.1 Soil temperature in controlled experiment.

- Wet cycle

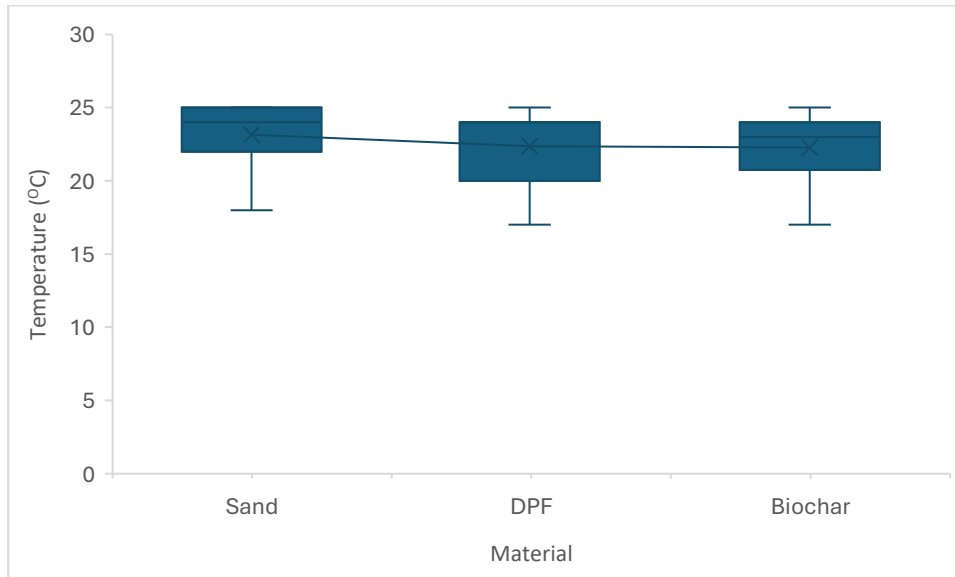


Figure 4.21. Boxplot of the soil temperature relative to the Material factors measured during the wet cycle. Box-and-whisker plots show the interquartile range, with the box representing the first quartile (Q1) to the third quartile (Q3), and the whiskers extending from the minimum to the maximum values. The median is represented by a line within the box, and the cross symbol (x) indicates the mean soil temperature.

Under controlled wet cycle conditions, sand exhibited the highest quartile median soil temperature, reaching (25°C) (Figure 4.21). As for the DPF and biochar share the same median soil temperature at (25°C). The UAE sand exhibited the highest mean soil temperature recorded (23°C), followed by DPF and biochar, which both recorded (22 °C). Statistical analysis indicated that unamended material had a significant effect on soil temperature during the wet cycle under controlled conditions ($p < 0.05$).

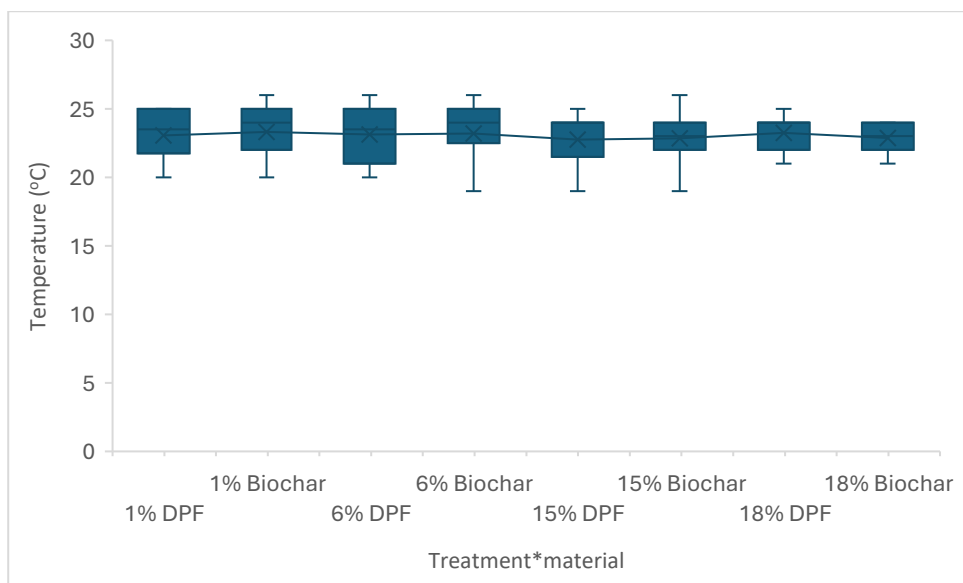


Figure 4.22. Boxplot of the soil temperature relative to the Treatment*Material interaction measured during the wet cycle. Box-and-whisker plots show the interquartile range, with the box representing the first quartile (Q1) to the third quartile (Q3), and the whiskers extending from the minimum to the maximum values. The median is represented by a line within the box, and the cross symbol (x) indicates the mean soil temperature.

Under controlled wet cycle conditions, four treatments - 1% biochar, 6% DPF, 6% biochar, and 15% biochar - shared the highest median soil temperature of (25°C) (Figure 4.22). The 18% biochar showed the lowest median soil temperature at (24°C) (Figure 4.22). The 6% biochar exhibited the highest mean plant height recorded (23°C), followed by the lowest plant height, the 15% DPF recorded (22°C). Statistical analysis indicated that amended treatment material had a significant effect on soil temperature height during the wet cycle under controlled conditions ($p < 0.05$).

- Dry cycle

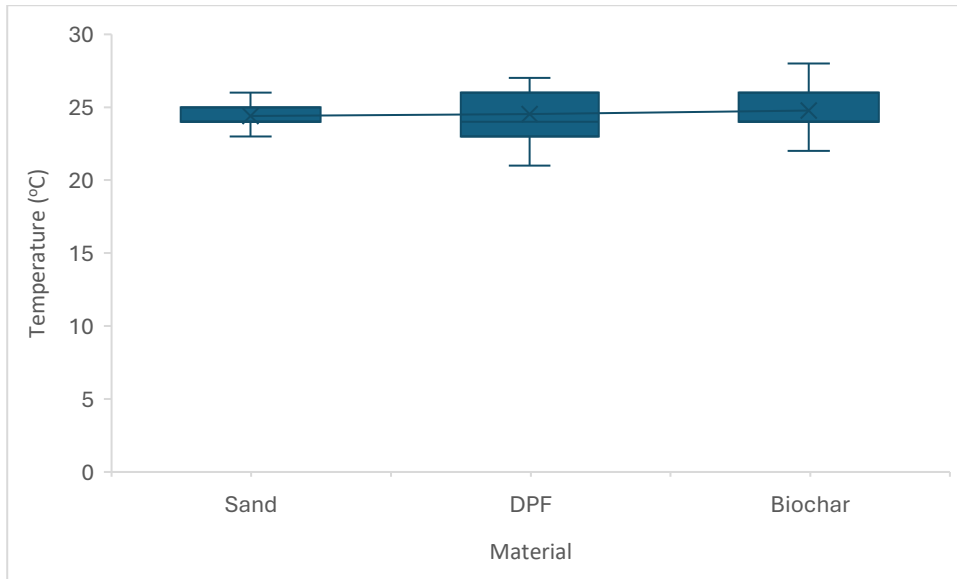


Figure 4.23. Boxplot of the soil temperature relative to the Material factors measured during the dry cycle. Box-and-whisker plots show the interquartile range, with the box representing the first quartile (Q1) to the third quartile (Q3), and the whiskers extending from the minimum to the maximum values. The median is represented by a line within the box, and the cross symbol (x) indicates the mean soil temperature.

Under controlled dry cycle conditions, biochar exhibited the highest median soil temperature, reaching (28°C) followed by DPF at (27) (Figure 4.23). Conversely, sand showed the lowest median soil temperature of (26°C) (Figure 4.23). The biochar exhibited the highest mean soil moisture recorded (25°C), followed by DPF (24.5°C) and UAE sand (24.4°C). Statistical analysis indicated that unamended material had a significant effect on soil temperature during the wet cycle under controlled conditions ($p < 0.05$).

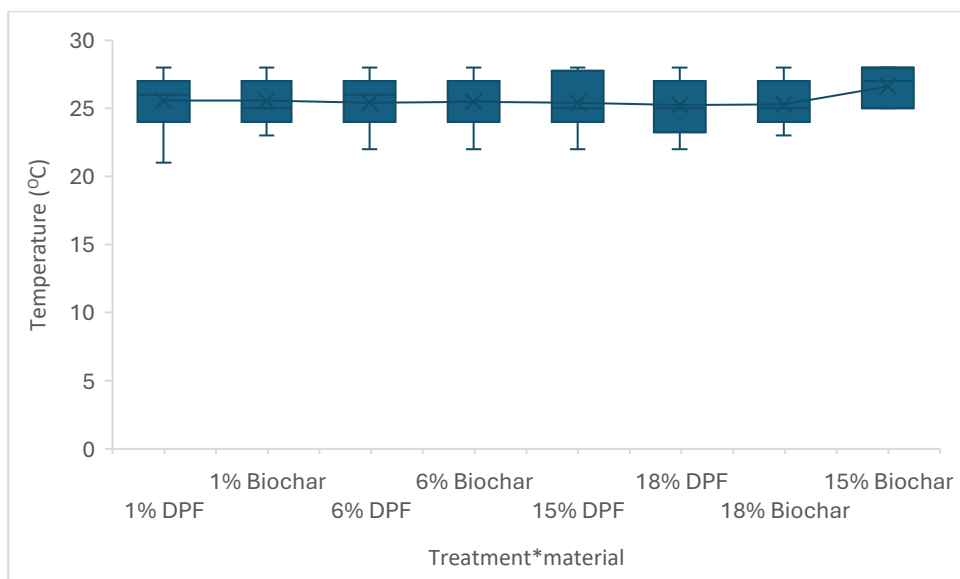


Figure 4.24. Boxplot of the soil temperature relative to the Treatment*Material interaction measured during the dry cycle. Box-and-whisker plots show the interquartile range, with the box representing the first quartile (Q1) to the third quartile (Q3), and the whiskers extending from the minimum to the maximum values. The median is represented by a line within the box, and the cross symbol (x) indicates the mean soil temperature.

Under controlled dry cycle conditions, all treatments except 15% DPF reached the highest median quartile soil temperature recorded (28°C) (Figure 4.24). The remaining treatments share the same lower median whisker plots at (28°C) (Figure 4.24). The 15% biochar exhibited the highest mean soil temperature recorded (26°C), followed by the lowest soil temperature, the 18% DPF (25.25°C). Statistical analysis indicated that amended treatment material had a significant effect on soil temperature during the wet cycle under controlled conditions ($p < 0.05$).

4.4.3.2 Soil temperature in uncontrolled experiment

- Wet cycle

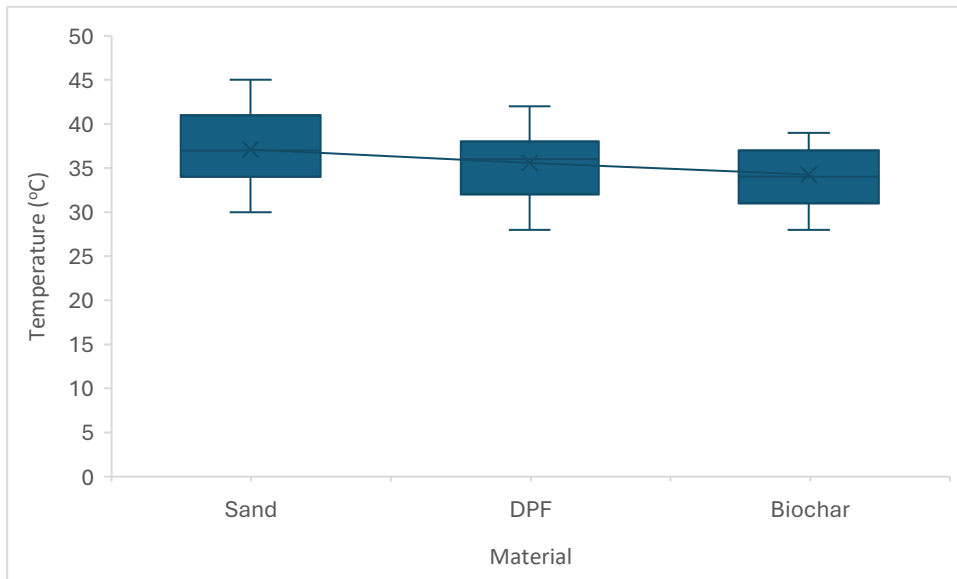


Figure 4.25. Boxplot of the uncontrolled soil temperature relative to the Material factors measured during the wet cycle. Box-and-whisker plots show the interquartile range, with the box representing the first quartile (Q1) to the third quartile (Q3), and the whiskers extending from the minimum to the maximum values. The median is represented by a line within the box, and the cross symbol (x) indicates the mean soil temperature.

Under uncontrolled wet cycle conditions, sand exhibited the highest median soil temperature, reaching (45°C) (Figure 4.25). Conversely, biochar had the lowest median soil temperature of (39°C) (Figure 4.25). The UAE sand exhibiting the highest mean soil temperature recorded was (37°C), followed by DPF (36°C) and biochar (34 °C). Statistical analysis indicated that unamended material had a significant effect on soil temperature during the wet cycle under uncontrolled conditions ($p < 0.05$).

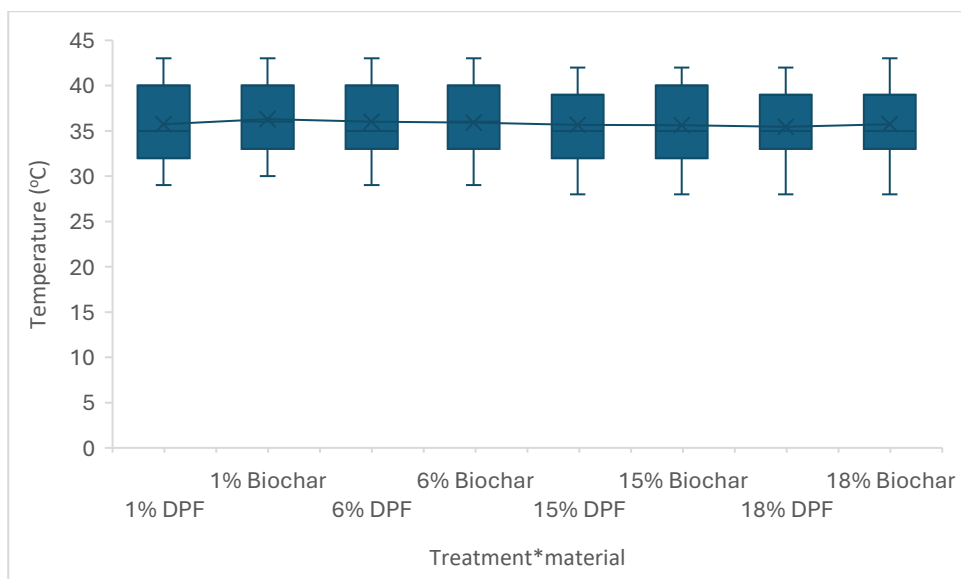


Figure 4.26. Boxplot of the soil temperature relative to the Treatment*Material interaction measured during the wet cycle. Box-and-whisker plots show the interquartile range, with the box representing the first quartile (Q1) to the third quartile (Q3), and the whiskers extending from the minimum to the maximum values. The median is represented by a line within the box, and the cross symbol (x) indicates the mean soil temperature.

Under uncontrolled wet cycle conditions, five treatments, 1% DPF, 1% biochar, 6% DPF, 6% biochar, and 18% biochar, exhibited the highest median soil temperature of (43°C) (Figure 4.26). Conversely, all other treatments (15% DPF, 15% biochar, 18% DPF, and 18% biochar) had the lowest median soil temperature (42°C) (Figure 4.26). The 1% biochar exhibited the highest mean soil temperature recorded (36°C), followed by the lowest soil temperature, the 18% DPF recorded as (35°C). Statistical analysis indicated that amended treatment material had a significant effect on soil temperature during the wet cycle under uncontrolled conditions ($p < 0.05$).

- Dry cycle

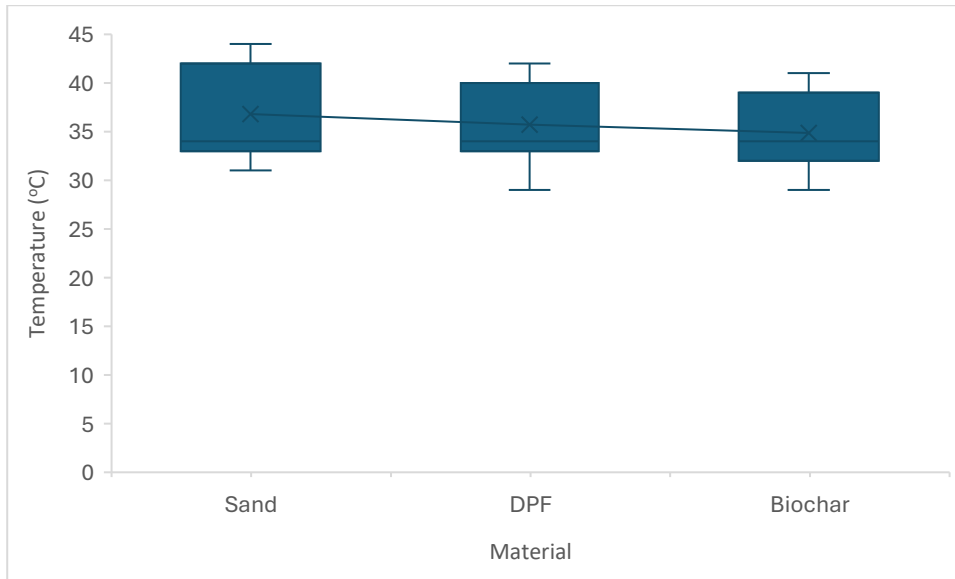


Figure 4.27. Boxplot of the soil temperature relative to the Material factors measured during the dry cycle. Box-and-whisker plots show the interquartile range, with the box representing the first quartile (Q1) to the third quartile (Q3), and the whiskers extending from the minimum to the maximum values. The median is represented by a line within the box, and the cross symbol (x) indicates the mean soil temperature.

Under uncontrolled dry cycle conditions, and with respect to the Materials factor, sand exhibited the highest median soil temperature (44°C), while biochar had the lowest soil temperature at (41°C) (Figure 4.27). The UAE sand exhibited the highest mean soil temperature recorded (37°C), followed by DPF (36°C) and biochar (35°C). Statistical analysis indicated that unamended material had a significant effect on soil temperature during the dry cycle under uncontrolled conditions ($p < 0.05$).

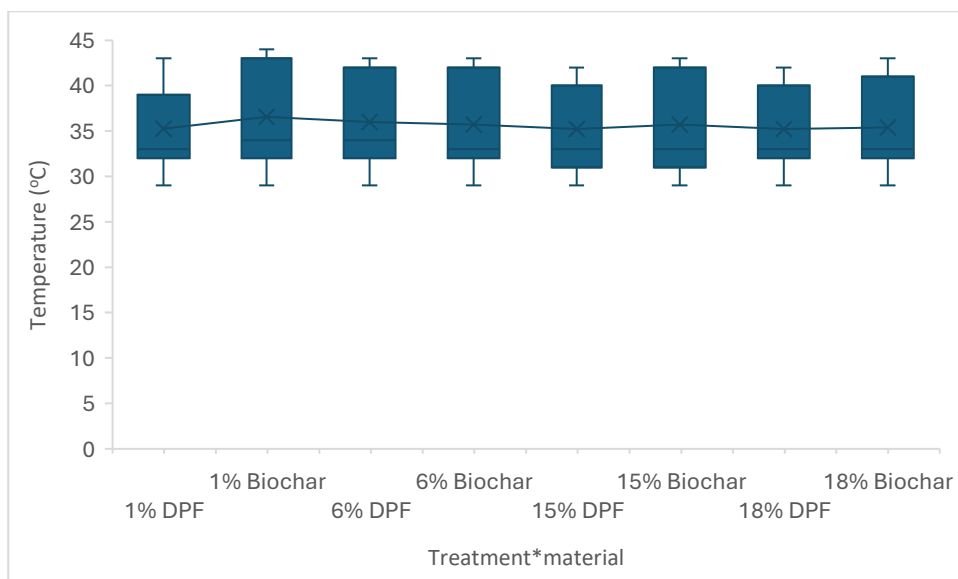


Figure 4.28. Boxplot of the soil temperature relative to the Treatment*Material interaction measured during the dry cycle. Box-and-whisker plots show the interquartile range, with the box representing the first quartile (Q1) to the third quartile (Q3), and the whiskers extending from the minimum to the maximum values. The median is represented by a line within the box, and the cross symbol (x) indicates the mean soil temperature.

With respect to the Treatment factor, and under uncontrolled dry cycle conditions, 1% biochar exhibited the highest median soil temperature, reaching (44°C) (Figure 4.28). The lowest soil temperatures were the 15% and 18% DPFs at (41°C) (Figure 4.28). The 1% biochar exhibited the highest mean soil temperature recorded (37°C), followed by the lowest soil temperature, the 1% DPF recorded as (35°C). Statistical analysis indicated that amended treatment material had a significant effect on soil temperature during the dry cycle under uncontrolled conditions ($p < 0.05$).

4.4.4 Soil pH

4.4.4.1 Soil pH in controlled experiment

- Wet cycle

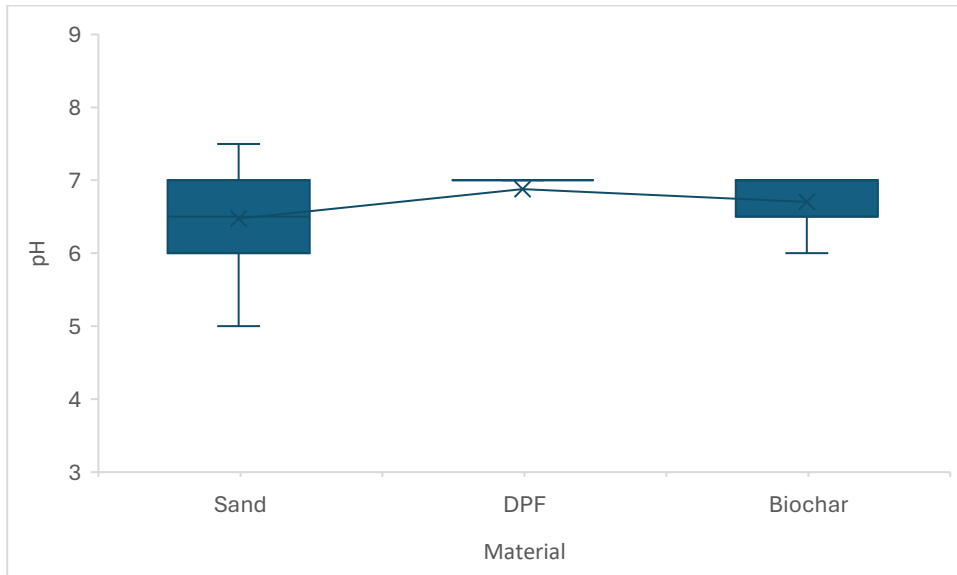


Figure 4.29. Boxplot of the soil pH relative to the Material factors measured during the wet cycle. Box-and-whisker plots show the interquartile range, with the box representing the first quartile (Q1) to the third quartile (Q3), and the whiskers extending from the minimum to the maximum values. The median is represented by a line within the box, and the cross symbol (x) indicates the mean soil pH.

Under a controlled wet cycle condition, and with respect to the Material factor, DPF exhibited the highest median soil pH at 7, compared to the lowest soil pH, which was the sand at 6.5 (Figure 4.29). The DPF exhibited the highest mean soil pH recorded (6.88), followed by biochar (6.70) and UAE sand (6.48). Statistical analysis indicated that unamended material had a significant effect on soil pH during the wet cycle under controlled conditions ($p < 0.05$).

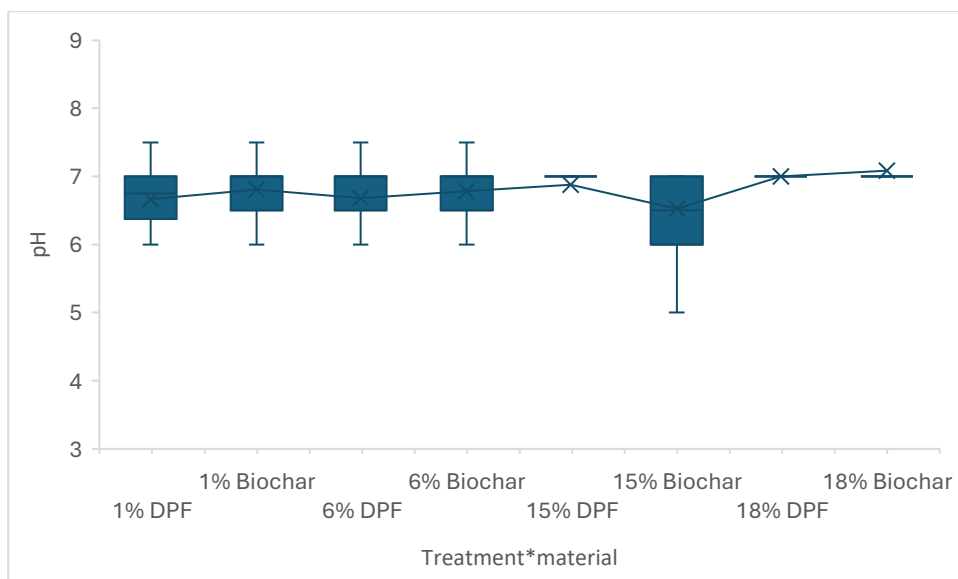


Figure 4.30. Boxplot of the soil pH relative to the Treatment*Material interaction measured during the wet cycle. Box-and-whisker plots show the interquartile range, with the box representing the first quartile (Q1) to the third quartile (Q3), and the whiskers extending from the minimum to the maximum values. The median is represented by a line within the box, and the cross symbol (x) indicates the mean soil pH.

With respect to the Treatment*Material factor, and under controlled condition during the wet cycle, 1% DPF, 1% biochar, 6% DPD and 6% biochar exhibited the highest median soil pH at 7.5 (Figure 4.30). The lowest median soil pH, it was observed in the 15% biochar at 5 (Figure 4.30). The 18% biochar exhibited the highest mean soil pH recorded (7.08), followed by the lowest soil pH, the 15% biochar (6.52). Statistical analysis indicated that amended treatment material had a significant effect on soil pH during the wet cycle under controlled conditions ($p < 0.05$).

- Dry cycle

The soil pH of the materials and treatments in the controlled condition during the dry cycle showed that all the materials (sand, DPF and biochar) had a neutral soil pH of 7.

4.4.4.2 Soil pH in an uncontrolled experiment

- Wet cycle

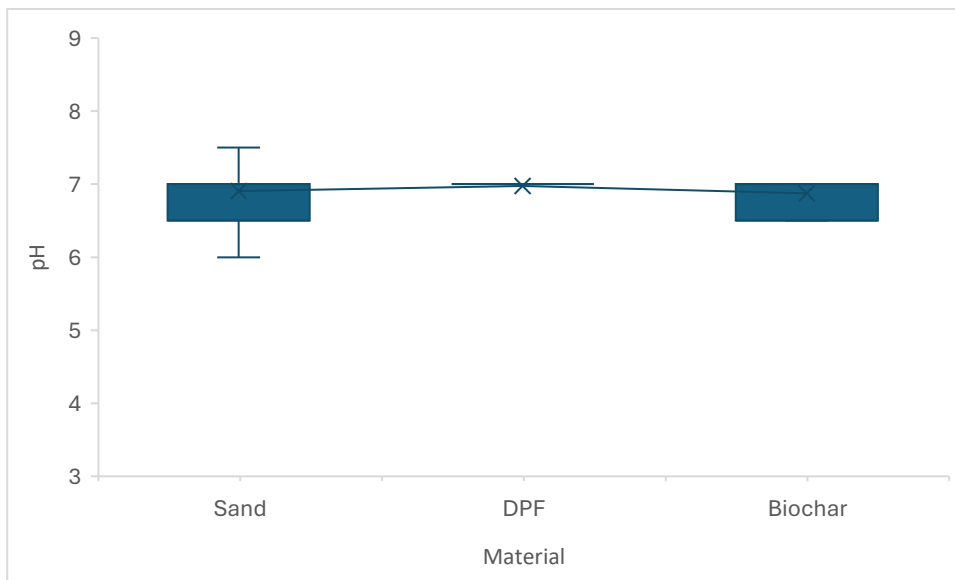


Figure 4.31. Boxplot of the soil pH relative to the material factors measured during the wet cycle. Box-and-whisker plots show the interquartile range, with the box representing the first quartile (Q1) to the third quartile (Q3), and the whiskers extending from the minimum to the maximum values. The median is presented by a line within the box, although in some cases the median coincides with the quartile boundary and may not be visually distinguishable. The cross symbol (x) indicates the mean soil pH.

During the uncontrolled wet cycle condition, and with respect to the Material factor, sand exhibited the highest median soil pH at 7.5 (Figure 4.31). Compared to the lowest median soil pH, both DPF and biochar were at 7 (Figure 4.31). The DPF exhibited the highest mean soil pH recorded (6.98), followed by UAE (6.90) sand and biochar (6.87). Statistical analysis indicated

that unamended material had a significant effect on soil pH during the wet cycle under controlled conditions ($p < 0.05$).

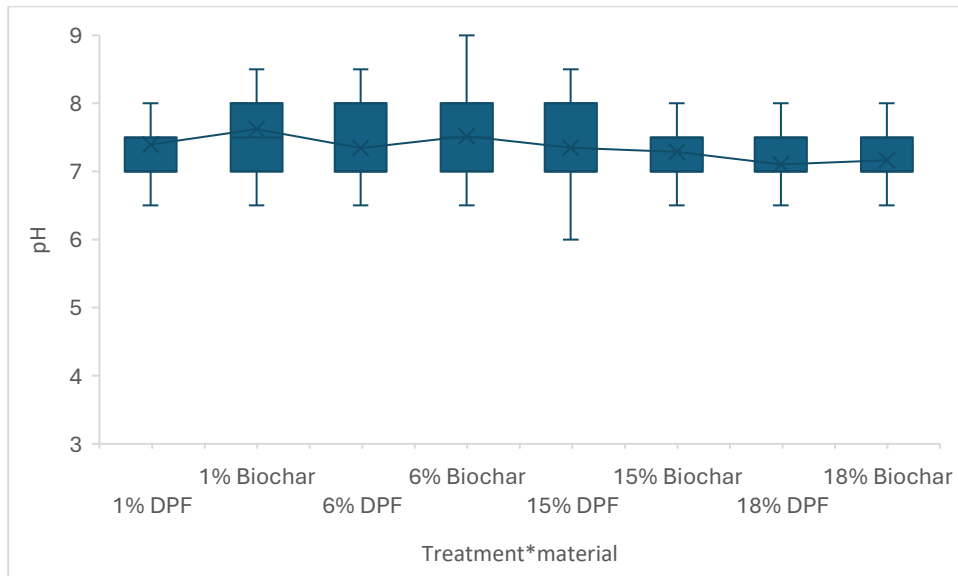
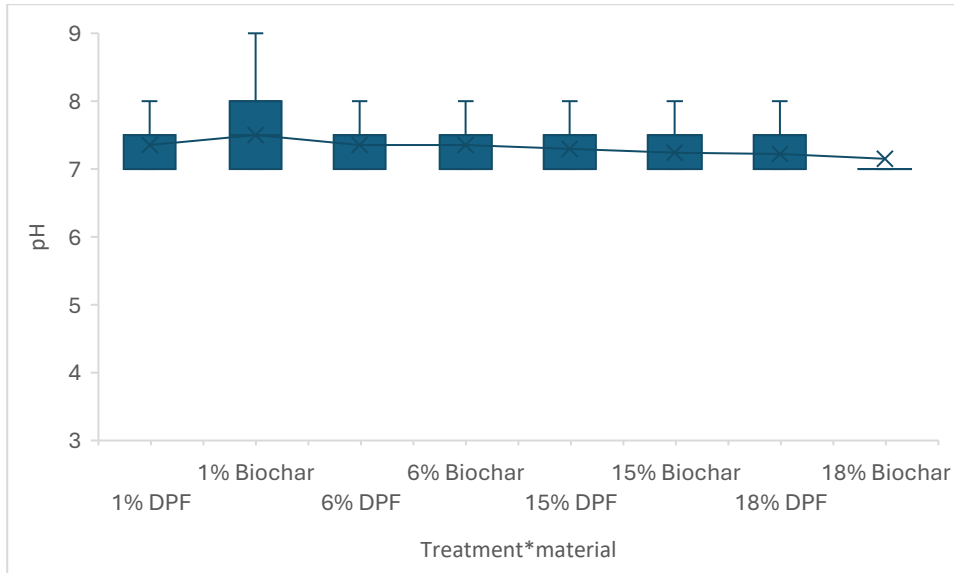


Figure 4.32. Boxplot of the soil pH relative to the Treatment*Material interaction measured during the wet cycle. Box-and-whisker plots show the interquartile range, with the box representing the first quartile (Q1) to the third quartile (Q3), and the whiskers extending from the minimum to the maximum values. The median is represented by a line within the box, and the cross symbol (x) indicates the mean soil pH.

Under uncontrolled wet cycle conditions, the 6% biochar exhibited the highest median soil pH at 9 (Figure 4.32). The lowest soil pH observed was the 1% DPF at 7.62 (Figure 4.32). The 1% biochar exhibited the highest mean soil pH recorded (7.62), followed by the lowest soil temperature, the 18% DPF recorded (7.10). Statistical analysis indicated that amended treatment material had a significant effect on soil pH during the wet cycle under controlled conditions ($p < 0.05$).

- Dry cycle

During the dry cycle, there was no observed difference in the soil pH; all were soil pH 7.



*Figure 4.33. Boxplot of the soil pH relative to the Treatment*Material interaction measured during the dry cycle. Box-and-whisker plots show the interquartile range, with the box representing the first quartile (Q1) to the third quartile (Q3), and the whiskers extending from the minimum to the maximum values. The median is represented by a line within the box, and the cross symbol (x) indicates the mean soil pH.*

With respect to Treatment*Material factor, and under uncontrolled dry cycle conditions, 1% biochar exhibited the highest median soil pH at (7.5) (Figure 4.33). Compared to the lowest median soil pH was the 18% biochar at 7 (Figure 4.33). The 1% biochar exhibiting the highest mean soil pH recorded (7.5), followed by the lowest soil pH the 18% biochar recorded (7.15). Statistical analysis indicated that amended treatment material had a significant effect on soil pH during the dry cycle under uncontrolled conditions ($p < 0.05$).

4.4.5 Light

4.4.5.1 Light in a controlled experiment

The light in these experiments was measured as a covariate and as a check upon the conditions being experienced.

- Wet cycle
- The light level observed was Dry cycle.

The pot trial in the laboratory-based experiment resulted in a low light exposure in all pot samples: there was no observed difference in both wet and dry cycles.

4.4.5.2 Light in an uncontrolled experiment

- Wet cycle

During the wet cycle, the light intensity experienced by all the control and treatments was measured to be the same at level 2.

4.4.6 Canopeo

Table 4.2. The percentage coverage of the canopy monitored during the controlled pot trial experiment.

| <i>Week/ Cycle</i> | <i>Canopy cover %</i> |
|--------------------|-----------------------|
| <i>Week 1/ Wet</i> | <i>1.53</i> |
| <i>Week 2/ Wet</i> | <i>5.6</i> |
| <i>Week 3/ Wet</i> | <i>7.43</i> |
| <i>Week 4/ Dry</i> | <i>0.30</i> |

For those measurements taken during the wet cycle, the highest percentage of green canopy cover was in the final week of measurement, and the second highest was during week 2 (Table 4.2). During the final week of the dry cycle, the cat grass had dried out and resulted in a no green canopy cover (% of 0.30 - Table 4.2). Data collection for canopy cover was discontinued due to the limited canopy coverage observed in this experiment.

4.4.7 ANOVA results

4.4.7.1 Controlled

- Height

The Anderson-Darling test and the QQ' plot (Figure 4.34) showed that the data were not normally distributed, and so the data were log transformed. The QQ' plot could indicate that some samples could be considered as outliers, and 1.90% of the samples were removed.

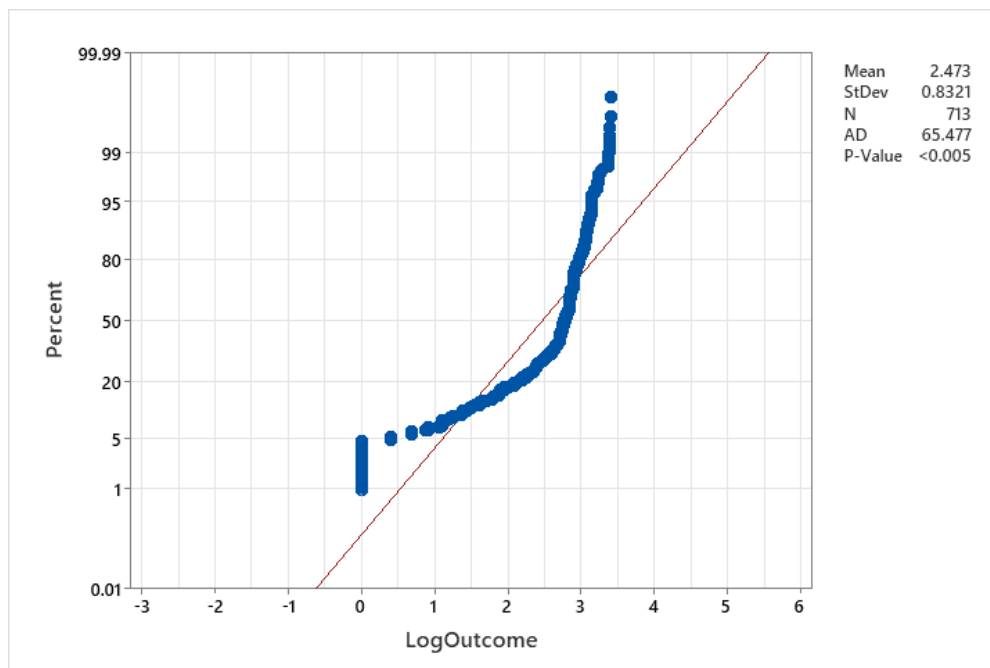


Figure 4.34. QQ' plot of the observed value of the height.

Table 4.3. The percentage of variance explained for significant ($P < 0.05$) factors and interactions for the Treatment, Material, Cycle, and Day factors for height.

| <i>Source</i> | <i>DF</i> | <i>P-Value</i> | <i>% of variance explained</i> |
|---------------------------|-----------|----------------|--------------------------------|
| <i>Treatment</i> | 4 | 0 | 6.54 |
| <i>Material</i> | 1 | 0 | 4.65 |
| <i>Cycle</i> | 1 | 0 | 28.03 |
| <i>Day</i> | 9 | 0 | 21.91 |
| <i>Treatment*Material</i> | 4 | 0.143 | 0.60 |
| <i>Treatment*Cycle</i> | 4 | 0.512 | 0 |
| <i>Treatment*Day</i> | 36 | 1 | 0 |
| <i>Material*Cycle</i> | 1 | 0.858 | 0 |
| <i>Material*Day</i> | 9 | 0.993 | 0 |
| <i>Cycle*Day</i> | 9 | 0 | 22.21 |
| <i>Error</i> | 634 | 0 | 16.06 |

The ANOVA, including all factors and two-way interactions, had an R^2 of 83.95%.

As measured by proportion of the original variance explained, the most important factor was Cycle, which explained 28.03% of the original variance in the dataset (Table 4.3). There were only two levels of the Cycle factor, and so post hoc analysis was not necessary.

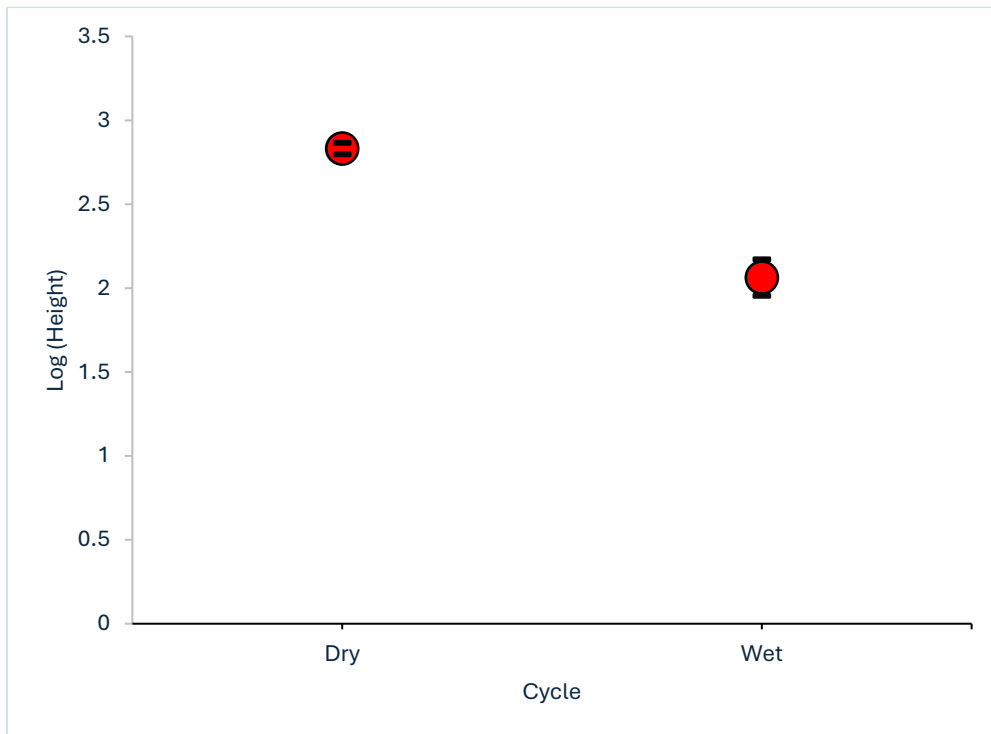


Figure 4.35. Main effects plot of the Cycle factor on height. Error bars are the 95% confidence interval.

The main effects plot of the Cycle factor showed that the vegetation height was slightly higher on the dry cycle than on the wet cycle (Figure 4.35).

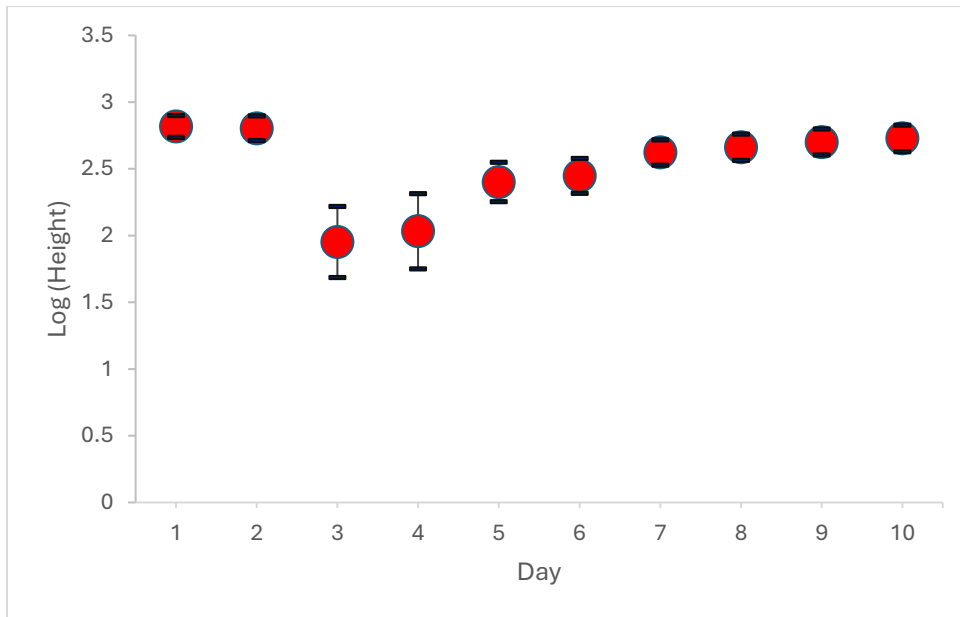


Figure 4.36. The main effect plot of the Day factor on height. Error bars are the 95% confidence interval and may be smaller than the plotted point.

The main effects plot of the Day factor shows that the vegetation height of the first and second days were the highest (Figure 4.36). The second highest vegetation height was the tenth day, followed by other days such as the ninth, eighth and the seventh days. The lowest values of vegetation height were on the third and the fourth days (Figure 4.36).

Table 4.4. Results of Tukey's post hoc test for height between levels of the Day factor. Levels not significantly different from each other share a common letter grouping.

| <i>Day</i> | <i>N</i> | <i>Mean</i> | <i>Grouping</i> | | |
|------------|----------|-------------|-----------------|---|---|
| 1 | 58 | 2.8171 | A | | |
| 2 | 60 | 2.8043 | A | | |
| 10 | 65 | 2.7276 | A | | |
| 9 | 65 | 2.7009 | A | | |
| 8 | 65 | 2.6623 | A | | |
| 7 | 71 | 2.6221 | A | | |
| 6 | 65 | 2.4477 | A | | |
| 5 | 85 | 2.4013 | A | B | |
| 4 | 89 | 2.032 | | B | C |
| 3 | 90 | 1.952 | | | C |

The post hoc analysis between the levels of the Days factor showed that there were 3 groups: A, B, and C. Day 1 showed a higher mean of vegetation compared to Day 5. Although Days 5, 4 and 3 have different groupings and some overlaps with each other, there were no significant differences except for Day 3 and Day 4 (Table 4.4).

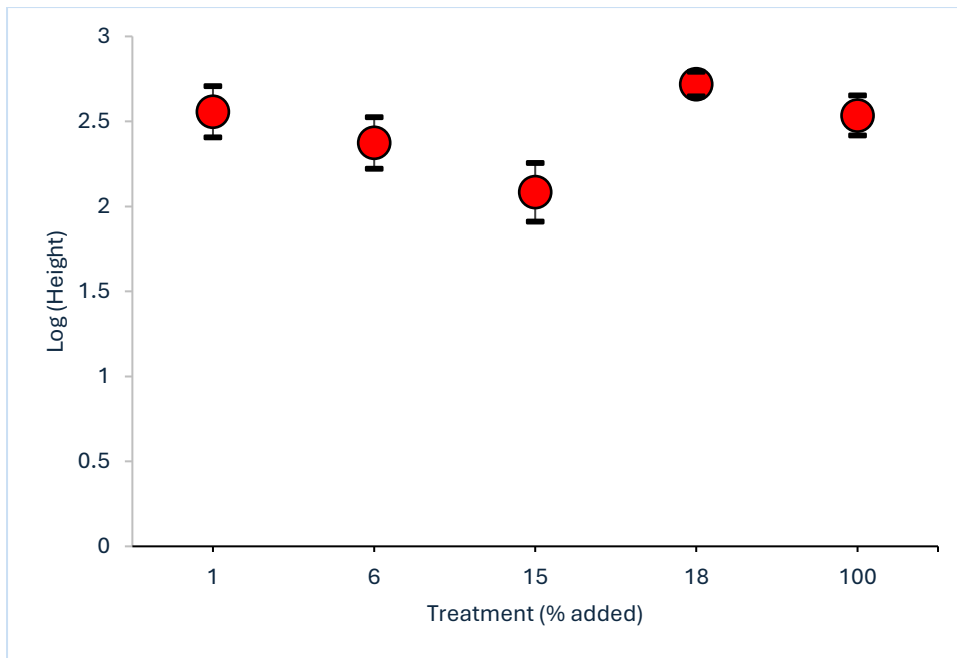


Figure 4.37. The main effect plot of the Treatment factor on height. Error bars are the 95% confidence interval but may be smaller than the plotted point.

The main effects plot of the Treatment factor showed that the vegetation height of the 18% treatment was the highest, and the lowest effect was for the 15% treatment (Figure 4.37).

Table 4.5. Results of Tukey's post hoc test for the height between levels of the Treatment factor. Levels not significantly different from each other share a common letter grouping.

| <i>Treatment</i> | <i>N</i> | <i>Mean</i> | <i>Grouping</i> | |
|------------------|----------|-------------|-----------------|---|
| 18 | 150 | 2.7196 | A | |
| 1 | 137 | 2.5566 | A | B |
| 100 | 172 | 2.5349 | A | B |
| 6 | 138 | 2.3733 | | B |
| 15 | 116 | 2.084 | | C |

The post hoc analysis between the levels of the Treatments factor showed that there were 3 groups: A, B and C (Table 4.5.). The 18% treatment showed a higher mean vegetation compared to the 1% treatment. However, treatments that showed significance were 1 and 100 (Table 4.5.).

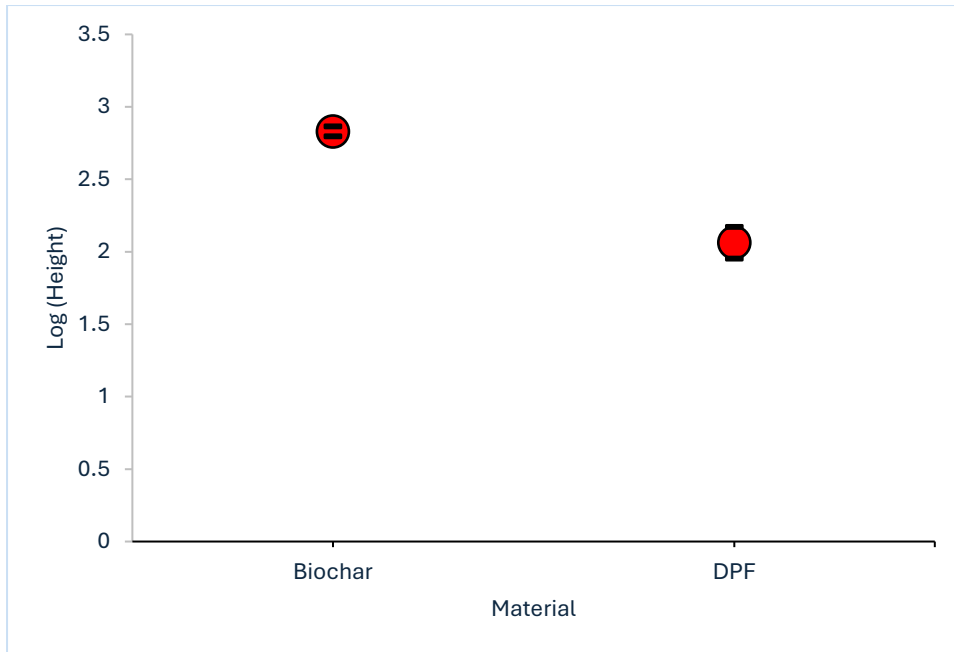


Figure 4. 38. The main effect plot of the Material factor on height. Error bars are the 95% confidence interval and may be smaller than the plotted point.

The main effect plot of the Material factor showed that biochar amended soil had greater plant height than DPF (Figure 4. 38).

- Moisture

The Anderson-Darling test and the QQ' plot showed that the moisture content data were not normally distributed (Figure 4.39). This plot could indicate that some samples could be considered as outliers, and 0.57% of the samples were removed.

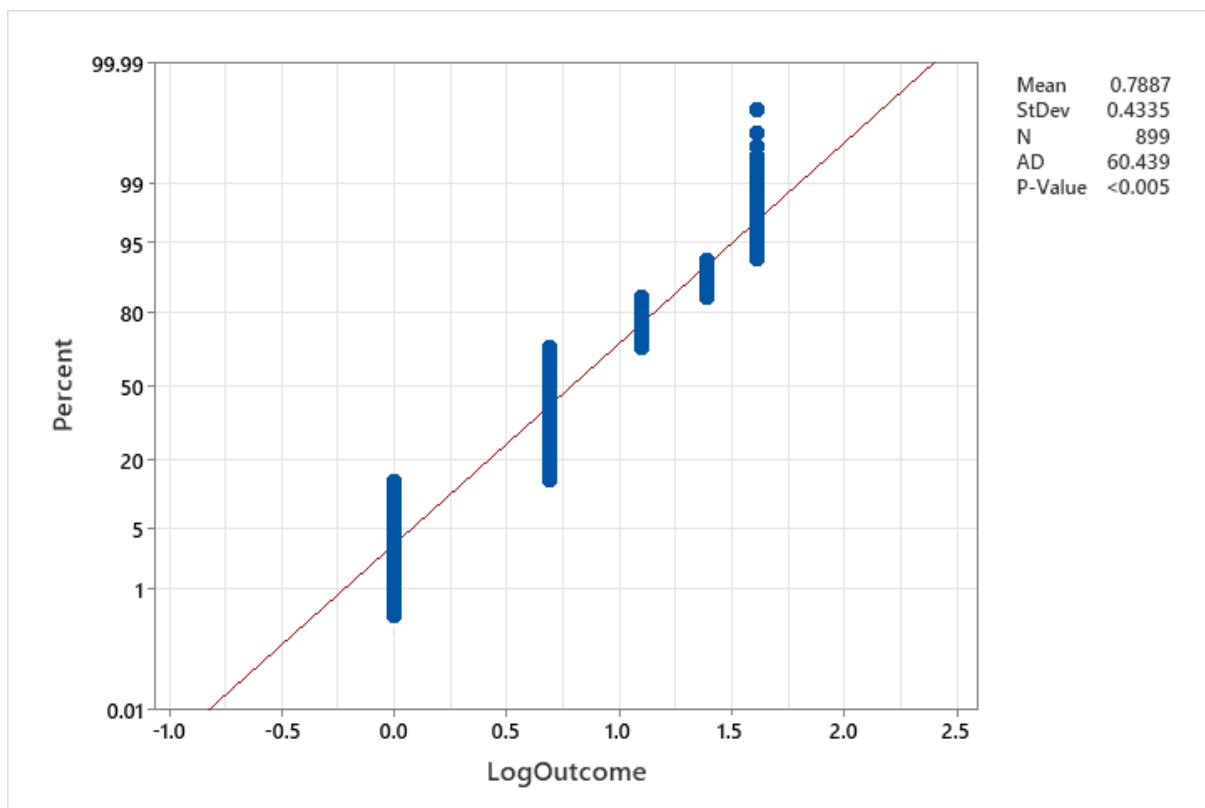


Figure 4.39. QQ' plot of the observed value of the moisture.

The ANOVA, including all factors and two-way interactions, had an R^2 of 87.25%.

Table 4.6. The percentage of variance explained for significant ($P < 0.05$) factors and interactions for the Treatment, Material and Cycle factors on the moisture content.

| <i>Source</i> | <i>DF</i> | <i>P-Value</i> | <i>% of variance explained</i> |
|---------------------------|-----------|----------------|--------------------------------|
| <i>Treatment</i> | 4 | 0 | 49.63 |
| <i>Material</i> | 1 | 0.003 | 6.26 |
| <i>Cycle</i> | 1 | 0 | 30.11 |
| <i>Treatment*Material</i> | 4 | 0.226 | 1.25 |
| <i>Treatment*Cycle</i> | 4 | 0.39 | 0 |
| <i>Material*Cycle</i> | 1 | 0.379 | 0 |
| <i>Error</i> | 898 | 0 | 12.75 |

As measured by proportion of the original variance explained, the most important factor was Treatment, which explained 49.63% of the original variance in the dataset (Table 4.6). There were only two levels of the Cycle factor, and so post hoc analysis was not necessary.

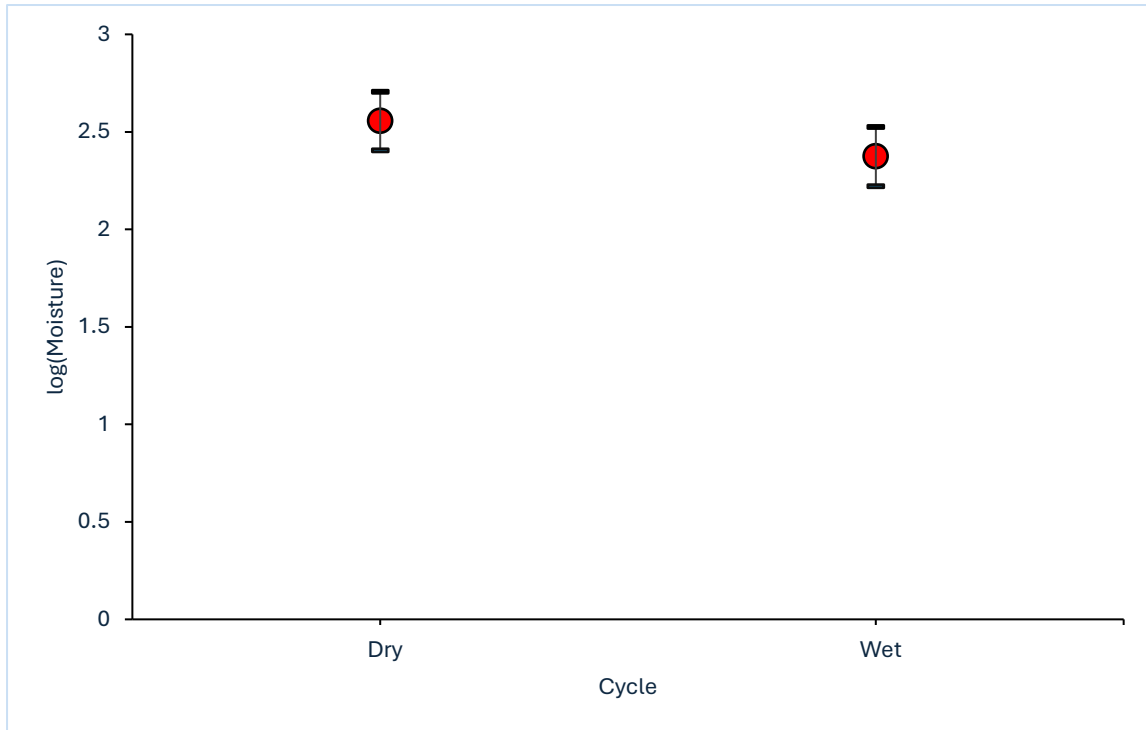


Figure 4.40. Main effects plot of the Cycle factor on moisture content. Error bars are the 95% confidence interval.

The main effects plot of the Cycle factor shows that the moisture content was higher on the dry cycle than the wet cycle by 1.58% (Figure 4.40).

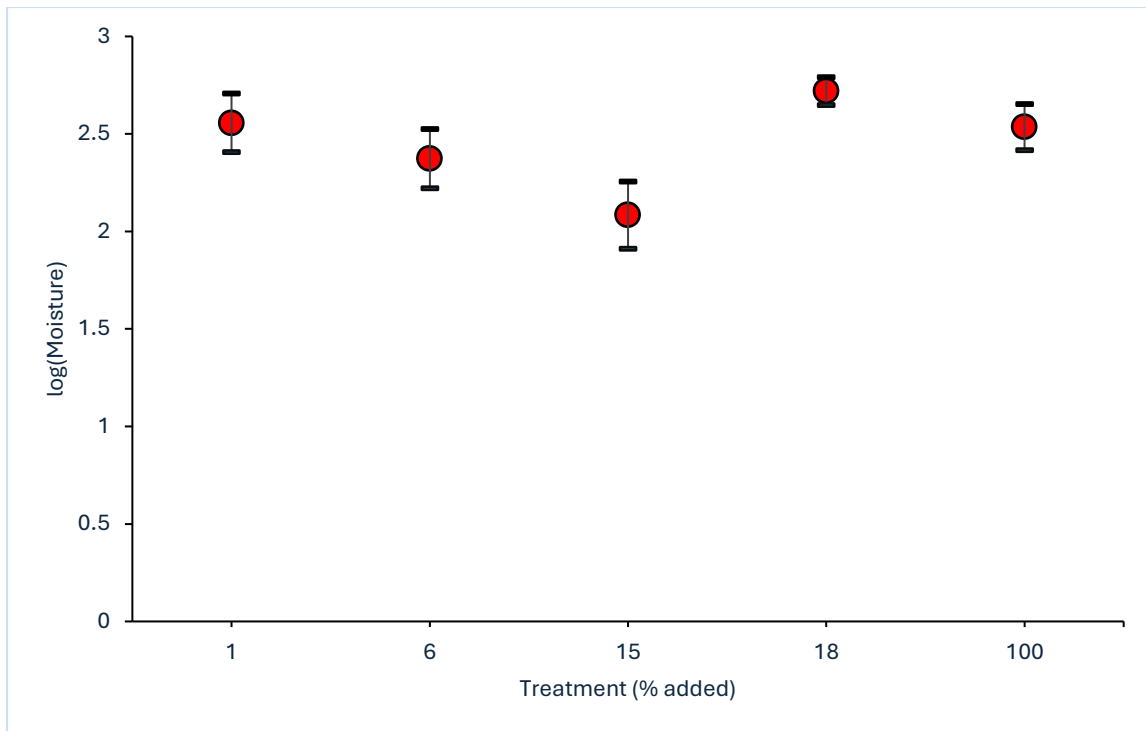


Figure 4.41. Main effects plot of the Treatment factor on moisture content. Error bars are the 95% confidence interval and may be smaller than the plotted point.

The main effects plot of the Treatment factor shows that soil moisture of the 18% and 1% treatments was the highest. The lowest moisture content was for the 15% treatment (Figure 4.41).

Table 4.7. Results of Tukey's post hoc test for the Moisture between levels of the Treatment factor. Levels not significantly different from each other share a common letter grouping.

| <i>Treatment</i> | <i>N</i> | <i>Mean</i> | <i>Grouping</i> |
|------------------|----------|-------------|-----------------|
| 18 | 180 | 0.9 | A |
| 15 | 180 | 0.8663 | A |
| 6 | 180 | 0.8345 | A |
| 1 | 179 | 0.7857 | A |
| 100 | 180 | 0.5569 | B |

The post hoc analysis between the levels of the Treatment factor showed there were two groups: A and B (Table 4.7). The 18% treatment showed a higher mean moisture content compared to 100% treatment (Table 4.7).

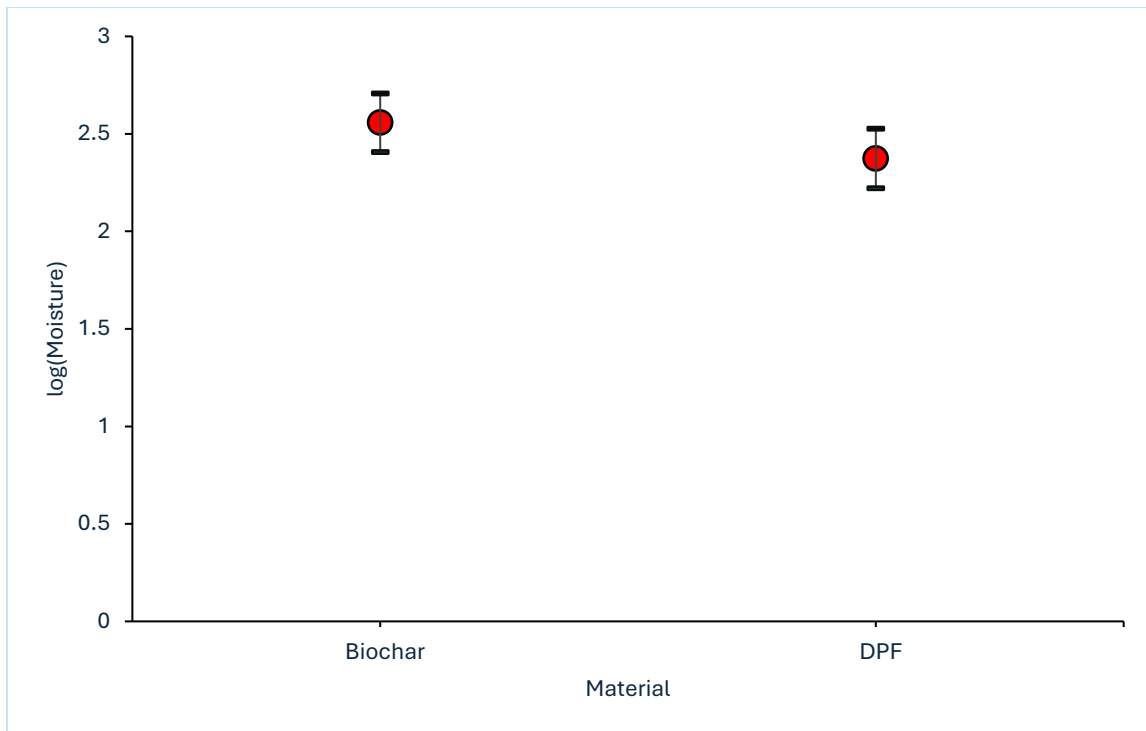


Figure 4.42. Main effects plot of the Material factor on moisture content. Error bars are the 95% confidence interval.

The main effects plot of the Material factor shows that the soil moisture of the biochar was slightly higher than DPF by 0.2% (Figure 4.42).

- pH

The Anderson-Darling test and the QQ' plot showed that the pH content data were not normally distributed (Figure 4.43). This plot could indicate that some samples could be considered as outliers, and 0.27% of the samples were removed.

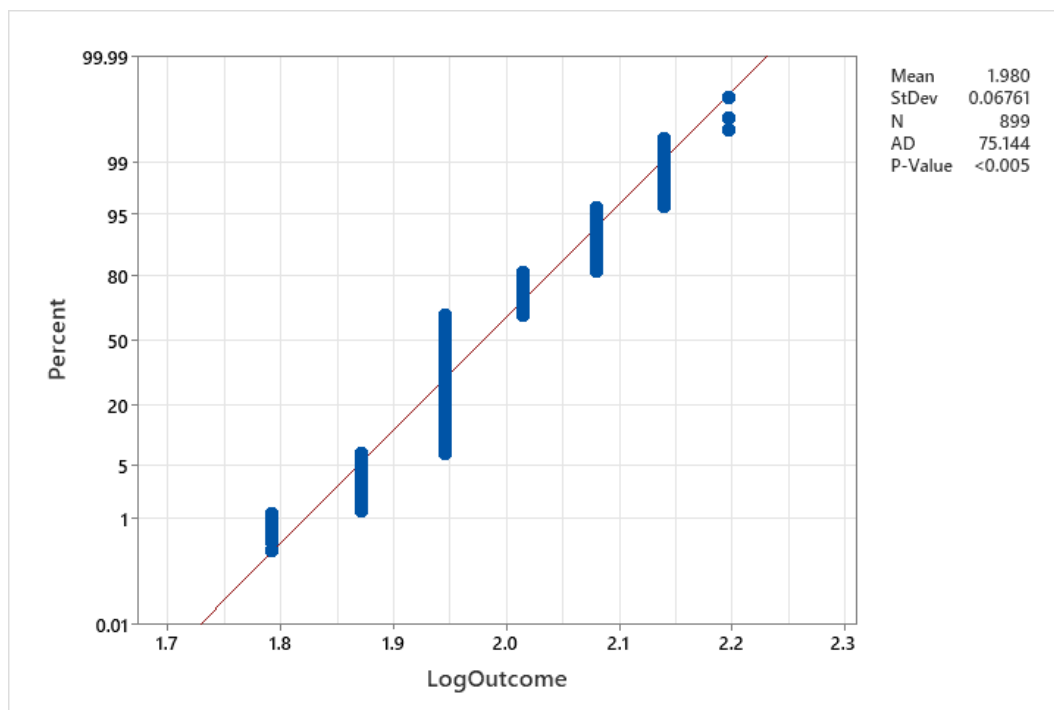


Figure 4.43 QQ' plot of the observed values of the pH.

The ANOVA, including all factors and two-way interactions, had an R^2 of 83.21%.

Table 4.8. The percentage of variance explained for significant ($P < 0.05$) factors and interactions for the Treatment, Material and Cycle factors on the pH.

| <i>Source</i> | <i>DF</i> | <i>P-Value</i> | <i>% of variance explained</i> |
|---------------------------|-----------|----------------|--------------------------------|
| <i>Treatment</i> | 4 | 0 | 76.76 |
| <i>Material</i> | 1 | 0.576 | 0 |
| <i>Cycle</i> | 1 | 0.885 | 0 |
| <i>Treatment*Material</i> | 4 | 0.013 | 6.45 |
| <i>Treatment*Cycle</i> | 4 | 0.328 | 0 |
| <i>Material*Cycle</i> | 1 | 0.306 | 0 |
| <i>Error</i> | 799 | 0 | 16.28 |

As measured by proportion of the original variance explained, the most important factor was Treatment, which explained 76.76% of the original variance in the dataset (Table 4.8). There were only two levels of the Treatment factor, and so post hoc analysis was unnecessary.

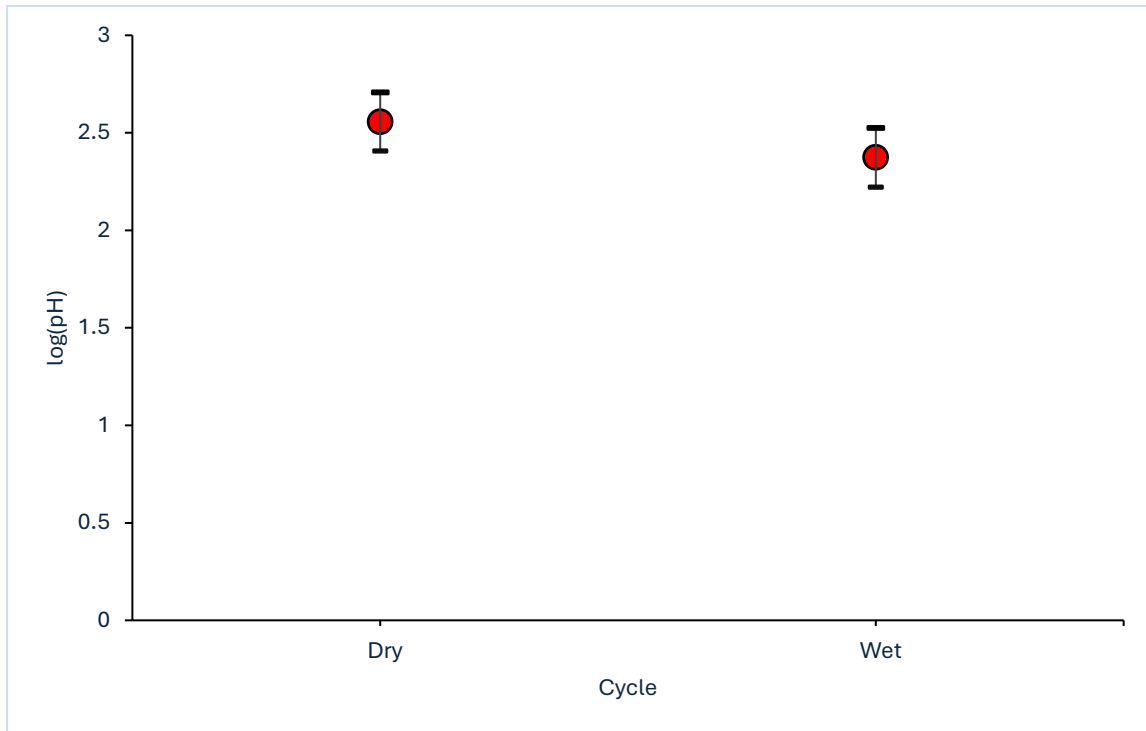


Figure 4.44. Main effects plot of the Cycle factor on moisture content. Error bars are the 95% confidence interval.

The main effects plot of the Cycle factor shows that the pH vegetation was slightly higher on the dry cycle than the wet cycle (Figure 4.44).

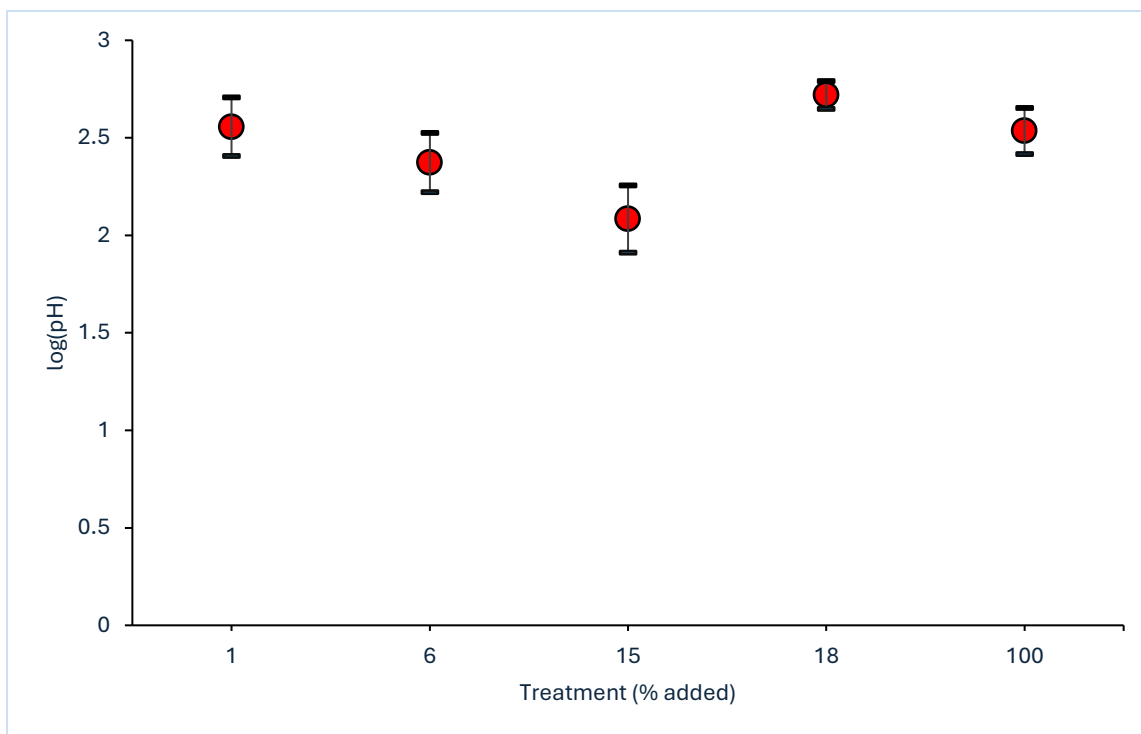


Figure 4.45. Main effects plot of the Treatment factor on moisture content. Error bars are the 95% confidence interval and may be smaller than the plotted point.

The main effects plot of the Treatment factor showed that the soil pH of the 18% treatment was the highest. The lowest soil pH was for the 15% treatment (Figure 4.45).

Table 4.9. Results of Tukey's post hoc test for the pH between levels of the Treatment factor. Levels not significantly different from each other share a common letter grouping.

| <i>Treatment</i> | <i>N</i> | <i>Mean</i> | <i>Grouping</i> | |
|------------------|----------|-------------|-----------------|---|
| <i>1</i> | 179 | 2.01022 | A | |
| <i>6</i> | 180 | 1.99983 | A | B |
| <i>15</i> | 180 | 1.98613 | | B |
| <i>18</i> | 180 | 1.96475 | | C |
| <i>100</i> | 180 | 1.93866 | | D |

The pH was compared in different treatments using post hoc analysis, and Table 4.9 shows there were 4 groupings: A, B, C and D (Table 4.9). Where group A and B overlap on the 6% treatment. Although it might show overlaps, group A was significant on the 1% treatment, and group B was significant on the 15% treatment.

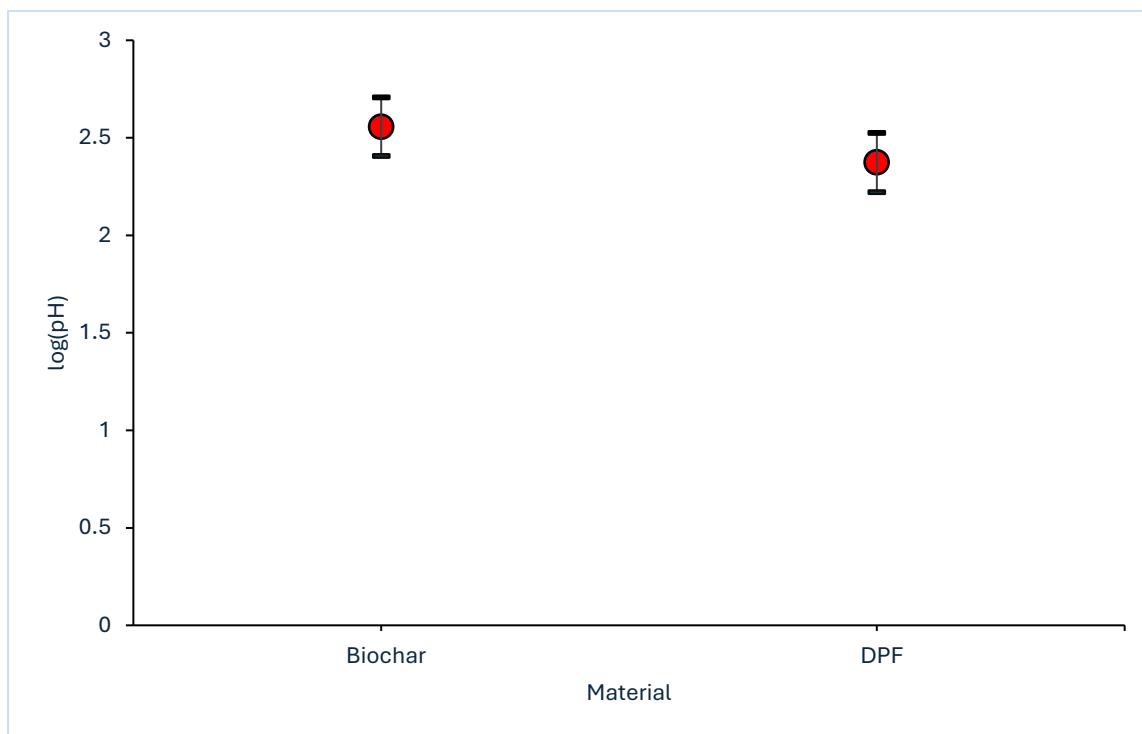


Figure 4.46. Main effects plot of the Material factor on moisture content. Error bars are the 95% confidence interval.

The main effects plot of the Material factor shows that the pH of the biochar treatment was slightly higher than DPF (Figure 4.46).

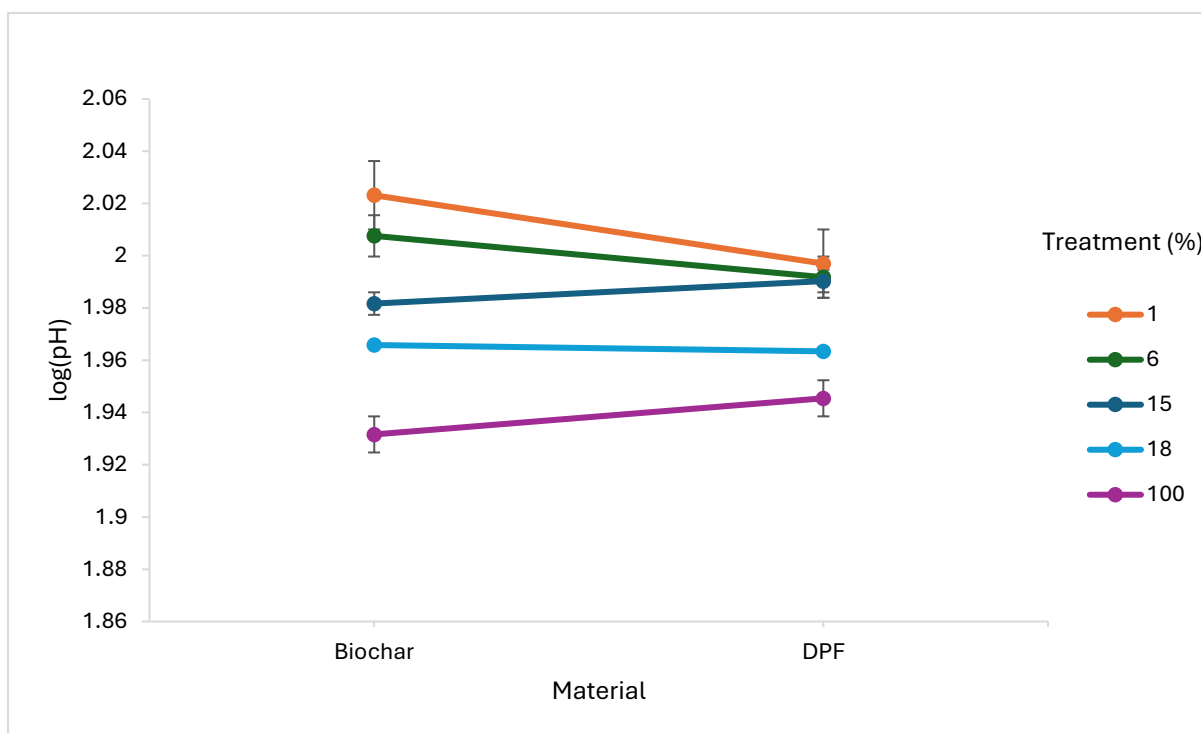


Figure 4.47. The interaction plot of the soil pH between Materials and Treatment factors.

The Treatment*Material interaction was found to be significant (Table 4.8 & Figure 4.47). The plot suggests that some of the soil pH of biochar was higher than DPF. The highest biochar treatments were 1%, 6% and 18% soil pH. As for the soil pH of DPF were higher than biochar on treatments like 6% and 100%. Both materials, the biochar and DPF, share the highest treatment was 1% soil pH, and the lowest was the control 100% (Figure 4.47).

- Soil temperature

The Anderson-Darling test and the QQ' plot showed that the soil temperature data were not normally distributed (Figure 4.48). This plot could indicate that some samples could be considered as outliers, and 0.57% of the data were removed.

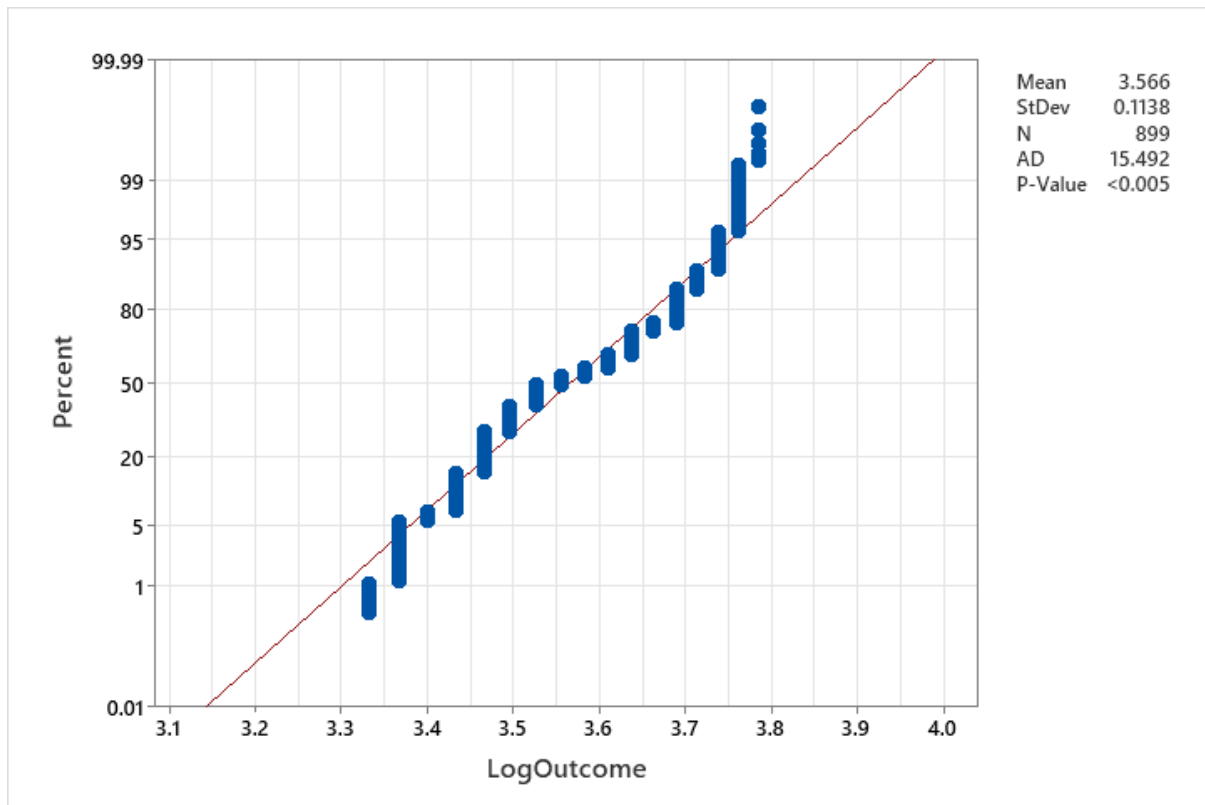


Figure 4.48. QQ' plot of the observed value of the temperature.

The ANOVA, including all factors and two-way interactions, had an R^2 of 1.37%.

Table 4.10. The percentage of variance explained for significant ($P < 0.05$) factors and interactions for the Treatment, Material and Cycle factors on the temperature.

| <i>Source</i> | <i>DF</i> | <i>P-Value</i> | <i>% of variance explained</i> |
|---------------------------|-----------|----------------|--------------------------------|
| <i>Treatment</i> | 4 | 0.426 | 8.94 |
| <i>Material</i> | 1 | 0.996 | 62.21 |
| <i>Cycle</i> | 1 | 0.526 | 15.43 |
| <i>Treatment*Material</i> | 4 | 0.262 | 0 |
| <i>Treatment*Cycle</i> | 4 | 0.951 | 0 |
| <i>Material*Cycle</i> | 1 | 0.67 | 13.42 |
| <i>Error</i> | 883 | 0 | 0 |

As measured by proportion of the original variance explained, the most important factor was Material, which explained 62.21% of the original variance in the dataset (Table 4.10). However, this effect was not significant. There were only two levels of the Cycle factor, and so no post hoc analysis was necessary.

4.4.7.2 Uncontrolled

- Height

The Anderson-Darling test and the QQ' plot showed that the height data were not normally distributed (Figure 4.49). This plot could indicate that some samples could be considered as outliers, and 34.26% were necessarily removed.

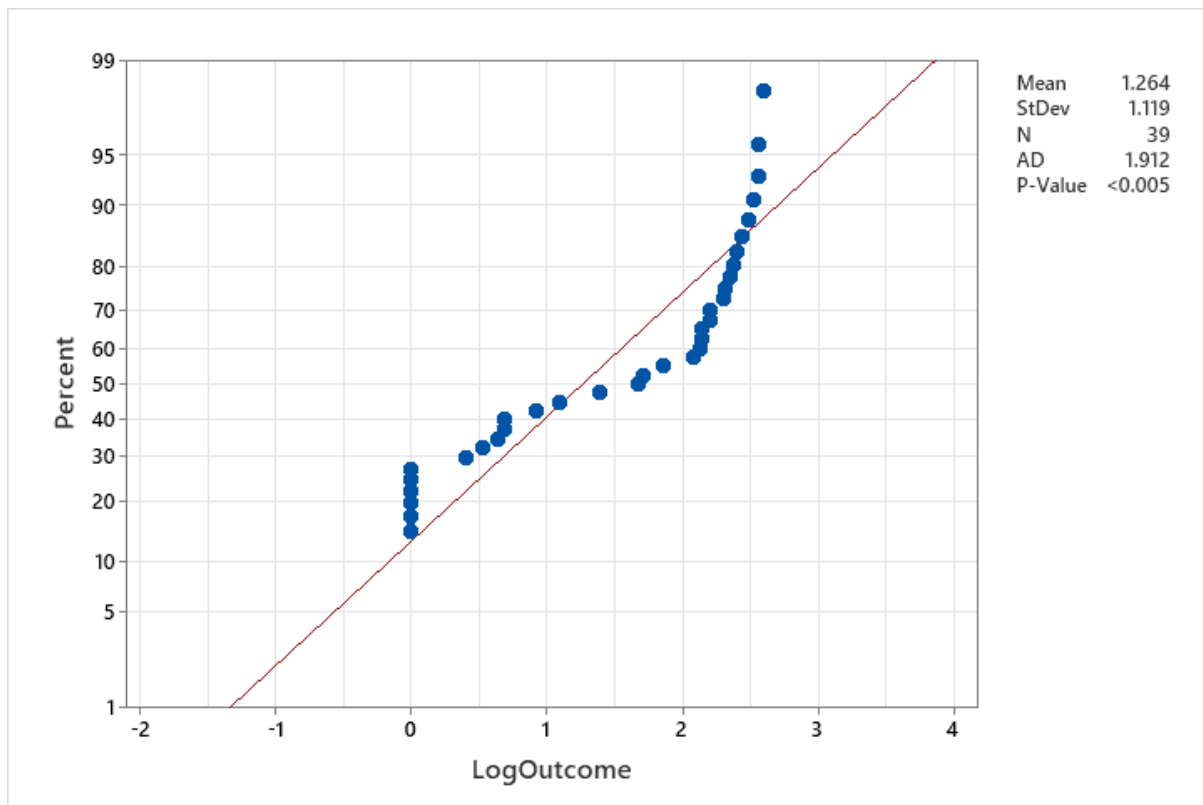


Figure 4.49. QQ' plot of the observed value of the height.

The ANOVA, including all factors and two-way interactions, had an R^2 of 77.2 % (Table 4.11).

Table 4.11. The proportion of significant ($P < 0.05$) factors for the treatment, material, cycle and day.

| <i>Source</i> | <i>DF</i> | <i>P-Value</i> | <i>% of variance explained</i> |
|---------------------|-----------|----------------|--------------------------------|
| <i>Treatment</i> | 4 | 0 | 67.7 |
| <i>Cycle</i> | 1 | 0.169 | 1.76 |
| <i>Material*Day</i> | 7 | 0.861 | 2.77 |
| <i>Error</i> | 26 | 0 | 22.81 |

As measured by proportion of the original variance explained, the most important factor was Treatment, which explained 67.7% of the original variance in the dataset. Therefore, the post hoc analysis was necessary (Table 4.11).

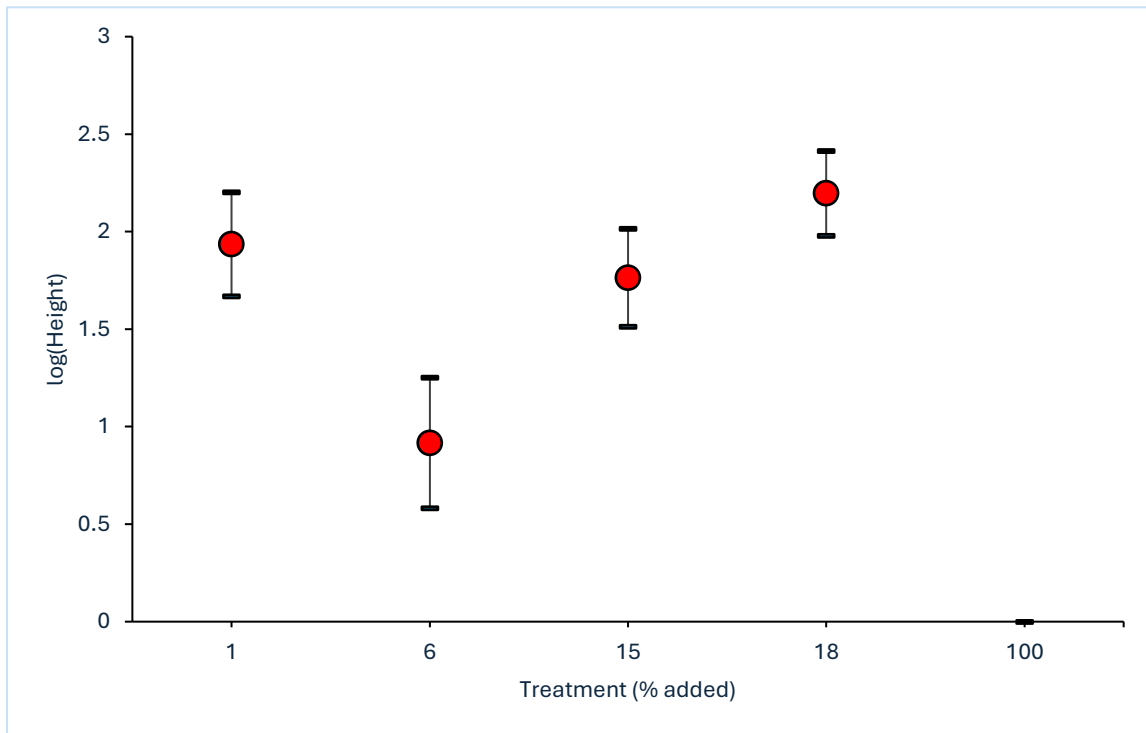


Figure 4.50. Main effects plot of the Treatment factor on plant height. Error bars are the 95% confidence interval and may be smaller than the plotted point.

The main effects plot of the Treatment factor showed that the 18% treatment was the highest.

The lowest height shown was the 100% treatment (Figure 4.50).

Table 4.12. Results of Tukey's post hoc test for the height of the Treatment factor. Levels not significantly different from each other share a common letter grouping.

| <i>Treatment</i> | <i>N</i> | <i>Mean</i> | <i>Grouping</i> |
|------------------|----------|-------------|-----------------|
| <i>1</i> | 8 | 220 | A |
| <i>6</i> | 6 | 1.94 | A |
| <i>15</i> | 7 | 1.78 | A |
| <i>18</i> | 4 | 0.92 | B |
| <i>100</i> | 14 | -0.32 | C |

The height was compared in different treatments using post hoc analysis, and Table 4.12 shows there were 3 groupings: A, B and C. Groups B and C were mostly significant, but there was a slight difference between both treatments (Table 4.12).

- Soil moisture

The Anderson-Darling test and the QQ' plot showed that the moisture data were not normally distributed (Figure 4.51). This plot could indicate that some samples could be considered as outliers, and 0.57% of the data were removed.

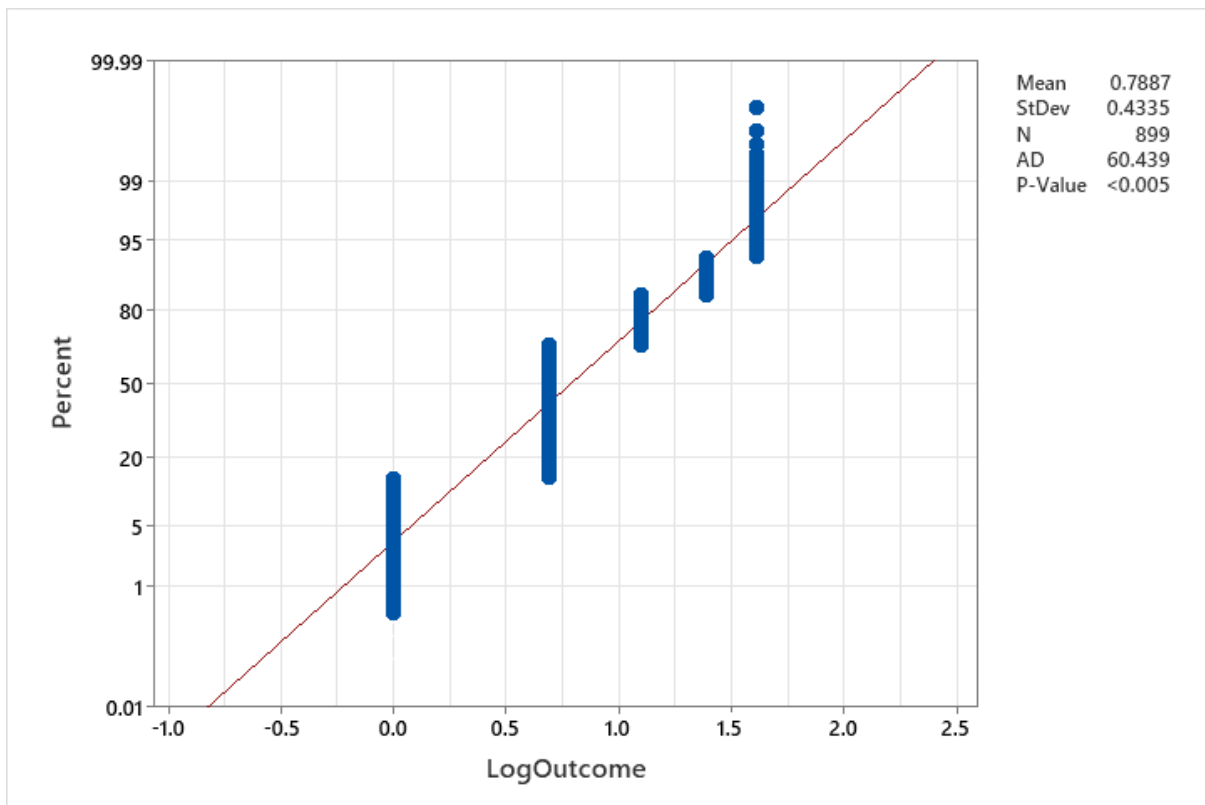


Figure 4.51. QQ' plot of the observed value of the soil moisture.

The ANOVA, including all factors and two-way interactions, had an R^2 of 15.20 % (Table 4.13).

Table 4.13. The proportion of significant ($P < 0.05$) factors for the treatment, material, and cycle.

| <i>Source</i> | <i>DF</i> | <i>P-Value</i> | <i>% of variance explained</i> |
|---------------------------|-----------|----------------|--------------------------------|
| <i>Treatment</i> | 4 | 0 | 7.92 |
| <i>Material</i> | 1 | 0.005 | 0.78 |
| <i>Cycle</i> | 1 | 0 | 3.70 |
| <i>Material*Treatment</i> | 4 | 0.239 | 0.56 |
| <i>Material*Day</i> | 9 | 0.982 | 0.25 |
| <i>Treatment*Day</i> | 36 | 0.986 | 1.98 |
| <i>Error</i> | 843 | 0 | 84.81 |

As measured by the proportion of the original variance explained, the most important factor was the Treatment factor, which explained 7.92% of the original variance in the dataset. There were only two levels of the Treatment factor, and so no post hoc analysis was necessary.

- Soil pH

The Anderson-Darling test and the QQ' plot showed that the pH data were not normally distributed (Figure 4.52). This plot could indicate that some samples could be considered as outliers, of 0.57% were necessarily removed.

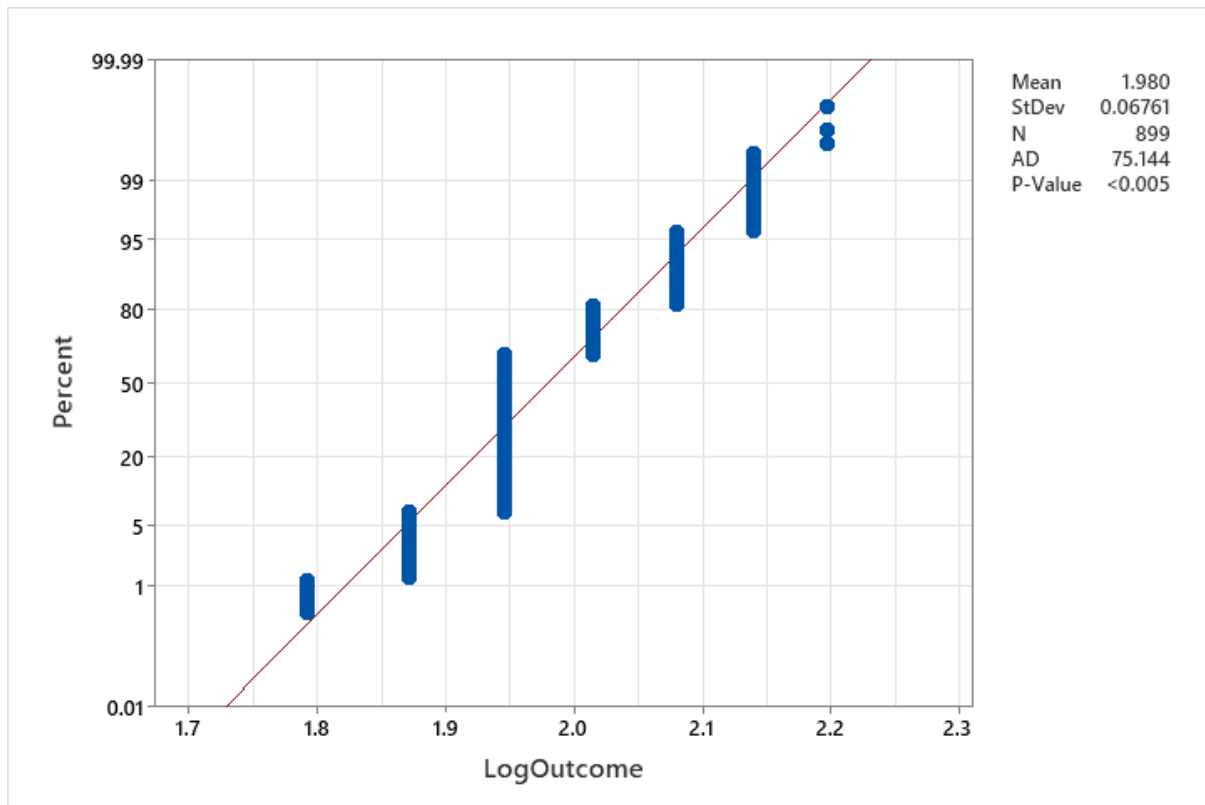


Figure 4.52. QQ' plot of the observed value of the pH.

The ANOVA, including all factors and two-way interactions, had an R^2 of 16.26 % (Table 4.14).

Table 4.14. The proportion of significant ($P < 0.05$) factors for the treatment, material and cycle.

| <i>Source</i> | <i>DF</i> | <i>P-Value</i> | <i>% of variance explained</i> |
|---------------------------|-----------|----------------|--------------------------------|
| <i>Treatment</i> | 4 | 0 | 10.34 |
| <i>Material</i> | 1 | 0.576 | 0.03 |
| <i>Cycle</i> | 1 | 0.885 | 0.002 |
| <i>Treatment*Material</i> | 4 | 0.013 | 1.22 |
| <i>Treatment*Cycle</i> | 4 | 0.328 | 0.44 |
| <i>Material*Cycle</i> | 1 | 0.306 | 0.10 |
| <i>Error</i> | 883 | 0 | 83.74 |

As measured by proportion of the original variance explained, the most important factor was Treatment, which explained 10.34% of the original variance in the dataset. There were only two levels of the Treatment factor, and so no post hoc analysis was necessary.

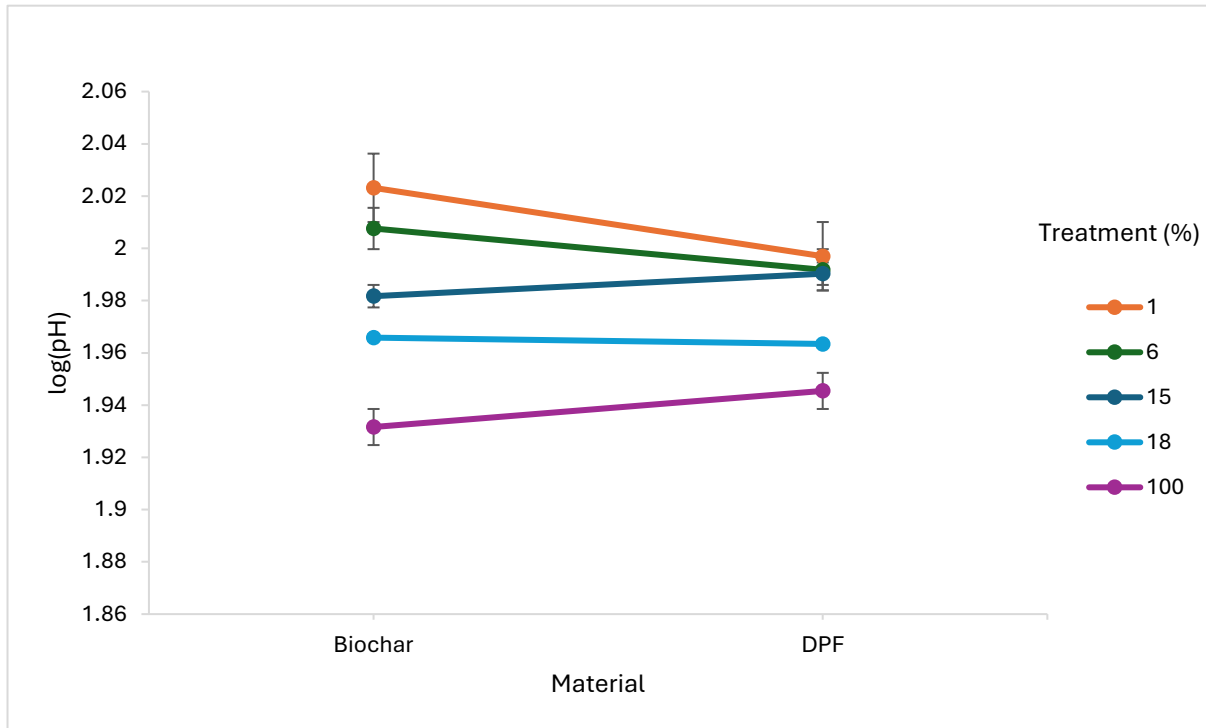


Figure 4.53. The interaction plot for pH between Material and Treatment factor.

The highest pH was 1% biochar, and the lowest was the 18% control DPF. The lowest from the control was the 100% DPF treatment (Figure 4.53).

- Soil Temperature

The Anderson-Darling test and the QQ' plot showed that the Temperature data were not normally distributed (Figure 4.54). This plot could indicate that some samples could be considered as outliers, of 0.57% were necessarily removed.

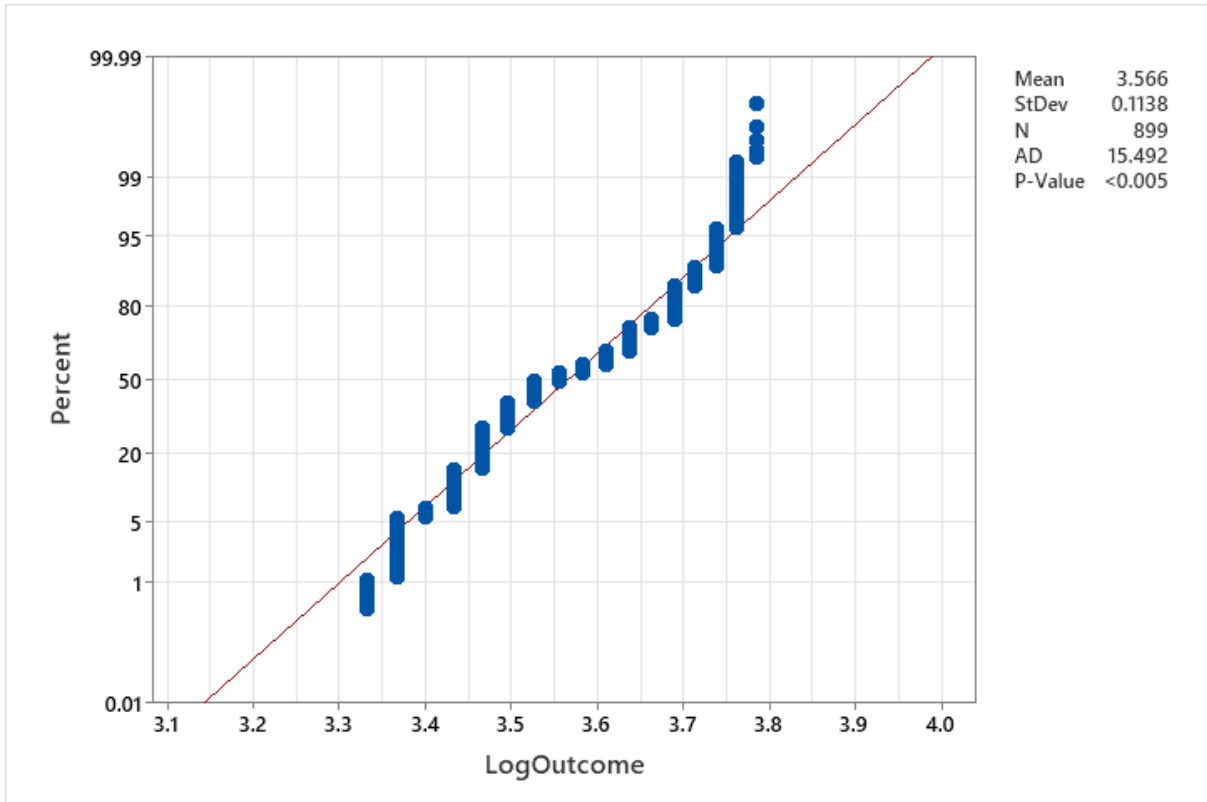


Figure 4.54. QQ' plot of the observed value of the temperature.

The ANOVA, including all factors and two-way interactions, had an R^2 of 1.37 % (Table 4.15).

Table 4.15. The proportion of significant ($P < 0.05$) factors for the treatment, material and cycle.

| <i>Source</i> | <i>DF</i> | <i>P-Value</i> | <i>% of variance explained</i> |
|---------------------------|-----------|----------------|--------------------------------|
| <i>Treatment</i> | 4 | 0.426 | 22.39 |
| <i>Material</i> | 1 | 0.996 | 5.60 |
| <i>Cycle</i> | 1 | 0.526 | 22.40 |
| <i>Treatment*Material</i> | 4 | 0.262 | 22.37 |
| <i>Treatment*Cycle</i> | 4 | 0.951 | 22.42 |
| <i>Material*Cycle</i> | 1 | 0.67 | 5.60 |
| <i>Error</i> | 883 | 0 | 0 |

As measured by proportion of the original variance explained, the most important factor was Treatment*Cycle, which explained 22.42% of the original variance in the dataset. There were only two levels of the Treatment factor, and so no post hoc analysis was necessary.

4.5 Discussion

The aim of this study was to examine the plant growth responses to soil amendments under different environmental conditions and moisture regimes. The results presented in this chapter demonstrated that soil amendments influenced plant growth, soil moisture dynamics and soil properties under both controlled laboratory and uncontrolled field conditions. These findings provide insight into how biochar and date palm fronds (DPF) amendments interact with sandy soils and environmental stress factors such as high temperatures and limited water availability.

The results indicated that amended soil with biochar did increase plant growth. Such as the 1% biochar application impacted plant growth particularly under controlled condition. Other treatments noticed were mostly the 1% DPF, 1% biochar, 6% DPF and 6% biochar. These findings align with the studies of Laird et al (2010) and Major et al. (2010), which reported enhanced plant growth with biochar application due to improved soil structure and nutrient availability. Increasing the carbon content of the soil, increases aggregation and decreases the bulk density (Badawi, 2020). Biochar could also change the sand texture and become more organic carbon dominated, which changes the minerals in the soil (Badawi, 2020). However, other studies contradict our findings, like Karbout et al. (2019), who found no significant improvements or benefits of biochar application to soil and had less yield growth.

Although biochar improved plant growth under controlled conditions, the same was not observed in the uncontrolled condition. In the uncontrolled field pot trials, plant growth was limited across most treatments, and biochar amendments did not consistently enhance plant development. In contrast, some growth was observed in pots containing DPF. This difference is likely related to the extreme environmental conditions during the field experiment, including high temperatures and intense solar radiation, which may have limited seed germination and early plant establishment. Under such conditions, the potential benefits of biochar amendments may be overshadowed by environmental stress, particularly during the early stages of plant

growth. The low amendment levels improved soil structure and moisture retention, such as 1% biochar amendment, as shown in this study. Compared to higher amendment rates, biochar alters soil aeration, nutrient availability, and water distribution within the pot environment. Previous studies have similarly reported that moderate to low biochar application rates often produce more favourable plant responses than high amendment levels, particularly in sandy soils where small changes in soil structure can significantly influence plant growth. The main effects plot suggested that plant height was higher during the dry cycle; this reflects cumulative growth from the preceding wet cycle rather than increased growth during the dry cycle period itself. When plant growth is considered relative to the start of each cycle, growth during the dry cycle was reduced, indicating that limited water availability constrained plant development. These amendment levels demonstrated consistent and meaningful effects on plant growth and soil moisture retention compared to other treatments. Based on the findings from this chapter and the mesocosm experiment presented in Chapter 3, amendment levels of 1% and 18% were identified as representing effective low and high application rates, respectively. These amendment levels were therefore selected for further investigation in Chapter 6 to enable a more focused evaluation of amendment performance and to explore the potential combined effects of biochar and DPF on soil properties and plant growth.

The moisture content indicated that sand had higher moisture levels during a controlled wet cycle, while biochar and DPF showed higher moisture retention during dry cycles, particularly at 1%, 6% and 18% concentrations. Although our study proved that sand can retain water in controlled condition, other studies have shown the opposite, that sand in the United Arab Emirates lacks organic matter and soil structure, which means the soil does not aggregate to retain water (Baïamonte *et al.*, 2019). Other studies that support our findings of biochar application to soil indicate that biochar has capabilities in retaining water (Sun *et al.*, 2023). Others suggest that the biochar effect on moisture content could be negligible in certain types

of soils (Rabbi *et al.*, 2021). During the uncontrolled condition, the water retention remained challenging despite the addition of biochar and DPF. The changing of weather and humidity made it challenging to maintain the moisture levels.

The soil pH of biochar treatments resulted in higher soil pH compared to DPF, with the highest pH observed at 1% biochar treatment. This result aligns with studies of Tusar *et al.* (2023) and Zubairu *et al.* (2023), which found that biochar application to acidic soils can raise soil pH. Another study showed that the type of feedstock and pyrolysis conditions used to produce biochar can influence soil pH (Tomczyk, *et al.*, 2020).

The study found that biochar had higher soil temperatures during dry cycles, while DPF showed higher temperatures during wet cycles. A study showed that changes in soil temperature when mixed with biochar are minimal, depending on specific environmental conditions and the rates at which biochar is applied (Feng *et al.*, 2021). However, the soil temperature observed differences between biochar and DPF treatments relate to the differences in material composition between charred and uncharred organic materials. Raw DPF contains natural plant composition such as waxes, lignin and cellulose, which may influence heat transfer and moisture interactions in the soil. In contrast to biochar, which undergoes pyrolysis, resulting in a more porous carbon structure with different thermal properties. These differences in material structure may partly explain the variation in soil temperature observed between the two amendments. The small differences observed in soil temperature. These interpretations should be considered exploratory and would benefit from further investigation using more precise thermal measurements.

The probe moisture meter played a vital role in the research, but its prolonged use caused some values to stabilise, particularly in pH level and light exposure measurements. Consequently, it was decided to monitor the pot trial for a limited period. Moreover, monitoring light exposure

under uncontrolled conditions proved to be difficult due to intense sunlight, necessitating experimentation during late afternoon hours. Another challenge encountered was the seed germination under these conditions. Despite using cat grass, carrots, and watermelon seeds, success was not achieved due to exposure to open air, leading to heat exhaustion. To overcome this, a shed was constructed to reduce heat exposure, ultimately resulting in successful watermelon germination after several weeks.

The outcomes of this research are applicable to various regions globally, particularly those experiencing extreme weather conditions or water scarcity. This study identifies strategies that can be utilised in indoor settings more than outdoor settings. Before starting crop production, farmers and researchers must carefully evaluate the current weather patterns and select crop varieties that are well-suited to the existing seasonal conditions. Notably, the results of this investigation highlight the importance of taking such precautionary measures, as demonstrated by the successful cultivation of watermelons during the summer season in the United Arab Emirates. Additionally, the research highlights the role of biochar, particularly when derived from Date Palm Fronds (DPF), in enhancing plant growth. The study reveals that biochar and DPF can significantly improve plant growth in indoor environments, especially when applied to sandy soils. The effectiveness of biochar in retaining water is more pronounced under controlled conditions than in uncontrolled settings, suggesting its potential utility in sheltered environments, even under harsh climates. It is also important to consider that the effects of biochar and organic amendments such as DPF may become more pronounced over longer time periods. Biochar can gradually interact with soil minerals, organic matter and microbial communities, potentially improving soil aggregation, nutrient retention and water holding capacity over time. Similarly, organic residues such as PDF may undergo decomposition processes that influence soil structure and nutrient cycling. Because the pot trials conducted in this study were relatively short-term experiments, some of these longer-term biogeochemical

processes may not have been fully captured. Long-term field experiments would therefore provide valuable insight into how these soil amendments influence soil properties and crop productivity over extended periods. Some limitations should be considered when interpreting the results of this study. The pot trial experiments were conditioned over relatively short time periods and under uncontrolled container conditions, which may not fully replicate field-scale agricultural systems. In addition, the uncontrolled field experiment experienced extreme environmental conditions that limited germination for several plant species, resulting in successful growth primarily for watermelon. Despite these constraints, the experiment provides useful insights into how soil amendments interact with sandy soils and environmental stress factors. This chapter adds to the discussion on sustainable agriculture by offering ideas that could help create better ways to grow crops in dry regions. Further research, including the investigation presented in Chapter 6, can expand on these findings to evaluate the long-term and combined effects of biochar and DPF amendments under different environmental conditions. In addition to further studies, it could include growth metrics such as biomass or leaf area measurements to provide a more comprehensive assessment of plant responses to soil amendments. Potentially leading to more sustainable farming methods in difficult environments.

4.6 Conclusion

This chapter investigated the effects of biochar and date palm fronds (DPF) amendments on plant growth and soil properties in sandy soils under both controlled and uncontrolled conditions. The results demonstrated that soil amendments influenced plant growth, moisture dynamics and soil properties, but the magnitude of these effects varied depending on environmental conditions and amendment levels.

This research confirms the impact of biochar on plant growth across different weather conditions, aligning with the chapter's aim. It highlights the potential for water retention during extreme temperatures in both summer and winter seasons. The study also explains the differences between biochar and Date Palm Fronds (DPF), suggesting that while biochar may improve plant growth more effectively than DPF, the extent of its water retention capability in arid climates remains uncertain. Although biochar is often credited with superior water retention, this explores whether DPF might offer a viable alternative without the need for charring. Ultimately, this study not only deepens our understanding of biochar's role in promoting plant growth but also provides a basis for exploring sustainable soil enhancement strategies in arid regions.

Chapter 5: Thermal Gravimetric Analysis (TGA) of moisture holding capacity.

5.1 Introduction

The overall aim of this chapter was to assess the benefits of biochar in an arid climate with particular emphasis on understanding the moisture-holding capacity of different materials. Chapter 3 examined the moisture content of the study materials under different conditions using a mesocosm experimental approach in which the materials were mixed with sand at different proportions. Chapter 4 focused on crop response to DPF and biochar application.

The objective of this chapter is to evaluate how biochar, date palm fronds (DPF) and sandy soils differ in their ability to retain and release moisture when analysed using thermogravimetric analysis (TGA). TGA was selected because it provides continuous high-resolution measurements of mass loss, enabling the distinction between surface moisture, physically bound water and water held within the material structure. The technique offers insight into thermal behaviour and the strength of water binding within each material.

This chapter also incorporates a novel adaptation by analysing both dry and water amendment samples, unlike traditional techniques, where most studies examine only dry materials. By integrating this approach, the chapter contributes to the broader thesis aim of understanding how biochar and DPF can enhance moisture retention and improve the performance of arid soils.

5.2 Approach

This chapter employs a quantitative research approach to investigate the moisture retention properties of the materials studied in the previous chapters (sharp sand, UAE sand, DPF, and biochar) under both dry and wet conditions. The materials were subject to different heating rates in a thermogravimetric analyser (TGA), and their moisture retention characteristics were assessed through continuous measurement of mass loss.

The main research question for this chapter is:

What are the comparative moisture holding capacities of DPF, biochar and sandy soils and how can these materials contribute to improving the moisture retention of UAE soils?

5.3 Materials and methods

The TGA was used in this section for analysing the mass loss of organic matter and inorganic matter of the materials considered and analysed in previous chapters: biochar, DPF, UAE sand and sharp sand. The instrument used for conducting TGA was the SGA TGH 1200. In the first experiment, the sample' masses were between 100mg and 300mg and run from ambient to 700°C using different heat ramp rates within a micro furnace in the presence of an inert atmosphere – N₂ at between 1 and 2 atm atmosphere. There were five temperatures ramp rates used for each material, and these were: 5 K/min, 10 K/min, 15 K/min, 20 K/min and 25 K/min. The measured values were adjusted to a common temperature scale and cut to a common temperature range between 50°C and 700°C. To start up the experiment, the alumina pan was placed to balance in a controlled furnace at a temperature. Then the TGA experiment was run using the organic (DPF and Biochar) and inorganic materials (Sandy soil, Sharp sand and UAE sand) and (water). The water holding capacity of the organic and inorganic materials was assessed by adding water to the samples.

5.4 Results

5.4.1 DPF

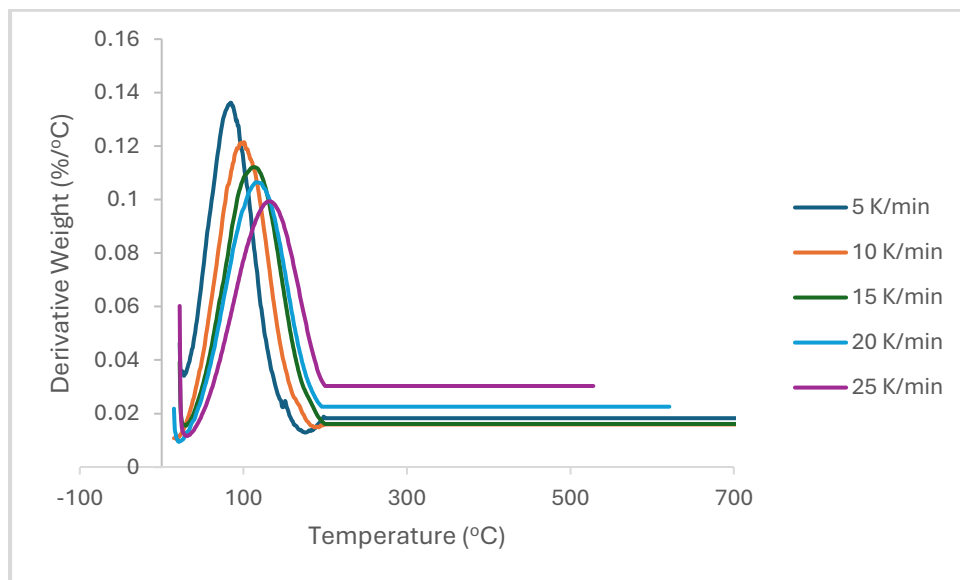


Figure 5.1. The rate of mass loss of Date Palm Fronds (DPF) at different heat rates (K/min).

The Date Palm Fronds (DPF) showed that the rate of mass loss varies with heating rates. At a higher heating rate of 25 K/min, the rate of mass loss is higher between 40°C and 250°C including rapid decomposition within this temperature range (Figure 5.1). At the lowest heating rate of 5 K/min, the rate of mass loss is slower, showing a more gradual decomposition process over a similar temperature range (Figure 5.1).

5.4.2 Biochar

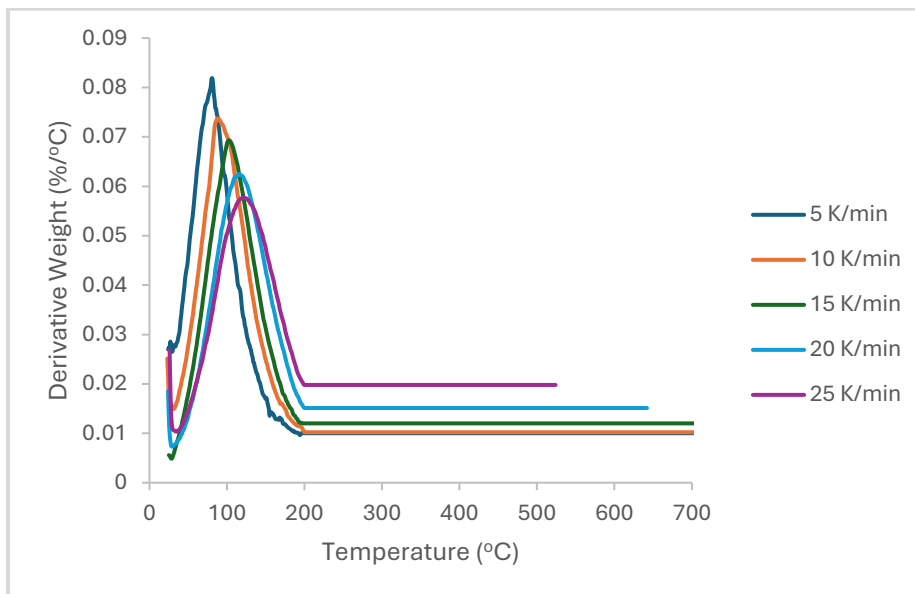


Figure 5.2. The rate of mass loss of biochar at different heat rates (K/min).

The biochar presented that the rate of mass loss increases with higher heating rates. At 25 K/min, the rate of mass loss is highest between 26°C and 226°C. In contrast, at 5 K/min, the rate of mass loss was the lowest mass loss occurred (Figure 5.2).

5.4.3 Water

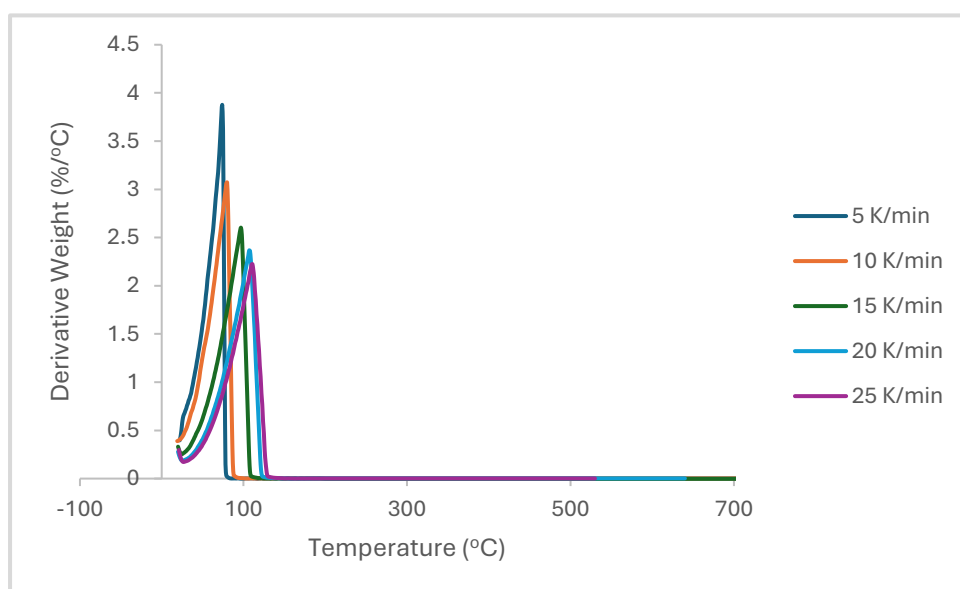


Figure 5.3. The rate of mass loss of water in different heat rates (K/min).

The water showed that the rate of mass loss due to evaporation varies according to heating rate. At 10 K/min, the rate of mass loss is highest, with rapid evaporation occurring between 39°C and 141°C. At 5 K/min, the evaporation rate is lower, showing a prolonged period of mass loss over the temperature range (Figure 5.3).

5.4.4 Wet DPF

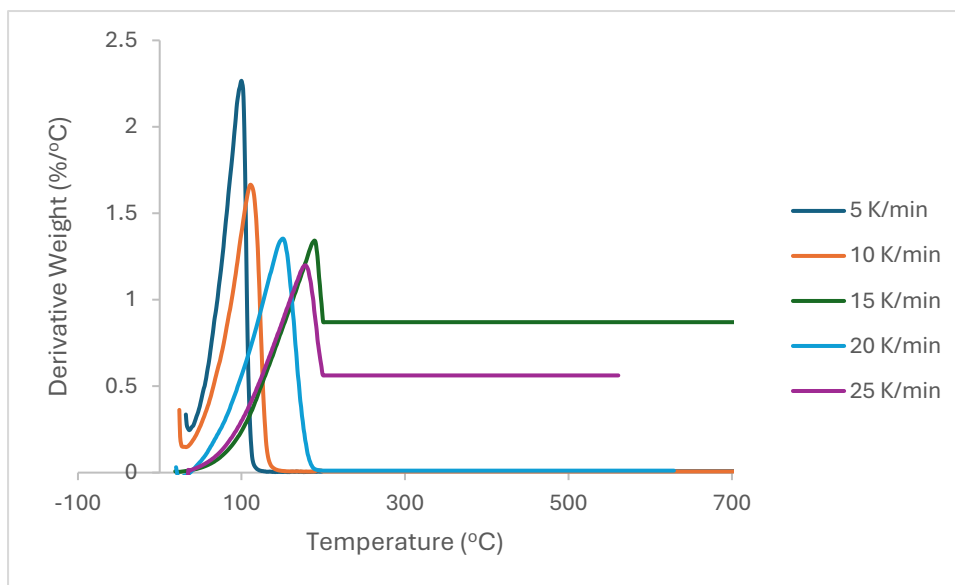


Figure 5.4. The rate of mass loss of wet DPF in different heat rates (K/min).

The wet DPF showed that at 25 K/min, the rate of mass loss is higher between 47°C and 200°C with a rapid moisture evaporation followed by decomposition. In contrast, at 5 K/min, the rate of mass loss is more gradual, extending over a broader temperature range (Figure 5.4).

5.4.5 Wet Biochar

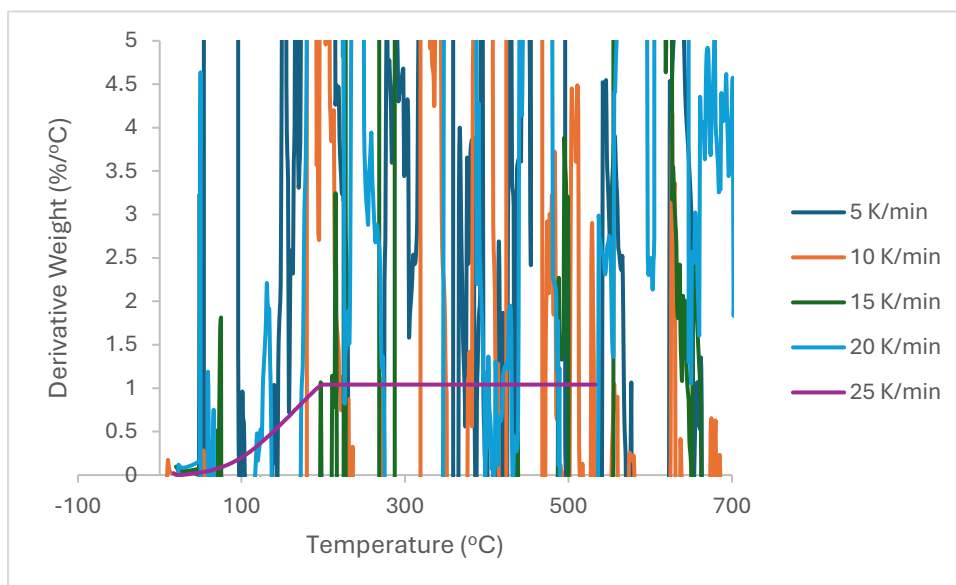


Figure 5.5. The rate of mass loss of wet biochar in different heat rates (K/min).

The wet biochar at most heating rates showed significant fluctuation, making the data difficult to interpret. Expecting 25 K/min produced a gradual, consistent curve of mass loss between 89°C – 531°C (Figure 5.5).

5.4.6 Wet Sharp Sand

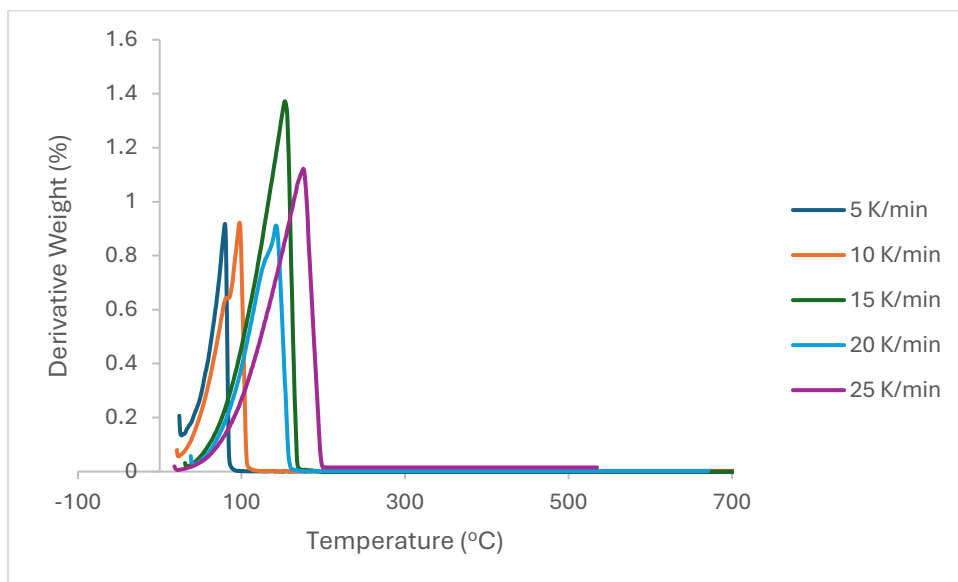


Figure 5.6. The rate of mass loss of wet sharp sand in different heat rates (K/min).

The wet, sharp sand showed that the rate of mass loss remains relatively low across different heating rates. At 25 K/min, there was a slight increase in the rate of mass loss between 25°C and 214°C. The lowest heating rate was at 5 K/min, the mass loss was slightly less (Figure 5.6).

5.4.7 Wet UAE Sand

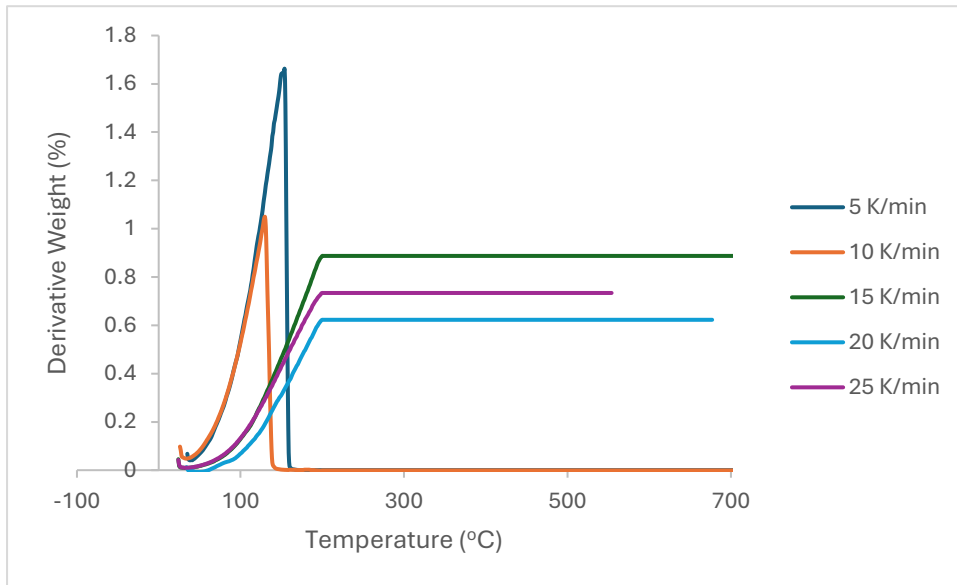


Figure 5.7. The rate of mass loss of wet UAE sand in different heat rates (K/min).

The wet UAE sand showed that the rate of mass loss varied across different heating rates. The highest rate was observed at 20 K/min, extending over a wide temperature range from with 50°C and 700°C. The rate of mass loss remained low at a heating rate of 5L/min (Figure 5.7).

5.5 Discussion

This chapter focused on utilising thermal gravimetric analysis (TGA) to evaluate the water holding capacity of various materials (DPF, biochar, sharp sand, UAE sand and water) under different heating rates in both dried and wet conditions. Mixing the materials with water in a TGA experiment was necessary to determine the performance of the materials to understand their heating rate differences in mass loss and potential applications in environmental contexts.

The TGA analysis revealed that both Date Palm Fronds (DPF) and biochar exhibited a correlation between heating rate and mass loss, suggesting a potential for water retention due to their organic composition. In contrast to the inorganic materials, sharp sand and UAE sand demonstrated minimal mass loss even in the presence of moisture, including their limited water holding capacity. While the water holding capacity was the primary focus of this study, the TGA results suggest that DPF and biochar, when wet, may have superior water retention properties compared to the inorganic sands.

The findings from the TGA experiments provide valuable insights into the thermal behaviour of the studied materials. Notably, DPF exhibited significant mass loss, particularly evident at higher heating rates, indicating pronounced thermal degradation. This observation aligns with previous research highlighting the susceptibility of organic materials such as agricultural residues to thermal decomposition under elevated temperature (Chen[‡] *et al.*, 2024).

On the other hand, biochar demonstrated remarkable mass loss, characterised by minimal mass loss even at elevated temperatures. This finding corroborates existing literature on the thermal properties of biochar, emphasising its potential as a stable carbonaceous material for diverse

applications, including soil improvement and carbon sequestration (Tengku Yasim-Anuar *et al.*, 2022).

Furthermore, the addition of water influenced the decomposition kinetics of both DPF and biochar, underscoring the importance of moisture content in modulating their thermal behaviour. This observation resonates with studies exposing the impact of moisture on the pyrolysis characteristics of biomass-derived materials, highlighting its role in promoting secondary reactions and altering product yields (Demirbas, 2007).

Moreover, the inorganic materials, namely sharp sand and UAE sand, exhibited slight mass loss, even in the presence of moisture. This behaviour highlights their main inert nature and reinforces their suitability for applications demanding mass loss and resistance to environmental factors (Wang, et al., 2016). Adding water to sand could also play a role in the materials, porosity and evaporation at different heating rates.

In interpreting these findings, it is important to consider how TGA compares with other techniques for investigating moisture retention, such as soil moisture release curves or pressure plate techniques (Stenke, et al., 2015). The TGA provides continuous, high-resolution measurements of mass loss as temperature increases, enabling differentiation between free water, surface adsorbed water, physically bound water held within pore structure and more strongly bound structural water associated with the material matrix. This allows detailed evaluation of the strength and stability of water retention mechanisms within organic and inorganic materials, which cannot be directly observed using conventional equilibrium-based soil moisture techniques.

The moisture release curve does not capture the thermal energy associated with water desorption. Therefore, TGA produces complementary information. The agreement between different moisture analysis techniques depends on how water is retained within the materials.

Conventional methods, such as moisture release curves, primarily measure water held by capillary and surface forces. In contrast, TGA can also detect more strongly bound water associated with the material structure. Therefore, materials such as biochar, which contain water retained within their pore network and internal structure, are more effectively characterised using TGA, as it provides additional information on the strength of water retention.

Despite the valuable insights collected from this study, several limitations deserve consideration. Foremost among these is the potential for experimental error or instrument malfunction during the TGA analysis. Such factors may have contributed to the observed difference in water holding capacity, particularly in the case of biochar. Our findings indicate that biochar exhibits different water holding capacity when mixed with water and compared with other materials. Therefore, we recommend repeating the experiment to ensure the accuracy of the results, given that the machine experienced some issues during the testing process.

This research provides key insights that have implications for various practical applications, ranging from renewable energy to waste management. For instance, understanding the thermal behaviour and water-holding capacity of materials like biochar and agricultural residue can inform decision-making processes in these sectors. For example, biochar's potential as a stable carbonaceous material for soil improvement and carbon sequestration in agricultural systems is highlighted, contributing to enhanced soil fertility and mitigating greenhouse gas emissions (Lehmann and Joseph, 2015). Additionally, insights into thermal stability of organic materials like DPF can inform the design and optimisation of biomass conversion processes, including pyrolysis and gasification, for renewable energy generation and biofuel production (Bridgwater, 2021). By exposing the thermal properties and response to moisture content of these materials, this research helps identify their potential uses in areas like resource

management and environmental conservation. For example, materials like biochar with its strong water holding capacity and thermal stability, can be useful in improving soil quality and capturing carbon, while understanding the thermal behaviour of DPF can guide its use in renewable energy production.

5.6 Conclusion

This chapter demonstrated differences in the moisture retention and thermal behaviour of the materials analysed using thermogravimetric analysis (TGA). Thereby fulfilling the objective of evaluating how biochar, DPF and sandy soils differ in their ability to retain and release moisture. The results showed that biochar and date palm fronds (DPF) exhibited greater mass loss associated with moisture release compared to sharp sand and UAE sand, indicating a higher capacity to retain water. This behaviour is attributed to the porous structure and organic composition of biochar and DPF, which provide greater surface area and internal pore space for water retention. In contrast, the sandy materials showed minimal moisture retention, reflecting their limited pore structure and lower capacity to retain water.

The results demonstrated that moisture retention behaviour varied with heating rate, with organic materials showing more pronounced mass loss across a wider temperature range. This observation indicates the presence of both weakly and strongly bound water within biochar and DPF, confirming their enhanced moisture retention capacity compared to inorganic sandy materials. These findings support the potential use of biochar and DPF as soil amendments to improve water retention in arid soils, where moisture availability is a major limiting factor for plant growth.

This study also demonstrated the effectiveness of TGA as a technique for evaluating moisture retention behaviour. By analysing both dry and water-amended samples, this research provided additional insight into the moisture desorption process and the strength of water retention

within different materials. This methodological approach extends the application of TGA beyond conventional dry sample analysis and contributes to a more detailed understanding of water material interactions.

Overall, the findings of this chapter contribute to the broader thesis objectives of evaluating the potential of biochar and DPF to enhance moisture retention and improve soil performance in arid environments such as the UAE. These results provide a mechanism basis for the use of organic amendments to improve soil water availability and support sustainable agricultural practices in water-limited environments.

Building on these findings, the next chapter investigates the combined effects of biochar and DPF on water retention and plant growth in mesocosm and pot trial experiments, providing further evaluation of their suitability as soil amendments.

Chapter 6: The combination of DPF and Biochar

6.1 Introduction

The results presented in Chapter 3 examined the effects of biochar and Date Palm Date (DPF) on soil water retention using a mesocosm experiment. Chapter 4 investigated the effects of these amendments on plant growth when applied to soil under controlled and uncontrolled conditions. The findings showed that biochar generally promoted greater plant growth, whereas DPF demonstrated a higher capacity for water retention. As both materials influenced soil properties in different ways, it was important to examine where combining them could produce complementary or synergistic effects. Therefore, this chapter investigates the combined application of biochar and DPF to determine whether mixed amendments can further improve soil moisture retention and plant growth.

The specific objective of this chapter is to evaluate the effects of combined biochar-DPF treatments on soil moisture retention and plant growth under different moisture conditions.

6.2 Approach

In this chapter, a quantitative research approach was conducted using both mesocosms and pot trials to examine the combined materials (biochar and DPF). The main research questions for this chapter were:

- Did the combination of biochar and DPF make a difference in retaining water?
- Did the combination of biochar and DPF make a difference in plant growth?

6.3 Materials and methods

6.3.1 *Sample collection*

The samples of Date Palm Fronds and UAE soils were collected in the UAE. The sharp sand was bought locally in the UK. Chapters 2, 3 and 4 give the details of the sample collection and the biochar production.

6.3.2 *Mesocosms*

For understanding the water retention in mixed treatment mesocosms. Chapter 3 gave details of the mesocosm experimental design. For this chapter, the aim was to apply the same experimental design but combining both biochar and Date Palm Fronds (DPF) into one treatment. The samples of 1% mixed amendment, contained 0.5% DPF and 0.5% biochar, were weighed and mixed equally when applied to mesocosms. Similarly, samples with 18% mixed amendment, contained 9% DPF and 9% biochar, were prepared in the same manner. These mixed materials were then incorporated with sandy soils in different proportions- the proportions were 1% and 18% mixed amendment treatments. The 1% and 18% amendment levels were selected based on their performance in the experiments described in Chapters 3 and Chapter 4. For this experiment, there were two experiments that took place for the mixed materials. The mesocosm experiment conducted a four-factor experimental design where the factors were: (i) the material; (ii) the wetting cycle; (iii) the treatment; and (iv) time.

In total, there were 3 materials (DPF, biochar and sand) and 2 treatments (1% and 18%). The wetting cycle factor had three levels: wet cycle, dry cycle, dry cycle with a water bowl known henceforward as dry cycle waw. The wet cycle was watered daily with 1 ml of tap water into each mesocosm. The dry cycle had no water added. The dry cycle waw was like the dry cycle, but a water bowl was added into the oven to increase the humidity, and therefore, the soil

moisture content. The final factor was time. Each cycle of treatment was run in the oven for a week separately in an electrical heater (oven) at 40°C. The mesocosms were weighed each day for a week, and the data were collected and converted to percentage moisture content.

The mesocosms were 33 PVC tubes that were chopped into sections of 9-10 cm long and 4 cm in diameter. The plastic bungs were placed at the bottom of each tube to hold in the materials and the treatments. The mesocosms material or treatment was triplicated in each cycle.

6.3.3 Pot trial

Chapter 4 explained a detailed pot trial experiment that took place in the laboratory and in the field. For this chapter, the aim was to apply the same experimental design but combine both biochar and DPF treatments into one pot. The samples of 1% mixed amendment, contained 0.5% DPF and 0.5% biochar, were weighed and mixed equally when applied to the pot trial experiment, which took place in the laboratory (controlled experiment). Similarly, samples with 18% mixed amendment, contained 9% DPF and 9% biochar, were prepared in the same manner. These mixed materials were then incorporated with sandy soils in different proportions- the proportions were 1% and 18% mixed amendment treatments. The sand was used as a neutral amendment that would be hypothesised to have negligible water holding capacity and so was used to see the impact of a physical amendment on a soil. The dimension of the pot used was length 7.6 cm, top width 7.8 cm and bottom width 5.1 cm. The plant grown was cat grass (sp. *Avena sativa*): grown from seed. All treatments were triplicated in this experiment.

The pot trial experiment was conducted as a four-factor experiment: soil amendment, treatment, wetting cycle, and time in the experiment. The treatment factor (henceforward referred to as Treatment) had two levels of mixed materials (biochar and Date Palm Fronds (DPF) and

treatments were 1% and 18% of each amendment in the UAE sandy soil. The wetting cycle factor (henceforward as Cycle) had two levels: the wet cycle and the dry cycle. The time in the experiment, referred to as the day factor, had up to 60 levels (i.e., 60 days). The wetting cycle factor in the mesocosm experiment included three levels: wet cycle, dry cycle and dry cycle with a water bowl (waw). In contrast, the pot trial experiment included only two levels: wet cycle and dry cycle, as for the waw treatment was not used. This approach was adopted to maintain consistency with the pot trial experiment done in Chapter 4. The primary objective of the pot trial experiment was to assess plant growth responses under alternating watering conditions, rather than to simulate additional humidity conditions. Therefore, the waw treatment was not considered necessary for this experiment.

The mixed pots were kept in a growth tent (dimension: 129.5 cm height, 75 cm width and length), and an LED light was set to increase air temperature to 26° C and maintain a fixed light condition. The LED system was operated at its maximum output at 26°C which was the highest achievable temperature under the laboratory conditions. Although this temperature was lower than the 40°C used in the mesocosm experiment, the pot trial was designed to assess plant growth under controlled conditions, whereas the mesocosm experiment aimed to simulate accelerated soil drying. Soil temperature can influence soil moisture dynamics and plant growth. The temperature range used in this experiment (approximately 26°C) falls within the typical environmental temperatures observed in the UAE, where seasonal temperature commonly ranges between 25°C- 40°C. Therefore, although temperature differed from that used in the mesocosm experiment, it remains representative of real-world conditions and allows valid comparisons between treatments within the experiment. The period of the experiment was 5 weeks, and this period was divided into two cycles: the wet cycle was for 10 days, and the dry cycle was for 10 days. During the wet cycle, 10 ml of tap water was added to each pot daily, then soil moisture was checked using a moisture probe. After the completion of the wet

cycle, the dry cycle began by not adding water, but the probe analysis of the pots was continued until the end of each cycle. The moisture probe used in this experiment was the Beslands Soil Tester 4 in 1 for measuring moisture (made in China). The probe measures moisture (5 levels), pH (4.0- 9.0), temperature (8.89° C- 50° C), and light intensity (9 levels).

The soil moisture levels were recoded to numbers to deliver detailed data analysis. Moisture levels: dry + (1), dry (2), normal (3), wet (4) and wet + (5). Light was also recoded: low + (1), low (2), nor (3), nor + (4), high (5) and high + (6). The plant growth was measured as plant height vertically using a 30 cm ruler.

The amendment treatment combinations used in both the mesocosms and the pot trial experiment are summarised in (Table 6.1).

Table 6.1. Mixed amendment treatments used in the mesocosm and pot trial experiments (composition by dry weight).

| <i>Material type</i> | <i>Treatment level (%)</i> | <i>Composition (% by dry weight)</i> | <i>Description</i> |
|------------------------------|----------------------------|--------------------------------------|----------------------|
| <i>Mixed (DPF + Biochar)</i> | 1 | 0.5% DPF + 0.5% biochar + 99% | Low mixed amendment |
| <i>Mixed (DPF + Biochar)</i> | 18 | 9% DPF + 9% biochar + 82% | High mixed amendment |

6.3.4 *Statistical Analysis*

The results of both experiments were analysed by analysis of variance (ANOVA). The results were judged as statistically significant if their probability of being zero was ≤ 0.05 . Before any ANOVA was performed, the data were tested for normality using the Anderson-Darling test (Anderson and Darling, 1952), and QQ plots were also generated to visually assess the normality of the data distribution. It did not prove necessary to transform the data for any of the metrics in this study. The homogeneity of the variance was tested using the Levene test, and if the test failed, the data were log-transformed and re-tested. As for the normality test, this did not prove necessary. The magnitude of the effects of each significant factor and interaction was calculated using the generalised ω^2 (Olejnik and Algina, 2003), and values were presented as least-square means (otherwise known as marginal means). Post hoc assessment of factors and interactions was carried out using the Tukey test.

6.4 Results

6.4.1 Mesocosms experiment

6.4.1.1 Moisture content

- Wet Cycle

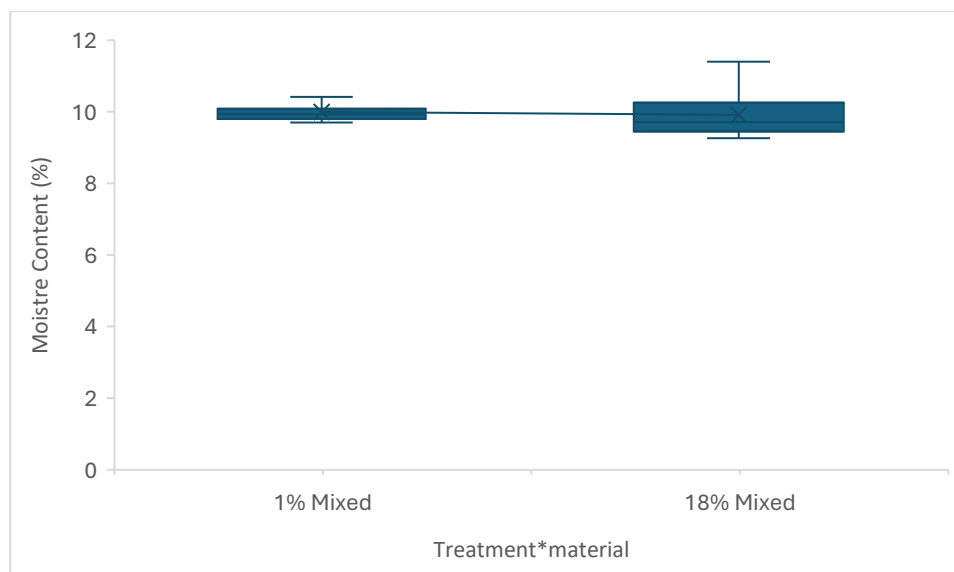


*Figure 6.1. The boxplot of the moisture content (% by weight) of the Treatment*Materials interaction measured during the wet cycle. Box-and-whisker plots show the interquartile range, with the box representing the first quartile (Q1) to the third quartile (Q3), and the whiskers extending from the minimum to the maximum values. The median is represented by a line within the box, and the cross symbol (x) indicates the mean moisture content.*

During the wet cycle, moisture content differed between treatment levels (Figure 6.1). The 1% mixed amendment treatment exhibited the highest median (9.93%), while the lowest moisture content was the 18% recorded (9.71%) (Figure 6.1). The mixed 1% exhibiting the highest mean moisture content recorded (10%), followed by mixed 18% (9.91%), which was the lowest moisture content. Statistical analysis confirmed that treatment level had a significant effect on moisture content ($p < 0.05$).

- Dry Cycle

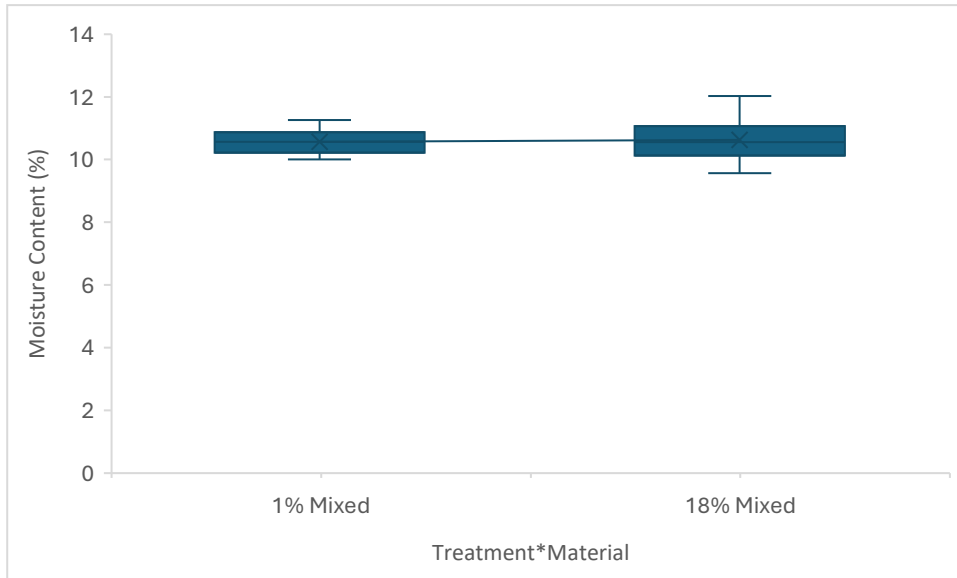


Figure 6.2. The boxplot of the moisture content (% by weight) of the Treatment*Materials interaction measured during the dry cycle. Box-and-whisker plots show the interquartile range, with the box representing the first quartile (Q1) to the third quartile (Q3), and the whiskers extending from the minimum to the maximum values. The median is represented by a line within the box, and the cross symbol (x) indicates the mean moisture content.

During the dry cycle, moisture content differed between treatment levels (Figure 6.2). The 1% mixed amendment treatment exhibited the highest median (10.57%), while the lowest moisture content was the 18% recorded (10.55%) (Figure 6.2). The mixed 18% exhibited the highest mean moisture content recorded (10.63%), followed by mixed 1% (10.56%), which was the lowest moisture content. Statistical analysis confirmed that treatment level had a significant effect on moisture content ($p < 0.05$).

- Dry Cycle (waw)

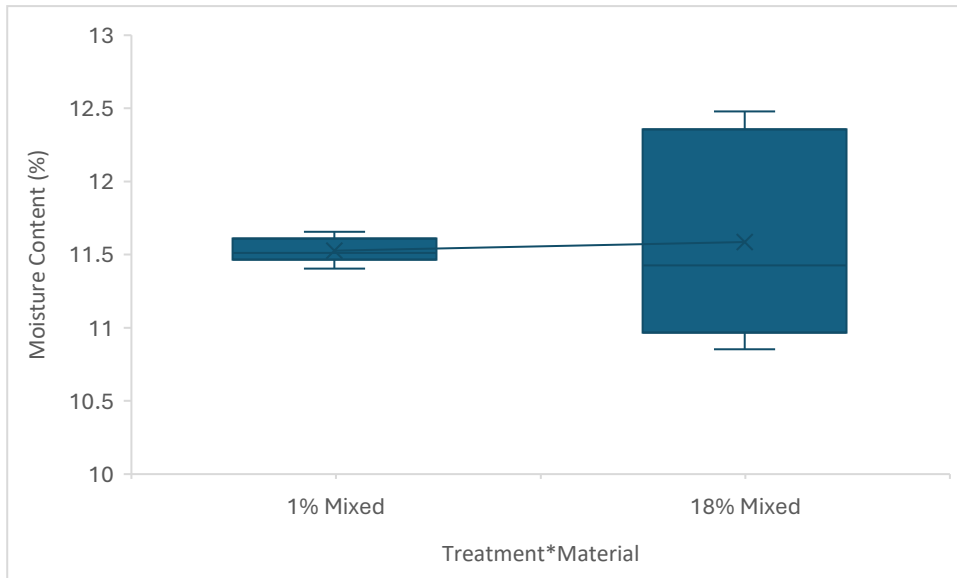


Figure 6.3. The boxplot of the moisture content (% by weight) of the Treatment*Materials interaction measured during the dry cycle waw. Box-and-whisker plots show the interquartile range, with the box representing the first quartile (Q1) to the third quartile (Q3), and the whiskers extending from the minimum to the maximum values. The median is represented by a line within the box, and the cross symbol (x) indicates the mean moisture content.

During the dry cycle waw, moisture content differed between treatment levels (Figure 6.3). The 1% mixed treatment exhibited the highest median (11.51%), while the lowest moisture content was the 18% recorded (11.43%) (Figure 6.3). The mixed 18% exhibited the highest mean moisture content recorded (11.59%), followed by mixed 1% (11.53%) was the lowest moisture content. Statistical analysis confirmed that treatment level had a significant effect on moisture content ($p < 0.05$).

6.4.2 Pot trial experiment

6.4.2.1 Plant height

- Wet cycle

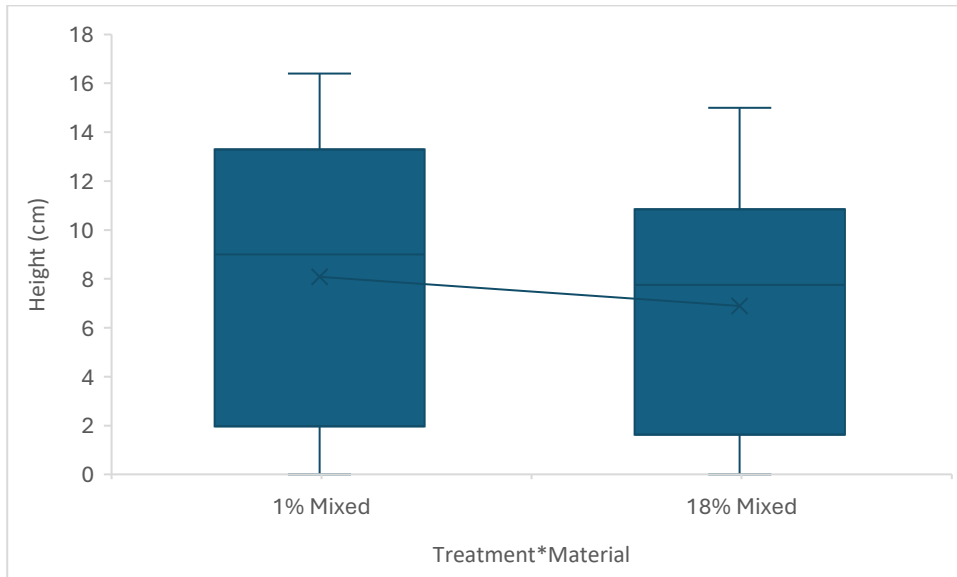


Figure 6.4. The boxplot of the height (cm) of the Treatment*Material interaction measured during the wet cycle. Box-and-whisker plots show the interquartile range, with the box representing the first quartile (Q1) to the third quartile (Q3), and the whiskers extending from the minimum to the maximum values. The median is represented by a line within the box, and the cross symbol (x) indicates the mean plant height.

During the wet cycle, plant height differed between treatment levels (Figure 6.4). The median plant height was highest at the 1% Treatment*Material (9 cm), and the lowest plant height was the 18% Treatment*Material (7.75 cm) (Figure 6.4). The 1% Treatment*Material exhibited the highest mean plant growth recorded (8.08 cm), followed by 18% Treatment*Material (6.89%) was the lowest plant growth. Statistical analysis confirmed that treatment level had a significant effect on moisture content ($p < 0.05$).

- Dry Cycle

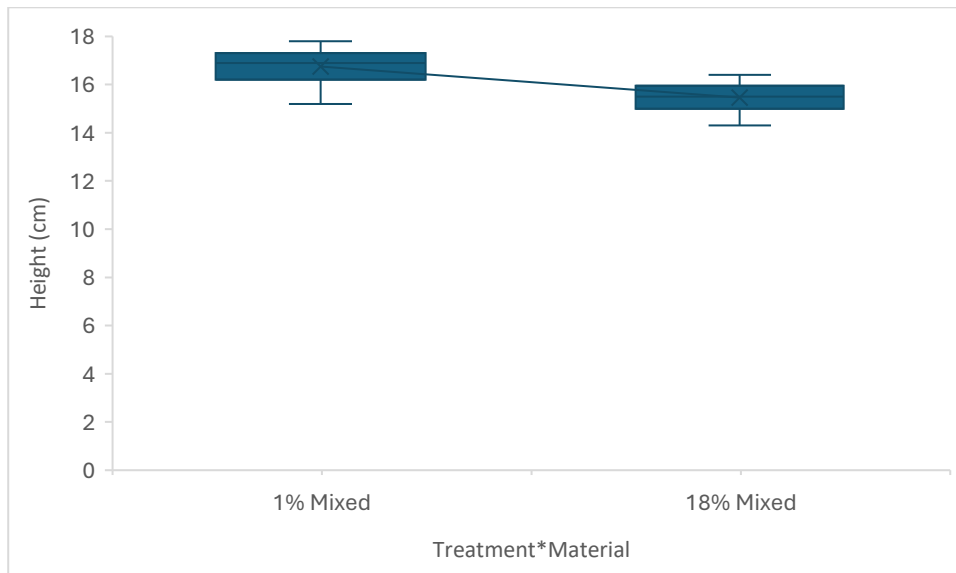


Figure 6.5. The boxplot of the height (cm) of the Treatment*Material interaction measured during the dry cycle. Box-and-whisker plots show the interquartile range, with the box representing the first quartile (Q1) to the third quartile (Q3), and the whiskers extending from the minimum to the maximum values. The median is represented by a line within the box, and the cross symbol (x) indicates the mean plant height.

During the dry cycle, plant height differed between treatment levels (Figure 6.5). The median plant height was highest at the 1% Treatment*Material (16.9 cm), and the lowest plant height was the 18% Treatment*Material (15.5 cm) (Figure 6.5). The 1% Treatment*Material exhibited the highest mean moisture content recorded at (16.75 cm), followed by 18% Treatment*Material (15.46 cm), which had the lowest plant growth. Statistical analysis confirmed that treatment level had a significant effect on moisture content ($p < 0.05$).

- **Growth rate calculation**

Plant growth was calculated using the incremental growth rate method described in **Chapter 4**, which estimates the change in plant height per day between measurement intervals (cm/day). This approach allows for a more accurate comparison of plant development under different moisture regimes. A summary of the calculation growth rates is shown in Table 6.2.

Table 6.2. Summary of plant growth rates (cm/day) during wet and dry cycles in the mixed treatment material pot trial experiment. Growth rate was calculated from changes in plant height between measurement intervals.

| <i>Day</i> | <i>Wet Cycle (cm/day)</i> | <i>Dry Cycle(cm/day)</i> |
|------------|---------------------------|--------------------------|
| 2 | | 0.65 |
| 4 | | -0.12 |
| 5 | 1.10 | |
| 7 | | 0.03 |
| 10 | 1.26 | |
| 14 | 1.02 | |

A negative growth rate observed during the dry cycle indicates a slight reduction in measured plant height between sampling intervals, which may occur due to plant wilting or minor measurement variability under low moisture conditions.

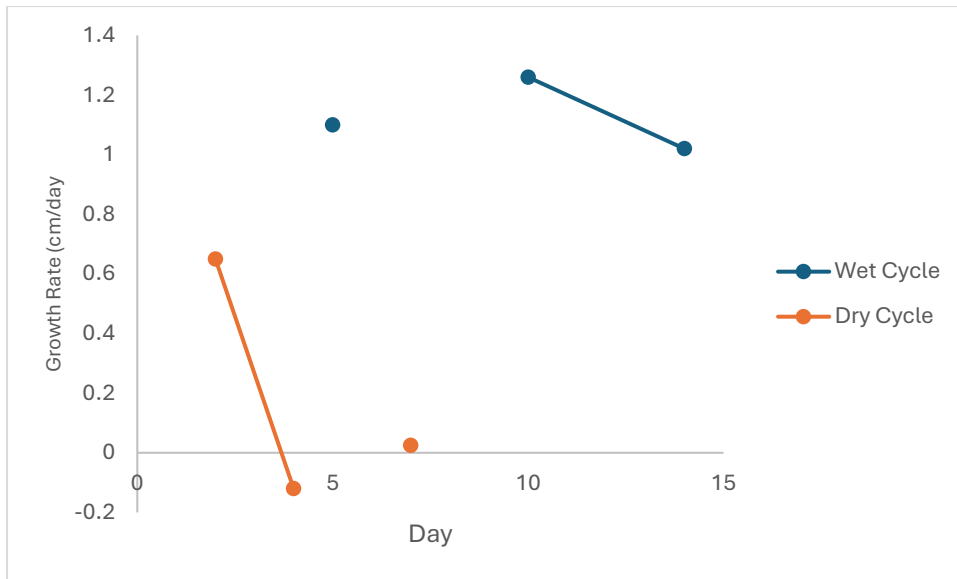


Figure 6.6. Plant growth rate (cm/day) during wet and dry cycles in the mixed amendment pot trial experiment. Growth rates were calculated from incremental changes in plant height over time.

Plant growth rates differed between wet and dry cycles. During the wet cycle, growth rates ranged from 1.02- 2.26 cm/day, whereas during the dry cycle, growth rates ranged from -0.12- 0.65 cm/day. Overall, plant growth was greater under wet conditions than under dry conditions (Figure 6.6).

6.4.2.2 Moisture level

The soil moisture level shows that the 1% and 18% mixed treatments had the same moisture level, of 1, during both wet and dry cycles.

Although level 1 is considered low soil moisture, it does support the research question of this study, which examines the mixed treatment 1% and 18% maintained moisture during both cycles.

6.4.2.3 Soil temperature

- Wet cycle

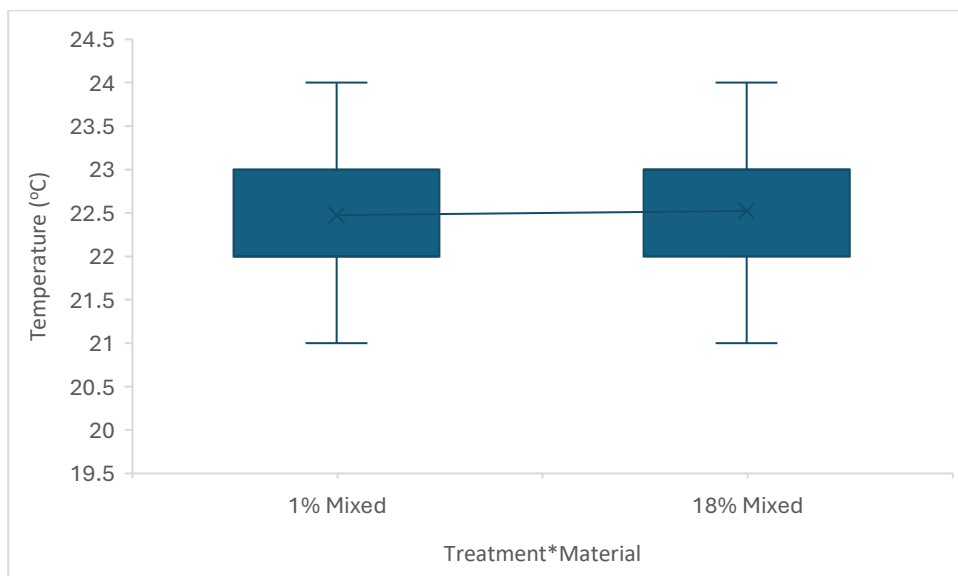


*Figure 6.7. The boxplot of the soil temperature of the Treatment*Material interaction measured during the wet cycle. Box-and-whisker plots show the interquartile range, with the box representing the first quartile (Q1) to the third quartile (Q3), and the whiskers extending from the minimum to the maximum values. The median is represented by a line within the box, and the cross symbol (x) indicates the mean soil temperature.*

During the wet cycle, soil temperature differed between treatment levels (Figure 6.7). The 1% and 18% Treatment*Materials median shared the same soil temperature at (25°C) (Figure 6.7). The 18% Treatment*Material exhibited the highest mean soil temperature recorded (23°C), 1% Treatment*Material had the lowest mean soil temperature (22°C). Statistical analysis confirmed that treatment level had a significant effect on moisture content ($p < 0.05$).

- Dry Cycle

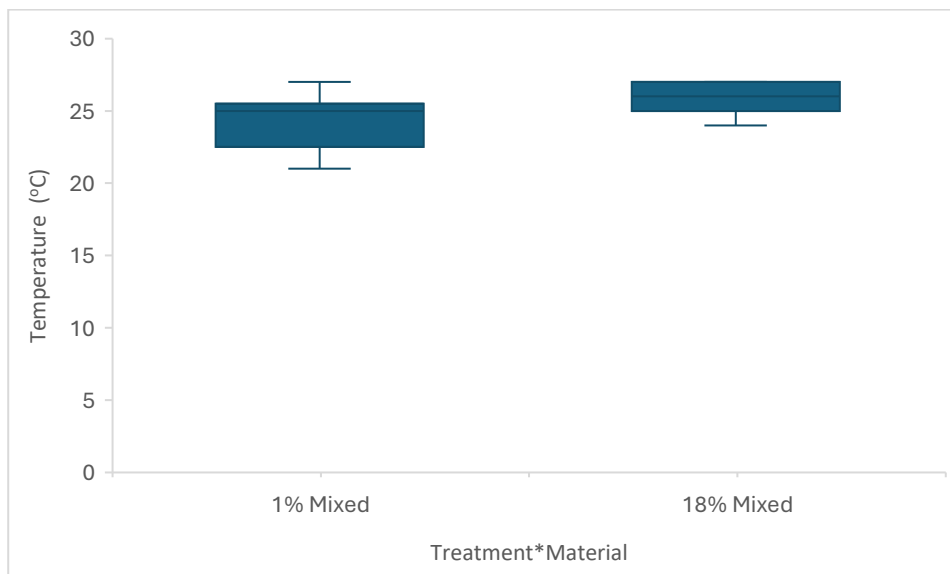


Figure 6.8. The boxplot of the soil temperature of the Treatment*Material interaction measured during the dry cycle. Box-and-whisker plots show the interquartile range, with the box representing the first quartile (Q1) to the third quartile (Q3), and the whiskers extending from the minimum to the maximum values. The median is represented by a line within the box, and the cross symbol (x) indicates the mean soil temperature.

During the dry cycle, soil temperature differed between treatment levels (Figure 6.8). The 18% Treatment*Material had the highest median soil temperature at (26°C). The lowest median soil temperature was the 1% Treatment*Material median at (25°C) (Figure 6.8). The 18% Treatment*Material exhibited the highest mean soil temperature recorded (26°C), the lowest mean soil temperature 1% Treatment*Material (24°C). Statistical analysis confirmed that treatment level had a significant effect on moisture content ($p < 0.05$).

6.4.2.4 Soil pH

The soil pH of the 1% and 18% mixed treatments was the same as the level 7 soil pH during both wet and dry cycles.

6.4.2.5 Light

The light of the 1% and 18% mixed treatments resulted in the same light levels at 2 during both wet and dry cycles.

Soil moisture and light intensity were recorded using a semi-quantitative probe and are presented as relative categorical levels as described in Chapter 4. These measurements provide an indication of relative soil moisture and light conditions and are not directly comparable to absolute measurements such as gravimetric water content or photosynthetically active radiation (PAR), but allow consistent comparison between treatments within the experiment.

Summary

Moisture content analysis showed that both the 1% and 18% mixed treatments retained water across all cycles (wet, dry and waw). During both wet and dry cycles, the 18% treatment recorded the highest moisture content, whereas the 1% treatment showed slightly higher median moisture values, indicating more consistent moisture retention.

Plant height analysis indicated that cumulative plant height was greater during the dry cycle than the wet cycle. Plant height analysis indicated that cumulative plant height was greater during the dry cycle than the wet cycle. However, growth rate analysis showed that actual plant growth was higher during the wet cycle, while growth during the dry cycle was lower. This demonstrates that the higher plant height observed in the dry cycle reflects accumulated growth over time rather than increased growth during the dry period.

Soil properties remained relatively stable across treatments. Soil moisture levels were consistently low (level 1), soil pH remained neutral (pH 7), and light levels were constant throughout the experiment. Soil temperature showed slight variation, with higher temperatures observed during the dry cycle.

Overall, the mixed treatments supported soil moisture retention and plant growth under both wet and dry conditions. However, when compared with the non-mixed treatments presented in Chapter 3 and Chapter 4, the 1% mixed treatment showed improved water retention, while 18% mixed treatment retained less water and plant growth in mixed treatments, which was generally lower than in single amendment treatments.

6.4.3 ANOVA results

6.4.3.1 Mesocosm experiment

- Moisture

The Anderson-Darling test and the QQ' plot (Figure 6.9) showed that the data were not normally distributed, and so the data were log transformed. The QQ' plot indicates that some samples could be considered as outliers, and 1.89% of the samples were removed.

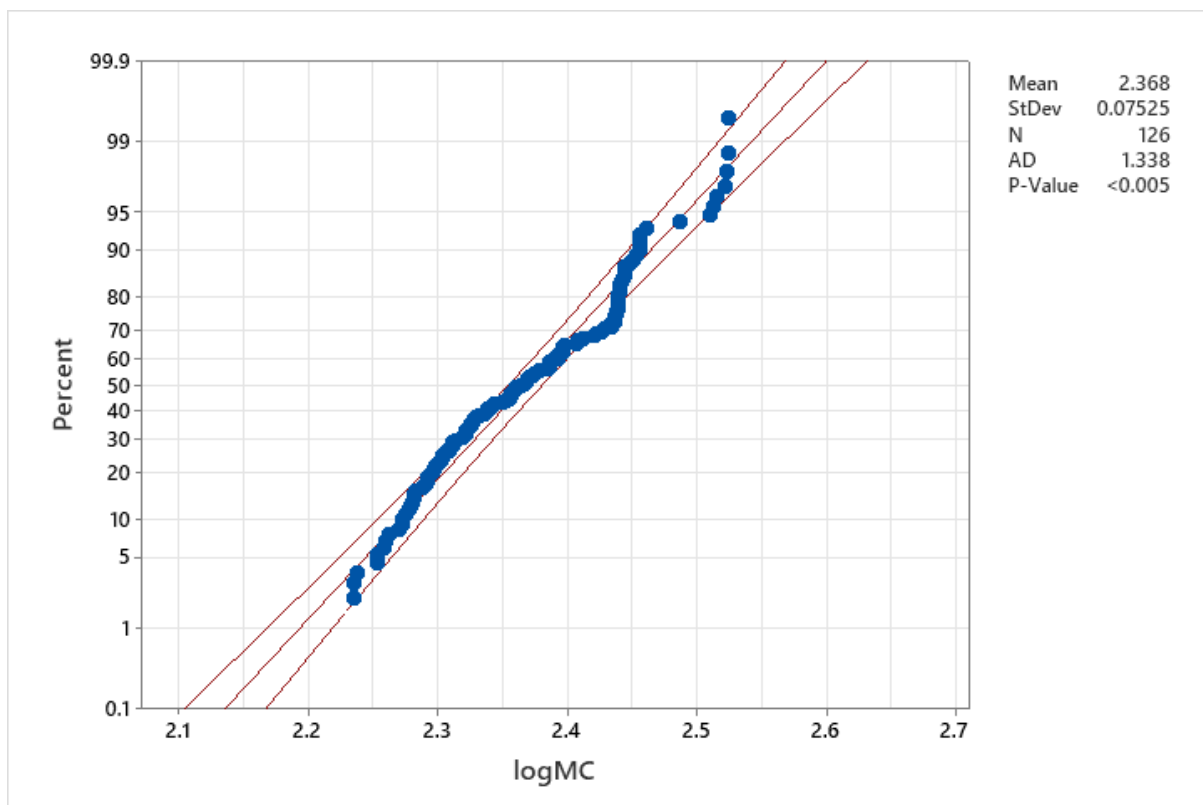


Figure 6.9. QQ' plot of the observed value of the moisture content. $\text{Log MC} = \log(\text{Moisture Content})$.

The ANOVA, including all factors and two-way interactions, had an R^2 of 81%.

Table 6.3. The percentage of variance explained for factors and interactions of the Day, Treatment and Cycle factors for on the moisture content.

| <i>Source</i> | <i>DF</i> | <i>P-Value</i> | <i>% of variance explained</i> |
|------------------------|-----------|----------------|--------------------------------|
| <i>Treatment</i> | 1 | 0.95 | 0 |
| <i>Cycle</i> | 2 | 0 | 66.92 |
| <i>Day</i> | 6 | 0.33 | 1.39 |
| <i>Treatment*Cycle</i> | 3 | 0.61 | 0.20 |
| <i>Treatment*Day</i> | 6 | 1 | 0.04 |
| <i>Cycle*Day</i> | 12 | 0 | 12.45 |
| <i>Error</i> | 96 | 0 | 19 |

As measured by the proportion of the original variance explained, the most important factor was Cycle, which explained 66.92% of the variance explained by the model (Table 6.5). As there were three levels of the Cycle factor, post hoc analysis was necessary for that factor.

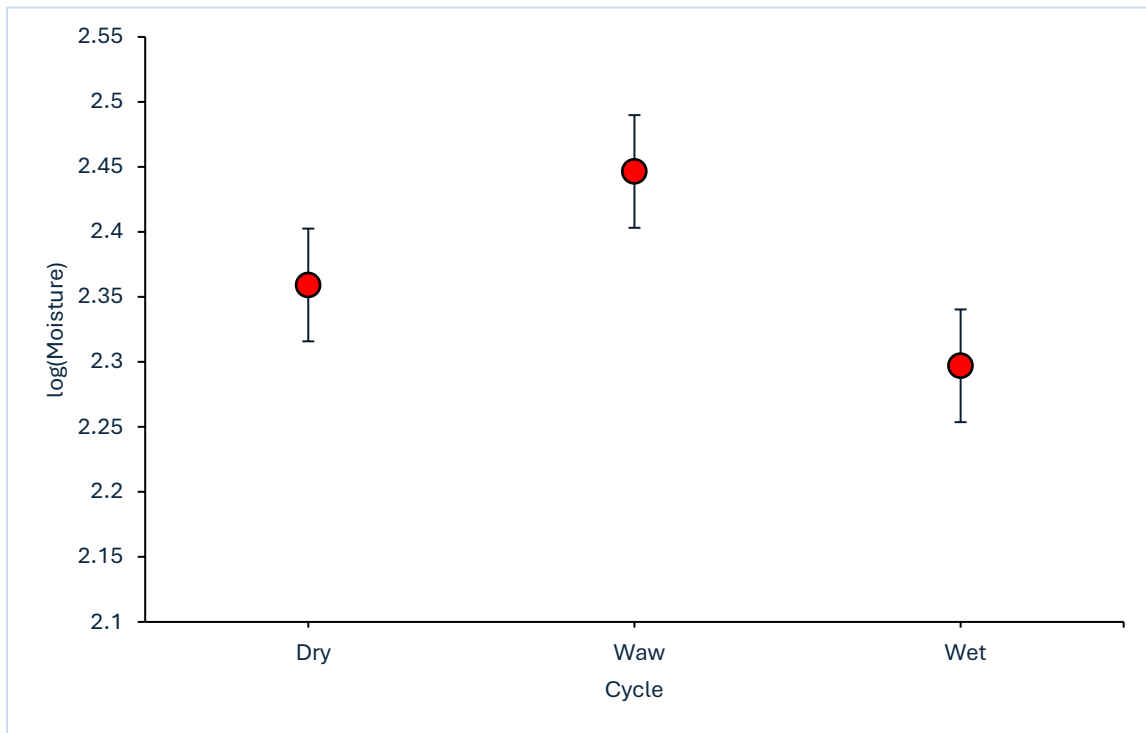


Figure 6.10. Main effects plot of the Cycle factor with respect to moisture content. Error bars are the 95% confidence interval.

The main effects plot of the Cycle factor showed that there is a significant difference between different cycles: wet, dry and waw. The highest moisture content was for the waw cycle, and the lowest moisture content was for the wet cycle (Figure 6.10).

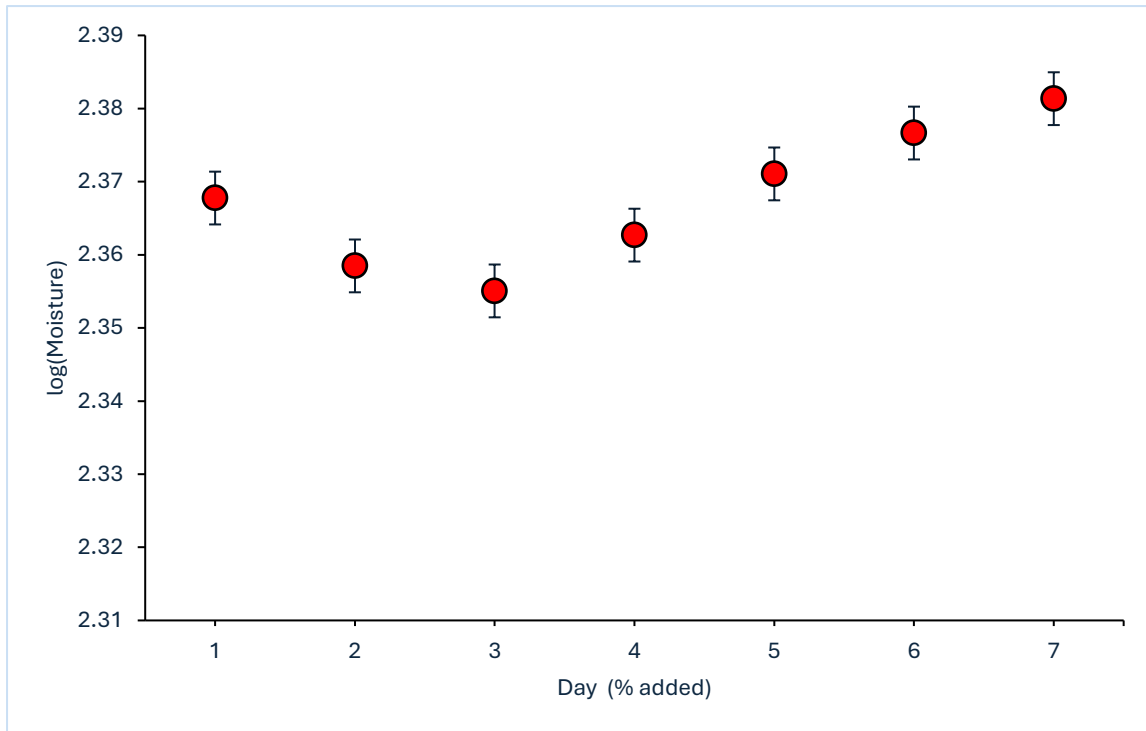


Figure 6.11. Main effects plot of the Day factor with respect to moisture content. Error bars are the 95% confidence interval.

The main effects plot of the Day factor showed that there was a significant difference between different days. The highest moisture content was on day 7, and the day with the lowest moisture content was on day 3 (

Figure 6.11).

Table 6.4. Results of post hoc analysis on Moisture content between the cycle factor.

| <i>Cycle</i> | <i>N</i> | <i>Mean</i> | <i>Grouping</i> |
|--------------|----------|-------------|-----------------|
| <i>Waw</i> | 42 | 2.45 | <i>A</i> |
| <i>Dry</i> | 42 | 2.36 | <i>B</i> |
| <i>Wet</i> | 42 | 2.30 | <i>C</i> |

The post hoc analysis showed that for the Cycle Factor, there were significant differences between all factor levels (Table 6.4).

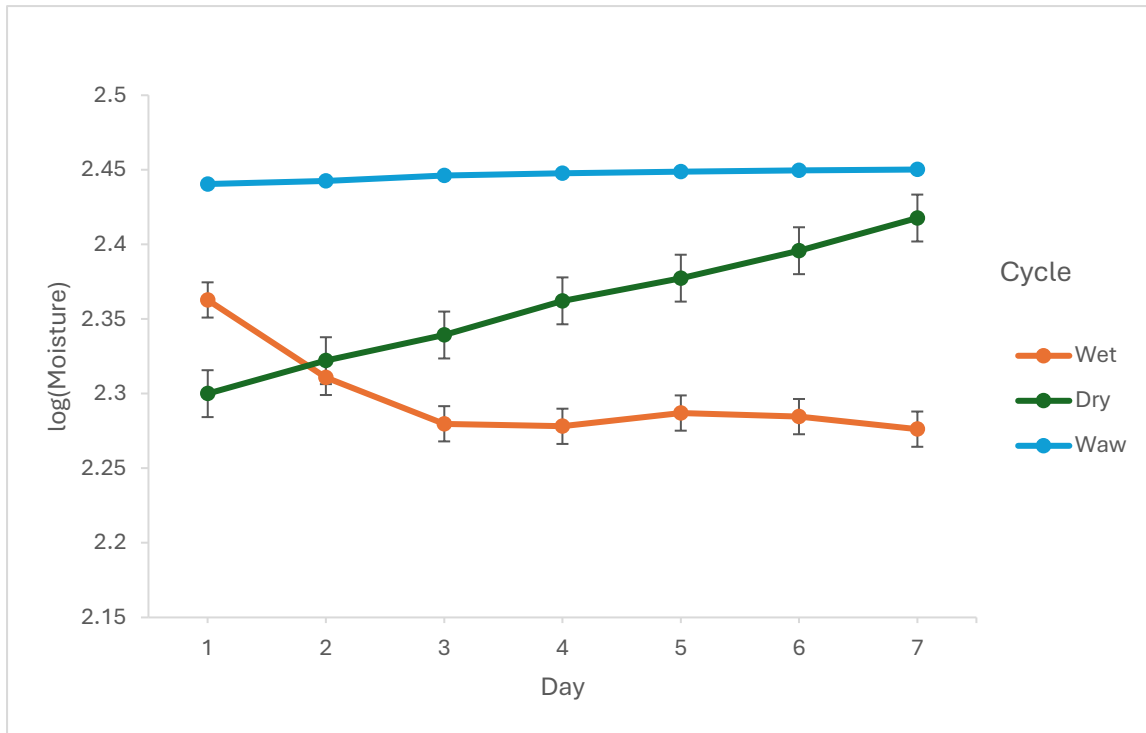


Figure 6.12. The interaction plot of moisture content between Day and Cycle factors.

One interaction was found to be significant (Day*Cycle-

Table 6.3 & Figure 6.12). The plot suggests that throughout the 7 days, the waw cycle had a higher moisture content than the dry and wet cycles. The lowest moisture content was on day 1 for the dry cycle, but from day 2- day 7 the wet cycle had the lowest moisture content.

- Plant Height

The Anderson-Darling test and the QQ' plot (

Figure 6.11) showed that the data were not normally distributed, and so the data were log transformed. The QQ' plot could indicate that some samples could be considered as outliers, and 4.71% of the samples were removed.

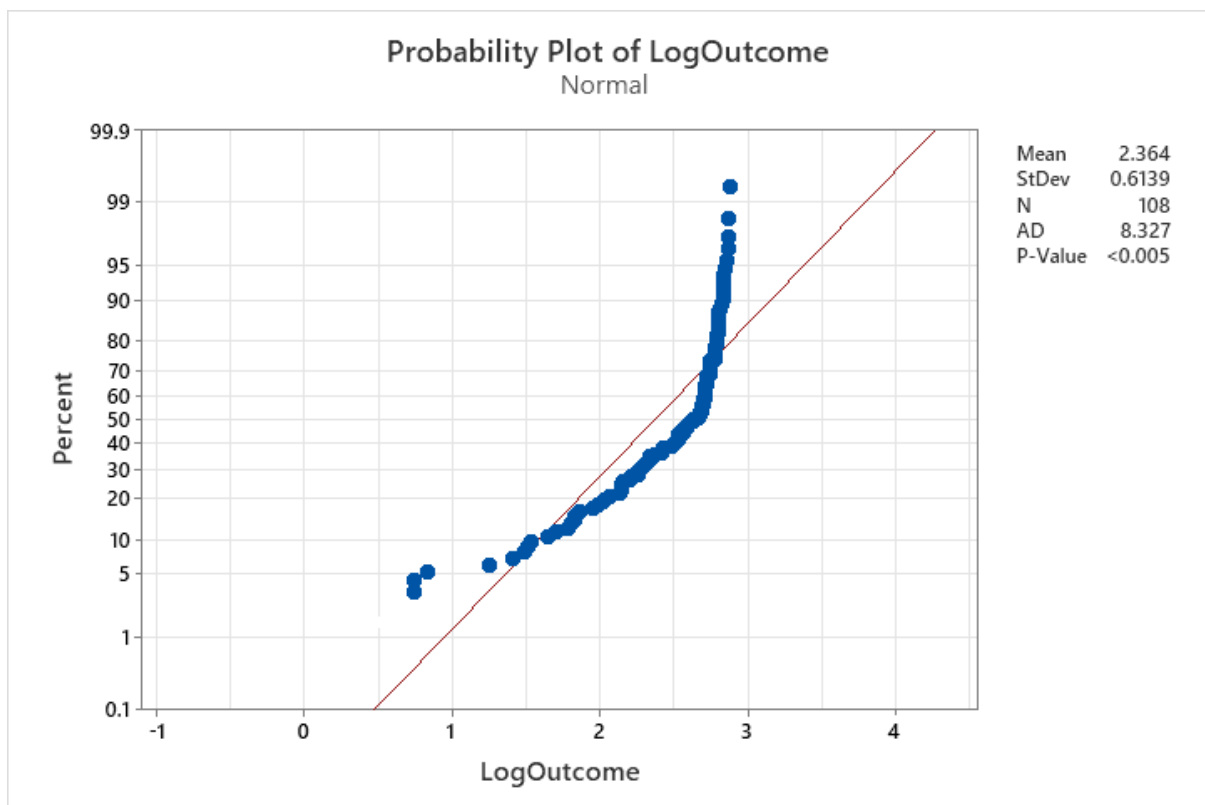


Figure 6.13. QQ' plot of the observed value of plant height. LogOutcome is log(Height).

The ANOVA, including all factors and two-way interactions, had an R^2 of 46.46%.

Table 6.5. The percentage of variance explained for factors and interactions of the Day, Treatment and Cycle factors for the plant height.

| <i>Source</i> | <i>DF</i> | <i>P-Value</i> | <i>% of variance explained</i> |
|------------------------|-----------|----------------|--------------------------------|
| <i>Treatment</i> | 1 | 0.21 | 0.99 |
| <i>Cycle</i> | 1 | 0 | 27.61 |
| <i>Day</i> | 9 | 0.008 | 15.10 |
| <i>Treatment*Cycle</i> | 1 | 0.542 | 0.23 |
| <i>Treatment*Day</i> | 9 | 1 | 0.20 |
| <i>Error</i> | 86 | 0 | 53.76 |

As measured by the proportion of the original variance explained, the most important factor was Cycle, which explained 27.61% of the variance explained by the model (Table 6.5). As there were two levels of the Cycle factor, post hoc analysis was unnecessary.

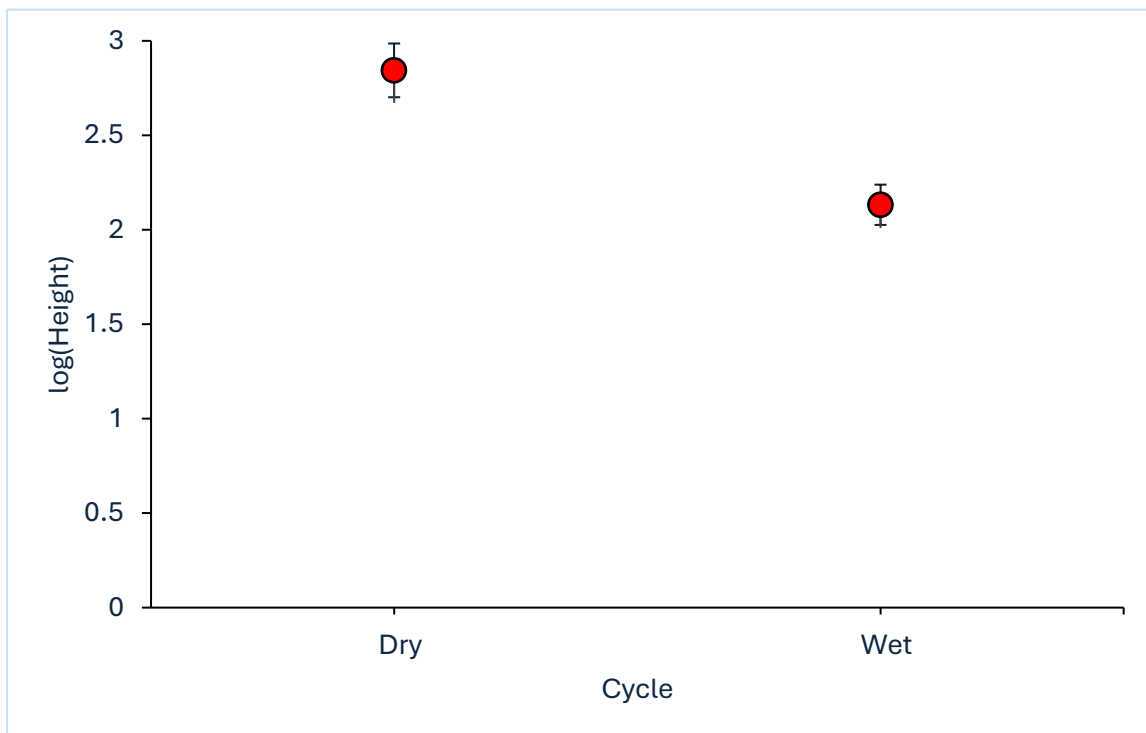


Figure 6.14. Main effects plot of the Cycle factor with respect to plant height. Error bars are the 95% confidence interval.

The main effects plot of the Cycle factor shows that cumulative plant height was higher during the dry cycle than the wet cycle (Figure 6.14). However, this reflects the greater cumulative height of plants later in the experiment and should not be interpreted as indicating higher growth during the dry cycle.

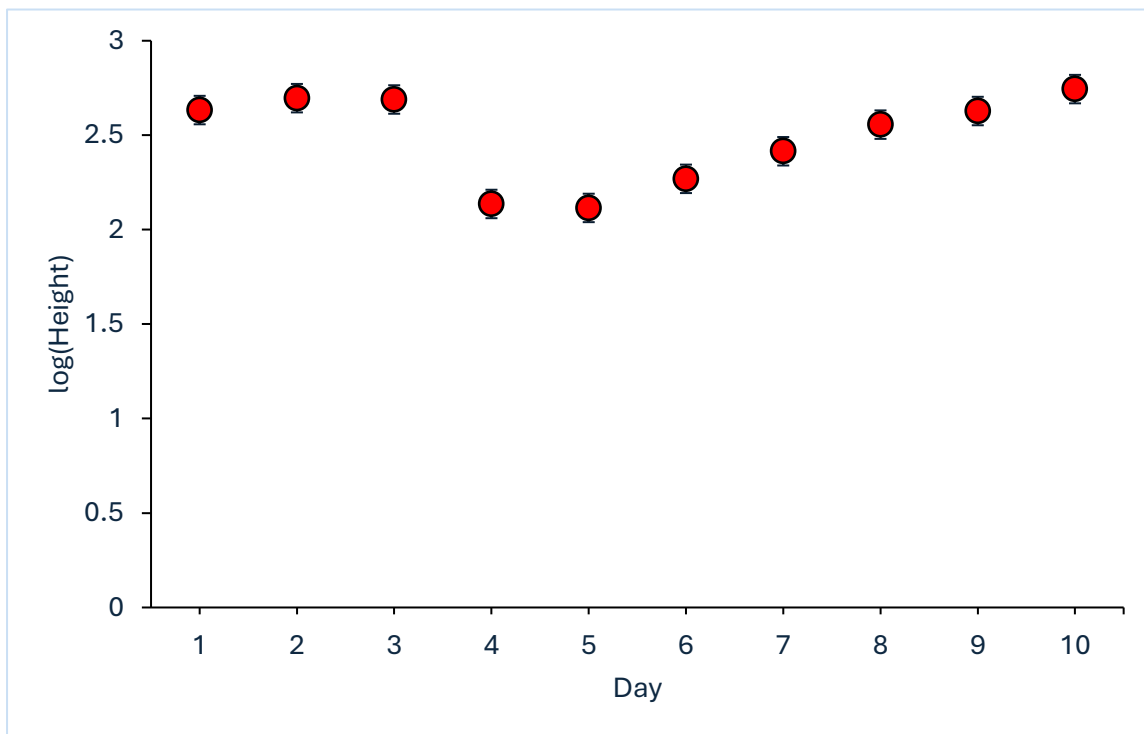


Figure 6.15. Main effects plot of the Day factor with respect to moisture content. Error bars are the 95% confidence interval. Sometimes the error bars are smaller than the plotted point.

The highest mean plant height for the Day factor was on Day 10, and the lowest mean recorded was on Day 5 (Figure 6.15).

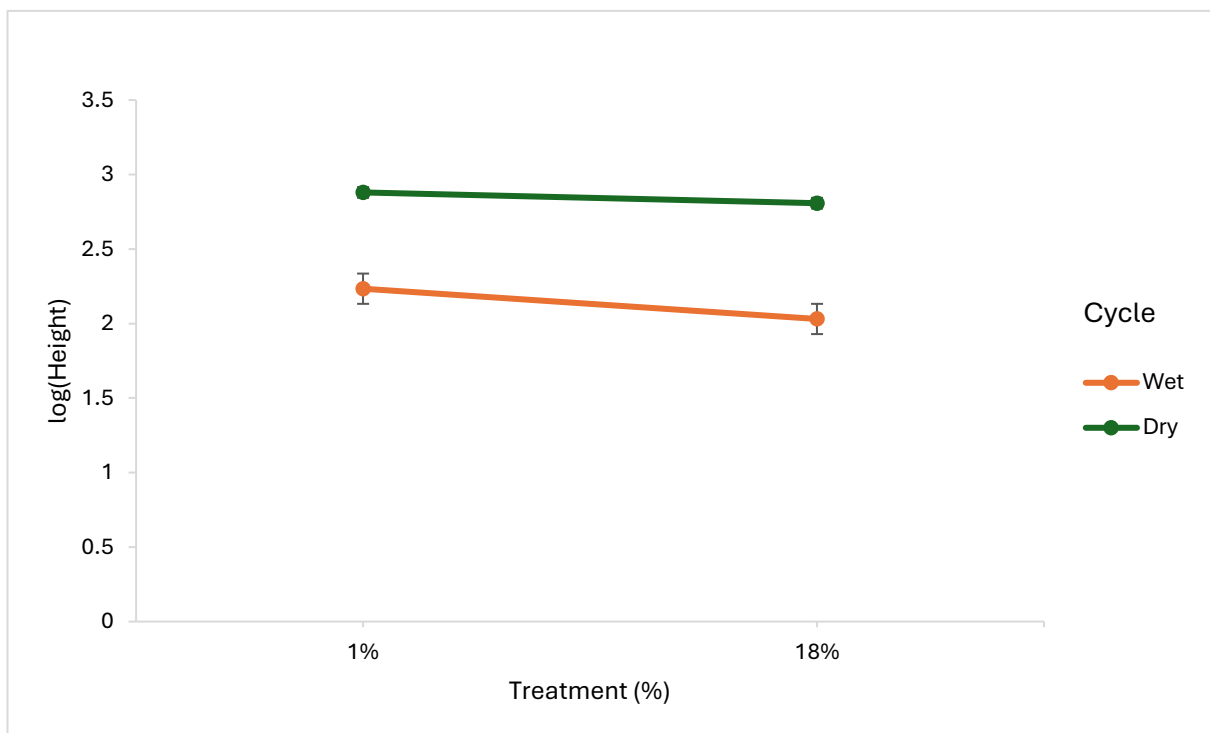


Figure 6.16. The interaction plot of plant height between Cycle and Treatment factors.

The two interactions were found to be significant (Table 6.5 & Figure 6.16). The plot suggests that the plant height of the 1% treatment was higher than that of the 18% during the dry and wet cycles (Figure 6.16).

- Moisture

The Anderson-Darling test and the QQ' plot (Figure 6.17) showed that the data were not normally distributed, and so the data were log transformed. The QQ' plot could indicate that some samples could be considered as outliers, and 1.89% of the samples were removed.

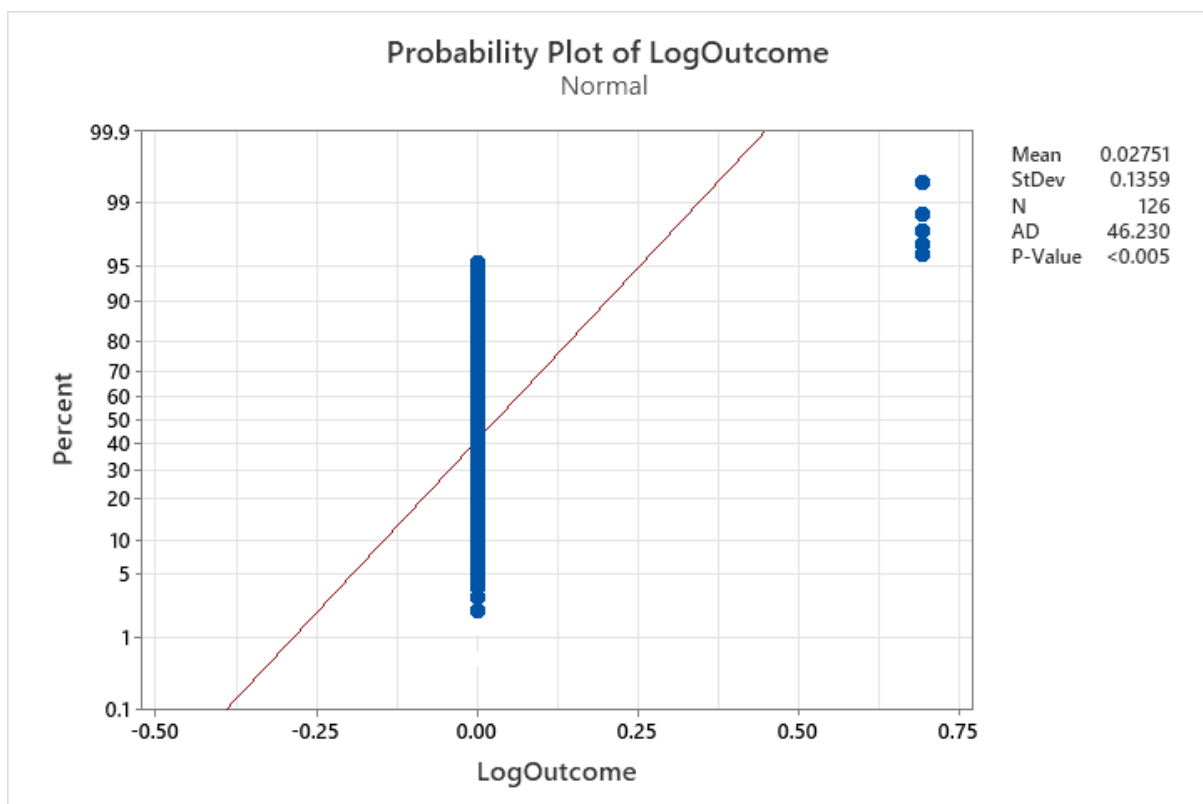


Figure 6.17. QQ' plot of the observed value of the moisture content. $\text{LogOutcome} = \log(\text{Moisture Content})$.

The ANOVA, including all factors and two-way interactions, had an R^2 of 26.41%.

Table 6.6. The percentage of variance explained for factors and interactions of the Day, Treatment and Cycle factors for the moisture content.

| <i>Source</i> | <i>DF</i> | <i>P-Value</i> | <i>% of variance explained</i> |
|------------------------|-----------|----------------|--------------------------------|
| <i>Treatment</i> | 1 | 0.639 | 0.16 |
| <i>Cycle</i> | 1 | 0.049 | 2.8 |
| <i>Day</i> | 9 | 0.008 | 16.85 |
| <i>Treatment*Cycle</i> | 1 | 0.208 | 1.13 |
| <i>Treatment*Day</i> | 9 | 0.593 | 5.27 |
| <i>Error</i> | 104 | 0 | 73.59 |

As measured by the proportion of the original variance explained, the most important factor was Day, which explained 16.85% of the variance explained by the model (Table 6.6). As there were two levels of the Cycle factor, post hoc analysis was unnecessary for that factor.

The analysis showed predominantly negative values in the main effect and interaction plots, which was unexpected given the nature of our response variable. Despite thoroughly verifying the data and ensuring the model assumptions were met, these negative values remained. Therefore, ANOVA was not appropriate for this type of data distribution.

- Soil Temperature

The Anderson-Darling test and the QQ' plot (Figure 6.18) showed that the data were not normally distributed, and so the data were log transformed. The QQ' plot could indicate that some samples could be considered as outliers, and 1.89% of the samples were removed.

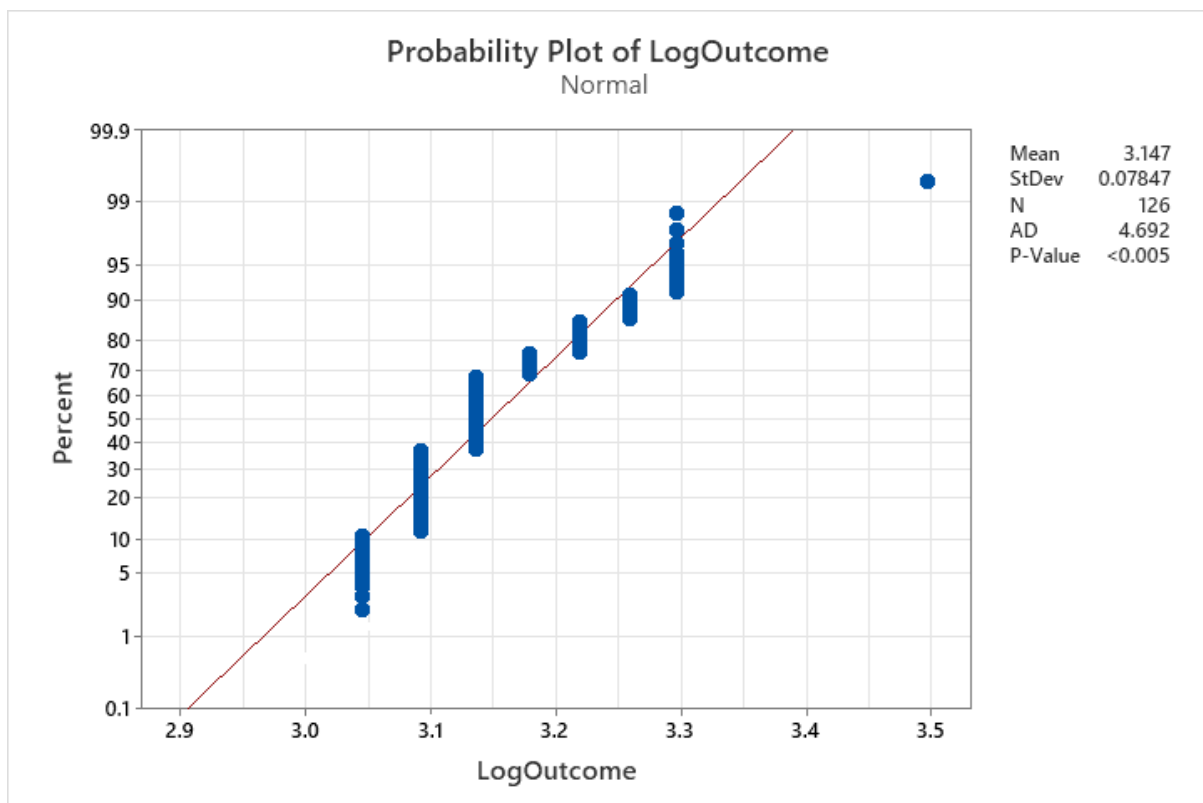


Figure 6.18. QQ' plot of the observed value of the soil temperature. $\text{LogOutcome} = \log(\text{Temperature})$.

The ANOVA, including all factors and two-way interactions, had an R² of 51.96%.

Table 6.7. The percentage of variance explained for factors and interactions of the Day, Treatment and Cycle factors for soil temperature.

| <i>Source</i> | <i>DF</i> | <i>P-Value</i> | <i>% of variance explained</i> |
|------------------------|-----------|----------------|--------------------------------|
| <i>Treatment</i> | 1 | 0.02 | 2.65 |
| <i>Cycle</i> | 1 | 0 | 36.01 |
| <i>Day</i> | 9 | 0.25 | 5.40 |
| <i>Treatment*Cycle</i> | 1 | 0.03 | 2.24 |
| <i>Treatment*Day</i> | 9 | 0.99 | 0.81 |
| <i>Error</i> | 104 | 0 | 48.04 |

As measured by proportion of the original variance explained, the most important factor was Cycle, which explained 36.01% of the variance explained by the model (Table 6.7). As there were two levels of the Cycle factor, post hoc analysis was unnecessary for that factor.

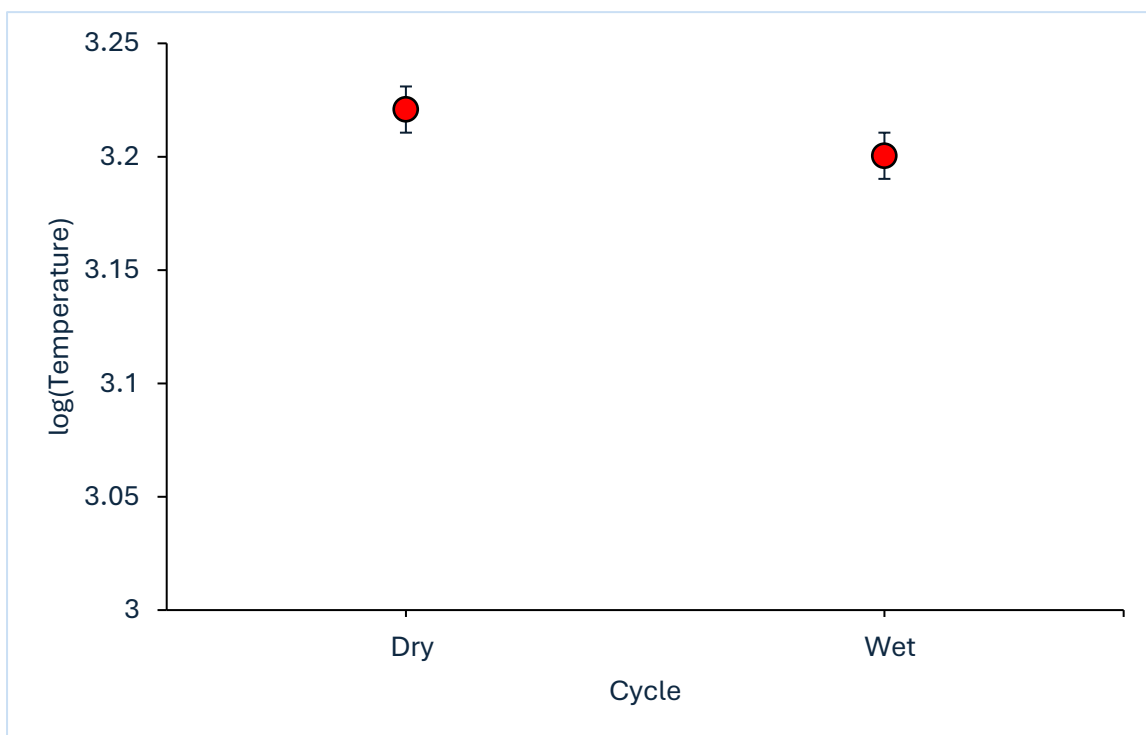


Figure 6.19. Main effects plot of the Cycle factor with respect to soil temperature. Error bars are the 95% confidence interval.

The main effects plot of the Cycle factor (Figure 6.19) shows that soil temperature during the dry cycle was higher than the wet cycle (Figure 6.19).

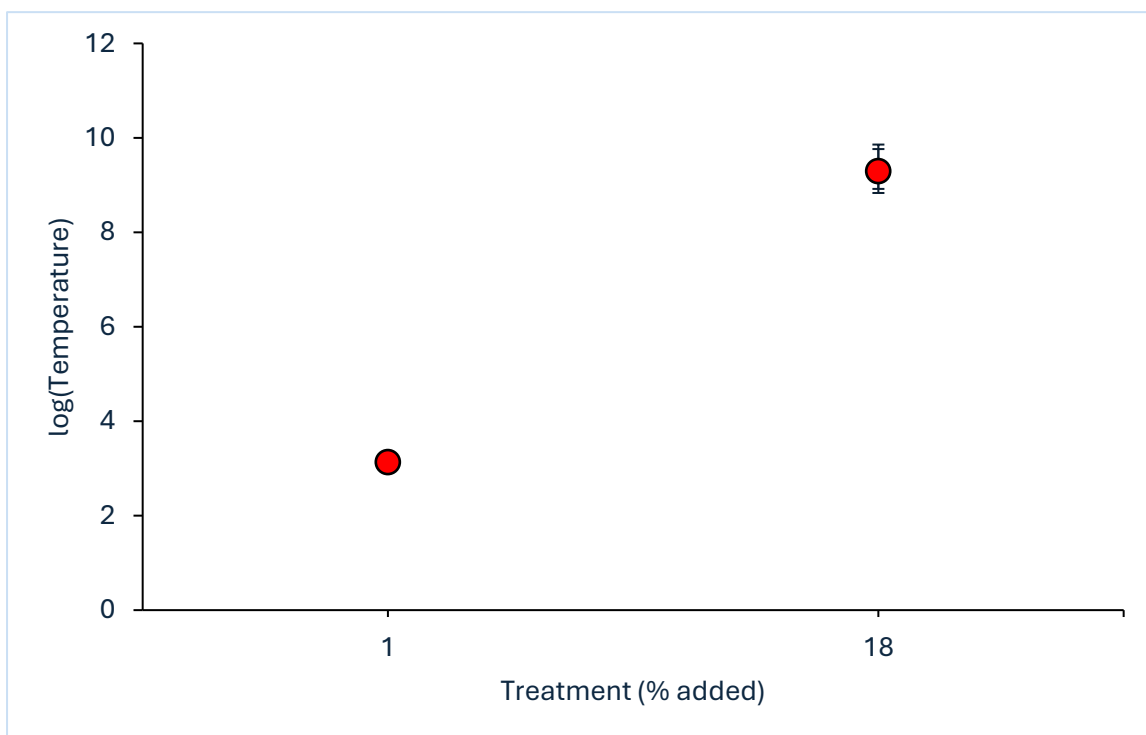


Figure 6.20. Main effects plot of the Treatment factor on soil temperature. Error bars are the 95% confidence interval and may be smaller than the plotted point.

The highest mean temperature recorded for the Treatment factor was for the 18% treatment (Figure 6.20).

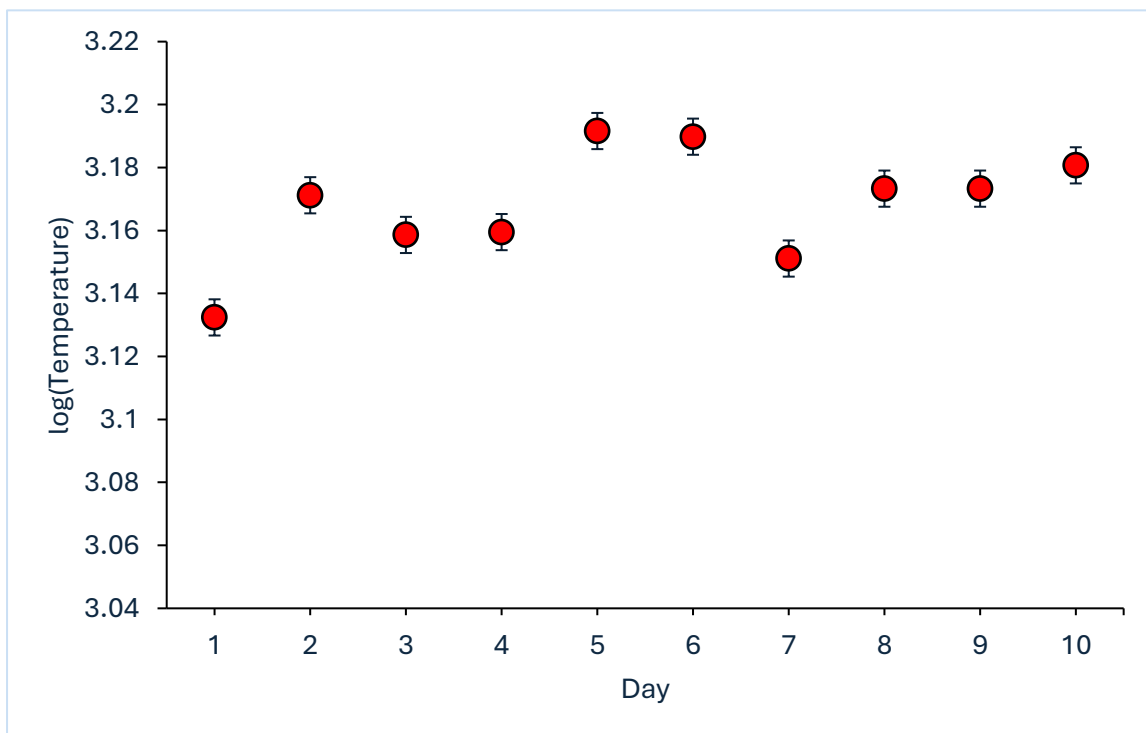


Figure 6.21. Main effects plot of the Day factor with respect to soil temperature. Error bars are the 95% confidence interval.

The highest mean soil temperature for the Day factor was on Day 5, and the lowest mean soil temperature was recorded on Day 1 (Figure 6.21).

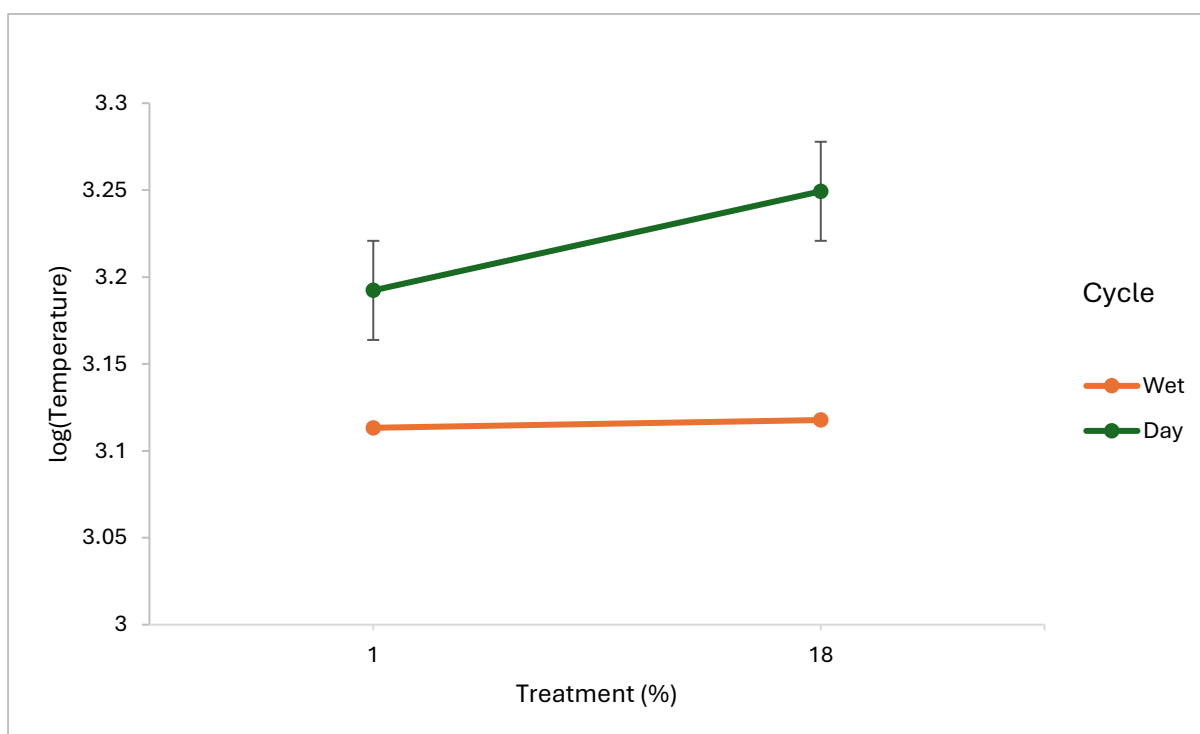


Figure 6.22. The interaction plot of soil temperature between Cycle and Treatment factors.

The one significant interaction was between Cycle and Treatment factors shown in Table 6.7 & Figure 6.22. The plot suggests that during the dry cycle, the 18% treatment was greater than

the 1% treatment. During the wet cycle, both treatments were not significantly different in soil temperatures (Figure 6.22).

- Soil pH

The Anderson-Darling test and the QQ' plot (Figure 6.23) showed that the data were not normally distributed, and so the data were log transformed. The QQ' plot could indicate that some samples could be considered as outliers, and 1.89% of the samples were removed.

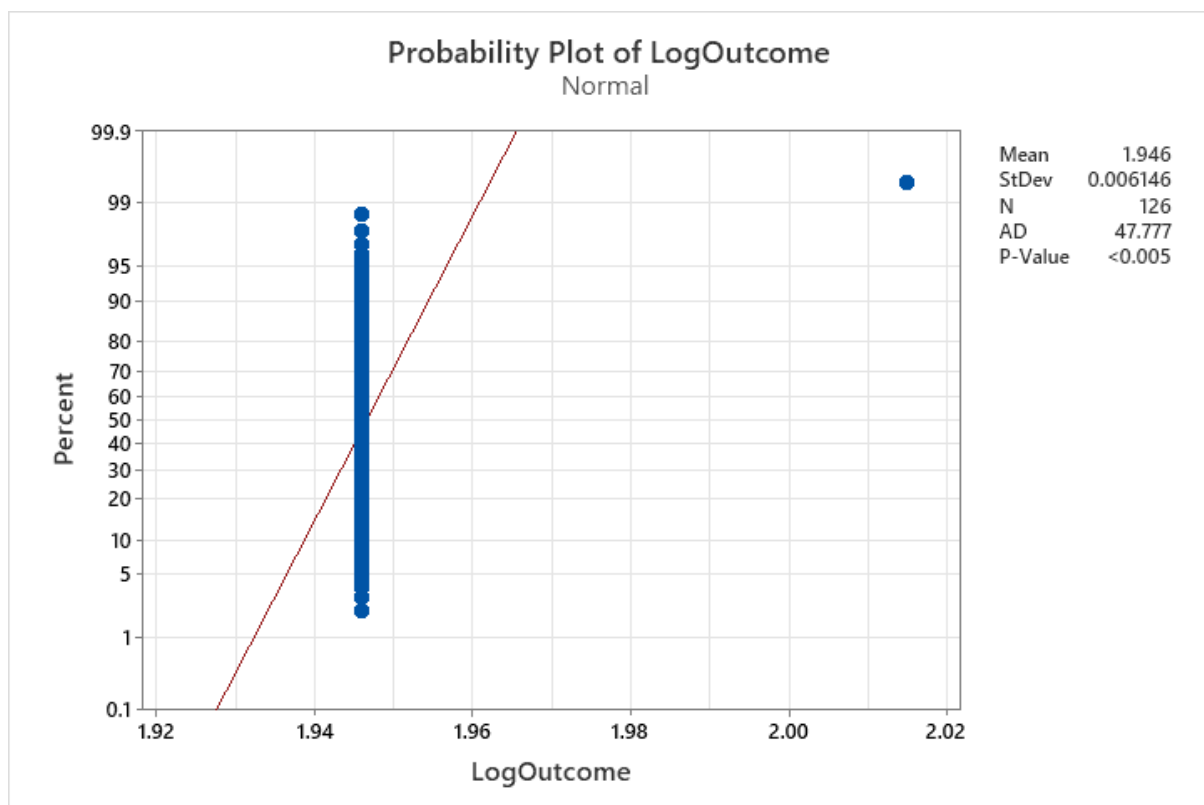


Figure 6.23. QQ' plot of the observed value of the soil pH. $\text{LogOutcome} = \log(\text{pH})$.

The ANOVA, including all factors and two-way interactions, had an R^2 of 18.02%.

Table 6.8. The percentage of variance explained for factors and interactions of the Day, Treatment and Cycle factors for the soil pH.

| <i>Source</i> | <i>DF</i> | <i>P-Value</i> | <i>% of variance explained</i> |
|------------------------|-----------|----------------|--------------------------------|
| <i>Treatment</i> | 1 | 0.68 | 0.15 |
| <i>Cycle</i> | 1 | 0.26 | 1.02 |
| <i>Day</i> | 9 | 0.33 | 8.22 |
| <i>Treatment*Cycle</i> | 1 | 0.26 | 1.02 |
| <i>Treatment*Day</i> | 9 | 0.33 | 8.22 |
| <i>Error</i> | 104 | 0 | 81.98 |

As measured by the proportion of the original variance explained, the most important factor was Day, which explained 8.22% of the variance explained by the model (Table 6.8). However, none of the factors was significant. As a result, no further discussion of specific factors or interactions was necessary.

- Light

The light was not included in the analysis because it could not be measured due to the ANOVA, as the same response and error occurred during the application analysis.

6.5 Discussion

The results of the mesocosm and pot trial experiments provide insight into the effects of combining biochar and Date Palm Fronds (DPF) on soil moisture retention and plant growth. The mesocosm experiment showed that both the 1% and 18% mixed amendments retained water during wet, dry and waw cycles, supporting the first research question of whether mixed amendments influence soil moisture retention. However, the 1% mixed amendment retained slightly more water than the 18% treatment, which was an unexpected result. The increasing proportion of organic amendments is expected to improve soil water holding capacity due to increased porosity and surface area (Dengxiao *et al.*, 2024). In sandy soils, the higher amendment levels can increase microporosity and promote faster drainage, which may reduce water retention under drying conditions. The higher moisture content observed in the waw cycle may be explained by the increased humidity within the oven due to the presence of the water bowl. Increased atmospheric pressure reduces evaporation from the soil surface because the difference in water vapour pressure between the soil and the surrounding air is smaller. Consequently, moisture loss from the soil is reduced, allowing the samples in the waw cycle treatment to retain higher water content compared with the wet and dry cycles. A similar mechanism may explain the contrasting trends observed between the wet and dry cycles. Despite the addition of water during the wet cycle, the high incubation temperature (40°C) likely increased evaporation rates, resulting in a net loss of moisture over time. In contrast, during the dry cycle, moisture loss may have slowed as the soil approached equilibrium with the surrounding air, leading to relatively stable or slightly increasing moisture content.

Although these results appear gradual over time, the ANOVA results confirmed that the Cycle factor had a significant effect on moisture content. These findings highlight the influence of temperature and atmospheric conditions on soil moisture dynamics under controlled experimental conditions.

The pot trial experiment further demonstrated that plant growth differed between treatments and moisture cycles. Growth rate analysis showed that plant growth was greater during the wet cycle, whereas plant height during the dry cycle was lower and occasionally negative. Although the ANOVA results indicated greater cumulative plant height during the dry cycle, the growth rate calculations suggest that this pattern reflects accumulated height rather than increased growth during the dry period. Adequate soil moisture promotes plant growth by supporting nutrient uptake and physiological processes (Gundale *et al.*, 2016).

When compared with the results in Chapter 4, plant growth in the mixed amendment was lower than in the single amendment treatments. This result may be due to interactions between biochar and DPF when applied together, which could alter soil structure, aeration or nutrient availability differently than when each material is applied individually. Previous studies have shown that combining organic amendments can influence soil physiological properties and microbial activity in different ways depending on amendment composition and soil type (Badawi, 2019). The soil temperature result indicated that the 1% mixed amendment showed slightly higher mean temperature during the dry cycle compared to the 18% mixed amendment, with a maximum temperature of 27°C. This temperature increase might be attributed to the lower water content in the soil, as water can play a part in the cooling effect due to its high specific heat capacity (Tisserant and Cherubini, 2019).

The soil pH remained constant at (level 7) for both 1% and 18% mixed amendments across all cycles, indicating that the combination of biochar and DPF did not significantly change soil pH. Maintaining neutral pH is beneficial for moist plant species as extreme pH

levels can limit nutrient availability and uptake (Soti *et al.*, 2015). A study done by (Badawi, 2019) showed that the pH level of sandy soil in the UAE was more alkaline (8.9) than biochar produced from DPF (6.8), which could make sense with our results in this study being neutral at (level 7).

The ANOVA results highlighted the significant interactions between treatment factors, particularly between Cycle and Day factors, explaining a substantial proportion of the variance in plant height and moisture content. Specifically, the analysis showed that plant height and water retention differed significantly between dry and wet cycles, with the dry cycle favouring plant growth and water retention. These interactions suggest that the combined treatment of biochar and DPF responds dynamically to changing environmental conditions, providing adaptive benefits for water retention and plant growth.

This study has several limitations. Although only two amendment levels (1% and 18%) were used, selected based on their good performance as discussed in the previous chapters, it would be interesting to compare these results with additional treatments, such as the 6% and 15% treatments. Comparative studies that examine a wider range of soil mixed treatment percentages could provide a more comprehensive understanding of the effects of these treatments. Another limitation is that further studies are needed to evaluate the pot trial under uncontrolled conditions. Applying these treatments in a field trial experiment setting would provide a better understanding of how the plants would behave under harsh weather conditions. Field trial experiments often present extreme and challenging environmental conditions, such as poor soil quality, fluctuating moisture levels, elevated temperatures, and exposure to harsh weather. These factors can simulate the stresses plants face in an arid environment. By testing biochar and Date Palm Fronds (DPF) in this setting, it will gain insight into their ability to improve soil structure, enhance water retention and support plant growth in extreme environments, making the findings more applicable in real-world scenarios. Given the

uniqueness of our study on the combination of biochar with DPF, it was challenging to identify prior research that has explored a similar approach.

This study demonstrates the broader relevance of mixed biochar and Date Palm Fronds (DPF) materials by highlighting their contributions to soil health and water retention, which are crucial for plant growth. Both charred (biochar) and non-charred (DPF) material offer advantages for agriculture and infrastructure. For agriculture, understanding green waste and utilising it in different treatment percentages could enhance waste management practices (Amalina *et al.*, 2022). For the infrastructure industry, biochar has been shown to improve water retention during floods, highlighting its potential benefits (Kumar *et al.*, 2022). Additionally, biochar's ability to enhance plant growth and health by enhancing soil structure and nutrient availability (Singh Yadav *et al.*, 2023). Although many studies have focused on biochar applications, this study also highlights that DPF can act the same whether it is a mixed treatment or a single treatment.

6.6 Conclusion

Soil moisture and light intensity were recorded using a semi-quantitative probe and are presented as relative categorical levels as described in Chapter 4. These measurements provide an indication of relative soil moisture and light conditions and are not directly comparable to absolute measurements such as gravimetric water content or photosynthetically active radiation (PAR) but allow consistent comparison between treatments within the experiment.

Chapter 7: Conclusion

7.1 Overview of thesis

The thesis has thoroughly explored the comprehensive application and benefits of biochar, focusing on its production through pyrolysis and its role in enhancing soil properties and the mitigation of climate change. By discovering its historical use in modern applications, this research has highlighted biochar's potential to increase crop yields and contribute to sustainable development goals, particularly in arid regions like the UAE.

7.2 Key objectives and findings

The primary objective of this research was to evaluate the properties of biochar and Date Palm Fronds (DPF), assess their impact on soil moisture retention, and determine their ability to improve plant growth under different environmental conditions. The key findings from the chapter can be summarised as follows:

1. **Chapter 1:** Established the foundation by detailing biochar's definition, production methods, and benefits, particularly its role in the UAE's sustainability efforts.
2. **Chapter 2:** Characterisation of biochar and DPF revealed biochar's greater porosity, higher Carbon (C) ratio, and greater thermal stability, underscoring its potential as an effective soil amendment.
3. **Chapter 3:** Mesocosm studies demonstrated that both biochar and DPF enhance soil water retention, with biochar showing greater potential during wet cycles.

4. **Chapter 4:** Indicated potential positive effects of biochar on plant growth under controlled conditions; however, these effects were not consistently observed under field conditions.
5. **Chapter 5:** Thermogravimetric analysis (TGA) featured biochar's stability and superior water holding capacity compared to DPF and sand, suggesting its suitability for environmental and industrial applications.
6. **Chapter 6:** The combination of biochar and DPF showed that the combination of treatments effectively improves water retention and plant growth, with lower concentration treatments (e.g., 1% mixed treatment) being more beneficial than higher concentrations.

7.3 Implications

The study offers critical insights for sustainable agriculture management, particularly in regions facing water scarcity and soil degradation. By examining the use of biochar and Date Palm Fronds (DPF) and the combination of both materials, this research highlights strategies for improving water retention and promoting plant growth, which is essential in arid climates like the UAE. The findings have significant implications for global agricultural practices, particularly biochar when derived from DPF, which has demonstrated enhanced water retention and nutrient availability, especially under controlled conditions in sandy soil. However, it is important to consider that the effectiveness of biochar may evolve over time. Ageing processes, including surface oxidation, pore structure modification and microbial colonisation, can alter its adsorption capacity, nutrient availability and overall interaction with soil systems. These changes may enhance or reduce its performance depending on environmental conditions and duration of application. This suggests that biochar could play a crucial role in optimising crop productivity in such challenging regions. Furthermore, biochar's stability in sequestering

carbon and improving soil structure positions it as a key player in mitigating climate change and enhancing renewable energy technologies. Its implication could reduce greenhouse gas emissions, promote carbon storage in agricultural soils and contribute to the United Nations Sustainable Development Goals (SDGs). Also, in line with the UAE 2050 vision and post-COP28 sustainability goals, biochar and DPF directly support the country's efforts to achieve net-zero emissions and promote sustainable land use. The results of this research are also applied to waste management practices in the reuse of agricultural residues like DPF, which can enhance soil properties while reducing waste. Additionally, biochar's thermal stability and moisture retention properties offer potential benefits for renewable energy products through biomass conversion processes like pyrolysis and gasification. By understanding the thermal characteristics and water-holding capacities of biochar and DPF, this research provides valuable insights for industries seeking to improve resource efficiency and sustainable land management.

7.4 Limitations

While the research provided valuable insights into the understanding of biochar and DPF's role in water retention and plant growth, several limitations must be considered. One of the primary limitations is the controlled environment in which the experiments were conducted. While the controlled conditions allow for precise measurements, they do not fully replicate the complex, variable conditions of outdoor environments. Real-world factors of biochar and DPF, in ways that were captured in this study, were very short-term. Therefore, the ecological validity of the findings is somewhat limited, and caution should be exercised when applying these results to uncontrolled settings and in the longer term. Although the research demonstrated positive impacts on soil moisture retention and plant growth for the shorter term in one season, it is suggested that future studies examine the impact over multiple growing seasons and beyond

the short term. Another limitation is that the measurements of soil pH were mostly neutral levels, which is expected for biochar produced from DPF, but after multiple uses of the probe, it was stuck on the same measurements on each sample.

7.5 Future work

Building on the implications and limitations of this research, future research is required to explore the long-term effects of biochar and DPF on soil health, plant growth and overall ecosystem sustainability. Conducting field trials in uncontrolled environments over multiple growing seasons would provide a more comprehensive understanding of the durability and effectiveness of these treatments. Such research could focus on how biochar and DPF interact with varying environmental conditions, including extreme temperatures, water scarcity and fluctuating moisture levels. Additionally, investigating the combined effects of biochar with other sustainable practices, such as organic fertilisers or crop rotation, to enhance agricultural resilience in arid regions. Further research is needed to investigate the economic feasibility and environmental impacts of large-scale biochar application and explore additional factors like soil microbial activity and nutrient cycling to further clarify its potential as a sustainable agricultural tool. Researchers should evaluate the different soil types and climates, focusing on optimising biochar properties to suit specific environmental conditions. Finally, further research can explore the potential of integrating biochar into renewable energy systems. For example, investigating its role in biochar conversion technologies, such as pyrolysis to produce biofuels and biogas. The findings of this research suggest that biochar not only improves soil quality but also holds promise for broader applications in energy and waste management, contributing to global efforts towards sustainability and climate resilience. Future studies should also investigate how ageing processes influence the long-term physicochemical properties of biochar and its effectiveness as a soil amendment under field conditions.

8.1 References

- Abdelfattah, M. A. *et al.* (2014) *United Arab Emirates Keys to Soil Taxonomy*. doi: 10.1007/978-94-007-7420-9.
- Abdelfattah, M., Shahid, S. and Othman, Y. (2009) 'Soil Salinity Mapping Model Developed Using RS and GIS - A Case Study from Abu Dhabi, United Arab Emirates', *European Journal of Scientific Research*, 26(3), pp. 342–351.
- AbdelRahman, M. A. E. (2023) *An overview of land degradation, desertification and sustainable land management using GIS and remote sensing applications*, *Rendiconti Lincei*. Springer International Publishing. doi: 10.1007/s12210-023-01155-3.
- Al-Rumaihi, A. *et al.* (2022) 'A review of pyrolysis technologies and feedstock: A blending approach for plastic and biomass towards optimum biochar yield', *Renewable and Sustainable Energy Reviews*. Elsevier Ltd, 167(March), p. 112715. doi: 10.1016/j.rser.2022.112715.
- Alotaibi, K. D. and Schoenau, J. J. (2019) 'Addition of Biochar to a Sandy Desert Soil : Effect on Crop Growth , Water Retention and Selected Properties', pp. 5–7.
- Alsuwaidi, A. H. and Ramos, E. (2017) 'Abu Dhabi State of Environment Report 2017', p. 97.
- Amalina, F. *et al.* (2022) 'Biochar production techniques utilizing biomass waste-derived materials and environmental applications – A review', *Journal of Hazardous Materials Advances*. Elsevier B.V., 7(July), p. 100134. doi: 10.1016/j.hazadv.2022.100134.
- Artiola, J. F. and Wardell, L. (2017) 'Guide to Making and Using Biochar for Gardens in Southern Arizona', *University of Arizona College of Agriculture Cooperative Extension*, (AZ1752). Available at: <https://extension.arizona.edu/pubs/guide-making-and-using-biochar-gardens-southern-arizona>.
- Badawi, M. A. (2019) 'Production of Biochar from Date Palm Fronds and its Effects on Soil Properties', 11, pp. 159–168.
- Badawi, M. A. (2020) 'Saving 45 % of Irrigation Water of Date Palm Tree Plantations Using Soil Amendments in UAE', 6(4), pp. 31–44.
- Baiamonte, G. *et al.* (2019) 'Effect of biochar on the physical and structural properties of a desert sandy soil', *Catena*. Elsevier, 175(April 2018), pp. 294–303. doi: 10.1016/j.catena.2018.12.019.
- Barrera-zapata, R. (2017) 'Morphological and physicochemical characterization of biochar produced by gasification of selected forestry species Caracterización morfológica y fisico-química de biocarbones producidos', 26(46), pp. 123–130.
- Bataillou, G. *et al.* (2022) 'Cedar Wood-Based Biochar: Properties, Characterization, and Applications as Anodes in Microbial Fuel Cell', *Applied Biochemistry and Biotechnology*. Springer US, 194(9), pp. 4169–4186. doi: 10.1007/s12010-022-03997-3.
- Benyoucef, S. *et al.* (2020) 'Preparation and characterization of novel microstructure cellulosic sawdust material: application as potential adsorbent for wastewater treatment', *Cellulose*. Springer Netherlands, 27(14), pp. 8169–8180. doi: 10.1007/s10570-020-03349-6.
- Bhaskar, U. *et al.* (2019) 'Modeling and Optimization of Product Profiles in Biomass Pyrolysis', (March), pp. 2016–2017.

- Bhat, S. *et al.* (2022) 'Application of Biochar for Improving Physical, Chemical, and Hydrological Soil Properties: A Systematic Review', *Sustainability (Switzerland)*, 14(17). doi: 10.3390/su141711104.
- Biederman, L. A. and Stanley Harpole, W. (2013) 'Biochar and its effects on plant productivity and nutrient cycling: A meta-analysis', *GCB Bioenergy*, 5(2), pp. 202–214. doi: 10.1111/gcbb.12037.
- Blanco-Canqui, H. (2017) 'Biochar and Soil Physical Properties', *Soil Science Society of America Journal*, 81(4), pp. 687–711. doi: 10.2136/sssaj2017.01.0017.
- Boraah, N., Chakma, S. and Kaushal, P. (2023) 'Optimum features of wood-based biochars: A characterization study', *Journal of Environmental Chemical Engineering*. Elsevier Ltd, 11(3), p. 109976. doi: 10.1016/j.jece.2023.109976.
- Borchard, N. *et al.* (2019) 'Biochar, soil and land-use interactions that reduce nitrate leaching and N₂O emissions: A meta-analysis', *Science of the Total Environment*. Elsevier B.V., 651, pp. 2354–2364. doi: 10.1016/j.scitotenv.2018.10.060.
- Brtnicky, M. *et al.* (2021) 'A critical review of the possible adverse effects of biochar in the soil environment', *Science of the Total Environment*. doi: 10.1016/j.scitotenv.2021.148756.
- Bruun, E. W. (2011) *Application of Fast Pyrolysis Biochar to a Loamy Soil*.
- Burezq, H. and Davidson, M. K. (2023) 'Biochar from date palm (*Phoenix dactylifera* L.) residues—a critical review', *Arabian Journal of Geosciences*. Springer International Publishing, 16(2). doi: 10.1007/s12517-022-11123-0.
- Chafik, Y. *et al.* (2024) 'Biochar characteristics and Pb²⁺/Zn²⁺ sorption capacities: the role of feedstock variation', *International Journal of Environmental Science and Technology*. Springer Berlin Heidelberg. doi: 10.1007/s13762-024-05646-0.
- Chatterjee, R. *et al.* (2020) 'Effect of Pyrolysis Temperature on PhysicoChemical Properties and Acoustic-Based Amination of Biochar for Efficient CO₂ Adsorption', *Frontiers in Energy Research*, 8(May), pp. 1–18. doi: 10.3389/fenrg.2020.00085.
- Chen†, M. *et al.* (2024) 'Achievement of efficient thermally activated delayed fluorescence materials based on 1,8-naphthalimide derivatives exhibiting piezochromic and thermochromic luminescence', *RSC Advances*. Royal Society of Chemistry, 14(25), pp. 17434–17439. doi: 10.1039/d4ra02981j.
- Chikri, R. *et al.* (2023) 'Two-step optimization of the preparation conditions of a high-quality activated carbon derived from sawdust', *Biomass Conversion and Biorefinery*. Springer Berlin Heidelberg, (123456789), pp. 9–14. doi: 10.1007/s13399-023-03965-9.
- Clough, T. J. *et al.* (2013) 'A review of biochar and soil nitrogen dynamics', *Agronomy*, 3(2), pp. 275–293. doi: 10.3390/agronomy3020275.
- Cybulska, I. *et al.* (2017) 'Organosolv delignification of agricultural residues (date palm fronds, *Phoenix dactylifera* L.) of the United Arab Emirates', *Applied Energy*. Elsevier Ltd, 185, pp. 1040–1050. doi: 10.1016/j.apenergy.2016.01.094.
- Daniel Bardsley (2017) *Date palm cloning ensures traditional UAE industry has a sweet future*, *The National*. Available at: <https://www.thenational.ae/uae/environment/date-palm-cloning-ensures-traditional-uae-industry-has-a-sweet-future-1.613482>.
- Davidson, E. A. and Janssens, I. A. (2006) 'Temperature sensitivity of soil carbon decomposition and feedbacks to climate change', *Nature*, 440(7081), pp. 165–173. doi: 10.1038/nature04514.

- Demirbas, A. (2007) 'Effects of moisture and hydrogen content on the heating value of fuels', *Energy Sources, Part A: Recovery, Utilization and Environmental Effects*, 29(7), pp. 649–655. doi: 10.1080/009083190957801.
- Dengxiao, Z. *et al.* (2024) 'Combined biochar and water-retaining agent application increased soil water retention capacity and maize seedling drought resistance in Fluvisols', *Science of the Total Environment*. Elsevier B.V., 907(October 2023), p. 167885. doi: 10.1016/j.scitotenv.2023.167885.
- Doan, T. T. *et al.* (2015) 'Impact of compost, vermicompost and biochar on soil fertility, maize yield and soil erosion in Northern Vietnam: A three year mesocosm experiment', *Science of the Total Environment*. Elsevier B.V., 514, pp. 147–154. doi: 10.1016/j.scitotenv.2015.02.005.
- Edeh, I. G. and Mašek, O. (2022) 'The role of biochar particle size and hydrophobicity in improving soil hydraulic properties', *European Journal of Soil Science*, 73(1). doi: 10.1111/ejss.13138.
- Eickemeier, P. *et al.* (2019) *IPCC, 2012: Summary for Policymakers, Planning for Climate Change*. doi: 10.4324/9781351201117-15.
- Elnour, A. Y. *et al.* (2019) 'Effect of pyrolysis temperature on biochar microstructural evolution, physicochemical characteristics, and its influence on biochar/polypropylene composites', *Applied Sciences (Switzerland)*, 9(6), pp. 7–9. doi: 10.3390/app9061149.
- Feng, W. *et al.* (2021) 'Effects of straw biochar application on soil temperature, available nitrogen and growth of corn', *Journal of Environmental Management*. Elsevier Ltd, 277(September 2020), p. 111331. doi: 10.1016/j.jenvman.2020.111331.
- Gao, Y. *et al.* (2021) 'Influences of soil and biochar properties and amount of biochar and fertilizer on the performance of biochar in improving plant photosynthetic rate: A meta-analysis', *European Journal of Agronomy*. Elsevier B.V., 130(July), p. 126345. doi: 10.1016/j.eja.2021.126345.
- Gašparovič, L., Koreňová, Z. and Jelemenský, L. (2010) 'Kinetic study of wood chips decomposition by TGA', *Chemical Papers*, 64(2), pp. 174–181. doi: 10.2478/s11696-009-0109-4.
- Geoengineering (2015) *Step-by-Step Guide for Grain Size Analysis*. Available at: <https://www.geoengineer.org/education/laboratory-testing/step-by-step-guide-for-grain-size-analysis#bstep-by-step-sieve-analysis-test-procedureb>.
- Gopal, M. *et al.* (2020) 'Biochars produced from coconut palm biomass residues can aid regenerative agriculture by improving soil properties and plant yield in humid tropics', *Biochar*. Springer Singapore, 2(2), pp. 211–226. doi: 10.1007/s42773-020-00043-5.
- Grünzweig, J. M. *et al.* (2022) 'Dryland mechanisms could widely control ecosystem functioning in a drier and warmer world'. Springer US, 6(August). doi: 10.1038/s41559-022-01779-y.
- Gundale, M. J. *et al.* (2016) 'The effect of biochar management on soil and plant community properties in a boreal forest', *GCB Bioenergy*, 8(4), pp. 777–789. doi: 10.1111/gcbb.12274.
- Hagemann, N. *et al.* (2017) 'Organic coating on biochar explains its nutrient retention and stimulation of soil fertility', *Nature Communications*. Springer US, 8(1), pp. 1–11. doi: 10.1038/s41467-017-01123-0.
- Haider, G. *et al.* (2017) 'Biochar reduced nitrate leaching and improved soil moisture content without yield improvements in a four-year field study', *Agriculture, Ecosystems and*

Environment. Elsevier B.V., 237, pp. 80–94. doi: 10.1016/j.agee.2016.12.019.

Heine, P. (2004) *Food Culture in the Near East, Middle East, and North Africa*. Greenwood Publishing Group. Available at: https://books.google.co.uk/books?id=1jE5k5qeKbgC&lpg=PR7&ots=1Fi4LC_bSv&dq=Food Culture in the Near East%2C Middle East%2C and North Africa by &lr&pg=PR7#v=onepage&q=Food Culture in the Near East, Middle East, and North Africa by&f=false.

Heydari, M. *et al.* (2023) 'Synergistic use of biochar and the plant growth-promoting rhizobacteria in mitigating drought stress on oak (*Quercus brantii* Lindl.) seedlings', *Forest Ecology and Management*, 531(January). doi: 10.1016/j.foreco.2023.120793.

Horák, J. *et al.* (2022) 'Mitigation of Greenhouse Gas Emissions with Biochar Application in Compacted and Uncompacted Soil', *Agronomy*, 12(3). doi: 10.3390/agronomy12030546.

Inayat, A. *et al.* (2023) 'Thermal degradation characteristics, kinetic and thermodynamic analyses of date palm surface fibers at different heating rates', *Fuel*. Elsevier Ltd, 335(November 2022), p. 127076. doi: 10.1016/j.fuel.2022.127076.

International Biochar Initiative (2015) 'Standardized Product Definition and Product Testing Guidelines for Biochar That Is Used in Soil', *International Biochar Initiative*, (November), p. 23. Available at: http://www.biochar-international.org/sites/default/files/Guidelines_for_Biochar_That_Is_Used_in_Soil_Final.pdf.

International Biochar Initiative (2018) *Biochar Is a Valuable Soil Amendment, Biochar International Initiative*. Available at: <https://biochar-international.org/biochar/>.

Ippolito, J. A., Laird, D. A. and Busscher, W. J. (2012) 'Environmental Benefits of Biochar', pp. 967–972. doi: 10.2134/jeq2012.0151.

Jeffery, S. *et al.* (2011) 'A quantitative review of the effects of biochar application to soils on crop productivity using meta-analysis', *Agriculture, Ecosystems and Environment*. Elsevier B.V., 144(1), pp. 175–187. doi: 10.1016/j.agee.2011.08.015.

Jha, S. *et al.* (2023) 'Biochar as Sustainable Alternative and Green Adsorbent for the Remediation of Noxious Pollutants: A Comprehensive Review', *Toxics*, 11(2), p. 117. doi: 10.3390/toxics11020117.

Jouiad, M. *et al.* (2015) 'Characteristics of slow pyrolysis biochars produced from rhodes grass and fronds of edible date palm', *Journal of Analytical and Applied Pyrolysis*. Elsevier B.V., 111, pp. 183–190. doi: 10.1016/j.jaap.2014.10.024.

K.R.Rajisha *et al.* (2011) 'Interface Engineering of Natural Fibre Composites for Maximum Performance', *Woodhead Publishing Series in Composites Science and Engineering*, pp. 241–274. Available at: <https://www.sciencedirect.com/science/article/pii/B9781845697426500095?via%3Dihub>.

Karbout, N. *et al.* (2019) 'Applying biochar from date palm waste residues to improve the organic matter, nutrient status and water retention in sandy oasis soils Applying biochar from date palm waste residues to improve the organic matter, nutrient status and water retention in s', (July 2020).

Karim, M. R. (2020) 'Biochar for Promoting Sustainable Agriculture', (June 2020), pp. 123–130. doi: 10.1007/978-3-319-95675-6_113.

Khalifa, N. and Yousef, L. F. (2015) 'A Short Report on Changes of Quality Indicators for a Sandy

- Textured Soil after Treatment with Biochar Produced from Fronds of Date Palm', *Energy Procedia*. Elsevier B.V., 74, pp. 960–965. doi: 10.1016/j.egypro.2015.07.729.
- Kochanek, J. *et al.* (2022) 'Biochar for intensification of plant-related industries to meet productivity, sustainability and economic goals: A review', *Resources, Conservation and Recycling*. Elsevier B.V., 179(December 2021), p. 106109. doi: 10.1016/j.resconrec.2021.106109.
- Kocsis, T., Ringer, M. and Biró, B. (2022) 'Characteristics and Applications of Biochar in Soil–Plant Systems: A Short Review of Benefits and Potential Drawbacks', *Applied Sciences (Switzerland)*, 12(8). doi: 10.3390/app12084051.
- Konneh, M. *et al.* (2021a) 'Adsorption and desorption of nutrients from abattoir wastewater: modelling and comparison of rice, coconut and coffee husk biochar', *Heliyon*. Elsevier Ltd, 7(11), p. e08458. doi: 10.1016/j.heliyon.2021.e08458.
- Konneh, M. *et al.* (2021b) 'Adsorption and desorption of nutrients from abattoir wastewater: modelling and comparison of rice, coconut and coffee husk biochar', *Heliyon*. Elsevier Ltd, 7(11), p. e08458. doi: 10.1016/j.heliyon.2021.e08458.
- Kumar, A. *et al.* (2022) 'A perspective on biochar for repairing damages in the soil–plant system caused by climate change-driven extreme weather events', *Biochar*. Springer Singapore, 4(1), pp. 1–23. doi: 10.1007/s42773-022-00148-z.
- Kumar, A. and Bhattacharya, T. (2021) 'Biochar: a sustainable solution', *Environment, Development and Sustainability*. Springer Netherlands, 23(5), pp. 6642–6680. doi: 10.1007/s10668-020-00970-0.
- Lehmann, J. and Joseph, S. (2009) *Biochar for Environmental Management: Science and Technology*. Available at: <https://www.semanticscholar.org/paper/Biochar-for-Environmental-Management%3A-Science-and-Lehmann-Joseph/8c7d4888bcb63d2200c1cfd7511626b36662486>.
- Lehmann, J. and Joseph, S. (2015) *Biochar for Environmental Management: Science, Technology and Implementation*. 2nd edn. Routledge, 2015.
- Liu, X. *et al.* (2013) 'Biochar's effect on crop productivity and the dependence on experimental conditions—a meta-analysis of literature data', *Plant and Soil*, 373(1), pp. 583–594. doi: 10.1007/s11104-013-1806-x.
- Liu, Z. *et al.* (2017) 'Biochar particle size, shape, and porosity act together to influence soil water properties', *PLoS ONE*, 12(6), pp. 1–19. doi: 10.1371/journal.pone.0179079.
- Malek, C. (2014) *UAE-made sand could save thousands of gallons of water*, *The National*. Available at: <http://www.thenational.ae/uae/environment/uae-made-waterproof-sand-that-is-worth-its-salt#ixzz2vJPNcJLM> (Accessed: 12 February 2014).
- Mecheri, G., Hafsi, S. and Gherraf, N. (2015) 'Preparation and Characterization of a Porous Material from Algerian Desert Sand', 7(1), pp. 69–74.
- Nair, V. D. and Mukherjee, A. (2022) 'The use of biochar for reducing carbon footprints in land-use systems: prospects and problems', *Carbon Footprints*, 1(2), p. 12. doi: 10.20517/cf.2022.13.
- Neogi, S. *et al.* (2022) 'Sustainable biochar: A facile strategy for soil and environmental restoration, energy generation, mitigation of global climate change and circular bioeconomy', *Chemosphere*. Elsevier Ltd, 293(December 2021), p. 133474. doi:

10.1016/j.chemosphere.2021.133474.

Novotný, M. *et al.* (2023) 'The use of biochar made from biomass and biosolids as a substrate for green infrastructure: A review', *Sustainable Chemistry and Pharmacy*. Elsevier B.V., 32(January), p. 100999. doi: 10.1016/j.scp.2023.100999.

Oni, B. A., Oziegbe, O. and Olawole, O. O. (2019) 'Significance of biochar application to the environment and economy', *Annals of Agricultural Sciences*, 64(2), pp. 222–236. doi: 10.1016/j.aoas.2019.12.006.

Ouarda, T. B. M. J. *et al.* (2014) 'Evolution of the rainfall regime in the united arab emirates', *Journal of Hydrology*. Elsevier B.V., 514, pp. 258–270. doi: 10.1016/j.jhydrol.2014.04.032.

Particle Size Distribution Curve (2019). Available at: <https://www.elementaryengineeringlibrary.com/civil-engineering/soil-mechanics/particle-size-distribution-curve>.

Patrignani, A. and Ochsner, T. E. (2015) 'Canopeo: A Powerful New Tool for Measuring Fractional Green Canopy Cover', (July). doi: 10.2134/agronj15.0150.

Quan, C. *et al.* (2023) 'Biomass-based carbon materials for CO₂ capture: A review', *Journal of CO₂ Utilization*. Elsevier Ltd, 68(September 2022), p. 102373. doi: 10.1016/j.jcou.2022.102373.

Rabbi, S. M. F. *et al.* (2021) 'Greater, but not necessarily better: The influence of biochar on soil hydraulic properties', *European Journal of Soil Science*, 72(5), pp. 2033–2048. doi: 10.1111/ejss.13105.

Ragula, U. B. R., Devanathan, S. and Subramanian, S. (2016) 'Modeling and Optimization of Product Profiles in Biomass Pyrolysis', *Intech*, pp. 225–240. Available at: <https://www.intechopen.com/books/advanced-biometric-technologies/liveness-detection-in-biometrics>.

Rosa, J. M. D. la (2020) *Biochar as soil amendment: Impact on soil properties and sustainable resource management*, *Mdpi*.

Rutherford, D. W. *et al.* (2012) 'Effect of formation conditions on biochars: Compositional and structural properties of cellulose, lignin, and pine biochars', *Biomass and Bioenergy*. Elsevier Ltd, 46, pp. 693–701. doi: 10.1016/j.biombioe.2012.06.026.

Saarnio, S., Heimonen, K. and Kettunen, R. (2013) 'Biochar addition indirectly affects N₂O emissions via soil moisture and plant N uptake', *Soil Biology and Biochemistry*. Elsevier Ltd, 58, pp. 99–106. doi: 10.1016/j.soilbio.2012.10.035.

Salem, I. Ben, Saleh, M. B., *et al.* (2021) 'Date palm waste pyrolysis into biochar for carbon dioxide adsorption', *Energy Reports*, 7, pp. 152–159. doi: 10.1016/j.egy.2021.06.027.

Salem, I. Ben, Gamal, M. El, *et al.* (2021) 'Utilization of the UAE date palm leaf biochar in carbon dioxide capture and sequestration processes', *Journal of Environmental Management*. Elsevier Ltd, 299(August), p. 113644. doi: 10.1016/j.jenvman.2021.113644.

Seyedsadr, S. *et al.* (2022) 'Biochar considerably increases the easily available water and nutrient content in low-organic soils amended with compost and manure', *Chemosphere*, 293(December 2021). doi: 10.1016/j.chemosphere.2022.133586.

Shahin, S. M. and Salem, M. A. (2015) 'The Challenges of Water Scarcity and the Future of Food Security in the United Arab Emirates (UAE)', *Natural Resources and Conservation*, 3(1), pp. 1–6. doi: 10.13189/nrc.2015.030101.

- Singh Yadav, S. P. *et al.* (2023) 'Biochar application: A sustainable approach to improve soil health', *Journal of Agriculture and Food Research*. Elsevier B.V., 11(January), p. 100498. doi: 10.1016/j.jafr.2023.100498.
- Sizirici, B. *et al.* (2021) 'The effect of pyrolysis temperature and feedstock on date palm waste derived biochar to remove single and multi-metals in aqueous solutions', *Sustainable Environment Research*. Sustainable Environment Research, 31(1). doi: 10.1186/s42834-021-00083-x.
- Som, A. M., Wang, Z. and Al-Tabbaa, A. (2012) 'Palm frond biochar production and characterisation', *Earth and Environmental Science Transactions of the Royal Society of Edinburgh*, 103(1), pp. 39–50. doi: 10.1017/S1755691012000035.
- Som, A. M., Wang, Z. and Al-Tabbaa, A. (2013) 'Palm frond biochar production and characterisation', *Earth and Environmental Science Transactions of the Royal Society of Edinburgh*, 103(1), pp. 39–48. doi: 10.1017/S1755691012000035.
- Soti, P. G. *et al.* (2015) 'Effect of soil pH on growth, nutrient uptake, and mycorrhizal colonization in exotic invasive *Lygodium microphyllum*', *Plant Ecology*. Springer Netherlands, 216(7), pp. 989–998. doi: 10.1007/s11258-015-0484-6.
- Stenke, F., David, T. and Gallipoli, D. (2015) 'Comparison of Water Retention Curves for Clayey Soils Using Different Measurement Techniques', pp. 1–11.
- Stewart, R. I. A. *et al.* (2013) *Mesocosm Experiments as a Tool for Ecological Climate-Change Research*, *Advances in Ecological Research*. Elsevier Ltd. doi: 10.1016/B978-0-12-417199-2.00002-1.
- Sun, J. *et al.* (2023) 'Biochar promotes soil aggregate stability and associated organic carbon sequestration and regulates microbial community structures in Mollisols from northeast China', *Soil*, 9(1), pp. 261–275. doi: 10.5194/soil-9-261-2023.
- Taheran, M. *et al.* (2016) 'Adsorption study of environmentally relevant concentrations of chlortetracycline on pinewood biochar', *Science of the Total Environment*. Elsevier B.V., 571, pp. 772–777. doi: 10.1016/j.scitotenv.2016.07.050.
- Tengku Yasim-Anuar, T. A. *et al.* (2022) 'Emerging application of biochar as a renewable and superior filler in polymer composites', *RSC Advances*, 12(22), pp. 13938–13949. doi: 10.1039/d2ra01897g.
- Thunberg, G. (2022) *The Climate Book*. Penguin Random House.
- Tisserant, A. and Cherubini, F. (2019) 'Potentials, limitations, co-benefits, and trade-offs of biochar applications to soils for climate change mitigation', *Land*, 8(12). doi: 10.3390/LAND8120179.
- Tomczyk, A., Sokołowska, Z. and Boguta, P. (2020) 'Biochar physicochemical properties: pyrolysis temperature and feedstock kind effects', *Reviews in Environmental Science and Biotechnology*. Springer Netherlands, 19(1), pp. 191–215. doi: 10.1007/s11157-020-09523-3.
- Tusar, H. M. *et al.* (2023) 'Biochar-Acid Soil Interactions—A Review', *Sustainability (Switzerland)*, 15(18). doi: 10.3390/su151813366.
- Usman, A. R. A. *et al.* (2015) 'Biochar production from date palm waste: Charring temperature induced changes in composition and surface chemistry', *Journal of Analytical and Applied Pyrolysis*. Elsevier B.V., 115, pp. 392–400. doi: 10.1016/j.jaap.2015.08.016.
- Vossen, R. (2022) *Microscopy of Sand, Microscopy of Nature*. Available at:

<https://microscopyofnature.com/microscopy-sand> (Accessed: 19 September 2022).

Wang, J., Xiong, Z. and Kuzyakov, Y. (2016) 'Biochar stability in soil: Meta-analysis of decomposition and priming effects', *GCB Bioenergy*, 8(3), pp. 512–523. doi: 10.1111/gcbb.12266.

Wang, Y. *et al.* (2017) 'Remediation of Petroleum-contaminated Soil Using Bulrush Straw Powder, Biochar and Nutrients', *Bulletin of Environmental Contamination and Toxicology*. Springer US, 98(5), pp. 690–697. doi: 10.1007/s00128-017-2064-z.

Wang, Y., Yin, R. and Liu, R. (2014) 'Characterization of biochar from fast pyrolysis and its effect on chemical properties of the tea garden soil', *Journal of Analytical and Applied Pyrolysis*. Elsevier B.V., 110(1), pp. 375–381. doi: 10.1016/j.jaap.2014.10.006.

Woolf, D. *et al.* (2010) 'Sustainable biochar to mitigate global climate change', *Nature Communications*. Nature Publishing Group, 1(5), pp. 1–9. doi: 10.1038/ncomms1053.

Yang, W. *et al.* (2019) 'Adsorption of copper(II) and lead(II) from seawater using hydrothermal biochar derived from *Enteromorpha*', *Marine Pollution Bulletin*, 149. doi: 10.1016/j.marpolbul.2019.110586.

Yu, H. *et al.* (2019) 'Biochar amendment improves crop production in problem soils: A review', *Journal of Environmental Management*. Elsevier, 232(September 2018), pp. 8–21. doi: 10.1016/j.jenvman.2018.10.117.

Zhang, J. *et al.* (2021) 'Biochar Addition Altered Bacterial Community and Improved Photosynthetic Rate of Seagrass: A Mesocosm Study of Seagrass *Thalassia hemprichii*', *Frontiers in Microbiology*, 12(December). doi: 10.3389/fmicb.2021.783334.

Zhang, Y. *et al.* (2022) 'Biochar as construction materials for achieving carbon neutrality', *Biochar*. Springer Nature Singapore, 4(1). doi: 10.1007/s42773-022-00182-x.

Zhang, Y. *et al.* (2023) 'Field verification of low-level biochar applications as effective ameliorants to mitigate cadmium accumulation into *Brassica campestris* L from polluted soils', *Frontiers in Environmental Science*, 10(January), pp. 1–8. doi: 10.3389/fenvs.2022.1114335.

Zheng, X. *et al.* (2022) 'The effects of biochar and its applications in the microbial remediation of contaminated soil : A review', *Journal of Hazardous Materials*. Elsevier B.V., 438(July), p. 129557. doi: 10.1016/j.jhazmat.2022.129557.

Zubairu, A. M., Kwari, S. J. and Buba, M. T. (2023) 'Exploring the effect of biochar on soil pH (A review) Colloquia Series Available Online at www.ssn.ng', (November).